Colorado – New Mexico
Regional Extreme Precipitation Study

Summary Report
Volume II
Deterministic Regional Probable Maximum Precipitation Estimation

November 30, 2018

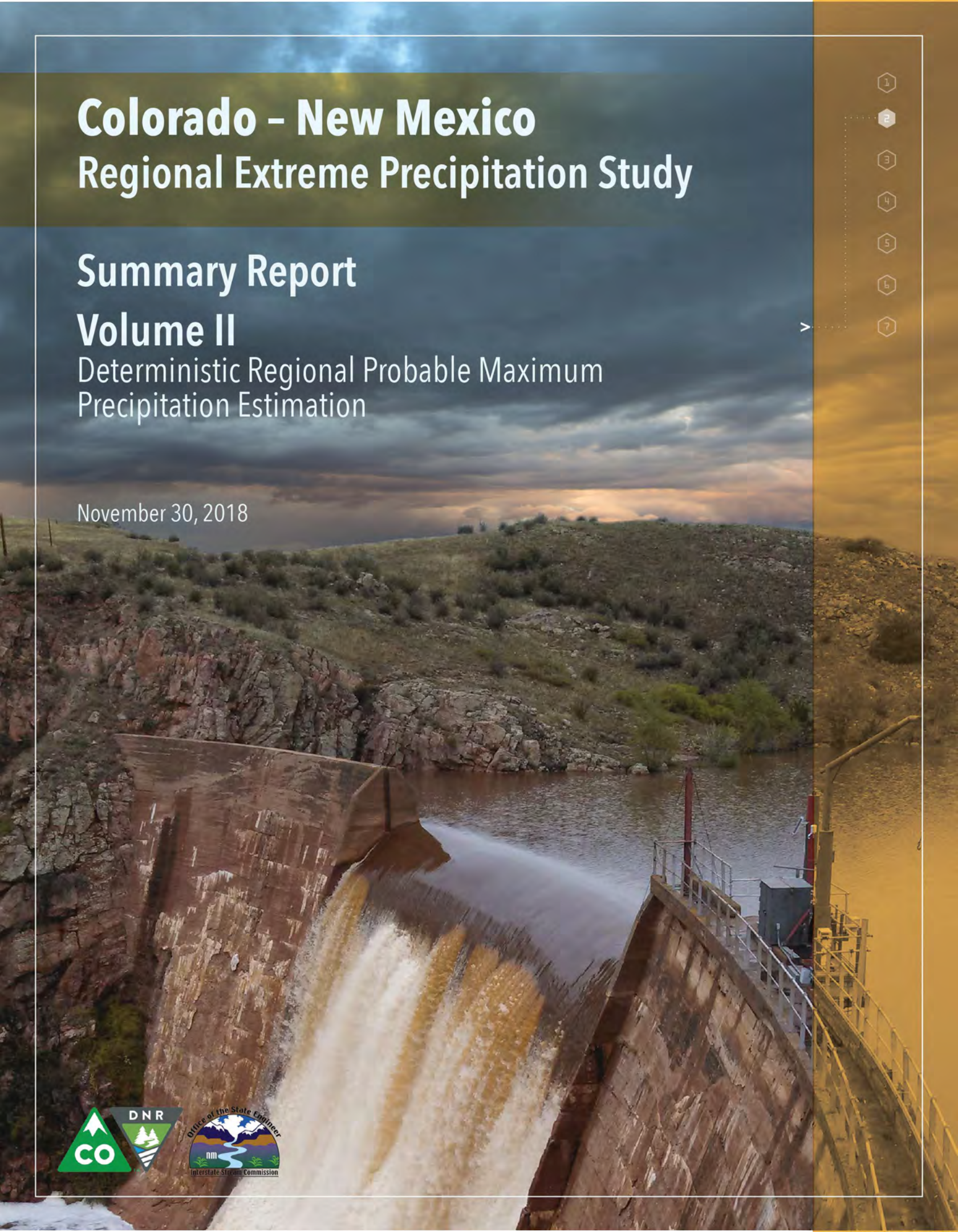

This page left intentionally blank

Colorado – New Mexico
Regional Extreme Precipitation Study

Summary Report

Volume II

Deterministic Regional Probable Maximum Precipitation Estimation

Prepared by:
Applied Weather Associates

November 30, 2018

COLORADO
Division of Water Resources
Department of Natural Resources

Office of the State Engineer
Interstate Stream Commission

This page left intentionally blank

Table of Contents

List of Figures

List of Tables

Appendices

Glossary

Adiabat: Curve of thermodynamic change taking place without addition or subtraction of heat. On an adiabatic chart or pseudo-adiabatic diagram, a line showing pressure and temperature changes undergone by air rising or condensation of its water vapor; a line, thus, of constant potential temperature.

Adiabatic: Referring to the process described by adiabat.

Advection: The process of transfer (of an air mass property) by virtue of motion. In particular cases, advection may be confined to either the horizontal or vertical components of the motion. However, the term is often used to signify horizontal transfer only.

Air mass: A body of air with horizontally uniform temperature, humidity, and pressure.

Barrier: A mountain range that partially blocks the flow of warm humid air from a source of moisture to the basin under study.

Basin centroid: The point at the exact center of the drainage basin as determined through geographical information systems calculations using the basin outline.

Basin shape: The physical outline of the basin as determined from topographic maps, field survey, or geographic information system (GIS).

Cold front: Front where relatively colder air displaces warmer air.

Convective rain: Rainfall caused by the vertical motion of an ascending mass of air that is warmer than the environment and typically forms a cumulonimbus cloud. The horizontal dimension of such a mass of air is generally of the order of 12 miles or less. Convective rain is typically of greater intensity than either of the other two main classes of rainfall (cyclonic and orographic), and is often accompanied by thunder. The term is more particularly used for those cases in which the precipitation covers a large area as a result of the agglomeration of cumulonimbus masses.

Convergence: Horizontal shrinking and vertical stretching of a volume of air, accompanied by net inflow horizontally and internal upward motion.

Cooperative station: A weather observation site where an unpaid observer maintains a climatological station for the National Weather Service (NWS).

Correlation coefficient: The average change in the dependent variable, the orographically transposed rainfall (P_o), for a 1-unit change in the independent variable, the in-place rainfall (P_i).

Cyclone: A distribution of atmospheric pressure in which there is a low central pressure relative to the surroundings. On large-scale weather charts, cyclones are characterized by a system of closed constant pressure lines (isobars), generally approximately circular or oval in form, enclosing a central low-pressure area. Cyclonic circulation is counterclockwise in the northern hemisphere and clockwise in the southern. (That is, the sense of rotation about the local vertical is the same as that of the earth's rotation).

Depth-Area curve: Curve showing the relation of maximum average depth to size of area within a storm or storms for a given duration.

Depth-Area-Duration: The precipitation values derived from Depth-Area and Depth-Duration curves at each time and area size increment analyzed for a probable maximum precipitation (PMP) evaluation.

Depth-Area-Duration curve: A curve showing the relation between an averaged areal rainfall depth and the area over which it occurs, for a specified time interval, during a specific rainfall event.

Depth-Area-Duration values: The combination of Depth-Area and Duration-Depth relations. Also called Depth-Duration-Area.

Depth-Duration curve: Curve showing the relation of maximum average depth of precipitation to duration periods within a storm or storms for a given area size.

Dew point: The temperature to which a given parcel of air must be cooled at constant pressure and constant water vapor content for saturation to occur.

Effective barrier height: The height of a barrier determined from elevation analysis that reflects the effect of the barrier on the precipitation process for a storm event. The actual barrier height may be either higher or lower than the effective barrier height.

Endorheic: A closed drainage basin that retains water and allows no outflow to other external bodies of water such as rivers or oceans, but converges instead into lakes or swamps, permanent or seasonal, that equilibrate through evaporation.

Envelopment: A process for selecting the largest value from any set of data. In estimating PMP, the maximum and transposed rainfall data are plotted on graph paper, and a smooth curve is drawn through the largest values.

Explicit transposition: The movement of the rainfall amounts associated with a storm within boundaries of a region throughout which a storm may be transposed with only relatively minor modifications of the observed storm rainfall amounts. The area

within the transposition limits has similar, but not identical, climatic and topographic characteristics throughout.

First-order NWS station: A weather station that is either automated, or staffed by employees of the National Weather Service and records observations on a continuous basis.

Front: The interface or transition zone between two air masses of different parameters. The parameters describing the air masses are temperature and dew point.

General storm: A storm event that produces precipitation over areas in excess of 500-square miles, has a duration longer than 6 hours, and is associated with a major synoptic weather feature.

Geographic Transposition Factor (GTF): A factor representing the comparison of precipitation frequency relationships between two locations which is used to quantify how rainfall is affected by physical processes related to location and terrain. It is assumed the precipitation frequency data are a combination of what rainfall would have accumulated without topographic affects and what accumulated because of the topography, both at the location and upwind of the location being analyzed.

Hydrologic unit: A hydrologic unit is a drainage area delineated to nest in a multi-level, hierarchical drainage system. Its boundaries are defined by hydrographic and topographic criteria that delineate an area of land upstream from a specific point on a river, stream or similar surface waters. A hydrologic unit can accept surface water directly from upstream drainage areas, and indirectly from associated surface areas such as remnant, non-contributing, and diversions to form a drainage area with single or multiple outlet points. Hydrologic units are only synonymous with classic watersheds when their boundaries include all the source area contributing surface water to a single defined outlet point

HYSPLIT: Hybrid Single-Particle Lagrangian Integrated Trajectory. A complete system for computing parcel trajectories to complex dispersion and deposition simulations using either puff or particle approaches. Gridded meteorological data, on one of three conformal (Polar, Lambert, or Mercator latitude-longitude grid) map projections, are required at regular time intervals. Calculations may be performed sequentially or concurrently on multiple meteorological grids, usually specified from fine to coarse resolution.

Implicit transpositioning: The process of applying regional, areal, or durational smoothing to eliminate discontinuities resulting from the application of explicit transposition limits for various storms.

Isohyets: Lines of equal value of precipitation for a given time interval.

Isohyetal pattern: The pattern formed by the isohyets of an individual storm.

Isohyetal orientation: The term used to define the orientation of precipitation patterns of major storms when approximated by elliptical patterns of best fit. It is also the orientation (direction from north) of the major axis through the elliptical PMP storm pattern.

Jet Stream: A strong, narrow current concentrated along a quasi-horizontal axis (with respect to the earth's surface) in the upper troposphere or in the lower stratosphere, characterized by strong vertical and lateral wind shears. Along this axis it features at least one velocity maximum (jet streak). Typical jet streams are thousands of kilometers long, hundreds of kilometers wide, and several kilometers deep. Vertical wind shears are on the order of 10 to 20 mph per kilometer of altitude and lateral winds shears are on the order of 10 mph per 100 kilometers of horizontal distance.

Local storm: A storm event that occurs over a small area in a short time period. Precipitation rarely exceeds 6 hours in duration and the area covered by precipitation is less than 500 square miles. Frequently, local storms will last only 1 or 2 hours and precipitation will occur over areas of up to 200 square miles. Precipitation from local storms will be isolated from general-storm rainfall. Often these storms are thunderstorms.

Low Level Jet stream: A band of strong winds at an atmospheric level well below the high troposphere as contrasted with the jet streams of the upper troposphere.

Mass curve: Curve of cumulative values of precipitation through time.

Mesoscale Convective Complex: For the purposes of this study, a heavy rain-producing storm with horizontal scales of 10 to 1000 kilometers (6 to 625 miles) which includes significant, heavy convective precipitation over short periods of time (hours) during some part of its lifetime.

Mesoscale Convective System: A complex of thunderstorms which becomes organized on a scale larger than the individual thunderstorms, and normally persists for several hours or more. MCSs may be round or linear in shape, and include systems such as tropical cyclones, squall lines, and MCCs (among others). MCS often is used to describe a cluster of thunderstorms that does not satisfy the size, shape, or duration criteria of an MCC.

Mid-latitude frontal system: An assemblage of fronts as they appear on a synoptic chart north of the tropics and south of the polar latitudes. This term is used for a continuous front and its characteristics along its entire extent, its variations of intensity, and any frontal cyclones along it.

Moisture maximization: The process of adjusting observed precipitation amounts upward based upon the hypothesis of increased moisture inflow to the storm.

Observational day: The 24-hour time period between daily observation times for two consecutive days at cooperative stations, e.g., 6:00PM to 6:00PM.

One-hundred-year rainfall event: The point rainfall amount that has a one-percent probability of occurrence in any year. Also referred to as the rainfall amount that has a 1 percent chance of occurring in any single year.

Polar front: A semi-permanent, semi-continuous front that separates tropical air masses from polar air masses.

Precipitable water: The total atmospheric water vapor contained in a vertical column of unit cross-sectional area extending between any two specified levels in the atmosphere; commonly expressed in terms of the height to which the liquid water would stand if the vapor were completely condensed and collected in a vessel of the same unit cross-section. The total precipitable water in the atmosphere at a location is that contained in a column or unit cross-section extending from the earth's surface all the way to the "top" of the atmosphere. The 30,000-foot level (approximately 300mb) is considered the top of the atmosphere in this study.

Persisting dew point: The dew point value at a station that has been equaled or exceeded throughout a period. Commonly durations of 12 or 24 hours are used, though other durations may be used at times.

Probable Maximum Flood: The flood that may be expected from the most severe combination of critical meteorological and hydrologic conditions that are reasonably possible in a particular drainage area.

Probable Maximum Precipitation: Theoretically, the greatest depth of precipitation for a given duration that is physically possible over a given size storm area at a particular geographic location at a certain time of the year.

Pseudo-adiabat: Line on thermodynamic diagram showing the pressure and temperature changes undergone by saturated air rising in the atmosphere, without ice-crystal formation and without exchange of heat with its environment, other than that involved in removal of any liquid water formed by condensation.

Rainshadow: The region, on the lee side of a mountain or mountain range, where the precipitation is noticeably less than on the windward side.

Saturation: Upper limit of water-vapor content in a given space; solely a function of temperature.

Shortwave: Also referred to as a shortwave trough, is an embedded kink in the trough / ridge pattern. This is the opposite of longwaves, which are responsible for synoptic

scale systems, although shortwaves may be contained within or found ahead of longwaves and range from the mesoscale to the synoptic scale.

Spatial distribution: The geographic distribution of precipitation over a drainage according to an idealized storm pattern of the PMP for the storm area.

Storm transposition: The hypothetical transfer, or relocation of storms, from the location where they occurred to other areas where they could occur. The transfer and the mathematical adjustment of storm rainfall amounts from the storm site to another location is termed "explicit transposition." The areal, durational, and regional smoothing done to obtain comprehensive individual drainage estimates and generalized PMP studies is termed "implicit transposition" (WMO, 1986).

Synoptic: Showing the distribution of meteorological elements over an area at a given time, e.g., a synoptic chart. Use in this report also means a weather system that is large enough to be a major feature on large-scale maps (e.g., of the continental U.S.).

Temperature inversion: An increase in temperature with an increase in height.

Temporal distribution: The time order in which incremental PMP amounts are arranged within a PMP storm.

Tropical Storm: A cyclone of tropical origin that derives its energy from the ocean surface.

Total storm area and total storm duration: The largest area size and longest duration for which depth-area-duration data are available in the records of a major storm rainfall.

Transposition limits: The outer boundaries of the region surrounding an actual storm location that has similar, but not identical, climatic and topographic characteristics throughout. The storm can be transpositioned within the transposition limits with only relatively minor modifications to the observed storm rainfall amounts.

Undercutting: The process of placing an envelopment curve somewhat lower than the highest rainfall amounts on depth-area and depth-duration plots.

Warm front: Front where relatively warmer air replaces colder air.

List of Acronyms

AMS: Annual maximum series

AWA: Applied Weather Associates

DAD: Depth-Area-Duration

dd: decimal degrees

EPRI: *Electric Power Research Institute*

F: Fahrenheit

GCS: Geographical coordinate system

GEV: Generalized extreme value

GIS: Geographic Information System

GRASS: Geographic Resource Analysis Support System

GTF: Geographic Transposition Factor

HMR: Hydrometeorological Report

HUC: Hydrologic Unit Code

HYSPLIT: Hybrid Single Particle Lagrangian Integrated Trajectory Model

IPMF: In-place Maximization Factor

mb: millibar

MCS: Mesoscale Convective System

MTF: Moisture Transposition Factor

NCAR: National Center for Atmospheric Research

NCDC: National Climatic Data Center

NCEP: National Centers for Environmental Prediction

NEXRAD: Next Generation Radar

NOAA: National Oceanic and Atmospheric Administration

NWS: National Weather Service

NRCS: Natural Resources Conservation Service

PMF: Probable Maximum Flood

PMP: Probable Maximum Precipitation

PRISM: Parameter-elevation Relationships on Independent Slopes

PW: Precipitable Water

SPAS: Storm Precipitation and Analysis System

TAF: Total Adjustment Factor

USACE: US Army Corps of Engineers

USBR: Bureau of Reclamation

USGS: United States Geological Survey

WBD: Watershed Boundary Database

WMO: World Meteorological Organization

1. PMP Development Background

Probable Maximum Precipitation (PMP) depths developed during this study utilized the storm-based process to derive deterministic values (WMO, 2009). This requires the identification and analysis of PMP-type storm events that have occurred over the region of interest and regions of similar meteorology and topography. This study covered the two-state region of Colorado and New Mexico and immediately adjacent areas for which the state dam safety offices are responsible for regulating (Figure 1). This region is covered by Hydrometeorological Reports (HMRs) 49 (Hansen et al., 1977), 51 (Schreiner and Riedel, 1978), and 55A (Hansen et al., 1988). Results of this study replace HMR PMP values for Colorado and New Mexico dam safety programs.

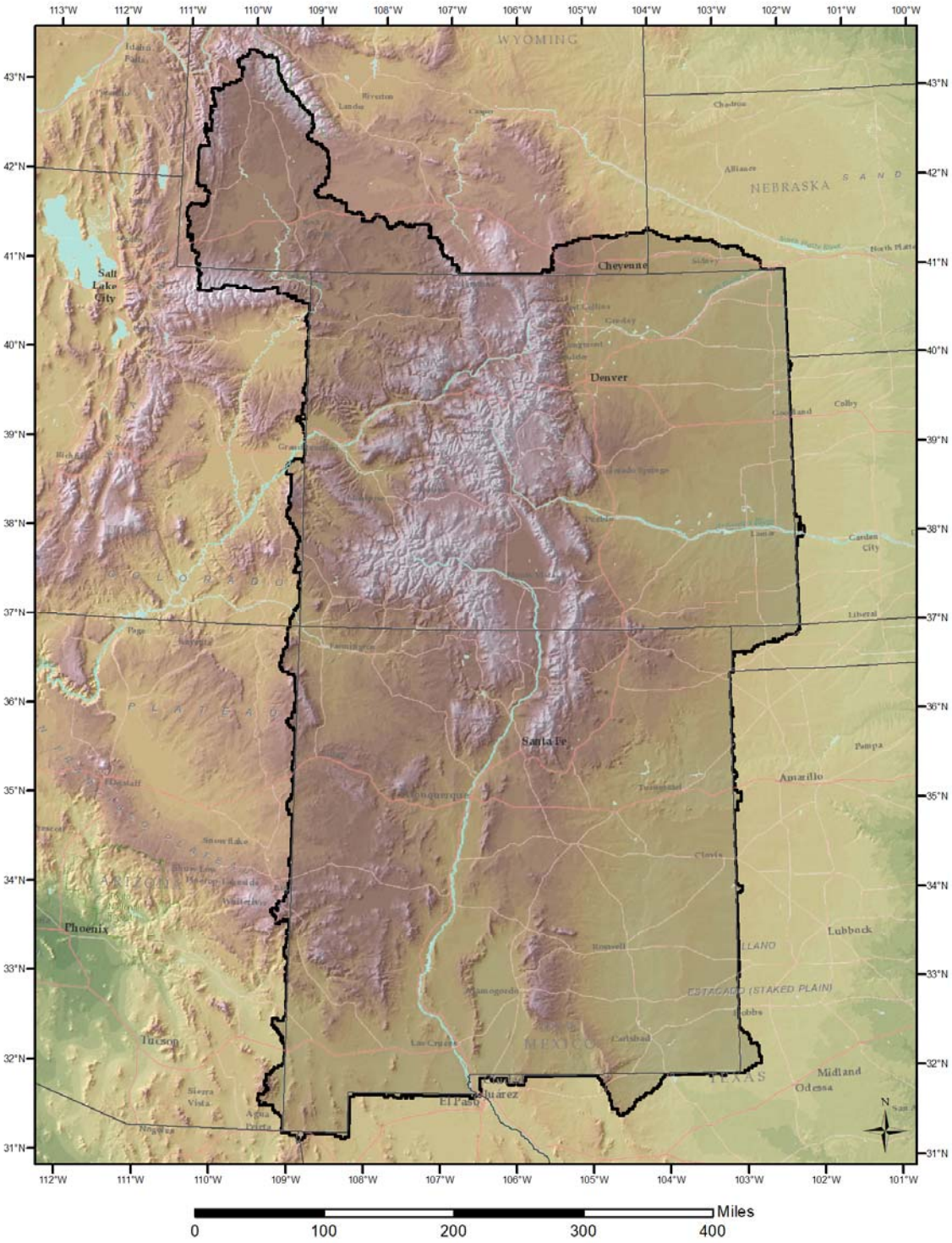

Figure 1: Probable Maximum Precipitation study domain

2. Methodology

The storm-based approach used in this study is consistent with many of the procedures that were used in the development of the HMRs and as described in the World Meteorological Organization PMP documents (WMO, 2009), with updated procedures implemented where appropriate. Methodologies reflecting the current standard of practice were applied in this study considering the unique meteorological and topographical interactions within the region as well as the updated scientific data and procedures available. Updated procedures are described in detail later in this report. Figure 2 provides the general steps used in deterministic PMP development utilizing the storm-based approach. Terrain characteristics are addressed as they specifically affect rainfall patterns spatially, temporally, and in magnitude.

This study identified major storms that occurred within the region and areas where those storms were considered transpositionable within the study region. Each of the main storm types capable of producing PMP-level rainfall were identified and investigated. The main storm types included local storms, general storms, and for some regions remnant tropical storms. The "short list" of storms was extensively reviewed, quality controlled, and accepted. This short list of storms was utilized to derive the PMP depths for all locations.

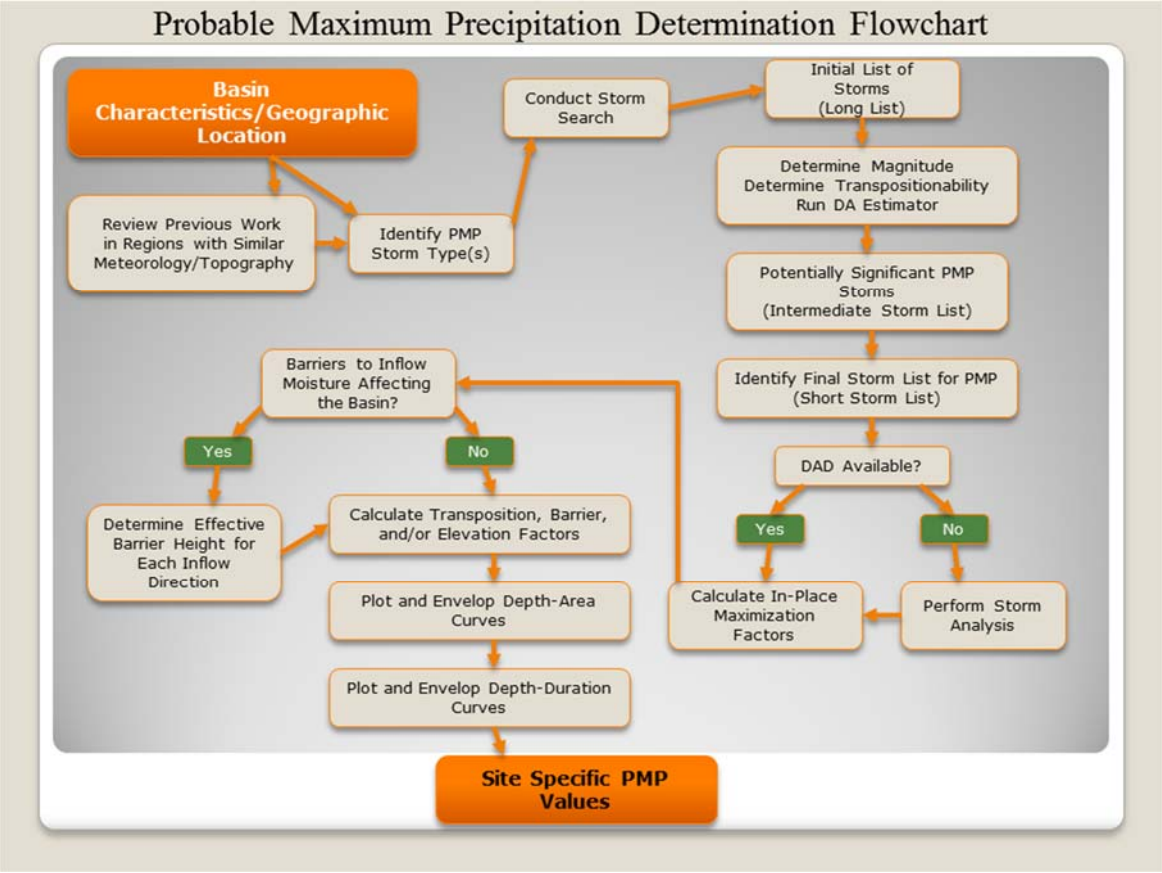

Figure 2: Probable Maximum Precipitation calculation steps

The moisture content of each of these storms was maximized to provide worst-case rainfall accumulation for each storm at the location where it occurred (in-place storm location). Storms were then transpositioned to regions with similar meteorological and topographical characteristics. Locations where each storm was transpositioned were determined using meteorological judgment, comparison of adjustment factors, comparisons of PMP depths, comparison against previous transposition limits from HMRs and AWA, discussions with the PRB, discussion with the Project Sponsors, and comparisons against precipitation frequency climatologies. Adjustments were applied to each storm as it was transpositioned to each grid point to calculate the amount of rainfall each storm would have produced at each grid point versus what it produced at the original location. These adjustments were combined to produce the total adjustment factor (TAF) for each storm for each grid point.

The TAF is applied to the observed precipitation values at the area size of interest to each storm. The Storm Precipitation Analysis System (SPAS) is utilized to analyze the rainfall associated with each storm used for PMP development. SPAS has been used to analyze more than 700 extreme rainfall events since 2002. SPAS analyses are used in PMP development as well as other numerous meteorological applications. SPAS has been extensively peer reviewed and accepted as appropriate for use in analyzing precipitation accumulation by numerous independent review boards and as part of the Nuclear Regulatory Commission (NRC) software certification process. Appendix E provides a detailed description of the SPAS program. The TAF is a product of the In-Place Maximization Factor (IPMF), the Moisture Transposition Factor (MTF), and the Geographic Transposition Factor (GTF). For this study, extensive discussion took place regarding the use of the MTF and whether it was already accounted for with the GTF process. Discussions among the PRB, Project Sponsors, and AWA did not produce conclusive evidence. Evaluation of the MTF process is ongoing currently and will be continued as a topic of future research. Therefore, it was as agreed to utilize a conservative approach and allow the MTF to be limited to 1.00 or greater.

The governing equation used for computation of the Total Adjusted Rainfall (TAR), for each storm for each grid cell for each duration, is given in Equation 1.

$$TAR_{xhr} = P_{xhr} \times IPMF \times MTF \times GTF \qquad \text{(Equation 1)}$$

where:

TAR_{xhr} is the Total Adjusted Rainfall value at the x-hour (x-hr) duration for the specific grid cell at each duration at the target location;

P_{xhr} is the x-hour precipitation observed at the historic in-place storm location (source location) for the basin-area size;

In-Place Maximization Factor (*IPMF)* is the adjustment factor representing the maximum amount of atmospheric moisture that could have been available to the storm for rainfall production;

Moisture Transposition Factor (MTF) is the adjustment factor accounting for the difference in available moisture between the location where the storm occurred and each grid cell in the basin;

Geographic Transposition Factor (GTF) is the adjustment factor accounting for precipitation frequency relationships between two locations. This is used to quantify all processes that effect rainfall, including terrain, location, and seasonality.

Note, the largest of these values at each duration becomes PMP at each grid point. The values are run at the area size specified through user input. The PMP output depths are then provided for durations required for Probable Maximum (PMF) analysis at a given location by storm type and provided as a basin average. These data have a spatial pattern and temporal pattern associated with them for hydrologic modeling implementation. The spatial and temporal patterns are based on climatological patterns (spatial) and a synthesis of historic storm accumulation patterns (temporal). Alternative spatial and temporal patterns are also possible at a given location. The user should consult with the Colorado and New Mexico dam safety offices for guidance regarding the use of alternative spatial and/or temporal patterns beyond what is provided in the tool.

2.1 Regional Climatological Characteristics Affecting PMP Storm Types

Weather patterns in the region are characterized by three main types:

1. Areas of low pressure often moving through the region from the northwest through the southwest or redeveloping along the lee slopes of the Front Range (general storms);
2. Remnant tropical moisture either from the Gulf of California or Gulf of Mexico (tropical storms); and
3. Isolated thunderstorms/Mesoscale Convective Systems (local storms).

General storms are most frequent in the fall and spring in Colorado, with winter becoming important further south into New Mexico. Remnant tropical storms occur from June through October. Local storms are most active in the spring through fall, with a distinct increase in activity during the North American Monsoon (NAM) pattern providing moisture for increased thunderstorm activity from early July through September. For more detailed descriptions of the NAM see Grantz et al., (2007), Higgins et al., (2004), Higgins et al., (1999), Adams and Comrie (1997), Higgins et al., (1997), Douglas (1995), Douglas (1993), Smith (1989), and Hales (1972).

No large bodies of water are in the region to moderate the climate and its location in proximity to the center of the continent along with elevated terrain all play a role in the weather patterns. Detailed discussion on the weather and climate of the region can be found from numerous sources, for example:

- https://wrcc.dri.edu/Climate/narrative_co.php
- https://wrcc.dri.edu/Climate/narrative_nm.php
- http://climate.colostate.edu

- https://weather.nmsu.edu

2.2 Storm Types

The PMP storm types investigated during the study were local thunderstorms/ Mesoscale Convective Systems (MCS) where the main rainfall occurs over short durations and small area sizes, general storms where main rainfall occurs over large areas sizes and longer durations, and remnant tropical systems which occur less frequently and have accumulation characteristics similar to the general storm type. The unique temporal patterns associated with each of these storms types was explicitly investigated. The development of these temporal patterns is described in Section 10.5.

The classification of storm types, and hence PMP development by storm type used in this study, is similar to descriptions provided in HMR 55A Section 1.5. Storms were classified by rainfall accumulation characteristics, while trying to adhere to previously used classifications. Several discussions took place with the PRB to ensure acceptance of the storm classifications. In addition, the storm classifications were cross-referenced with the storm typing completed as part of Precipitation Frequency Task to ensure consistency between storms.

Local storms were defined using the following guidance:

- The main rainfall accumulation period occurred over a 6-hour period or less
- Were previously classified as local storms by the USACE or in the HMRs
- Were not associated with overall synoptic patterns leading to rainfall across a large region
- Exhibited high intensity accumulations
- Occurred during the appropriate season, April through October

General storms were defined using the following guidance:

- The main rainfall accumulation period lasted for 24 hours or longer
- Occurred with a synoptic environment associated with a low-pressure system, frontal interaction, and regional precipitation coverage
- Was previously classified as a general storm by the USACE or in the HMRs
- Exhibited lower rainfall accumulation intensities compared to local storms

Tropical storms were defined using the following guidance:

- The rainfall was a direct result of a previously landfalling tropical system
- Was previously classified as a tropical storm by the USACE or in the HMRs
- Occurred during the appropriate season, June through October

It should be noted that some of the storms exhibit characteristics of more than one storm type and are therefore have been included for PMP development as more than one type. These are classified as hybrid storms.

2.2.1 Local Storms

Localized thunderstorms and MCSs are capable of producing extreme amounts of precipitation for short durations and over small area sizes, generally 6 hours or less over area sizes of 500 square miles or less. During any given hour, the heaviest rainfall only covers very small areas, generally less than 100 square miles. The PMP tool developed in this study limits the local storm PMP to 100-square miles or less. Previous statewide PMP studies in Arizona (Kappel et al., 2013) and Wyoming (Kappel et al., 2014) as well as the Precipitation Frequency Task from this study applies a 50-square mile limit was applied to the local storm PMP. Therefore, the use of a 100-square mile limitation is a conservative application for this storm type. However, it was felt this was necessary to be able to capture events with a larger footprint of rainfall. This most often occurs over the eastern plains of Colorado and New Mexico where low-level moisture sources can sustain these types of storms for longer durations and larger area sizes. Examples of this storm type are often classified as MCSs.

These are termed MCS because they are relatively small in areal extent (10s to 100s of square miles), whereas synoptic storm events are 100s to 1000s of square miles. MCSs are clusters of thunderstorms that exhibit a somewhat organized structure and contain lines or regions of thunderstorms that are often generated by adjacent thunderstorms. This will often form across the eastern plains regions of Colorado and New Mexico where individual thunderstorms that have formed over the higher elevations of the Front Range and Rocky Mountains move east in the afternoon and evening and interact with higher levels of low-level moisture and instability. These previously isolated thunderstorms will then congeal into a more organized structure as they continue a general eastward movement away from the region. These are considered hybrid type storms in this study because they can produce rainfall accumulation for durations greater than 6 hours and can be influenced by synoptic patterns and front systems.

Thunderstorms can be isolated from the overall general synoptic weather patterns and fueled by localized moisture sources. The local storm type in the Colorado-New Mexico region has a distinct seasonality, occurring during the warm season when the combination of moisture and atmospheric instability is at its greatest, most common from May through September. This is the time of the year when convective characteristics and moisture within the atmosphere are adequate to produce lift and instability needed for thunderstorm development and heavy rainfall. For regions west of the Continental Divide these processes are enhanced by the NAM. In Arizona and regions west of the Continental Divide, the NAM develops during June, reaches peak intensity during July and August, and then dissipates during September. For the region east of the Continental Divide, the NAM process also helps to increase the amount of atmospheric moisture available for storm initiation and rainfall production.

Local storm PMP values derived in this report are valid from April through October and can be associated with various synoptic conditions. Finally, local storm PMP depths should not be applied with snow pack on the ground as a snow pack would not allow

the atmospheric instability and moisture levels to occur in combination that would produce convective initiation and PMP level local storm rainfall.

2.2.2 General Storms

General storms occur in association with frontal systems and along boundaries between sharply contrasting air masses. Precipitation associated with frontal systems is enhanced when the movement of weather patterns slow or stagnates, allowing moisture and instability to affect the same general region for several days. In addition, when there is a larger than normal thermal contrast between air masses in combination with higher than normal moisture, PMP-level precipitation can occur. The processes are often enhanced by the effects of topography, with heavier precipitation occurring along and immediately upwind of upslope regions. Intense regions of heavy rain can also occur along a front as a smaller scale disturbance moving along the frontal boundary, called a shortwave, creates a region of enhanced lift and instability. These shortwaves are not strong enough to move the overall large-scale pattern, but instead add to the storm dynamics and energy available for producing precipitation.

This type of storm will usually not produce the highest rainfall rates over short durations, but instead leads to flooding situations as moderate rain continues to fall over the same region for an extended period of time.

The seasonality of general storms varies throughout the region. Although they can occur at almost any time of the year, they are generally strongest from fall through spring. Strong frontal systems do affect many parts of the region in winter. However, most of the precipitation occurs in the form of snow, especially at higher elevations. Therefore, the full general storm PMP depths are valid from May through November east of the Continental Divide and in transposition zones 9, 14, 15, and 16 (*cf: Section 7.3, Transposition Zones*). For the remaining transposition zones west of the Continental Divide (transposition zones 10-13) the full general storm PMP depths are valid October through March. Rainfall from frontal systems is generally less intense during the summer season when frontal dynamics and instability are less than the fall and spring seasons. This results in lower intensities and shorter durations. In addition, during the summer months, local and/or tropical storms dominate rainfall accumulations. Finally, the general storm PMP is assumed to be a rainfall only event where melting snow would not contribute significantly to runoff.

2.2.3 Tropical Storms

Tropical storms can affect southern portions of the study region, with the possibility of controlling PMP depths for regions south of 38.5°N latitude. These storms only form from June through October because of their reliance on warm water along with supporting synoptic and upper level weather patterns. They can originate from the Gulf of California, Eastern Pacific, and Gulf of Mexico prior to moving into the region. In addition, because of their reliance on moisture and warm ocean temperatures their influence decreases rapidly once they move inland and away from the moisture and energy sources. Therefore, tropical storm PMP was only developed for regions south of 38.5°N latitude. This is similar (although slightly further north, i.e. more

conservative) than limits used in HMR 55A. Figure 2.32 in HMR 55A shows remnant tropical systems that affected the region. This does not mean remnant tropical moisture has no effect on areas further north, however the magnitude of rainfall is significantly less than local or general storms and therefore does not control PMP depths. The remnant air mass from a tropical system can add high levels of moisture and potential convective energy to the atmosphere, while circulations associated with the original tropical system continue to persist at diminished levels within the atmosphere. When these systems move slowly over a region, large amounts of rainfall can be produced both in convective bursts and over longer durations.

2.3 Topographic Effects on Precipitation

Terrain plays a significant role in precipitation development and accumulation patterns in time and space. The terrain within the region both enhances and depresses precipitation depending on whether the terrain is forcing the air to rise (upslope effect) or descend (downslope). To account for the effect of precipitation by terrain features (called orographic effects), explicit evaluations were performed using precipitation frequency climatologies and investigations into past storm spatial and accumulation patterns across the region. The NOAA Atlas 14 precipitation frequency climatologies (Bonin et al., 2011 and Perica et al., 2013), the Wyoming statewide precipitation frequency data developed by AWA (Kappel et al., 2014), and the Texas statewide precipitation frequency data developed by AWA (Kappel et al., 2016) were used in this analysis. These climatologies were also used to derive the GTF and the spatial distribution of the PMP. This approach is similar to the use of the NOAA Atlas 2 100-year 24-hour precipitation frequency climatologies used in HMRs 55A (Section 6.3 and 6.4, Hansen et al., 1988), 57 (Section 8.1, Hansen et al., 1994), and 59 (Section 6.61. and 6.6.2, Corrigan et al., 1999) as part of the Storm Separation Method (SSM) to quantify orographic effects in topographically significant regions.

The quantification of orographic effects was completed by evaluating rainfall depths at the 100-year recurrence interval using the 6-hour duration for local storms and the 24-hour duration for tropical and general storms at both the source (storm center) and target (grid point) location. This comparison produced a ratio that quantified the differences of precipitation processes, including topography, between the two locations. The assumption is that the precipitation frequency data represent all aspects that have produced precipitation at a given location over time, including the effect of terrain both upwind and in-place. Therefore, if two locations are compared within regions of similar meteorological and topographical characteristics, the resulting difference of the precipitation frequency climatology should reflect the difference of all precipitation producing processes between the two locations, including topography.

This relationship between precipitation frequency climatology and terrain is also recognized in the WMO PMP Manual (WMO, 1986 pg. 54 and by the Australian Bureau of Meteorology (Section 3.1.2.3 of Minty et al., 1996). Although the orographic effect at a particular location may vary from storm to storm, the overall effect of the topographic influence (or lack thereof) is inherently included in the

climatology of precipitation that occurred at that location, assuming that the climatology is based on storms of the same type. In WMO 2009 Section 3.1.4 it is stated "since precipitation-frequency values represent equal probability, they can also be used as an indicator of the effects of topography over limited regions. If storm frequency, moisture availability, and other precipitation-producing factors do not vary, or vary only slightly, over an orographic region, differences in precipitation-frequency values should be directly related to variations in orographic effects." Therefore, by applying appropriate transposition limits, analyzing by storm type, and utilizing duration for storm typing, it is assumed the storms being compared using the precipitation frequency data are of similar moisture availability and other precipitation-producing factors.

This assumption was explicitly evaluated and determined to be acceptable during the course of this study through various sensitivities and discussions with the PRB and Project Sponsors. These included testing of the variance of the statistical fit, comparing the difference of using the single grid at the storm center location versus an area size of several grids around the storm center, model evaluations removing/adding topography, investigation of dimensionless growth curves, and the regionalization of a dimensionless GTF.

3. Data Description & Sources

An extensive storm search was conducted as part of this study to derive the list of storms to use for PMP development. This included investigating the storm lists from previous relevant studies in the region (e.g., statewide studies in Arizona, Wyoming, Nebraska, Texas, and several site-specific studies within the region). In addition, work completed as part of the Colorado Extreme Precipitation study (McKee and Doesken, 1997) and the EPAT study (2007) provided valuable information on storms in the region. The storm list and the updated storm search completed to augment those previous storm lists utilized data from the sources below:

1. Hydrometeorological Reports 49, 51, 55A, and 57, each of which can be downloaded from the Hydrometeorological Design Studies Center website at http://www.nws.noaa.gov/oh/hdsc/studies/pmp.html
2. Cooperative Summary of the Day / TD3200 through 2017. These data are published by the National Center for Environmental Information (NCEI), previously the National Climatic Data Center (NCDC). These are stored on AWA's database server and can be obtained directly from the NCEI.
3. Hourly Weather Observations published by NCEI, U.S. Environmental Protection Agency, and Forecast Systems Laboratory (now National Severe Storms Laboratory). These are stored on AWA's database server and can be obtained directly from the NCEI.
4. NCEI Recovery Disk. These are stored on AWA's database server and can be obtained directly from the NCEI.
5. U.S. Corps of Engineers Storm Studies (USACE, 1973).

6. United States Geological Society (USGS) Flood Reports (e.g., Follansbee and Jones, 1922; Follansbee and Speigel, 1937; Matthai, 1969; Rostvedt, 1970; Snipes, 1974; Vaill, 1999; Costa and Jarrett, 2008; Kohn et al., 2016).
7. Bureau of Reclamation storm data.
8. Other data published by NWS offices. These can be accessed from the National Weather Service homepage at http://www.weather.gov/.
9. Data from supplemental sources, such as Community Collaborative Rain, Hail, and Snow Network (CoCoRaHS), Weather Underground, Forecast Systems Laboratories, RAWS, and various Google searches.
10. Previous and ongoing PMP and storm analysis work (Tomlinson, 1993; Tomlinson et al., 2008-2013; Kappel et al., 2013-2018).
11. Peer reviewed journals (e.g., Maddox, 1980; Jarrett, 1987; Jarrett and Costa, 1987; Corrigan and Vogel, 1993; Jarrett, 1993; Jarrett and Tomlinson, 2000; Weaver et al., 2000; Doesken et al., 2003; Hidalgo and Dracup, 2003; England et al., 2006; Javier et al., 2007; Wu et al., 2009; Osborn and Reynolds, 2009; Reich and Shaby, 2012: Rutz et al., 2014; Mahoney et al., 2013; Mahoney et al., 2014; Alexander et al., 2015; Rutz et al., 2015; Tye and Cooley, 2015; Mueller, 2017;).

4. Data Quality Control and Quality Assurance

During the development of the deterministic PMP values, quality control (QC) and quality assurance (QA) measures were in-place to ensure data used were free from errors and process followed acceptable scientific procedures. QC/QA procedures were in-place internally from Applied Weather Associates and externally from the PRB and Project Sponsors.

The built in QA/QC checks that are part of the SPAS algorithms were utilized. These include gauge quality control, gauge mass curve checks, statistical checks, gauge location checks, co-located gauge checks, rainfall intensity checks, observed versus modeled rainfall checks, ZR relationship checks (if radar data are available), these data QA/QC measures help ensure accurate precipitation reports, ensure proper data analysis and compilation of values by duration and area size, and consistent output of SPAS results. For additional information on SPAS, the data inputs, modeled outputs, and QA/QC measures see Appendix E. For the storm adjustment process, internal QA/QC included validation that all IPMF were 1.00 or greater, that the MTF was set to 1.00 or higher, that upper (1.50) and lower (0.50) limits of the GTF were applied, and that any unique GTF/MTF limits were appropriate.

Maps of gridded GTF and MTF values were produced to cover the PMP analysis domain (Appendix B and Appendix C). These maps serve as a tool to spatially visualize and evaluate adjustment factors. Spot checks were performed at various positions across the REPS domain and hand calculations were done to verify adjustment factor calculations are consistent. Internal consistency checks were applied to compare the storm data used for PMP development against previous PMP studies including Nebraska (Tomlinson et al., 2008), Arizona (Kappel et al., 2013), Wyoming (Kappel et al.,

2014), and Texas (Kappel et al., 2016). Maps of each version of PMP depths were plotted at standard area sizes and durations to ensure proper spatial continuity of PMP depths. Updates were applied to ensure reasonable gradients and depths based on overall meteorological and topographical interactions. Comparisons were completed against previous PMP values from the appropriate HMRs, from the bordering PMP studies, and against various precipitation frequency climatologies. Updated precipitation frequency data from the REPS Precipitation Frequency Task were used to evaluate the Annual Exceedance Probability of the PMP. The PMP tool employs very few calculations, however the script utilizes Python's 'try' and 'except' statements to address input that may be unsuitable or incorrect.

The PRB and Project Sponsors completed external QA/QC on several important aspects of the PMP development. PRB members explicitly evaluated storms used for PMP development, the transposition limits of important storms, the storm representative values for each storm, and the PMP depths across the region. In addition, PRB and Project Sponsors provided extensive review and comment on the temporal accumulation pattern development, the GIS tool output, and report documentation.

5. Storm Selection

5.1 Storm Search Process

The initial search began with identifying storms that had been used in other PMP studies in the region covered by the storm search domain (Figure 3). These storm lists were combined to produce a long list of storms for this study. Previous lists analyzed included the Nebraska statewide PMP study (2008), the Arizona statewide PMP study (2013), the Wyoming state PMP study (2014), and the Texas statewide PMP study (2016) (Figure 4). These previous storms lists were updated with data through the course of this study and from other reference sources such as HMRs, USGS, USACE, USBR, EPAT, New Mexico and Colorado state climate center reports, and NWS reports. In addition discussions with the PRB, Project Sponsors, and other project participants were reviewed to identify dates with large rainfall amounts for locations within the storm search domain.

Storms from each of these sources were evaluated to see if they occurred within the initial storm search domain shown in Figure 3 and was previously important for PMP development. Next, each storm was analyzed to determine whether it was included on the short list for any of the previous studies, whether it was used in the relevant HMRs, and/or whether it produced an extreme flood event. Storms included on the initial storm list all exceeded the 100-year return frequency value for specified durations at the station location. Each storm was then classified by storm type (e.g., local, general, tropical) based on their accumulating characteristics and seasonality as discussed in Section 2. Storm types were discussed with the PRB to ensure concurrence and cross-referenced with Precipitation Frequency Task storm typing to ensure consistency. The storms were then grouped by storm type, storm location, and

duration for further analysis to define the final short list of storms used for PMP development. These storms were plotted and mapped using GIS to better evaluate the spatial coverage of the events throughout the region by storm type to ensure adequate coverage for PMP development.

The recommended storm list was presented to the PRB and Project Sponsors for discussion and evaluation. The recommended short list of storms was based on the above evaluations and experience with past studies and relevance for this project. The recommended short storm list was reviewed by the PRB and Project Sponsors and discussed in detail during Workshops 2, 3, and 4 and subsequently through the end of the project as various iterations of the PMP were developed. A few storms were removed from final consideration because of transposition limits and others were classified as hybrid events when they exhibit rainfall accumulation characteristics of more than one storm type. Iterations of how each storm was used can be found in the PMP Version log provided in Appendix I.

Table 1 provides the initial list of storms (known as the long list) considered during this study that passed these initial evaluations. Note, in some instances the storm location name, storm total amount, and/or start date of the rainfall may vary compared to previous studies. This occurs when updated information is applied or when a new SPAS analysis is completed subsequent to the previous study. This is a standard process in PMP development as each study completed reflects the most current information available at the time of analysis. Therefore, the storm list provided in this report represent the most current and up-to-date representation of each storm and supersede any previous lists. The extended tables of the long storm list can be found in Appendix M.

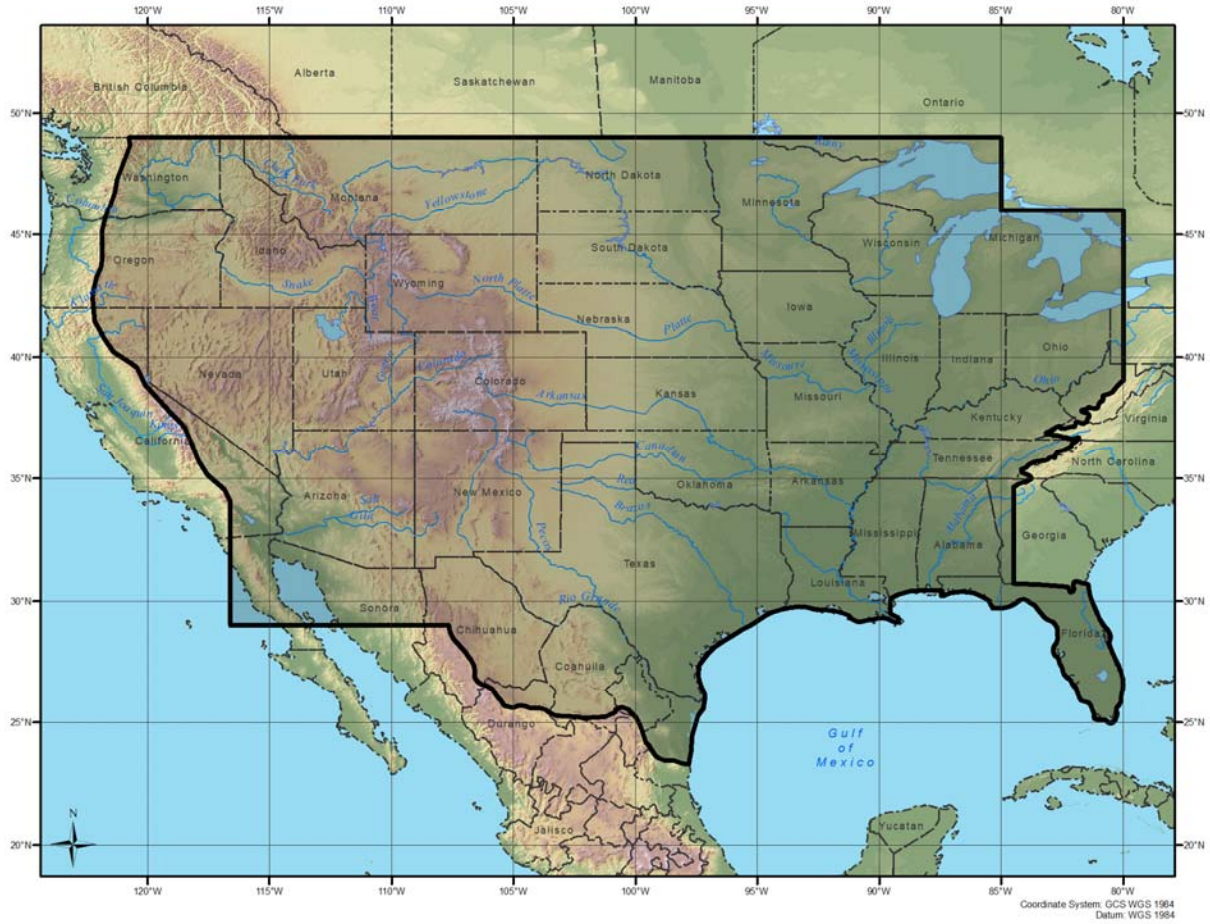

Figure 3: Initial storm search domain used for initial storm identification

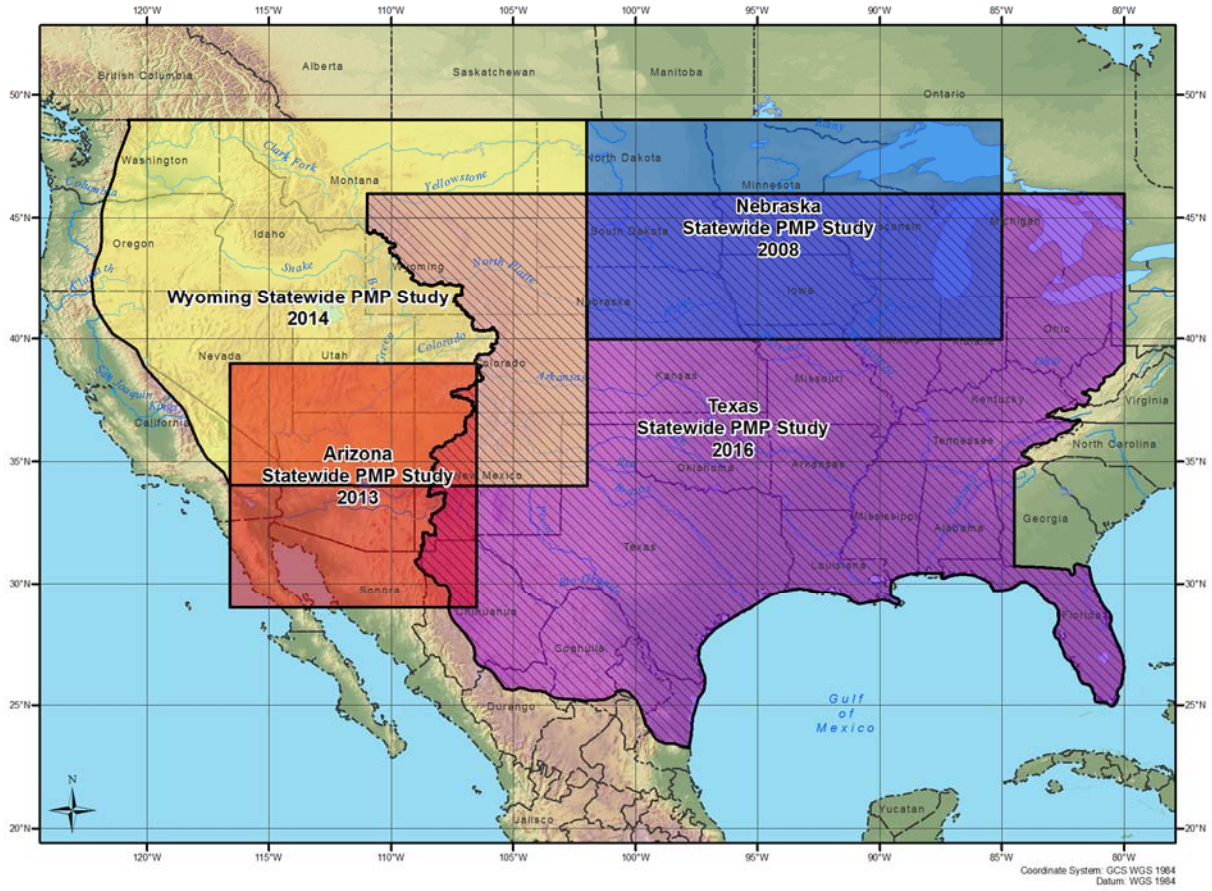

Figure 4: Previous AWA statewide PMP studies storm search domains

Table 1: Long storm list (extended tables in Appendix M)

STORM NAME	STATE	LAT	LON	YEAR	MONTH	DAY	MAXMIMUM TOTAL RAINFALL (in.)
RYE	CO	37.990	-104.921	1878	8	24	10.00
WARD DISTRICT	CO	40.138	-105.504	1894	5	29	8.54
LAKE MORAINE	CO	38.780	-105.010	1894	5	30	7.66
PARACHUTE	CO	39.450	-108.050	1899	10	10	5.00
BOXELDER	CO	40.983	-105.183	1904	5	20	8.00
ROCIADA	NM	35.850	-105.433	1904	9	26	7.32
ELK	NM	32.933	-105.283	1905	7	21	13.30
WARRICK	MT	48.079	-109.704	1906	6	5	13.69
RATTLESNAKE	ID	43.648	-115.744	1909	11	18	16.21
WAGON WHEEL	CO	37.663	-106.938	1911	10	3	7.88
FORT UNION	NM	35.933	-105.083	1913	6	6	7.90
CLAYTON	NM	36.450	-103.150	1914	4	29	9.60
TAJIQUE	NM	34.767	-106.333	1915	7	19	9.90
SUN RIVER CANYON	MT	47.683	-112.717	1916	6	19	9.27
LAKEWOOD	NM	32.633	-104.350	1916	8	7	6.00
CIBOLA NF	NM	35.113	-108.196	1916	1	14	8.45
MT ORD	AZ	33.904	-111.413	1916	1	14	10.63
SANTA CATALINA	AZ	32.429	-110.813	1916	1	14	10.63
MEEK	NM	33.683	-105.183	1919	9	15	9.80
FRY'S RANCH	CO	40.717	-105.717	1921	4	14	7.60
DENVER	CO	39.750	-105.017	1921	8	17	4.60
STEAMBOAT SPRINGS	CO	40.485	-106.832	1921	6	14	3.00
SPRINGBROOK	MT	47.364	-105.778	1921	6	17	15.20
PENROSE	CO	38.464	-105.070	1921	6	2	12.20
VIRSYLVIA (CERRO)	NM	36.733	-105.600	1922	8	17	7.50
GROVER	CO	39.750	-105.333	1922	7	27	4.00
SHERIDAN	WY	44.917	-106.917	1923	7	22	5.60
SAVAGETON	WY	43.846	-105.804	1923	9	27	17.56
MESA VERDE	CO	37.150	-108.517	1924	8	3	3.50
AMISTAD	NM	35.900	-103.167	1926	5	24	6.82
PRESCOTT	AZ	34.540	-112.469	1927	2	14	8.10
PALISADE LAKE	CO	37.450	-107.183	1927	6	26	7.00
PENNINGTON	NM	36.317	-103.583	1928	10	11	6.90
VALMORA	NM	35.817	-104.933	1929	8	6	6.60
GALINAS	NM	35.150	-105.650	1929	9	20	4.90
CHEESEMAN	CO	39.217	-105.283	1929	7	19	3.80
SILVER LAKE	CO	40.0333	-105.5833	1929	9	4	9.00
LEWERS RANCH	NV	39.250	-119.820	1930	11	12	10.00
COPE	CO	39.310	-107.470	1930	8	9	7.00
PORTER	NM	35.217	-103.283	1930	10	9	9.91

Table 1 (continued): Long storm list

STORM NAME	STATE	LAT	LON	YEAR	MONTH	DAY	MAXMIMUM TOTAL RAINFALL (in.)
WESTCLIFFE	CO	38.133	-105.467	1933	4	19	5.50
KASSLER	CO	39.500	-105.100	1933	9	9	4.50
CHEYENNE	OK	35.621	-99.679	1934	4	3	23.01
HORSE CREEK	CO	38.030	-102.070	1935	8	28	11.00
LAS CRUCES	NM	32.304	-106.796	1935	8	30	10.03
HALE	CO	39.613	-102.263	1935	5	30	18.00
GENOA	CO	39.329	-103.538	1935	5	30	12.65
ELBERT	CO	39.238	-104.488	1935	5	30	24.00
ROOSEVELT	TX	30.454	-100.038	1936	9	13	30.13
BROOME	TX	31.788	-100.854	1936	9	13	30.34
RAGLAND	NM	34.817	-103.733	1937	5	26	7.80
SMITH RANCH	CO	40.479	-105.229	1938	8	30	11.77
MASONVILLE	CO	40.454	-105.196	1938	9	10	7.03
CROSSMAN PEAK	AZ	34.546	114.196	1939	9	4	9.65
THATCHER	AZ	32.763	-109.829	1939	9	16	4.18
TULAROSA	NM	33.067	-106.033	1941	9	27	7.50
GRENVILLE	NM	36.600	-103.617	1941	9	21	10.42
PRAIRIEVIEW	NM	33.138	-103.079	1941	5	20	11.08
MCCOLLEUM RANCH	NM	32.146	-104.746	1941	9	20	21.81
RANCHO GRANDE	NM	34.933	-105.100	1942	8	29	8.00
BRIGHTON	UT	40.604	-111.582	1943	5	31	6.75
COLONY	WY	44.933	-104.200	1944	6	2	9.20
DUBOIS	ID	44.250	-112.193	1944	6	26	4.32
LAKE GEORGE	CO	38.980	-105.358	1945	7	31	**3.45**
BEAVER DAM SP	NV	37.515	-114.073	1946	10	27	7.50
GERING	NE	41.817	-103.683	1947	6	17	10.00
FORT COLLINS	CO	40.548	-105.133	1948	5	30	9.00
GOLDEN	CO	39.788	-105.288	1948	6	7	6.00
PROSPECT VALLEY	CO	40.083	-104.433	1949	6	12	14.50
MARSLAND	NE	42.600	-103.100	1951	7	27	7.00
CONWAY	TX	35.221	-101.396	1951	5	13	15.21
BRADSHAW CITY	AZ	34.204	112.354	1951	8	26	14.99
PHILMONT RANCH	NM	36.617	-105.050	1953	8	20	11.53
VIC PIERCE	TX	30.404	-101.438	1954	6	23	35.79
NEAR FORT LARAMIE	WY	42.250	-104.367	1955	4	24	9.50
ROCK SPRINGS	TX	29.912	-99.996	1955	9	23	24.09
LAKE MALOYA	NM	37.009	-104.341	1955	5	19	14.82
ENGLEWOOD	CO	39.650	-104.900	1956	7	30	12.00
GATEWAY	CO	38.682	-108.975	1957	8	21	3.00
SAN LUIS	CO	37.201	-105.424	1957	8	12	2.90

Table 1 (continued): Long storm list

STORM NAME	STATE	LAT	LON	YEAR	MONTH	DAY	MAXMIMUM TOTAL RAINFALL (in.)
MORGAN	UT	41.079	-111.654	1958	8	16	7.01
HORSESHOE DAM	AZ	33.938	-111.736	1959	10	27	10.86
DAWSON	NM	36.667	-104.783	1960	10	16	6.86
FORREST	NM	34.800	-103.600	1960	7	8	8.87
PYRAMID	CO	40.153	-107.224	1961	9	20	5.00
SONORA DESERT MUSEU	AZ	32.179	-111.388	1962	9	25	7.16
ALBUQUERQUE	NM	35.109	-106.622	1963	8	29	3.50
PAGE	AZ	36.917	-111.450	1963	8	30	2.03
GIBSON DAM	MT	48.354	-113.371	1964	6	6	19.16
NORTH TUCSON	AZ	32.304	-111.004	1964	9	5	5.28
SAHUARITA	AZ	32.006	-110.904	1964	9	9	6.77
MT LEMMON	AZ	32.438	-110.763	1965	11	22	6.75
ZILBETOD	AZ	36.813	-109.179	1965	11	22	6.31
YOUNG	AZ	33.821	-110.921	1965	11	22	11.58
PLUM CREEK	CO	39.188	-104.296	1965	6	15	14.25
RATON	NM	36.754	-104.538	1965	6	16	11.04
ELBERT	CO	39.188	-104.296	1965	6	16	16.29
HOLLY	CO	37.713	-102.404	1965	6	16	19.18
CARLSBAD	NM	32.254	-104.613	1966	8	22	17.35
ZILBETOD	AZ	36.821	-109.188	1966	12	4	4.26
JUNIPINE	AZ	36.229	-112.063	1966	12	4	10.74
PASTORA PEAK	AZ	36.821	-109.188	1966	12	4	4.26
ALTAR	MX	30.646	-111.771	1966	12	4	15.86
GRANTS	NM	35.189	-107.771	1967	9	8	4.00
DINERO	MX	28.254	-97.904	1967	9	19	35.01
SOMBRERETILLO	MX	26.279	-99.921	1967	9	19	35.87
JAKES CORNER	AZ	34.021	-111.379	1967	12	17	10.02
PAONIA	CO	38.868	-107.592	1968	8	8	5.00
BLANDING	UT	37.826	-109.543	1968	8	1	6.67
JOHN DAY	OR	44.446	-118.879	1969	6	9	7.09
BIG ELK MEADOW	CO	40.267	-105.417	1969	5	4	20.01
COLORADO SPRINGS	CO	38.817	-104.700	1970	8	20	11.00
ELKO RAILROAD	NV	40.776	-115.759	1970	8	27	4.68
SELIGMAN	AZ	35.317	-112.883	1970	7	21	5.89
BAYFIELD	CO	37.304	-107.413	1970	9	4	6.14
INDIAN WELLS	AZ	35.495	-110.421	1970	9	4	7.00
WORKMAN CREEK	AZ	33.820	-110.904	1970	9	4	12.13
MT LEMMON	AZ	32.411	-110.721	1970	9	4	9.31

Table 1 (continued): Long storm list

STORM NAME	STATE	LAT	LON	YEAR	MONTH	DAY	MAXMIMUM TOTAL RAINFALL (in.)
DURANGO	CO	37.275	-107.880	1972	10	19	5.00
RAPID CITY	SD	44.196	-103.488	1972	6	9	15.80
JOANNE	AZ	33.821	-110.921	1972	10	4	11.66
BROOMFIELD	CO	39.917	-105.100	1973	5	5	6.30
WATERTON RED ROCK	AB	49.088	-114.046	1975	6	18	14.46
SWEETWATER	CO	39.721	-107.038	1976	7	13	6.00
BIG THOMPSON CANYON	CO	40.479	-105.429	1976	7	31	12.52
PENA BLANCA	NM	35.566	-106.343	1977	7	8	4.00
NOGALES	AZ	31.339	-110.935	1977	10	6	15.97
WHITE SANDS	NM	32.387	-106.529	1978	8	19	10.43
BEAR SPRING	AZ	34.038	-111.488	1978	2	27	15.52
BIG PINE FLAT	AZ	33.675	-111.335	1978	12	16	10.37
CONRAD RANCH	UT	40.585	-111.590	1979	10	18	5.78
BELEN	NM	34.652	-106.772	1980	6	9	3.70
GRAND CANYON NP	AZ	36.313	-112.079	1980	2	13	10.67
CROWN KING	AZ	34.221	-112.346	1980	2	13	17.63
ROCK SPRINGS	AZ	34.013	-112.263	1980	2	13	11.10
FRIJOLE CREEK	CO	37.096	-104.379	1981	7	3	16.33
ALAMO	NV	36.554	-114.713	1981	8	10	6.50
CLYDE	TX	32.479	-99.479	1981	10	10	23.23
MT TIMPANOGOS	UT	40.404	-111.638	1982	9	26	10.13
FLAT TOP MOUNTAIN	UT	40.379	-112.204	1982	9	26	10.02
COTTONWOOD	UT	40.404	-111.638	1982	9	26	10.13
JIM CREEK	CO	37.271	-106.394	1983	7	20	2.00
MT GRAHAM	AZ	33.288	-109.104	1983	9	27	13.99
ALTAR	MX	30.646	-111.771	1983	9	27	13.86
PRESCOTT	AZ	34.621	-112.554	1983	9	23	17.95
REDSTONE	CO	39.181	-107.240	1984	6	5	3.00
LAKE GEORGE	CO	38.917	-105.483	1984	9	1	5.50
CREEDE	CO	37.850	-106.917	1985	9	11	8.79
CHEYENNE	WY	41.354	-104.819	1985	8	1	7.15
LOS LUNAS	NM	34.807	-106.736	1987	8	7	2.75
ALBUQUERQUE	NM	35.109	-106.622	1987	8	10	3.08
ALBUQUERQUE	NM	35.098	-106.482	1988	7	9	5.00
DEADMAN HILL	CO	40.811	-105.773	1989	8	1	2.80
VILLANUEVA	NM	35.275	-105.323	1989	8	17	7.00
OPAL	WY	41.738	-110.246	1990	8	16	7.16
DELTA	CO	38.742	-108.069	1993	8	10	4.00
RIFLE	CO	39.535	-107.783	1993	5	15	4.00
WOLF CREEK	CO	37.483	-106.799	1993	8	27	6.00

Table 1 (continued): Long storm list

STORM NAME	STATE	LAT	LON	YEAR	MONTH	DAY	MAXMIMUM TOTAL RAINFALL (in.)
KNOLES HOLE SPRING	AZ	33.829	-110.913	1993	1	5	13.36
MT LEMMON	AZ	32.413	-110.746	1993	1	5	11.15
SPIONKOP CREEK	AB	49.171	-114.163	1995	6	5	14.48
PUEBLO	CO	38.170	-104.390	1996	7	9	4.50
COTOPAXI	CO	38.479	-105.610	1996	8	1	1.50
CLIFTON	CO	39.064	-108.482	1996	8	8	4.00
TUCSON	AZ	32.390	-110.800	1996	9	3	7.37
RUXTON PARK	CO	38.850	-104.983	1997	6	6	6.40
VIRGINIA DALE	CO	40.966	-105.219	1997	7	28	7.21
FORT COLLINS	CO	40.548	-105.133	1997	7	28	14.48
PAWNEE CREEK	CO	40.775	-103.625	1997	7	29	13.58
CROOK	CO	40.862	-102.803	1998	7	23	7.06
JOSEPH CITY	AZ	34.945	-110.355	1998	7	31	4.20
COLORADO SPRINGS	CO	38.815	-104.716	1999	4	28	5.75
SAGUACHE	CO	38.205	-106.373	1999	7	25	5.00
RYE 1 SW	CO	37.914	-104.948	1999	4	29	7.80
DALLAS CREEK	CO	38.095	-107.915	1999	7	31	5.07
SABINO CANYON	AZ	32.385	-110.705	1999	7	14	7.87
GONZALEZ	MX	22.763	-98.613	2000	10	5	24.83
SANTA ROSA	NM	34.928	-104.856	2001	8	13	5.00
COLORADO SPRINGS	CO	38.873	-104.832	2001	8	31	6.00
PLACERVILLE	CO	38.005	-107.955	2001	8	8	5.66
BLUFF	UT	37.255	-109.575	2001	8	14	6.28
KAYCEE	WY	43.559	-106.707	2002	8	28	7.40
OGALLALA	NE	41.125	-101.717	2002	7	6	14.92
COLLBRAN	CO	39.285	-107.895	2003	8	15	4.27
ROOSEVELT LAKE	AZ	33.596	-111.065	2003	9	6	11.19
GOLDEN	CO	39.769	-105.126	2004	6	8	4.00
JAVIER	AZ	34.730	-113.020	2004	9	18	10.10
BIG PINE FLAT	AZ	33.685	-111.325	2005	2	10	8.72
CAMP CREEK	AZ	34.380	-111.180	2005	9	3	4.93
PENROSE	CO	38.562	-105.981	2006	7	5	6.00
EL PASO	TX	31.935	-106.515	2006	8	1	10.25
CEDAR CITY	UT	37.375	-113.075	2006	7	31	5.69
SAN LUIS VALLEY	CO	37.689	-105.942	2007	7	19	2.13
BEULAH	CO	38.122	-104.850	2007	8	1	6.40
MT LEMMON	AZ	32.440	-110.780	2007	11	30	6.54
LOST PEAK	AZ	37.470	-113.930	2007	11	30	4.70
COOKS MESA	AZ	34.460	-111.230	2007	11	30	8.60
MARSHALL SADDLE	AZ	32.440	-110.780	2007	11	30	6.54
MT HOPE	CO	37.540	-106.870	2007	11	30	6.69
PETRIFIED FOREST	AZ	34.725	-109.645	2007	7	27	7.18

Table 1 (continued): Long storm list

STORM NAME	STATE	LAT	LON	YEAR	MONTH	DAY	MAXMIMUM TOTAL RAINFALL (in.)
BONNY LAKE	CO	39.617	-102.183	2008	8	7	7.60
GLENDO 6NE	WY	42.528	-104.915	2008	5	22	7.83
SUNSPOT	NM	33.335	-105.795	2008	7	26	8.81
HAVASUPAI	AZ	35.155	-112.575	2008	8	15	4.49
ESTANZUELA_COAHUILA	MX	25.596	-100.204	2010	6	29	36.87
SPEARMAN	TX	36.135	-101.495	2010	6	13	13.89
ATLA	UT	40.590	-111.640	2010	10	25	6.01
DEER CREEK DAM	UT	41.360	-111.910	2010	10	25	5.58
ANDREW NYMAN MOUN	UT	42.050	-111.620	2010	10	25	5.97
SANTA RITA EXP RANGE	AZ	31.760	-110.840	2010	1	19	6.63
PETERSON RANCH	AZ	33.810	-110.910	2010	1	19	14.93
ROCK SPRINGS	AZ	34.080	-112.160	2010	1	19	7.77
CRYSTAL LAKE	MT	45.315	-107.175	2011	5	19	9.15
CHAPARRAL	NM	32.145	-105.995	2013	9	10	11.94
SUMNER LAKE	NM	34.595	-104.475	2013	9	10	9.63
GUADALUPE PASS	TX	32.035	-104.555	2013	9	10	18.34
CALGARY	AB	50.635	-114.855	2013	6	19	13.75
WHEELER	KS	39.765	-101.935	2013	9	8	9.78
AURORA	CO	39.705	-104.835	2013	9	8	15.45
CHEYENNE MOUNTAIN	CO	38.745	-104.865	2013	9	8	18.92
BOULDER	CO	40.015	-105.265	2013	9	8	20.41
EADS	CO	38.482	-102.783	2014	7	29	6.31
GAIL	TX	32.725	-101.405	2014	9	21	13.96
THE BOWL	TX	31.935	-104.825	2014	9	21	10.83
TRUCKTON	CO	38.654	-104.454	2015	8	10	9.74
ABILENE	TX	31.435	-99.115	2015	7	7	10.91
TAHOKA	TX	33.105	-101.825	2015	5	5	10.51

5.2 Short Storm List Development

From this initial storm list, the storms to be used for PMP were identified and moved to the recommended short storm list. Each storm was investigated using both published and unpublished references described above and AWA PMP studies to determine its significance in the rainfall and flood history of surrounding regions. Detailed discussions about each important storm took place with the PRB, Project Sponsors, and other study members. These included evaluations and comparisons of the storms, discussions of each storm's effects in the location of occurrence, discussion of storms in regions that were underrepresented, discussion of storms importance for PMF development in previous design analyses, and other meteorological and hydrological relevant topics.

Consideration was given to each storm's transpositionability within the overall domain and each storm's relative magnitude compared to other similar storms on the list and whether another storm of similar storm type was significantly larger. In this case, what is considered is whether after all adjustments are applied a given storm would still be smaller than other storms used. To determine this, several evaluations were completed. These included use of the storm in previous PMP studies, comparison of the precipitation values at area sizes relevant to the basin, and comparison of precipitation values after applying a 50 percent maximum increase to the observed values.

5.3 Gibson Dam, MT June 1964 Transposition Limit Discussions

Extensive discussion took place regarding the transposition limits of the Gibson Dam, MT June 1964 storm event. This storm is very important for setting PMP levels for the general storm type in mountainous locations of the northern Rocky Mountains in Wyoming and Montana. This storm was initially considered outside of the transposition limits used for this study. Explicit investigations into the transposition limits of the storm were completed as part of the Wyoming statewide PMP study (Kappel et al., 2014). The project review board and sponsors of that study agreed with AWA's recommended transposition limits that kept the storm out of the Colorado-New Mexico study region. In addition, the site-specific PMP study completed by AWA for the Gross Reservoir (Kappel et al., 2017) again revisited the transposition limits of this storm. That study included a Federal Energy Regulatory Commission Board of Consultants and Colorado dam safety engineers, many of whom were different from the review board that was part of the Wyoming study. Extensive evaluations of the transposition limits were again discussed. AWA's recommended transposition limits used in the Wyoming study were determined to be appropriate for the Gross Reservoir basin.

However, as part of this study, the PRB noted that in some previous work (e.g., HMR 55A and Flood Hazard Study for Pueblo Dam, Colorado, England et al., 2006) the storm was transpositioned to portions of Colorado. Therefore, additional evaluation of this storm's transposition limits took place as part of this study. The PRB Review Summary document provides the PRB analysis of the storm and potential transposition limits based on that analysis.

AWA provided several details regarding the meteorological and topographical interactions unique to the Gibson Dam storm location that supports a limited transposition region. These are relevant for the mountainous and other Front Range regions where the storm is not used in the study. The follow section provides those details and evaluations.

5.4 Gibson Dam Transposition Evaluations

This storm occurred from the first upslopes to the Continental Divide in northern Montana near Glacier National Park. The storm is a classic example of the general storm type in the region. The storm produced more than 19 inches of rainfall in a two-day period at relatively high elevations. Record flooding resulted from this event. This

storm is often controlling of PMP values where it is used for durations of 24 hours through 48 hours in HMR 55A, various site-specific PMP studies (e.g., Kappel et al., 2016; Kappel et al., 2018) and the Wyoming statewide PMP study. However, the storm center occurred at 47.6°N latitude. This places the storm beyond the 6° latitude constraint applied in the HMRs. This is discussed in HMR 57 Section 7.3 in the note at the bottom of page 69 and explicitly relates to the difference in the Coriolis parameter. In this case, the effect of this parameter (spin in the atmosphere) is >10 percent more at the Gibson Dam location versus northern portions of Colorado. This would therefore affect the storm dynamics differently than if the same storm occurred over Colorado. Specifically, HMR 57 states, "the latitudinal range of transposition was limited if necessary, so that the Coriolis parameter component of the absolute vorticity of the system would not change by more than 10 percent (about 5-6 degrees of latitude) between the original storm site and a proposed transposition location." Again, the latitudinal range between the Gibson Dam location and Colorado is greater than 6° and therefore violates the definition of transpositionability because the storm dynamics are now different as they are affected by the variation in the Coriolis parameter. However, model reanalysis investigations completed by the PRB demonstrated that similar storm dynamics and upward vertical velocity can occur in regions extending from northern Montana through southern New Mexico (see PRB Review Summary document). This helped in the final determination that this storm can be used over a limited portion of the northern Colorado Front Range.

The storm was well documented, including the meteorological environment that resulted in the rainfall. USGS Water Supply Paper 1840-B (Boner and Stermitz, 1967) provided an in-depth analysis of the synoptic meteorology and rainfall. This included analysis of the surface and upper level features that led to the rainfall and discussions of the interaction of the topography of the region. HMR 55A included an extensive evaluation of the synoptic meteorology of the storm (HMR 55A Section 2.4.1.6), as well as a discussion on the storm's transposition limits considered in that document (HMR 55A Section 8.2.2.1). In both the USGS and HMR 55A discussions, excellent reference is made to the connection of Gulf of Mexico moisture as an initial moisture input and combining with the surface and upper level meteorological features (e.g., cold upper level trough at 500mb and strong surface low pressure). These features are not unique to the Gibson Dam region. Similar combinations of upper level and surface meteorological parameters occur over the Colorado Front Range region as well. However, the combination of meteorological parameters associated with this event, specifically the strength of the upper level and surface features combined with the season of occurrence limit the transposition of the event. In this case, the cold upper level trough and strong jet stream, along with the intense area of low pressure at the surface would not occur with the same intensity and in the same combination over most of Colorado during the June timeframe.

During the Gibson Dam storm event, the inflow winds were from the east/northeast and included interaction with moisture and wind flow from the prairie and sub-Arctic regions of Canada. Figure 5 displays the HYSPLIT results associated with this storm and shows the inflow direction from the northeast, with a southeast inflow at the 700mb level 48-72-hours prior to the main rainfall event. This is the same as discussed

in HMR 55A Section 3.3. Figure 6 displays the inflow vectors associated with PMP-type storms throughout the HMR 55A region and explicitly demonstrates how the PMP-storm type inflow directions change from north to south across the region. The predominant low-level moisture inflow direction around the Gibson Dam region is east/northeast, while over Colorado, the low-level moisture inflow direction is from the east/southeast. This reflects the differences in general synoptic meteorology inflow patterns between the two regions. In addition, the positioning of the surface low pressure, upper level (500mb) trough, and influence of Pacific moisture occurred in a manner that would not occur in the same combination over most of Colorado during June. This limits the region of transpositionability to areas where these same features could combine together with the same intensity (storm dynamics and moisture) as observed.

These same considerations are discussed in the HMRs regarding transpositionability, specifically HMR 57 states, “Storm transposition involves the relocation of storm properties from the place where the storm occurred to places where the storm could have the same properties. Usually the storm property transposed is thought to be the attendant precipitation, however it is actually "the mechanisms" responsible for the precipitation that are transposed.” Further, HMR 57 Section 7.4 states, “The second step of horizontal storm transposition involves limiting the range of the storm mechanism by considering the specific thermal and moisture inflow characteristics of the given storm. As discussed in HMR 55A, if the boundary-layer moist inflow to the storm at a proposed location encounters significantly different topographic conditions than existed at the original site, the transposition would not be made.”

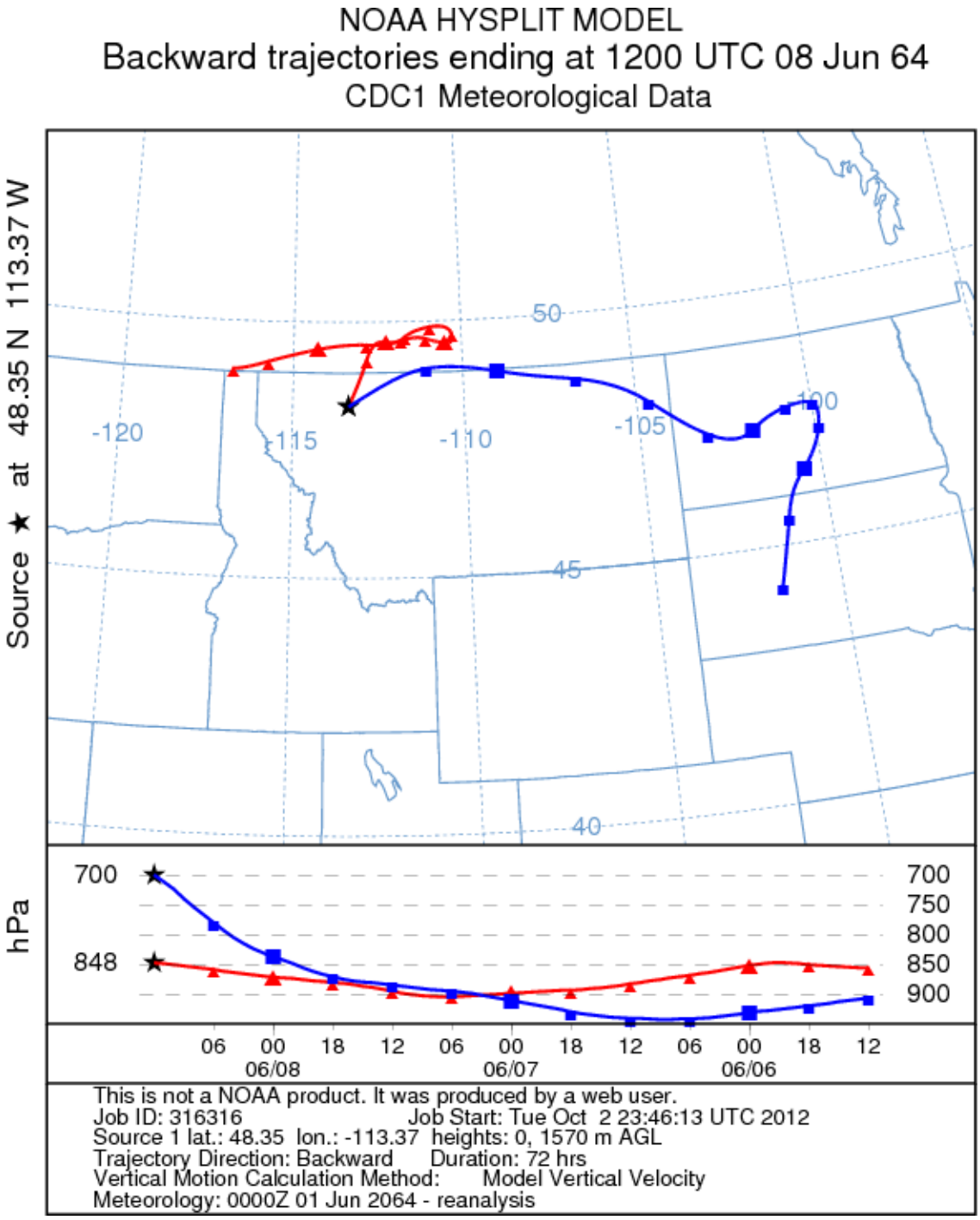

Figure 5: HYSPLIT analysis for Gibson Dam, MT June 1964 storm event. Red line represents the 700mb level inflow and blue line represents the 850mb level inflow that is also equivalent to the surface in this case.

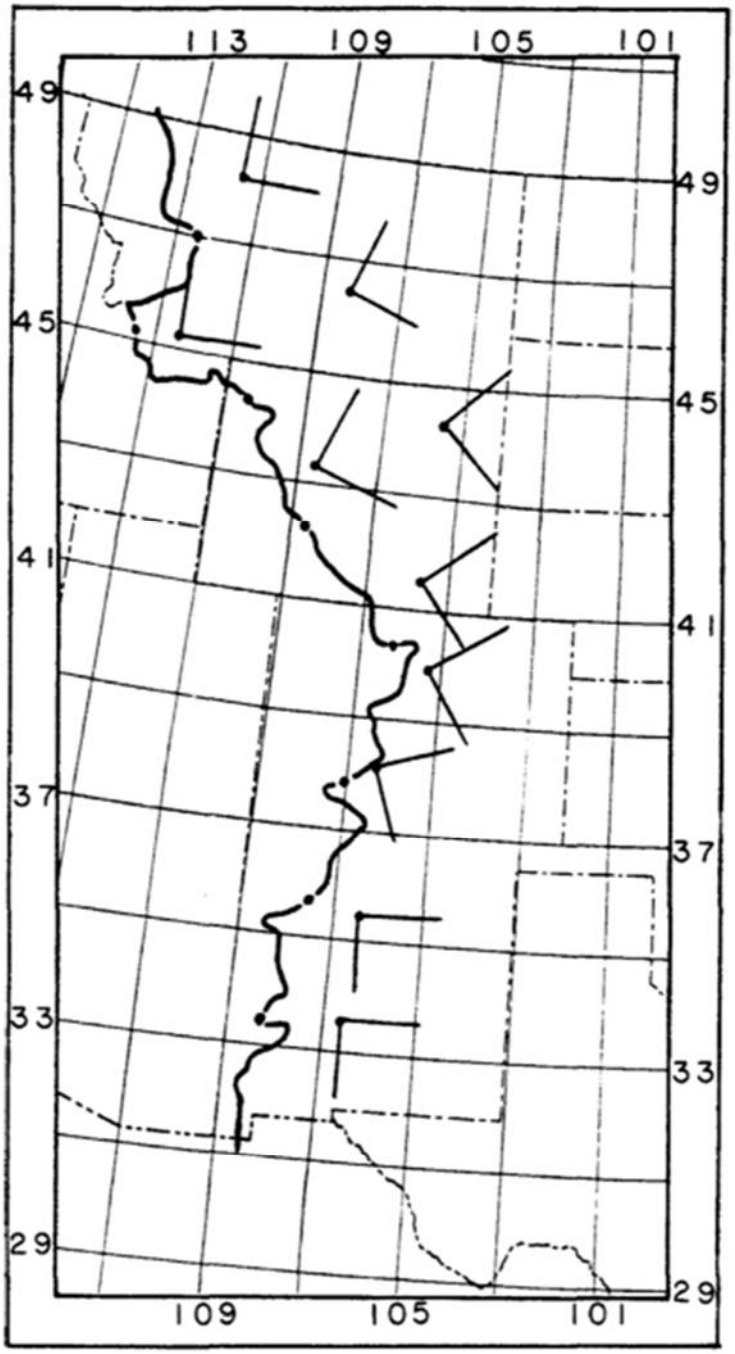

Figure 6: HMR 55A wind inflow directions maps for PMP-type storms (from HMR 55A Figure 3.3)

Figure 7 displays the transposition limits discussed in HMR 55A. This version takes the storm into the northern Colorado mountainous regions east of the Continental Divide. However, the final transposition limits applied are not explicitly known as that documentation is not provided in HMR 55A and this application of transposition limits would violate the discussions provided in the HMRs noted above. It is assumed that HMR 55A applied larger transposition limits than would be allowed considering the meteorology and topography at the Gibson Dam in-place location in order to ensure enough data are available from which to derive PMP values. For example, HMR 57 states, "A final consideration in horizontal transposition is the overall availability of record setting storms within the region. Where there are a sufficient number of such events, the procedure would be applied strictly; when there are few storms available, less restrictive application would be used." This is no longer the case in Colorado, as there are a sufficient number of high elevation storm events from which to derive PMP for this study.

In contrast to the transposition limits shown in HMR 55A, the NWS produced an explicit transposition limit map of the Gibson Dam storm that differs significantly from the HMR 55A map (Figure 8). These NWS transposition limit maps were obtained by AWA directly from the Hydrometeorological Design Studies Center where all HMR development took place and original data exist. Although it is not known exactly how these NWS transposition limit maps were ultimately utilized, they represent one of the only sets of working notes available from the original development of the HMRs. In all other cases where data in HMRs are available to cross reference against these maps (e.g., Figure 26 in HMR 52 and all storms listed in HMR 53 Table 2) the limits shown on the maps exactly match the HMR description. In addition, the information provided on the transposition limits maps regarding the storm designation number, date, and maximization match what is provided in the HMRs and USACE Storm Studies files (USACE, 1973). Given this information, it is assumed these transposition limit maps represent what the authors of the HMRs original intent was regarding each storm's explicit transposition limits where these maps exist. The image for the Gibson Dam storm shows they did not consider this storm to be transpositionable to any regions south of 47°N latitude. This is related to the unique interaction of storm dynamics, seasonality, moisture inflow direction, and the topography of the region as discussed above.

The same discussions and meteorological reasoning took place during evaluations performed as part of the Wyoming statewide PMP study which included representatives from the FERC), an independent BOC, representatives from the USACE, the Wyoming State Engineer's Office, the NRCS, and representatives from the University of Wyoming Atmospheric Sciences program. During these investigations, the transposition limits for the storm were further refined based on the meteorological conditions discussed previously and topographic considerations. Figure 9 provides the final transposition limits applied to the Gibson Dam storm as used in the Wyoming statewide PMP study. Further refinement of the transposition limits as discussed above as part of this study resulted in an update to the transposition limits used in the Wyoming statewide PMP study. These discussions explicitly demonstrate that the

Gibson Dam storm is only transpositionable to a very limited region along the Colorado Front Range as shown in Figure 10.

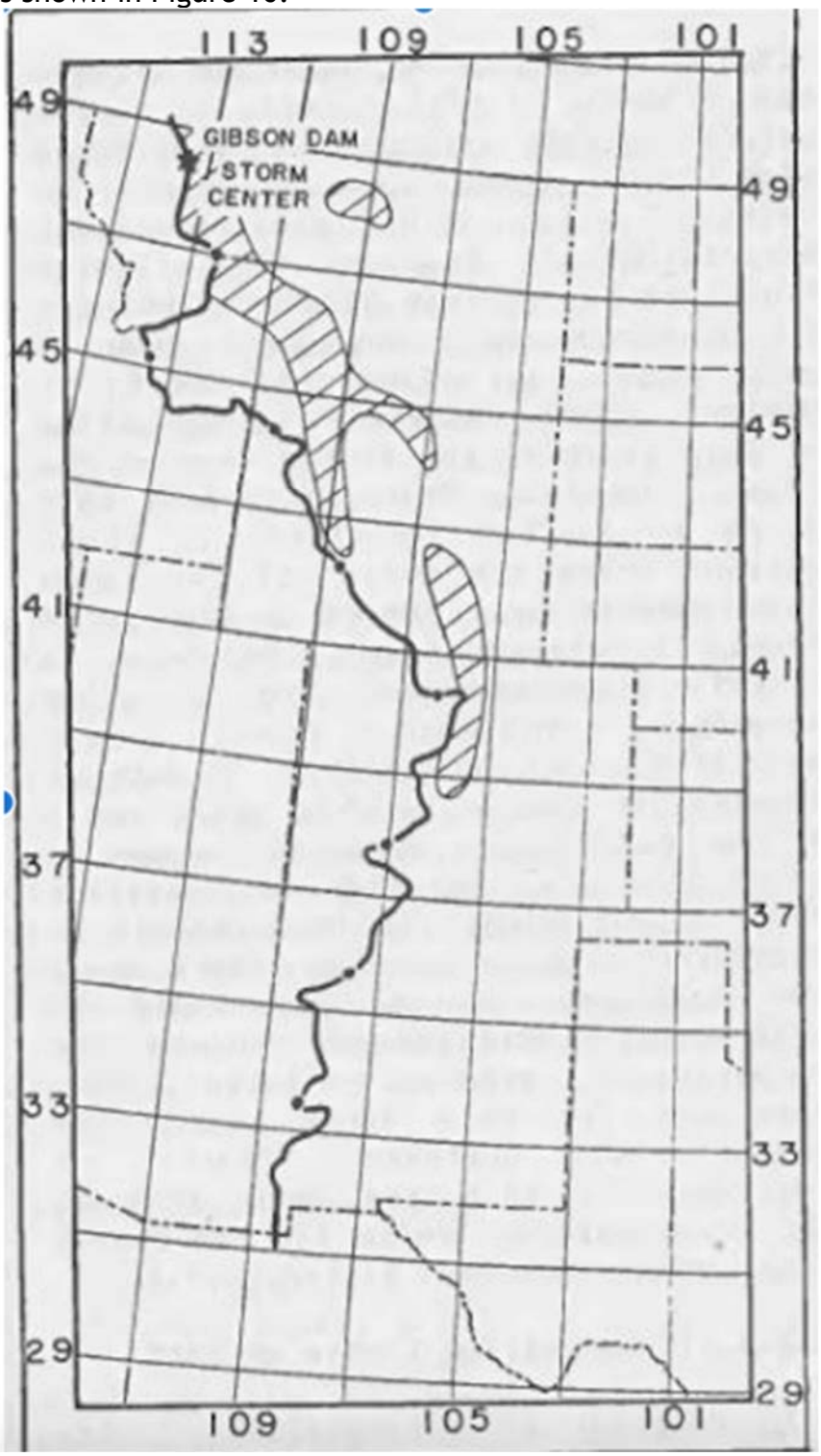

Figure 7: Transposition limits for Gibson Dam, MT June 1964 storm event as presented in HMR 55A Figure 8.3

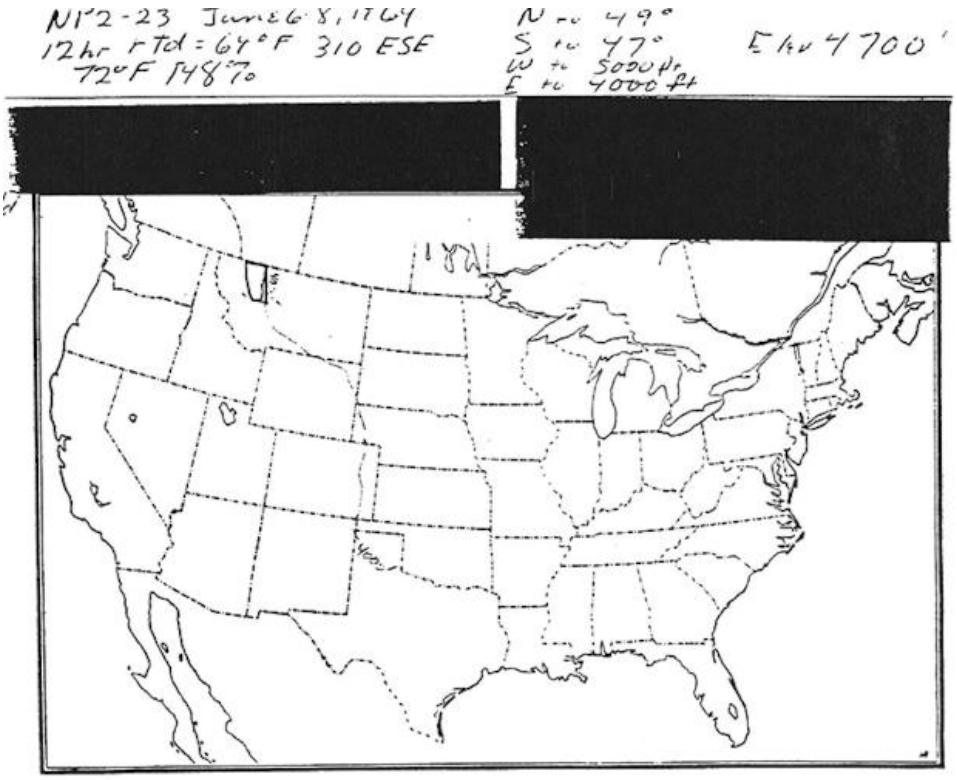

Figure 8: National Weather Service transposition limits for Gibson Dam, MT June 1964 storm event. Map recovered from the HDSC office transposition limits folder and now housed on AWA servers

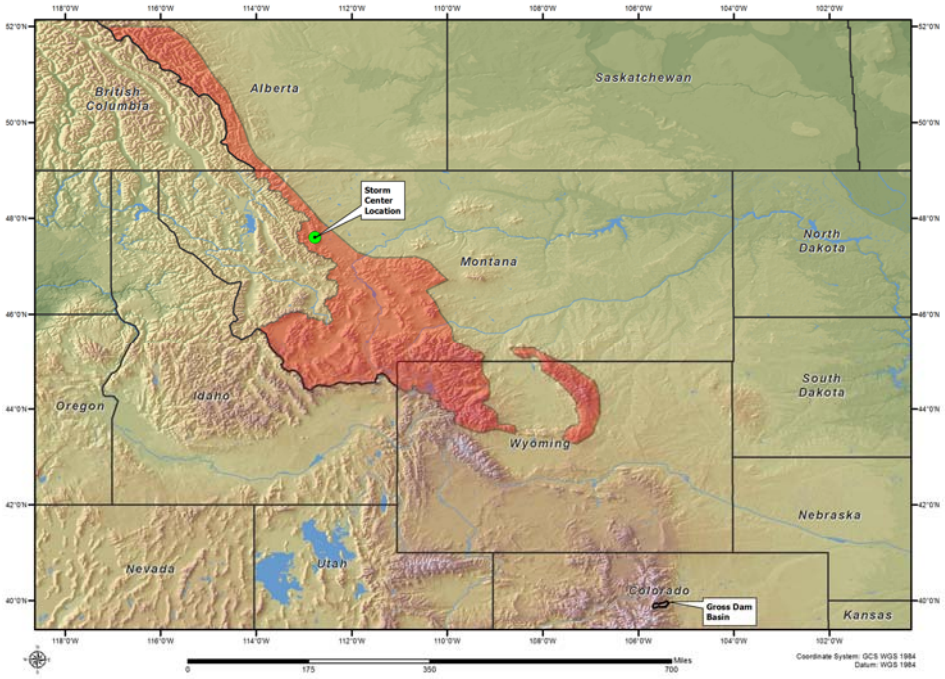

Figure 9: Updated transposition limits for Gibson Dam, MT June 1964 SPAS 1211 Zone 1 as developed during the Wyoming statewide PMP study and applied to the Gross Dam analysis

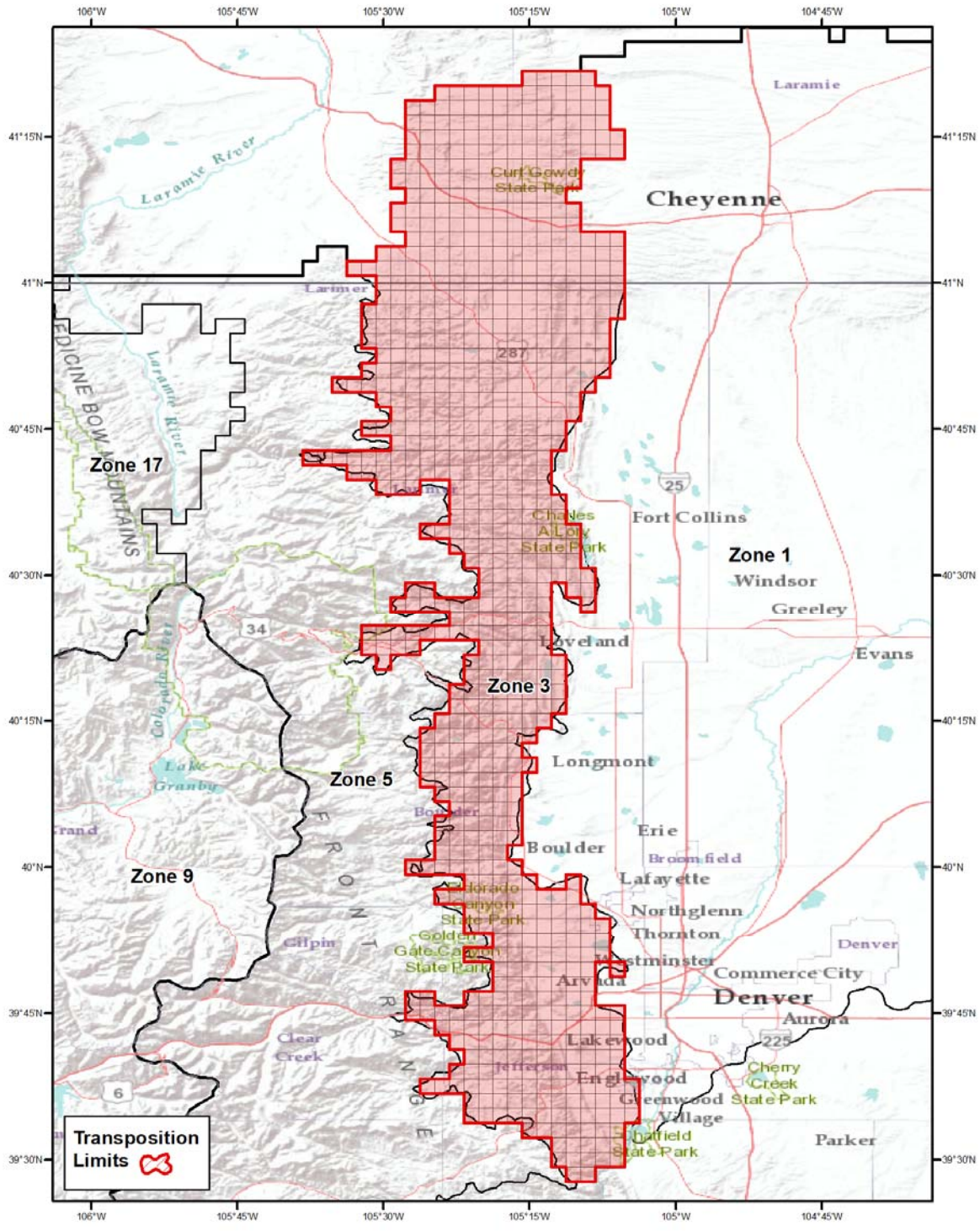

Figure 10: Gibson Dam transposition limits applied as to this study

5.5 Final PMP Storm List Development

The final short storm list used to derive PMP depths for this study considered each of the discussions in the previous sections in detail. Each storm on the final short storm list exhibited characteristics that were determined to be possible over some portion of the overall study domain. The storms that made it through these final evaluations were placed on the short storm list (Table 2 and Figure 11). Figure 12, Figure 13, and Figure 14 provide the short list storms by storm type with a callout providing the storm name and date that can be cross-referenced with the information provided in Table 2. Each of these storms was fully analyzed in previous PMP studies or as part of this study using the SPAS process (Appendix E). Ultimately, only a subset of the storms on the short list control PMP values at a given location for a given duration, with most providing support for the PMP values.

The short storm list contains more storms than were ultimately required to derive the PMP values to ensure no storms were omitted which could have affected PMP values after all adjustment factors were applied. This is because magnitude of the total adjustment factors was unknown at the beginning of the process. In other words, a storm with large point rainfall values may have a relatively small total adjustment factor, while a storm with a relatively smaller but significant rainfall value may end up with a large total adjustment factor. The combination of these calculations may provide a total adjusted rainfall value for the smaller rainfall event that is greater than the larger rainfall event after all adjustments are applied.

Several obvious patterns emerge from the location of these storm centers. The PMP-type general storms occur in topographically favored regions where these long duration storms have adequate time to interact with the terrain. The PMP-type local storms occur in both orographic and non-orographic regions signifying that terrain may not play as significant role in rainfall accumulation as general storms. PMP-type tropical storms strongly favor southern Arizona and southern New Mexico, as these are regions closer to the storm development areas. The short list of storms represents a relatively limited period of record of 140 years. Therefore, it is possible that each of these storms types may have occurred in other areas not represented on the current storm list before the observational record. However, this limitation is overcome by transpositioning storms over a wide range of locations and assuming those storms could have occurred in other regions of similar meteorological and topographical settings, essentially trading time for space.

Table 2: Short storm list

NAME	STATE	LAT	LON	YEAR	MONTH	DAY	MAXIMUM TOTAL RAINFALL (in)	ELEVATION (ft)	PMP STORM TYPE	STORM ANALYSIS DURATION	STORM REPRESENTATIVE VALUE (F°)	CLIMATOLOGICAL MAXIMUM VALUE (F°)	STORM ADJUSTMENT DATE	STORM REPRESENTATIVE LATITUDE	STORM REPRESENTATIVE LONGITUDE	INFLOW VECTOR	IN-PLACE MAX FACTOR
WARD DISTRICT	CO	39.804	-105.329	1894	5	29	11.15	8,336	General	24	66.0	77.0	15-Jun	36.45	-101.05	350SE	1.50
LAKE MORAINE	CO	38.804	-104.946	1894	5	30	8.91	10,380	General	24	66.0	77.0	15-Jun	36.45	-101.05	270SE	1.50
RATTLESNAKE	ID	43.673	-115.744	1909	11	18	17.20	3,297	General	SST	62.0	62.5	5-Nov	37.00	-126.00	700SW	1.03
WAGON WHEEL	CO	37.663	-106.938	1911	10	3	7.88	12,500	Tropical	24	68.0	74.5	20-Sep	34.50	-111.60	350SW	1.50
TAJIQUE 1 to 120h	NM	34.746	-106.413	1915	7	19	6.46	8,280	General	24	71.0	77.5	15-Jul	32.58	-105.50	160SSE	1.50
TAJIQUE 121 to 264h	NM	33.733	-106.968	1915	7	19	7.12	4,640	General	24	71.0	77.5	15-Jul	32.58	-105.50	115SE	1.43
MOGOLLON RIM	AZ	33.904	-111.413	1916	1	14	13.43	6,668	General	24	57.0	60.0	1-Feb	33.20	-113.42	130SW	1.20
CIBOLA NF	NM	35.113	-108.196	1916	1	14	8.45	8,720	General	24	57.0	60.0	1-Feb	33.20	-113.42	325WSW	1.22
SANTA CATALINA	AZ	32.429	-110.813	1916	1	14	10.63	7,863	General	24	57.0	60.0	1-Feb	33.20	-113.42	160WNW	1.23
PENROSE	CO	38.464	-105.070	1921	6	2	12.19	5,400	HYBRID (G/L)	6	74.0	79.5	20-Jun	34.25	-100.10	400SE	1.35
ADELAIDE	CO	38.630	-104.962	1921	6	2	9.27	8,465	HYBRID (G/L)	6	74.0	79.5	20-Jun	34.25	-100.10	400SE	1.38
VIRSYLVIA (CERRO)	NM	36.804	-105.604	1922	8	17	7.53	7,621	Local	6	67.0	79.0	3-Aug	35.69	-105.94	80SSW	1.50
SAVAGETON	WY	43.846	-105.804	1923	9	27	17.56	5,056	General	24	71.5	74.5	15-Sep	38.90	-100.08	450SE	1.19
HUNTERS	WY	44.421	-107.029	1923	9	27	10.13	9,330	General	24	71.5	74.5	15-Sep	38.90	-100.08	450SE	1.22
PALISADE LAKE	CO	37.454	-107.253	1927	6	26	6.37	8,211	General	24	67.0	77.0	10-Jul	35.38	-106.29	150SSE	1.50
ELBERT CHERRY CREEK	CO	39.238	-104.488	1935	5	30	24.00	6,800	Local	6	76.5	78.0	30-May	33.05	-99.80	500SSE	1.09
GENOA	CO	39.329	-103.538	1935	5	30	12.65	5,560	Local	6	76.5	78.0	30-May	33.05	-99.80	475SSE	1.09
HALE	CO	39.613	-102.263	1935	5	30	18.00	3,700	Local	6	76.5	78.0	30-May	33.05	-99.80	475SSE	1.08
LAS CRUCES	NM	32.304	-106.796	1935	8	30	10.03	3,890	Local	6	78.0	80.0	15-Aug	31.70	-106.30	50SE	1.10
SMITH RANCH	CO	40.479	-105.229	1938	8	30	11.77	5,471	General	24	73.0	78.0	16-Aug	38.61	-102.87	180SE	1.32
MASONVILLE	CO	40.454	-105.196	1938	9	10	7.03	5,392	Local	6	72.0	77.5	25-Aug	40.16	-103.21	105E	1.37
PRAIRIEVIEW	NM	33.138	-103.079	1941	5	20	11.08	3,805	General	24	71.0	78.5	9-Jun	29.46	-98.43	375SE	1.48
MCCOLLEUM RANCH	NM	32.146	-104.746	1941	9	20	21.81	5,840	General	24	74.0	78.0	10-Sep	29.50	-98.40	420ESE	1.25
GOLDEN	CO	39.788	-105.288	1948	6	7	6.00	7,109	Local	6	74.0	79.5	21-Jun	35.77	-100.73	370SE	1.37
CONWAY	TX	35.221	-101.396	1951	5	13	15.21	3,450	HYBRID (G/L)	24	71.5	78.0	1-Jun	30.51	-97.74	390SE	1.41
BRADSHAW CITY	AZ	34.204	-112.354	1951	8	26	14.99	6,222	Tropical	24	73.5	77.5	15-Aug	32.46	-112.35	120S	1.25
LAKE MALOYA	NM	37.009	-104.341	1955	5	19	14.82	7,954	General	24	70.5	78.0	5-Jun	31.50	-98.10	520SE	1.50
SAN LUIS	CO	37.179	-105.413	1957	8	12	3.03	8,017	Local	3	75.0	79.5	29-Jul	37.09	-107.05	90W	1.30
MORGAN	UT	41.079	-111.654	1958	8	16	7.01	7,311	Local	3	74.0	78.5	2-Aug	40.97	-112.00	20WSW	1.30
PYRAMID	CO	40.540	-106.721	1961	9	20	6.14	9,843	General	24	59.5	75.5	8-Sep	36.00	-112.00	425SW	1.50
GIBSON DAM	MT	48.354	-113.371	1964	6	6	19.16	8,000	General	24	66.0	73.0	22-Jun	48.40	-106.52	315E	1.30
PLUM CREEK	CO	39.221	-104.896	1965	6	15	14.25	7,007	HYBRID (G/L)	6	77.0	80.5	1-Jul	33.50	-100.00	480SE	1.21
RATON	NM	36.754	-104.538	1965	6	16	11.04	6,200	HYBRID (G/L)	6	77.0	80.5	1-Jul	33.50	-100.00	345SE	1.21
ELBERT	CO	39.188	-104.296	1965	6	16	16.28	6,207	HYBRID (G/L)	6	77.0	80.5	1-Jul	33.50	-100.00	460SE	1.20
HOLLY	CO	37.713	-102.404	1965	6	16	19.18	4,100	Local	6	77.0	80.5	1-Jul	33.50	-100.00	320SSE	1.20
CARLSBAD	NM	32.254	-104.613	1966	8	22	17.35	4,360	HYBRID (G/L)	24	74.0	79.0	7-Aug	31.95	-102.18	145E	1.30
JUNIPINE	AZ	34.979	-111.771	1966	12	4	10.74	6,710	General	SST	68.0	70.0	15-Nov	27.50	-124.50	950SW	1.13
PASTORA PEAK	AZ	36.821	-109.188	1966	12	4	4.26	8,189	General	SST	68.0	70.0	15-Nov	27.50	-124.50	1100SW	1.13
GRANTS	NM	35.188	-107.754	1967	9	8	4.00	7,654	Local	3	71.0	79.5	25-Aug	35.08	-108.78	60W	1.50
BLANDING	UT	37.826	-109.543	1968	8	1	6.67	10,367	Local	12	76.5	79.0	15-Aug	35.00	-112.00	240SW	1.24
BIG ELK MEADOW	CO	40.267	-105.417	1969	5	4	20.01	7,667	General	24	65.0	74.5	20-May	38.00	-99.00	375ESE	1.50

Table 2 (continued): Short storm list

NAME	STATE	LAT	LON	YEAR	MONTH	DAY	MAXIMUM TOTAL RAINFALL (in)	ELEVATION (ft)	PMP STORM TYPE	STORM ANALYSIS DURATION	STORM REPRESENTATIVE VALUE (F°)	CLIMATOLOGICAL MAXIMUM VALUE (F°)	STORM ADJUSTMENT DATE	STORM REPRESENTATIVE LATITUDE	STORM REPRESENTATIVE LONGITUDE	INFLOW VECTOR	IN-PLACE MAX FACTOR
BAYFIELD	CO	37.304	-107.413	1970	9	3	5.95	8,950	Tropical	24	75.0	77.5	20-Aug	32.79	-112.13	410SW	1.18
MT LEMMON	AZ	32.411	-110.721	1970	9	4	9.31	8,080	Tropical	24	75.0	77.5	20-Aug	32.79	-112.13	85WNW	1.17
WORKMAN CREEK	AZ	33.820	-110.904	1970	9	4	12.13	7,250	Tropical	24	75.0	77.5	20-Aug	32.79	-112.13	100SW	1.17
INDIAN WELLS	AZ	35.495	-110.421	1970	9	4	7.00	5,710	Tropical	24	75.0	77.5	20-Aug	32.79	-112.13	210SW	1.15
JOANNE	AZ	33.821	-110.921	1972	10	4	11.66	7,140	Tropical	24	73.0	75.0	20-Sep	32.77	-111.49	80SW	1.14
SWEETWATER	CO	39.721	-107.038	1976	7	13	6.00	6,278	Local	3	75.0	79.0	15-Jul	40.50	-107.25	55NNW	1.26
BIG THOMPSON CANYON	CO	40.479	-105.429	1976	7	31	12.52	8,133	Local	6	78.5	80.0	15-Jul	39.80	-102.40	165ESE	1.09
PENA BLANCA	NM	35.596	-106.429	1977	7	8	4.65	5,986	Local	6	68.5	79.0	22-Jul	35.33	-106.35	19SSE	1.50
NOGALES	AZ	31.339	-110.935	1977	10	6	15.97	3,924	Tropical	SST	77.0	79.5	20-Sep	23.00	-115.00	615SW	1.14
BEAR SPRING	AZ	34.038	-111.488	1978	2	27	15.52	7,000	General	24	58.5	61.0	15-Feb	32.60	-111.83	100SSW	1.19
WHITE SANDS	NM	32.387	-106.529	1978	8	19	10.43	4,604	Local	6	74.0	80.0	15-Aug	31.81	-106.38	40SSE	1.37
CONRAD RANCH	UT	40.585	-111.590	1979	10	18	5.78	9,712	General	24	55.0	63.5	5-Oct	38.80	-116.75	300WSW	1.50
ROCK SPRINGS	AZ	34.013	-112.263	1980	2	13	11.10	2,892	General	24	60.0	61.0	15-Feb	32.48	-112.35	120S	1.06
CROWN KING	AZ	34.221	-112.346	1980	2	13	17.63	6,445	General	24	60.0	61.0	15-Feb	32.48	-112.35	120S	1.07
BELEN	NM	34.654	-106.821	1980	6	9	4.21	5,181	Local	6	74.5	78.5	23-Jun	34.65	-106.82	270SE	1.24
FRIJOLE CREEK	CO	37.096	-104.379	1981	7	3	16.33	5,728	Local	6	77.0	78.5	25-Aug	35.40	-104.45	120S	1.09
CLYDE	TX	32.479	-99.479	1981	10	10	23.23	2,000	Tropical	24	76.0	77.5	25-Sep	29.50	-97.00	250SE	1.08
MT TIMPANOGOS	UT	40.404	-111.638	1982	9	26	10.13	10,555	General	24	69.0	73.0	10-Sep	38.50	-114.00	180SW	1.33
FLAT TOP MOUNTAIN	UT	40.379	-112.204	1982	9	26	10.02	9,062	General	24	69.0	73.0	10-Sep	38.50	-114.00	160SW	1.31
COTTONWOOD	UT	41.604	-112.012	1982	9	26	9.71	7,056	General	24	69.0	72.5	10-Sep	38.50	-114.00	240SSW	1.28
PRESCOTT	AZ	34.621	-112.554	1983	9	23	17.95	5,808	Local	SST	81.0	81.5	5-Sep	26.00	-113.00	600S	1.03
ALTAR	MX	30.646	-111.771	1983	9	27	13.86	2,770	Tropical	24	73.5	76.0	15-Sep	31.35	-110.00	115ENE	1.14
MT GRAHAM	AZ	33.288	-109.104	1983	9	27	13.99	6,371	Tropical	24	73.5	76.0	15-Sep	31.35	-110.00	140SSW	1.27
ALBUQUERQUE	NM	35.096	-106.479	1988	7	9	5.77	6,303	Local	6	72.5	79.5	23-Jul	35.00	-105.66	47E	1.49
OPAL	WY	41.738	-110.246	1990	8	16	7.16	6,924	Local	3	77.0	78.5	1-Aug	41.14	-112.00	100WSW	1.09
KNOLES HOLE SPRING	AZ	33.829	-110.913	1993	1	5	13.36	7,395	General	24	60.0	62.5	20-Dec	31.95	-110.91	130S	1.18
SPENCER CANYON	AZ	32.413	-110.746	1993	1	5	11.15	7,965	General	24	60.0	62.5	20-Dec	31.95	-110.91	130S	1.16
WOLF CREEK	CO	37.463	-106.721	1993	8	27	6.05	10,382	General	24	75.0	78.0	13-Aug	35.03	-106.14	170SSE	1.23
COTOPAXI	CO	38.455	-105.595	1996	8	1	2.03	7,652	Local	6	73.0	79.0	18-Jul	38.30	-104.72	50ESE	1.43
TUCSON	AZ	32.390	-110.800	1996	9	3	7.37	5,750	Local	3	77.5	82.0	18-Aug	32.65	-114.60	220W	1.27
RUXTON PARK	CO	38.855	-104.965	1997	6	6	5.04	9,009	HYBRID (G/L)	6	71.0	76.0	20-Jun	38.89	-104.39	30E	1.38
FORT COLLINS	CO	40.548	-105.133	1997	7	28	14.48	5,135	HYBRID (G/L)	12	76.5	78.5	15-Jul	40.00	-103.35	100ESE	1.12
PAWNEE CREEK	CO	40.775	-103.625	1997	7	29	13.58	4,500	Local	6	75.5	81.5	15-Jul	39.20	-100.15	215SE	1.38
JOSEPH CITY	AZ	34.945	-110.355	1998	7	31	4.20	5,000	Local	3	74.5	81.5	15-Aug	34.00	-111.50	90SW	1.45
SABINO CANYON	AZ	32.385	-110.705	1999	7	14	7.87	6,800	Local	12	75.0	79.0	1-Aug	32.12	-110.93	25SW	1.27
SAGUACHE	CO	38.215	-106.295	1999	7	25	6.68	8,900	Local	3	76.0	79.0	15-Jul	36.95	-107.99	130SW	1.21
DALLAS CREEK	CO	38.095	-107.915	1999	7	31	5.07	9,018	Local	3	76.0	79.0	17-Jul	40.43	-109.55	185NNW	1.21

Table 2 (continued): Short storm list

NAME	STATE	LAT	LON	YEAR	MONTH	DAY	MAXIMUM TOTAL RAINFALL (in)	ELEVATION (ft)	PMP STORM TYPE	STORM ANALYSIS DURATION	STORM REPRESENTATIVE VALUE (F°)	CLIMATOLOGICAL MAXIMUM VALUE (F°)	STORM ADJUSTMENT DATE	STORM REPRESENTATIVE LATITUDE	STORM REPRESENTATIVE LONGITUDE	INFLOW VECTOR	IN-PLACE MAX FACTOR
PLACERVILLE	CO	38.005	-107.955	2001	8	8	5.66	10,600	Local	3	75.5	80.5	15-Aug	36.16	-108.83	135SSW	1.38
BLUFF	UT	37.255	-109.575	2001	8	14	6.28	4,907	Local	3	77.5	81.0	15-Aug	34.50	-110.00	190SSW	1.20
OGALLALA	NE	41.125	-101.717	2002	7	6	14.92	3,215	Local	6	74.5	80.0	15-Jul	39.34	-101.97	125S	1.32
COLLBRAN	CO	39.285	-107.895	2003	8	15	4.27	7,694	Local	6	74.5	78.5	15-Aug	37.82	-107.03	110SSE	1.27
ROOSEVELT LAKE	AZ	33.596	-111.065	2003	9	6	11.19	2,700	Local	3	76.0	80.5	26-Aug	33.30	-111.70	40SW	1.25
JAVIER	AZ	34.730	-113.020	2004	9	18	10.10	5,600	Tropical	12	73.5	78.5	5-Sep	32.98	-115.10	170SW	1.32
CEDAR CITY	UT	37.375	-113.075	2006	7	31	5.69	8,000	Local	3	74.0	80.0	15-Aug	37.72	-113.10	25N	1.42
EL PASO	TX	31.935	-106.515	2006	8	1	10.25	4,818	Local	12	78.0	79.5	15-Aug	31.58	-110.33	225W	1.08
SAN LUIS VALLEY	CO	37.525	-105.945	2007	7	19	2.11	7,562	Local	6	76.0	78.5	2-Aug	38.48	-106.32	70NNW	1.16
PETRIFIED FOREST	AZ	34.725	-109.645	2007	7	27	7.18	5,500	Local	3	77.5	81.0	15-Aug	34.30	-110.36	50SW	1.20
COOKS MESA	AZ	34.460	-111.230	2007	11	30	8.60	7,472	General	24	63.5	65.0	15-Nov	31.70	-111.11	190S	1.11
MARSHALL SADDLE	AZ	32.440	-110.780	2007	11	30	6.54	8,834	General	24	63.5	65.0	15-Nov	31.70	-111.11	55SSW	1.13
MT HOPE	CO	37.540	-106.870	2007	11	30	6.69	12,055	General	24	63.5	65.0	15-Nov	31.70	-111.11	470SW	1.12
SUNSPOT	NM	33.335	-105.795	2008	7	26	8.81	9,339	Tropical	24	77.0	79.0	10-Aug	30.15	-103.05	275SE	1.12
HAVASUPAI	AZ	35.155	-112.575	2008	8	15	4.49	4,900	Local	3	74.5	81.0	1-Aug	34.65	-112.40	35SSE	1.41
PETERSON RANCH	AZ	33.810	-110.910	2010	1	19	14.93	7,450	General	SST	69.5	71.0	5-Jan	23.50	-123.00	1020SW	1.06
SANTA RITA EXP RANGE	AZ	31.760	-110.840	2010	1	19	6.63	4,576	General	SST	69.5	71.0	5-Jan	23.50	-123.00	935SW	1.09
SPEARMAN	TX	36.135	-101.495	2010	6	13	13.89	3,263	Local	6	76.5	79.5	27-Jun	35.00	-101.00	85SSE	1.17
ANDREW NYMAN MOUNTAIN	UT	42.050	-111.620	2010	10	25	5.97	8,290	General	24	59.0	63.5	8-Oct	38.32	-116.40	365SW	1.36
DEER CREEK DAM	UT	41.360	-111.910	2010	10	25	4.74	5,756	General	24	59.0	63.5	8-Oct	38.32	-116.40	325SW	1.32
ALTA	UT	40.590	-111.640	2010	10	25	6.01	8,680	General	24	59.0	64.5	8-Oct	38.32	-116.40	300SW	1.36
BOULDER	CO	40.015	-105.265	2013	9	8	20.41	5,308	General	24	75.5	76.5	31-Aug	37.00	-102.50	255SE	1.06
CHEYENNE MOUNTAIN	CO	38.745	-104.865	2013	9	8	18.92	9,323	General	24	75.5	76.5	31-Aug	37.00	-102.50	177SE	1.07
AURORA	CO	39.705	-104.835	2013	9	8	15.45	5,573	General	24	75.5	76.5	31-Aug	37.00	-102.50	225SE	1.06
COAL CREEK	CO	39.865	-105.285	2013	9	8	18.13	7,333	General	24	75.5	76.5	31-Aug	37.00	-102.50	225SE	1.07
GUADALUPE PASS	TX	32.035	-104.555	2013	9	10	18.34	3,986	General	24	74.0	79.0	25-Aug	29.50	-98.50	400ESE	1.30
SUMNER LAKE	NM	34.595	-104.475	2013	9	10	9.63	4,284	General	24	74.0	79.0	25-Aug	29.50	-98.50	495SE	1.30
CHAPARRAL	NM	32.145	-105.995	2013	9	10	11.94	4,718	General	24	74.0	79.0	25-Aug	29.50	-98.50	480ESE	1.30
GAIL	TX	32.725	-101.405	2014	9	21	13.96	2,575	Local	6	76.5	79.0	6-Sep	30.93	-100.12	145SSE	1.14
THE BOWL	TX	31.935	-104.825	2014	9	21	10.83	8,008	Tropical	24	76.5	77.5	7-Sep	30.40	-103.00	150SE	1.07
TAHOKA	TX	33.105	-101.825	2015	5	5	10.51	3,002	Local	6	71.0	77.5	18-May	29.29	-100.26	280SSE	1.40

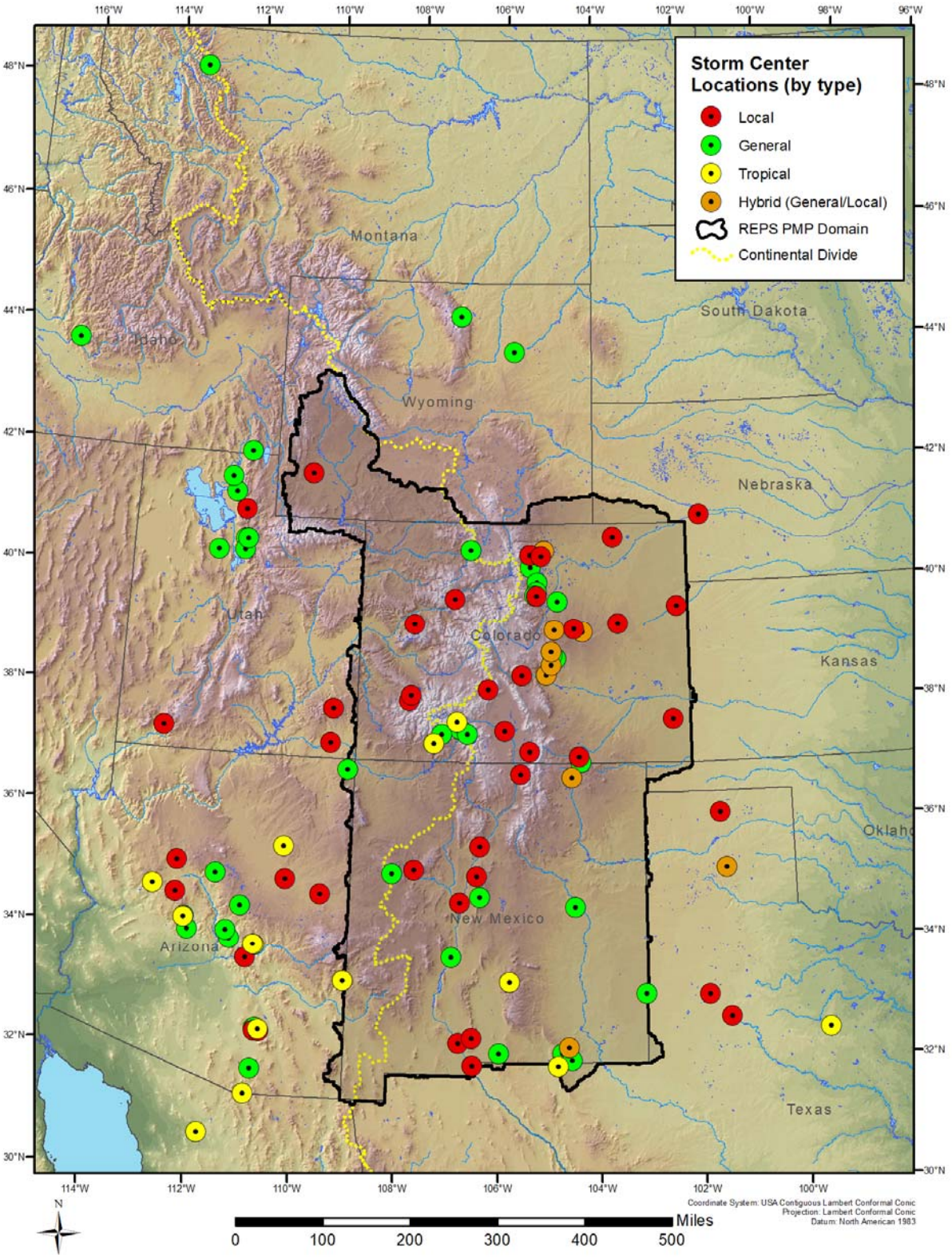

Figure 11: Short storm list locations

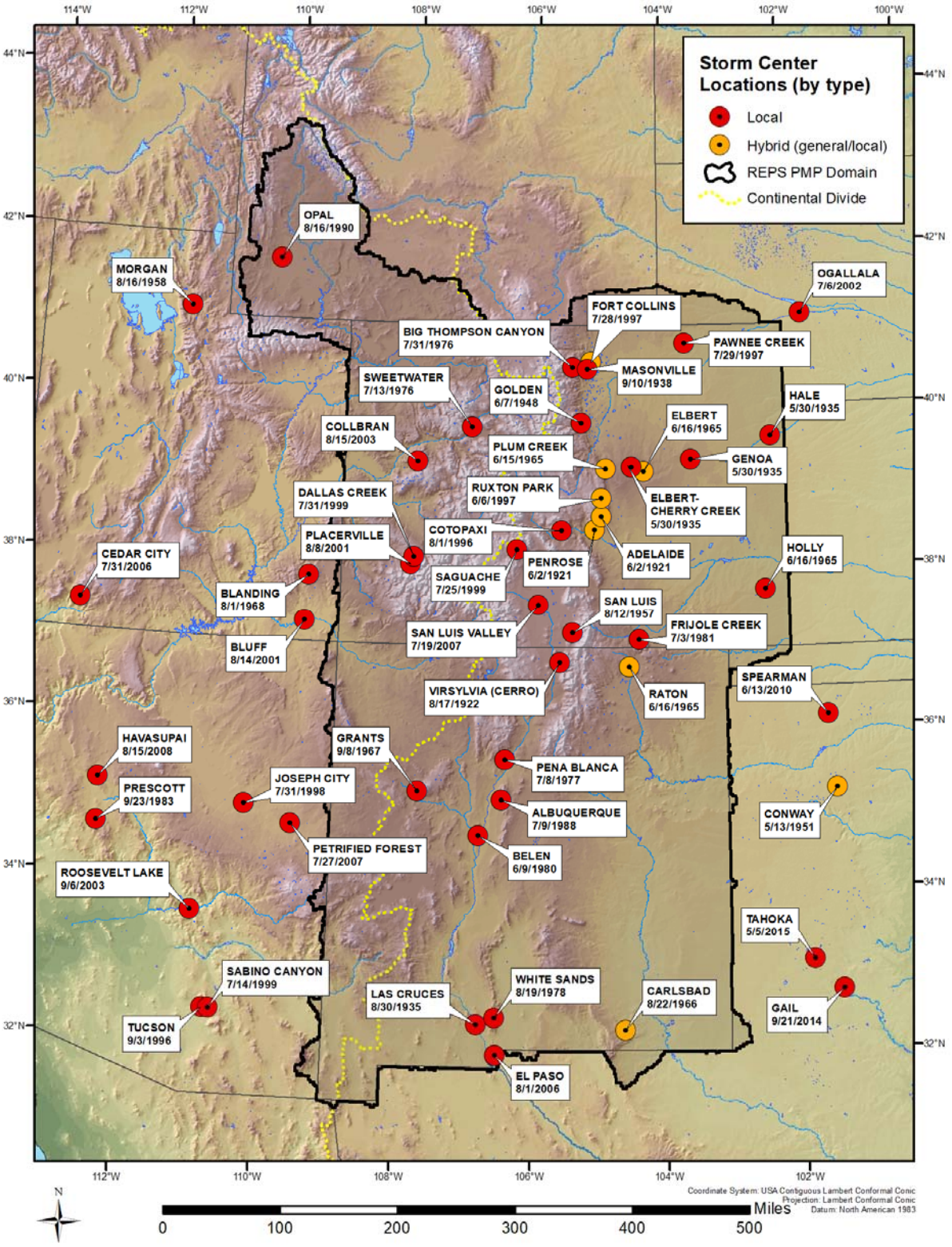

Figure 12: Short list of local storm locations

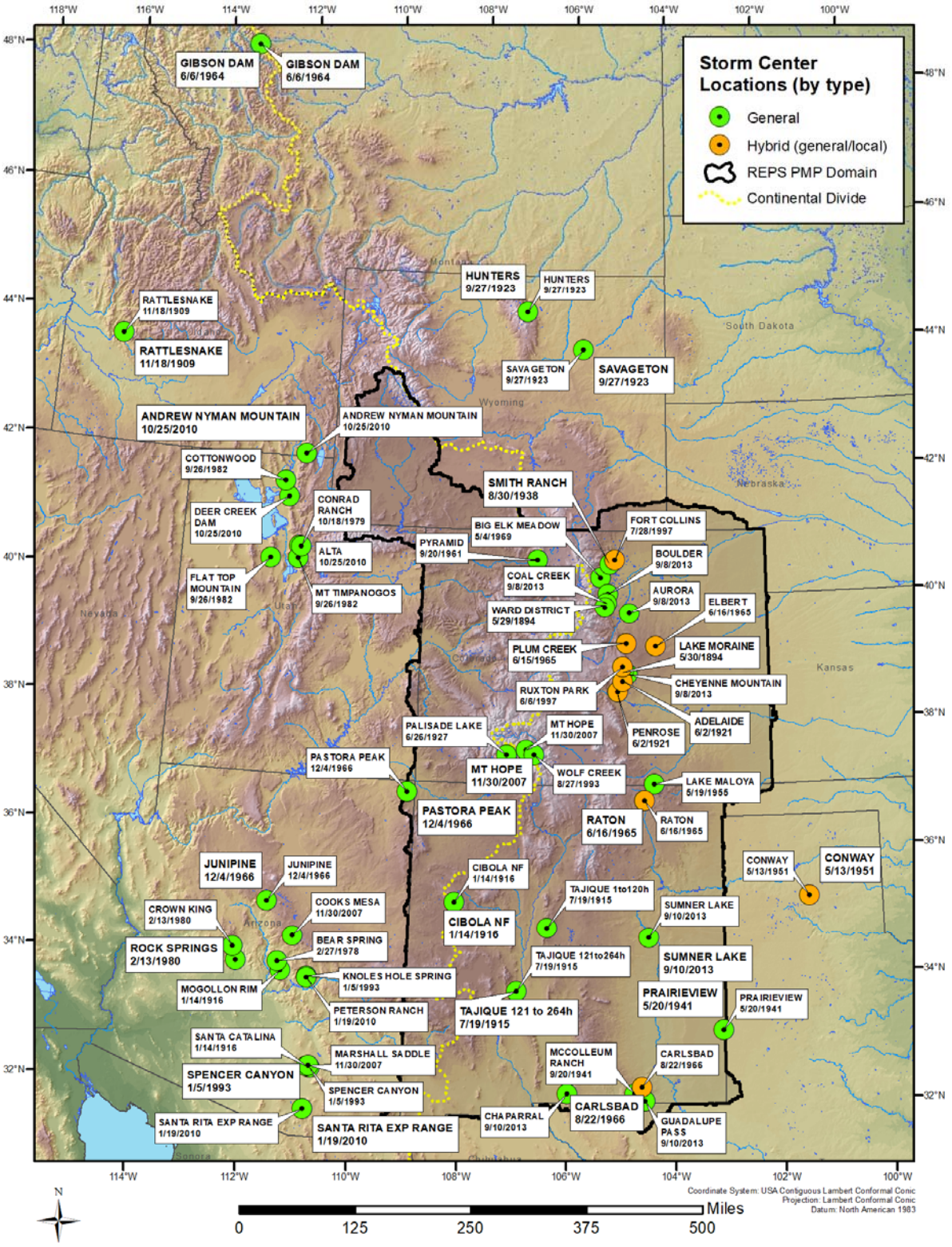

Figure 13: Short list of general storm locations

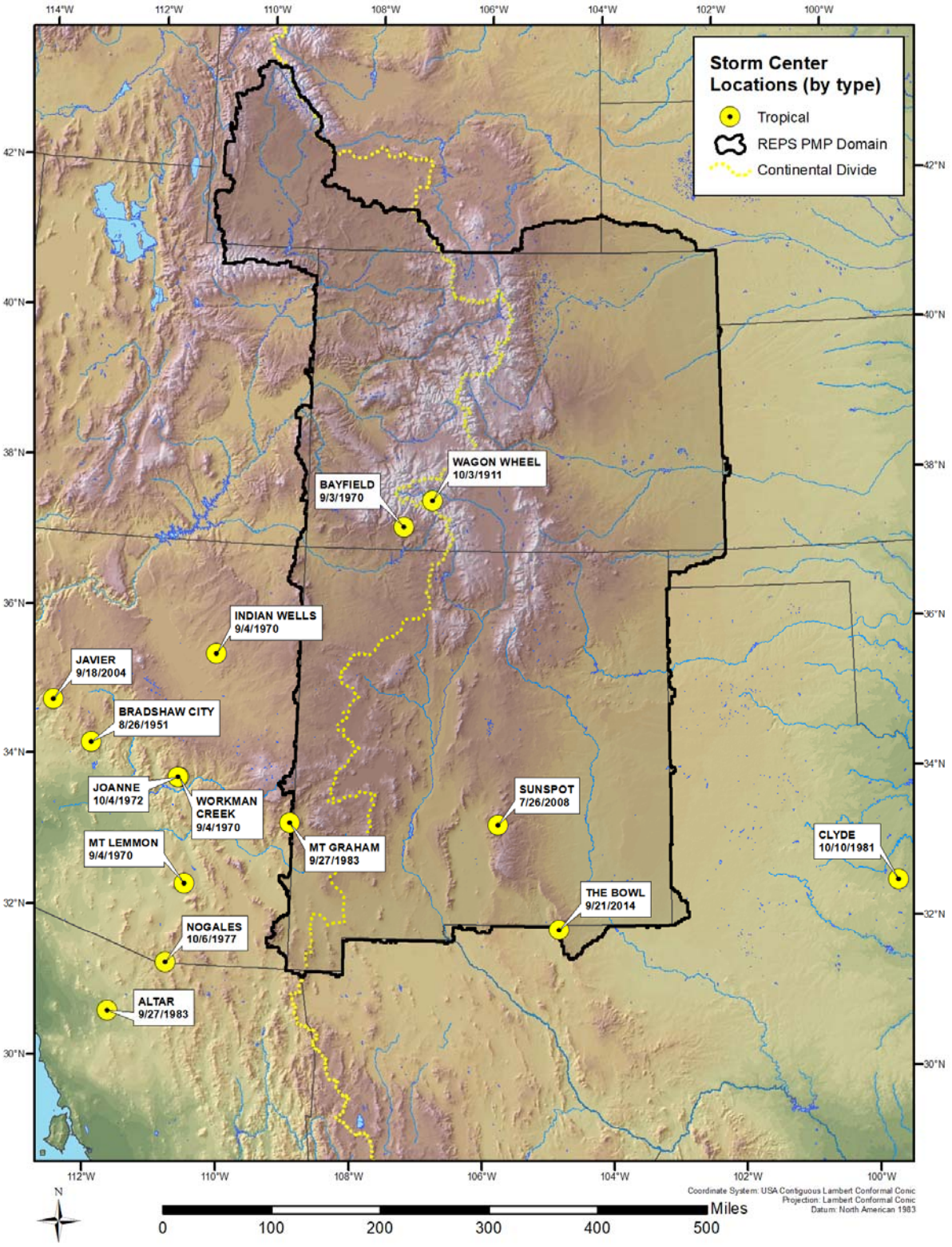

Figure 14: Short list of tropical storm locations

6. SPAS Analysis Results

For all storms identified as part of this study, Depth-Area-Duration (DADs) needed to be computed. Further, gridded rainfall information was required for all storms for the GTF calculations to be completed. SPAS was used to compute DADs for all of the storms used in this study. Results of all SPAS analyses used in the study are provided in Appendix F. This Appendix includes the standard output files associates with each SPAS analysis, including the following:

- SPAS analysis notes and description
- Total storm isohyetal
- DAD table and graph
- Storm center mass curve (hourly and incremental accumulation)

There are two main steps in the SPAS DAD analysis: 1) The creation of high-resolution hourly rainfall grids and 2) the computation of Depth-Area (DA) rainfall amounts for various durations, i.e. how the depth of the analyzed rainfall varies with area sizes being analyzed. The reliability of the results from step 2) depends on the accuracy of step 1). Historically the process has been very labor intensive. SPAS utilizes GIS concepts to create spatially-oriented and accurate results in an efficient manner (step 1). Furthermore, the availability of NEXRAD (NEXt generation RADar) data allows SPAS to better account for the spatial and temporal variability of storm precipitation for events occurring since the early 1990s. Prior to NEXRAD, the NWS developed and used a method based on Weather Bureau Technical Paper No. 1 (1946). Because this process has been the standard for many years and holds merit, the DAD analysis process developed for this study attempts to follow the NWS procedure as much as possible. By adopting this approach, some level of consistency between the newly analyzed storms and the hundreds of storms already analyzed by the USACE, USBR, and/or NWS can be achieved. Appendix E provides a detailed description of the SPAS program with the following sections providing a high-level overview of the main SPAS processes.

6.1 SPAS Data Collection

The areal extent of a storm's rainfall is evaluated using existing maps and documents along with plots of total storm rainfall. Based on the storm's spatial domain (longitude-latitude box), hourly and daily rain gauge data are extracted from the database for the specified area, dates, and times. To account for the temporal variability in observation times at daily stations, the extracted hourly data must capture the entire observational period of all extracted daily stations. For example, if a station takes daily observations at 8:00 AM local time, then the hourly data needs to be complete from 8:00 AM local time the day prior. As long as the hourly data are sufficient to capture all of the daily station observations, the hourly variability in the daily observations can be properly addressed.

The daily database is comprised of data from NCDC TD-3206 (pre-1948) and TD-3200 (generally 1948 through present). The hourly database is comprised of data from NCDC TD- 3240 and NOAA's Meteorological Assimilation Data Ingest System (MADIS).

The daily supplemental database is largely comprised of data from "bucket surveys," local rain gauge networks (e.g., ALERT, USGS, COCORAHS, etc.) and daily gauges with accumulated data.

6.2 SPAS Mass Curve Development

The most complete rainfall observational dataset available is compiled for each storm. To obtain temporal resolution to the nearest hour in the final DAD results, it is necessary to distribute the daily precipitation observations (at daily stations) into hourly bins. In the past, the NWS had accomplished this process by anchoring each of the daily stations to a single hourly station for timing. However, this may introduce biases and may not correctly represent hourly precipitation at locations between hourly observation stations. A preferred approach is to anchor the daily station to some set of nearest hourly stations. This is accomplished using a spatially based approach called the spatially based mass curve (SMC) process (see Appendix E).

6.3 Hourly and Sub-Hourly Precipitation Maps

At this point, SPAS can either operate in its standard mode or in NEXRAD-mode to create high resolution hourly or sub-hourly (for NEXRAD storms) grids. In practice both modes are run when NEXRAD data are available so that a comparison can be made between the methods. Regardless of the mode, the resulting grids serve as the basis for the DAD computations.

6.4 Standard SPAS Mode Using a Basemap Only

The standard SPAS mode requires a full listing of all the observed hourly rainfall values, as well as the newly created estimated hourly data from daily and daily supplemental stations. This is done by creating an hourly file that contains the newly created hourly mass curve precipitation data (from the daily and supplemental stations) and the "true" hourly mass curve precipitation. If not using a basemap, the individual hourly precipitation values are simply plotted and interpolated to a raster with an inverse distance weighting (IDW) interpolation routine in a GIS.

6.5 SPAS-NEXRAD Mode

Radar has been in use by meteorologists since the 1960s to estimate rainfall depth. In general, most current radar-derived rainfall techniques rely on an assumed relationship between radar reflectivity and rainfall rate. This relationship is described by the Equation 2 below:

$$Z = aR^b \qquad \text{Equation 2}$$

where Z is the radar reflectivity, measured in units of dBZ, R is the rainfall rate, a is the "multiplicative coefficient" and b is the "power coefficient". Both a and b are related to the drop size distribution (DSD) and the drop number distribution (DND) within a cloud (Martner et al., 2005).

The NWS uses this relationship to estimate rainfall through the use of their network of Doppler radars (NEXRAD) located across the United States. A standard default Z-R algorithm of $Z = 300R^{1.4}$ has been the primary algorithm used throughout the country and has proven to produce highly variable results. The variability in the results of Z vs. R is a direct result of differing DSD and DND, and differing air mass characteristics across the United States (Dickens 2003). The DSD and DND are determined by a complex interaction of microphysical processes in a cloud. They fluctuate hourly, daily, seasonally, regionally, and even within the same cloud (see Appendix E for a more detailed description).

Using the technique described above, also discussed in Appendix E, NEXRAD rainfall depth and temporal distribution estimates are determined for the area in question.

6.6 Depth-Area-Duration Program

The DAD extension of SPAS runs from within a Geographic Resource Analysis Support System (GRASS) GIS environment and utilizes many of the built-in functions for calculation of area sizes and average rainfall depths. The following is the general outline of the procedure:

1. Given a duration (e.g., x-hours) and cumulative precipitation, sum up the appropriate hourly or sub-hourly precipitation grids to obtain an x-hour total precipitation grid starting with the first x-hour moving window.
2. Determine x-hour precipitation total and its associated areal coverage. Store these values. Repeat for various lower rainfall thresholds. Store the average rainfall depths and area sizes.
3. The result is a table of depth of precipitation and associated area sizes for each x-hour window location. Summarize the results by moving through each of the area sizes and choosing the maximum precipitation amount. A log-linear plot of these values provides the depth-area curve for the x-hour duration.
4. Based on the log-linear plot of the rainfall depth-area curve for the x-hour duration, determine rainfall amounts for the standard area sizes for the final DAD table. Store these values as the rainfall amounts for the standard sizes for the x-duration period. Determine if the x-hour duration period is the longest duration period being analyzed. If it is not, analyze the next longest duration period and return to step 1.
5. Construct the final DAD table with the stored rainfall values for each standard area for each duration period.

6.7 SPAS DAD Zones

Several of the final SPAS analyses include more than one DAD zone. Individual SPAS DAD zones are developed when the timing and/or topographical interactions of a given SPAS analysis demonstrate that specific areas of the rainfall accumulation should not be grouped together. The DAD zones are delineated so that the final DAD depths represent an area of rainfall accumulation that occurred over the same time period and with the same topographical interactions. Meteorological judgment and

experience are applied to each SPAS analysis to determine the most appropriate DAD zone delineations.

DAD zone separation is completed so that the final DAD depths used in PMP analysis represent a physical possible rainfall accumulation pattern. Otherwise, the DAD depths would be a combination of rainfall from areas with significantly different topographical characteristics and/or significantly different timing. Separate DAD zones are needed because when DAD depths are calculated, spatial characteristics are lost as the process combines all data above a given threshold and area within a pre-defined domain regardless of timing or topographical location. Therefore, the DAD depths no longer represent those individual storm characteristics and those variations would not be represented in the DAD depths.

Many of the storms used in this study had multiple DAD zones. The DAD zones are treated as individual storm centers for PMP analysis. These are indicated in the storm lists as SPAS XXXX_X, where the X is the DAD zone. For example SPAS 1302_2 would represent SPAS storm number 1302 and DAD zone 2.

6.8 Comparison of SPAS DAD Output Versus Previous DAD Results

The SPAS process and algorithms have been thoroughly reviewed as part of many AWA PMP studies. Recently the SPAS program was reviewed as part of the NRC software verification and validation program to ensure that its use in developing data for use in NRC regulated studies was acceptable. The result of the NRC review showed that the SPAS program performed exactly as described and produced expected results.

As part of this study, the PRB asked that comparisons be provided comparing SPAS DAD and previously published DAD tables developed by the USACE, USBR, and/or NWS. AWA provided these comparison tables for all storms where previous DADs were available that covered the same domain as the SPAS analysis (see Appendix K). Table 3 provides an example comparison of a SPAS DAD from the analysis of the Big Thompson Canyon, CO July 1976 storm versus the USBR DAD previously developed for that storm. As expected, the differences between SPAS DAD depths and previously published depths varied by area size and duration. The difference were a result of one or more of the following:

- SPAS utilizes a more accurate basemap to spatially distribute rainfall between known observation locations. The use of a climatological basemap reflects how rainfall has occurred over a given region at a given time of the year and therefore how an individual storm pattern would be expected to look over the location being analyzed. Previous DAD analyses completed by the NWS and USACE often utilized simple IDW or Thiessen polygon methods that did not reflect climatological characteristics as accurately. In some cases the NWS and USACE utilized precipitation frequency climatologies to inform spatial patterns. However, these relied on NOAA Atlas 2 (Miller et al., 1973) patterns and data that are not as accurate as current data from PRISM (Daly et al., 1994 and Daly et al., 1997) and NOAA Atlas 14.

- In some cases updated sources of data uncovered during the data mining process were incorporated into SPAS that were not utilized in the original analysis.
- SPAS utilizes sophisticated algorithms to temporally and spatially distribute rainfall. In contrast, the isohyetal maps developed previously were hand drawn. Therefore, they reflected the best guess of the analyst of each storm, which could vary between each analyst's interpretations. Also, only a select few stations were used for timing, which limited the variation of temporal accumulation patterns throughout the overall domain being analyzed. SPAS uses the power of all the rainfall observations that have passed QA/QC measures to inform patterns over the entire domain. These temporal and spatial fits are evaluated and updated on an hourly basis for the entire duration.

Table 3: Comparison of SPAS 1231 DAD versus the USBR DAD, both representing the Big Thompson Canyon, CO July 1976 storm event

Storm 1231 Zone 1 MAXIMUM AVERAGE DEPTH OF PRECIPITATION (INCHES)					
areasqmi	1	2	3	4	Total
0.2	7.16	8.58	9.41	9.82	9.82
1	7.08	8.45	9.26	9.67	9.67
10	6.46	7.83	8.85	9.35	9.35
25	5.78	7.08	8.26	8.84	8.84
50	4.89	6.14	7.44	8.02	8.02
USBR **MAXIMUM AVERAGE DEPTH OF PRECIPITATION (INCHES)**					
areasqmi	1-hr	2-hr	3-hr	4-hr	Total
0.2	6.7	9.5	11.3	12.5	12.5
1	6.2	8.9	10.5	11.7	11.7
10	4.8	7.2	8.6	10.0	10.0
25	3.9	5.8	7.0	8.2	8.2
50	2.7	4.1	5.0	5.9	5.9
Difference (SPAS 1231 - USBR) **MAXIMUM AVERAGE DEPTH OF PRECIPITATION (INCHES)**					
areasqmi	1-hr	2-hr	3-hr	4-hr	Total
0.2	0.5	-0.9	-1.9	-2.7	-2.7
1	0.9	-0.5	-1.2	-2.0	-2.0
10	1.7	0.6	0.3	-0.7	-0.7
25	1.9	1.3	1.3	0.6	0.6
50	2.2	2.0	2.4	2.1	2.1
Percent Difference ((SPAS 1231 - USBR)/USBR) **MAXIMUM AVERAGE DEPTH OF PRECIPITATION (INCHES)**					
areasqmi	1-hr	2-hr	3-hr	4-hr	Total
0.2	7%	-10%	-17%	-21%	-21%
1	14%	-5%	-12%	-17%	-17%
10	35%	9%	3%	-7%	-7%
25	48%	22%	18%	8%	8%
50	81%	50%	49%	36%	36%

6.9 Utilization of WRF Model Re-analysis Fields as a SPAS Basemap

A significant improvement applied in this study was the use of model data from the REPS Dynamical Modeling Task. This included the ability to run Weather Research and Forecast (WRF) model re-analysis to recreate past extreme rainfall events. AWA provided the Dynamical Modeling Task with several storm events that could potentially benefit from this process. The storms which were run through the WRF reanalysis were Ward District, CO May 1894 (SPAS 1614); Rattlesnake, ID November 1909 (SPAS 1274); Penrose, CO June 1921 (SPAS 1294); Savageton, WY September 1923 (SPAS 1325); Elbert-Cherry Creek-Genoa-Hale May 1935 (SPAS 1295); Opal, WY August 1990 (SPAS 1264); and Virsylvia, NM August 1922. These were selected based on the following:

- Importance of each storm in previous PMP development
- Lack of observation data from which to derive a robust storm spatial pattern, temporal pattern and/or magnitude
- Uncertainty in the previous analysis results both from the USACE/USBR/NWS and AWA
- Uncertainty in the previous basemap utilized by AWA to accurately capture the spatial distribution
- Limited surface observation data for rainfall analysis and storm maximization

The results and usefulness of each WRF reanalysis varied significantly and were related to the accuracy of capturing the observed magnitude of each event. The WRF reanalysis often performed best in regions where topography played a significant role in rainfall spatial pattern and magnitude. Extensive discussion took place between AWA and the Dynamical Modeling Task lead Kelly Mahoney regarding the output of each WRF run for each storm. Specific evaluations of the spatial accumulation patterns and how they compared to previous patterns and to observed total storm accumulation depths were completed. Therefore the WRF results were most useful for the Rattlesnake, ID November 1909, Ward District, CO May 1894, and Penrose, CO June 1921 storms and were less useful for the other storms.

For the Rattlesnake, ID storm (SPAS 1274) the WRF precipitation (based on maximum value of 4-member runs) was utilized (Figure 15). In addition, because this storm occurred in November, where snowfall occurred at higher elevations, it was necessary to remove areas that were snow versus rain from the SPAS analysis. This was accomplished by utilizing the WRF snow (average based on 4-member runs) and removing those regions from the SPAS analysis domain (Figure 16). The WRF rainfall only basemap provided a more accurate spatial pattern for the data limited region, provided more accurate spatial patterns related to the topographical variations. This was used as the basemap to spatially distribute the rainfall between rain gauge observations for the updated SPAS analysis. Figure 17 provides the SPAS total storm isohyetal before WRF basemap application and Figure 18 provides the final pattern after application.

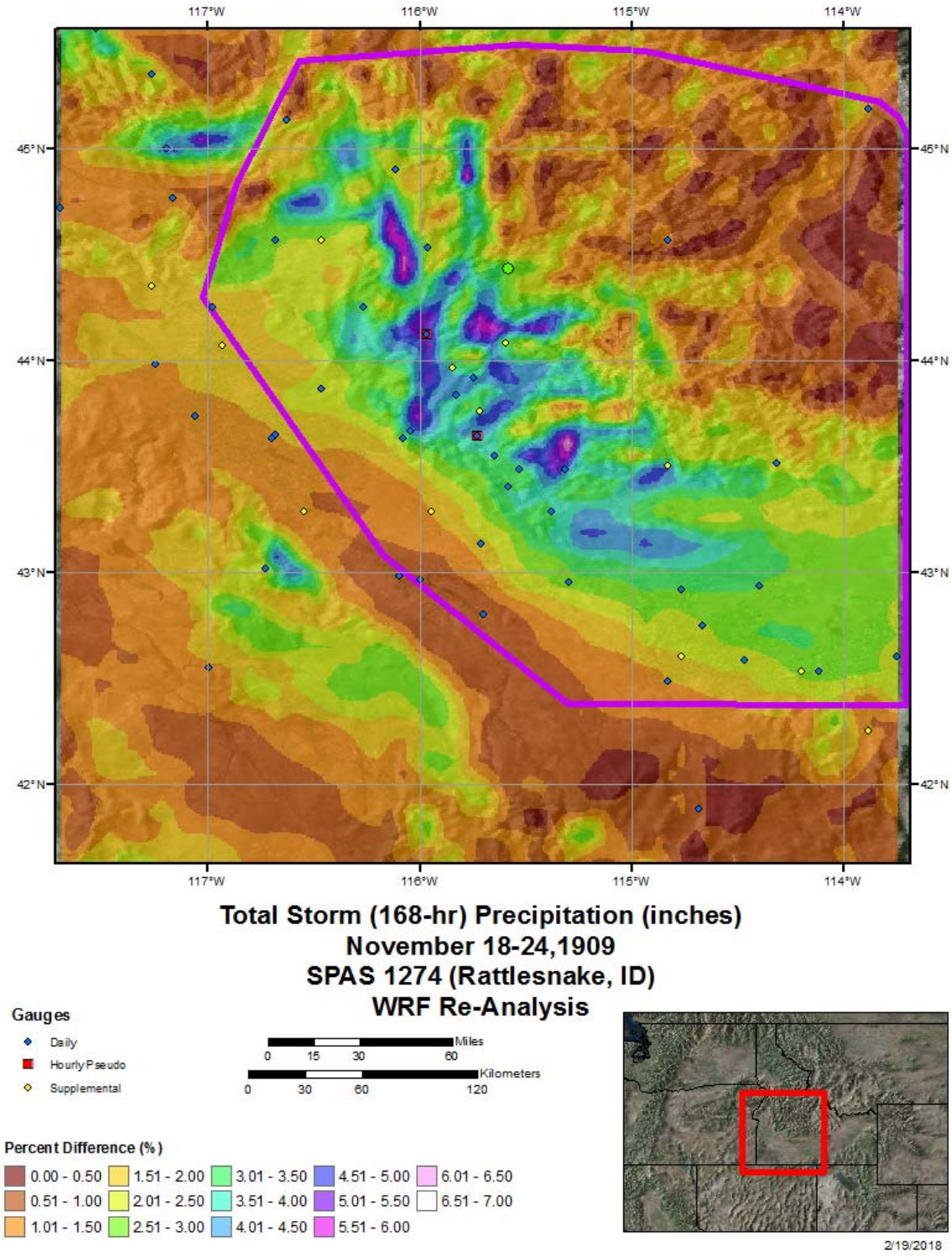

Figure 15: WRF reanalysis precipitation over the SPAS 1274 domain

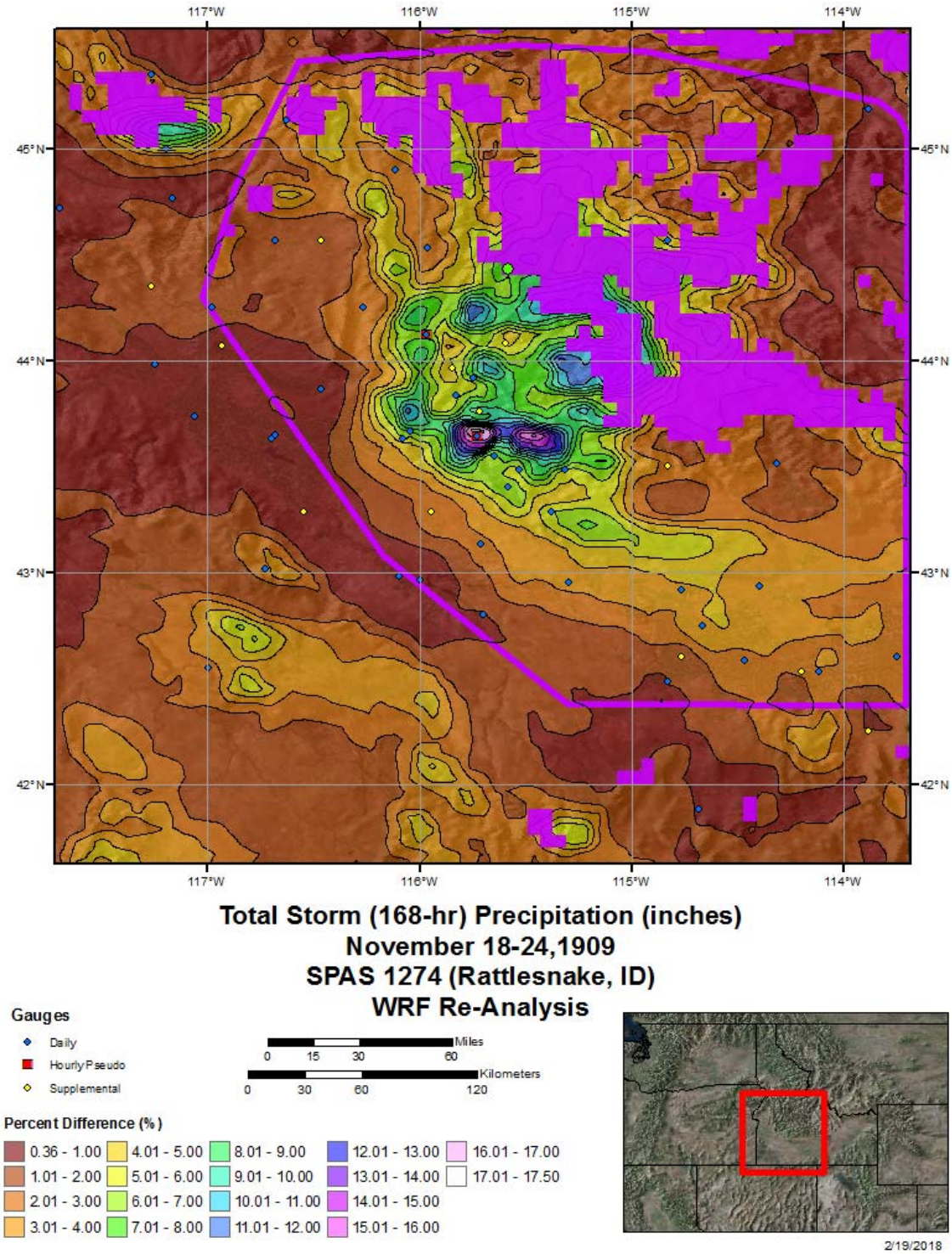

Figure 16: WRF reanalysis of regions showing frozen precipitation, shown in purple, over the SPAS 1274 domain

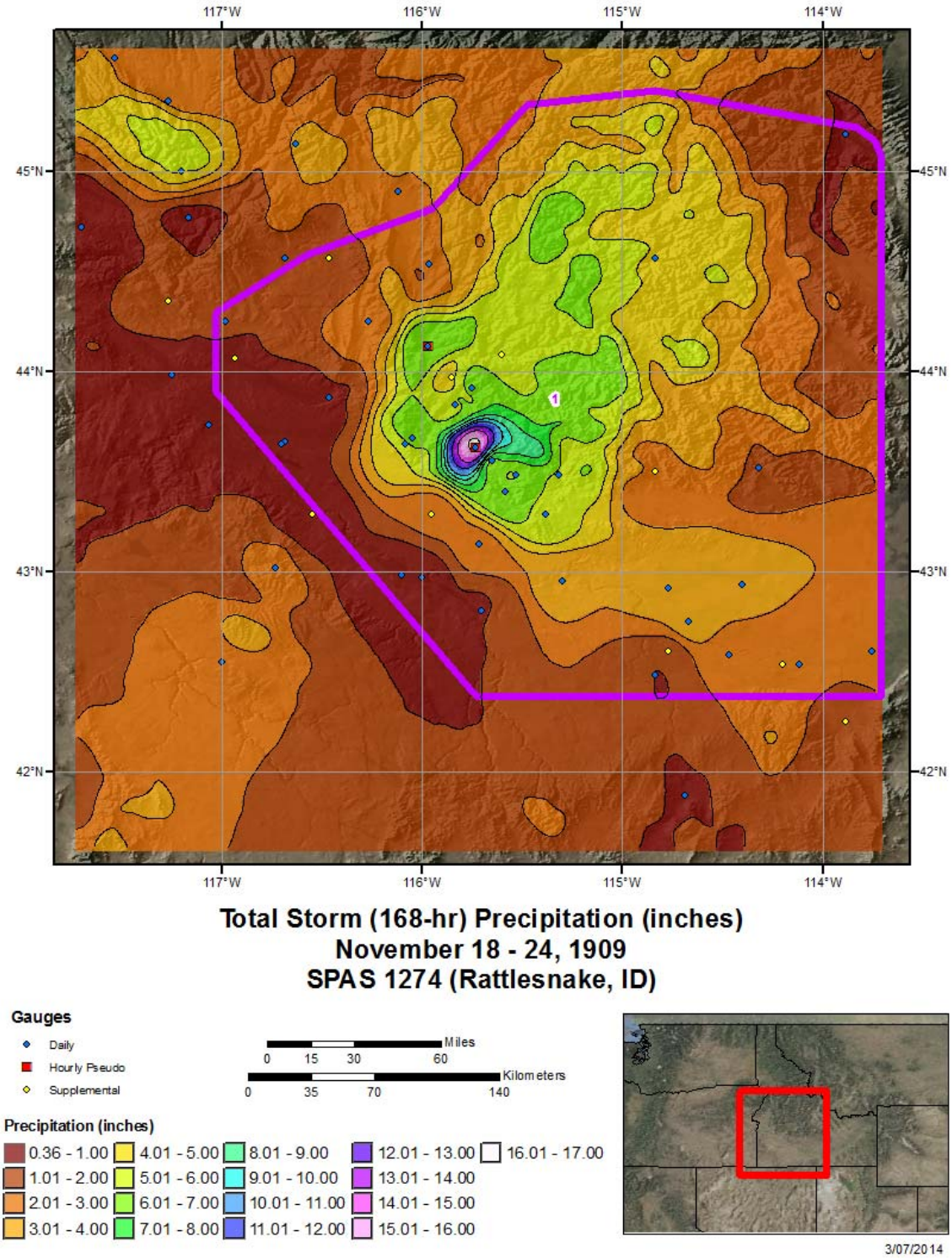

Figure 17: SPAS 1274 total storm isohyetal pattern prior to utilizing the WRF reanalysis information

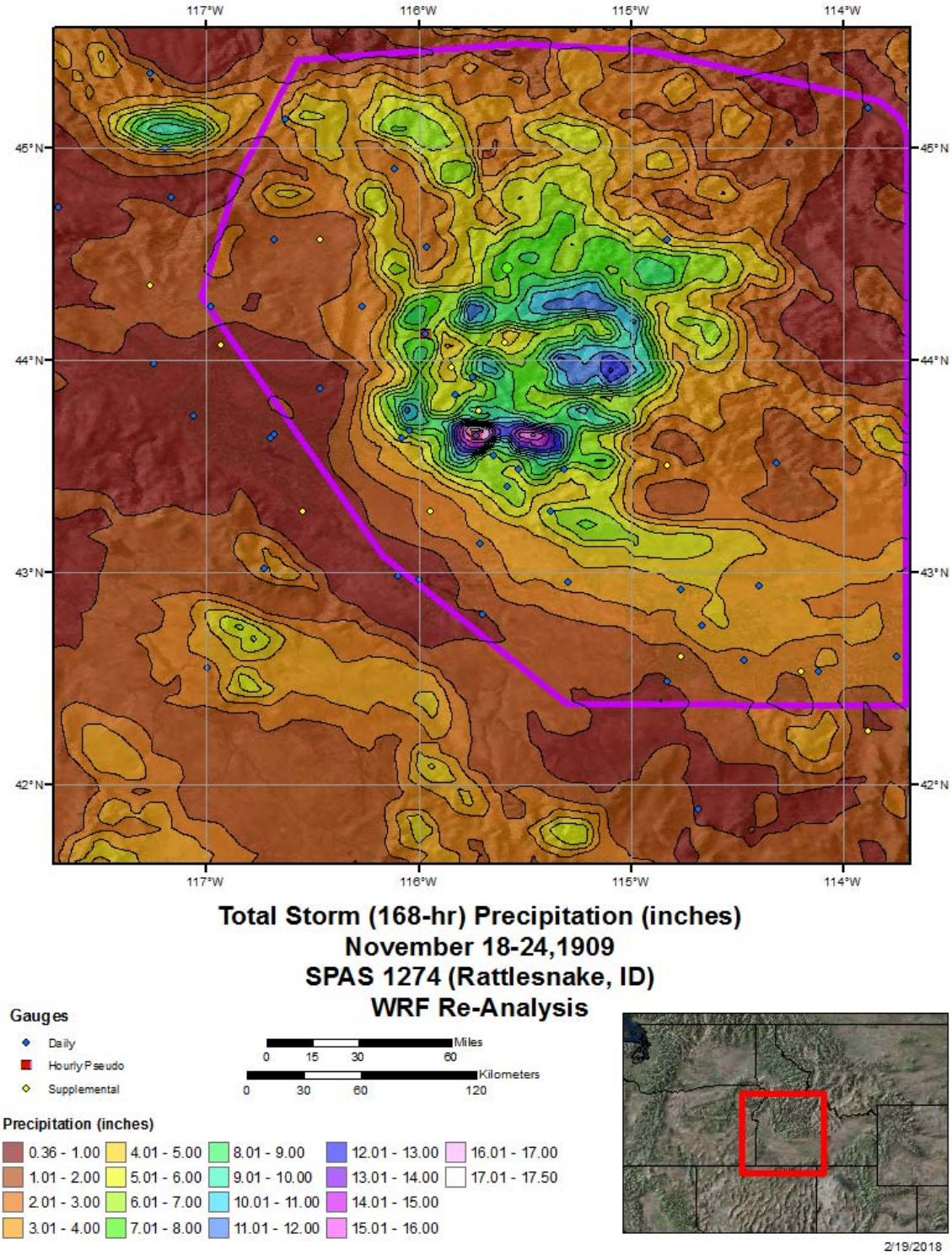

Figure 18: SPAS 1274 total storm isohyetal pattern after utilizing the WRF reanalysis information

For the Ward District, CO storm (SPAS 1614) the WRF spatial precipitation pattern (based on maximum value of 4-member runs) was used as a SPAS basemap (Figure 19). The WRF output showed a reasonable spatial pattern over the mountainous terrain given the expected interaction of topography and storm characteristics. The WRF pattern also matched well with the observed rainfall observations, although shifted slightly to the southeast. This provided significant improvement over the previous analysis where limited rainfall observations were available and therefore the spatial pattern was highly reliant on USGS hand drawn isohyetal pattern (Follansbee and Sawyer, 1948). Figures 20 and 21 provide the SPAS total storm isohyetal before WRF basemap application and after application. Notice the more realistic representation of the spatial pattern over the elevated terrain versus the previous SPAS analysis, which produced a more “bullseye” effect around the limited observational points. This mainly affected the overall volume of rainfall in the high elevation regions.

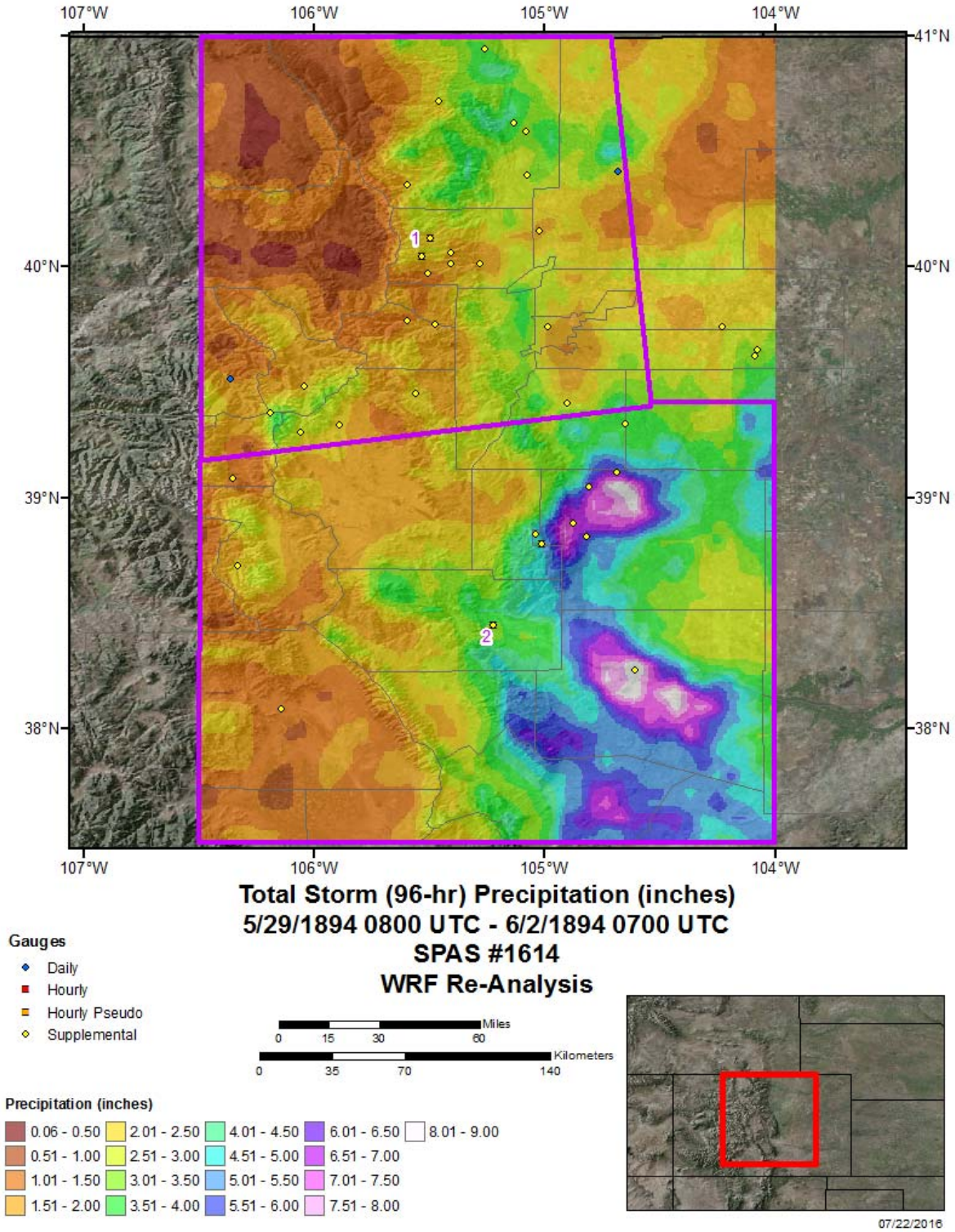

Figure 19: WRF reanalysis precipitation over the SPAS 1614 domain

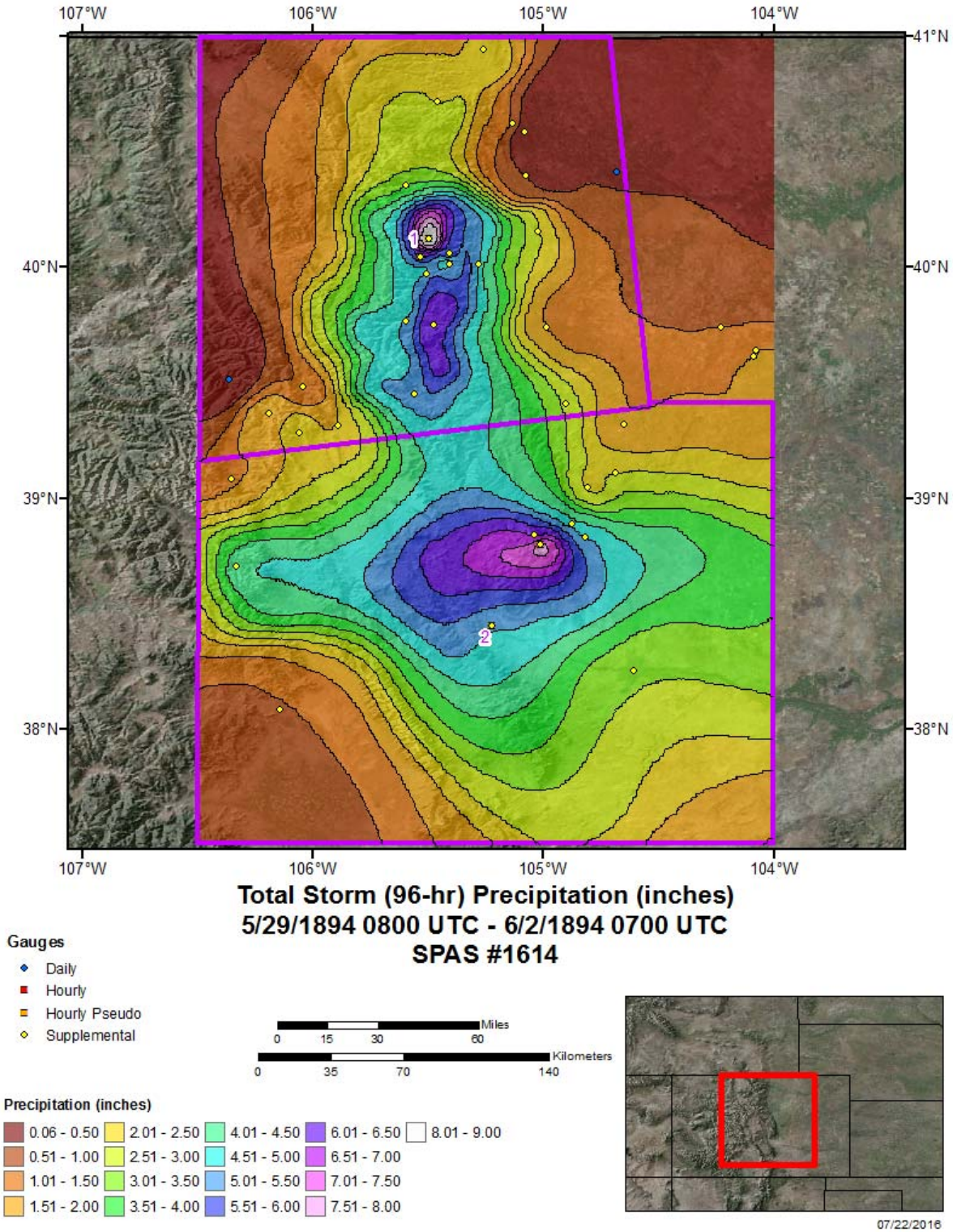

Figure 20: SPAS 1614 total storm isohyetal pattern prior to utilizing the WRF reanalysis information

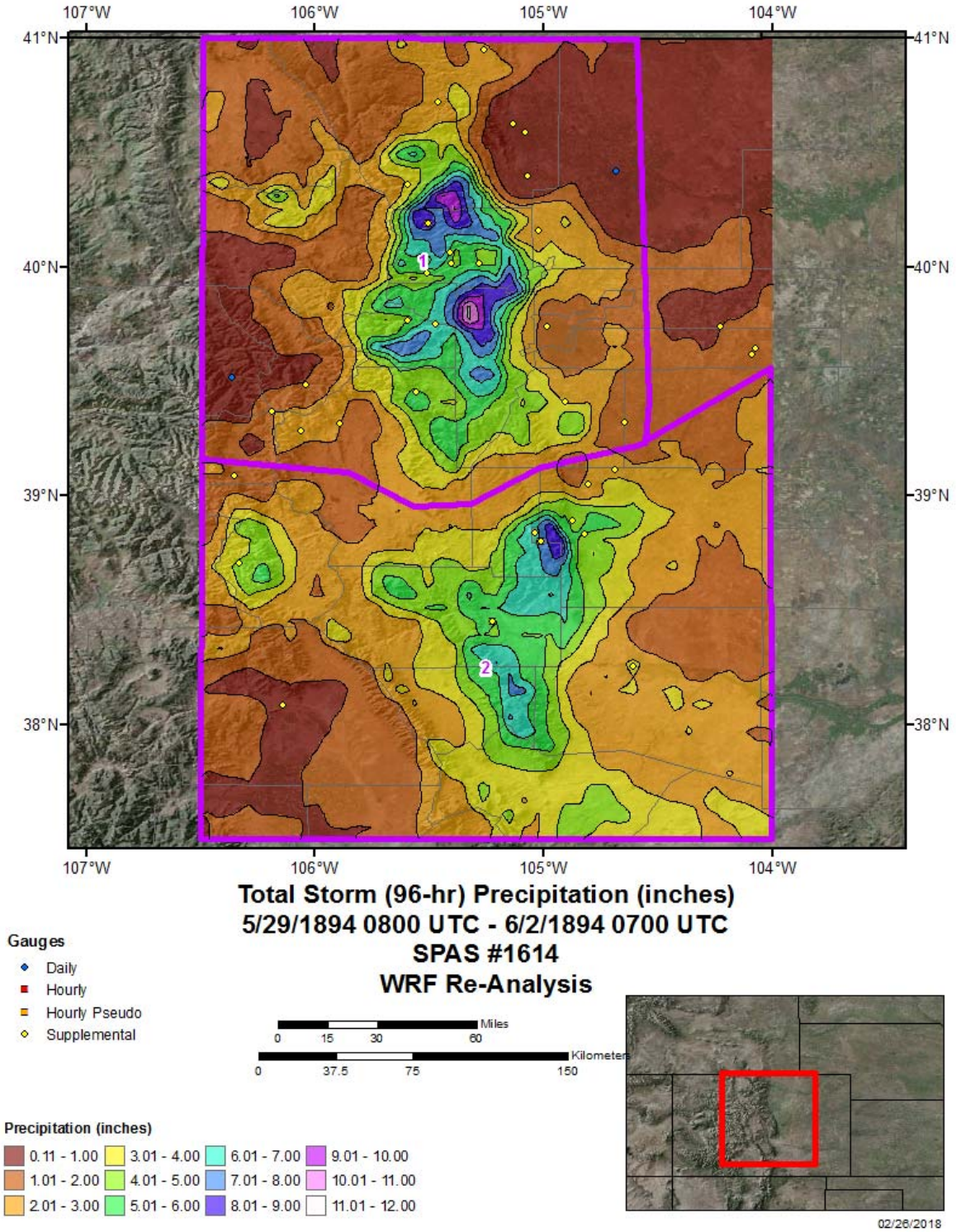

Figure 21: SPAS 1614 total storm isohyetal pattern after utilizing the WRF reanalysis information

DAD Zone 2 (the region above 7500 feet) of the Penrose, CO (SPAS 1294) storm was reevaluated with the aid the WRF reanalysis representing the maximum grids from the four-member ensemble grids. Reevaluation of the high elevation DAD for this storm occurred after evaluating the results of site-specific basin analyses. Results of these investigation produced anomalously high rainfall depths at 6 and 12-hours. Evaluations of the cause for the anomalously high values showed two causes. First, the GTF calculations for this storm had used the 24-hour duration. However, based on the hourly rain gauge near the storm center as well as eye witness reports and bucket survey data (Follansbee and Jones, 1922), the majority of the rainfall accumulation occurred over a 5-hour period (Figure 22). Therefore, the GTF calculations were corrected to use the 6-hour values. Second, the high elevation spatial patterns were investigated. This analysis demonstrated that the spatial patterns were significantly influenced by the PRISM June 1921 climatological basemap (Figure 23). This basemap produced anomalously high values over the highest elevations (e.g., the top of Pikes Peak). To correct the spatial pattern, the WRF reanalysis of the June 1921 storm was investigated.

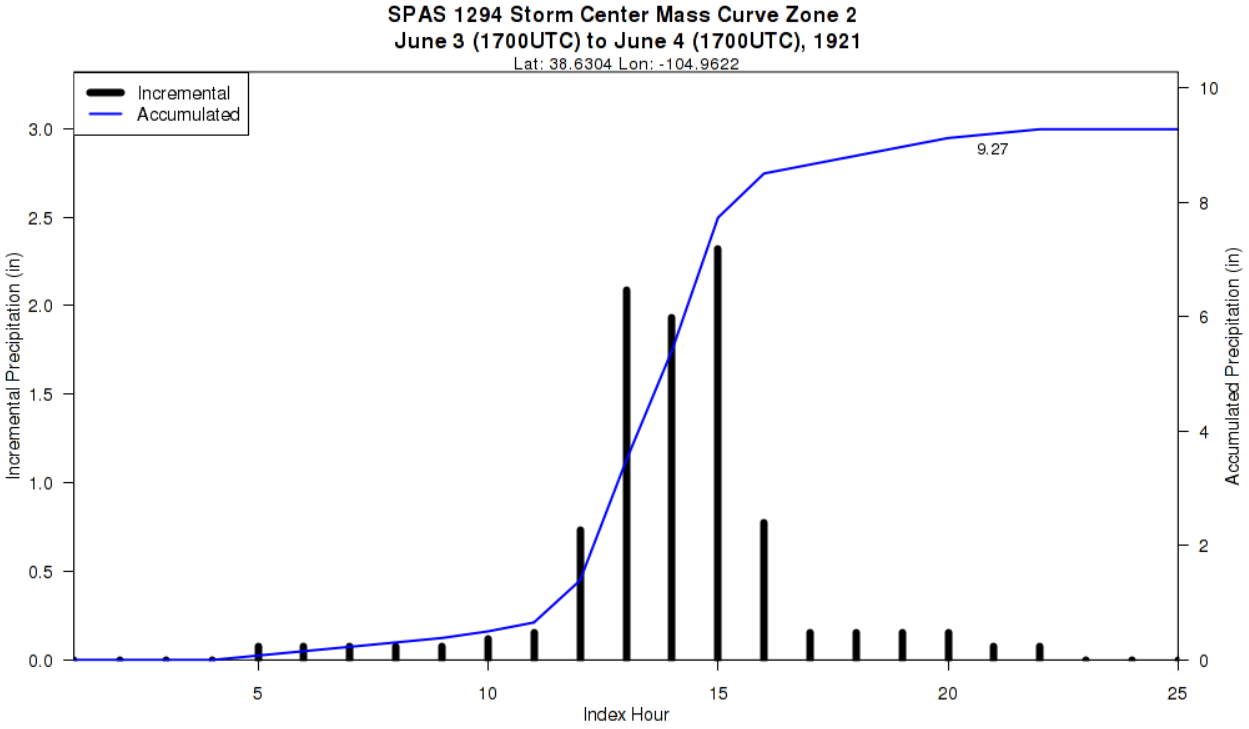

Figure 22: SPAS 1294 DAD Zone 2 storm center mass curve

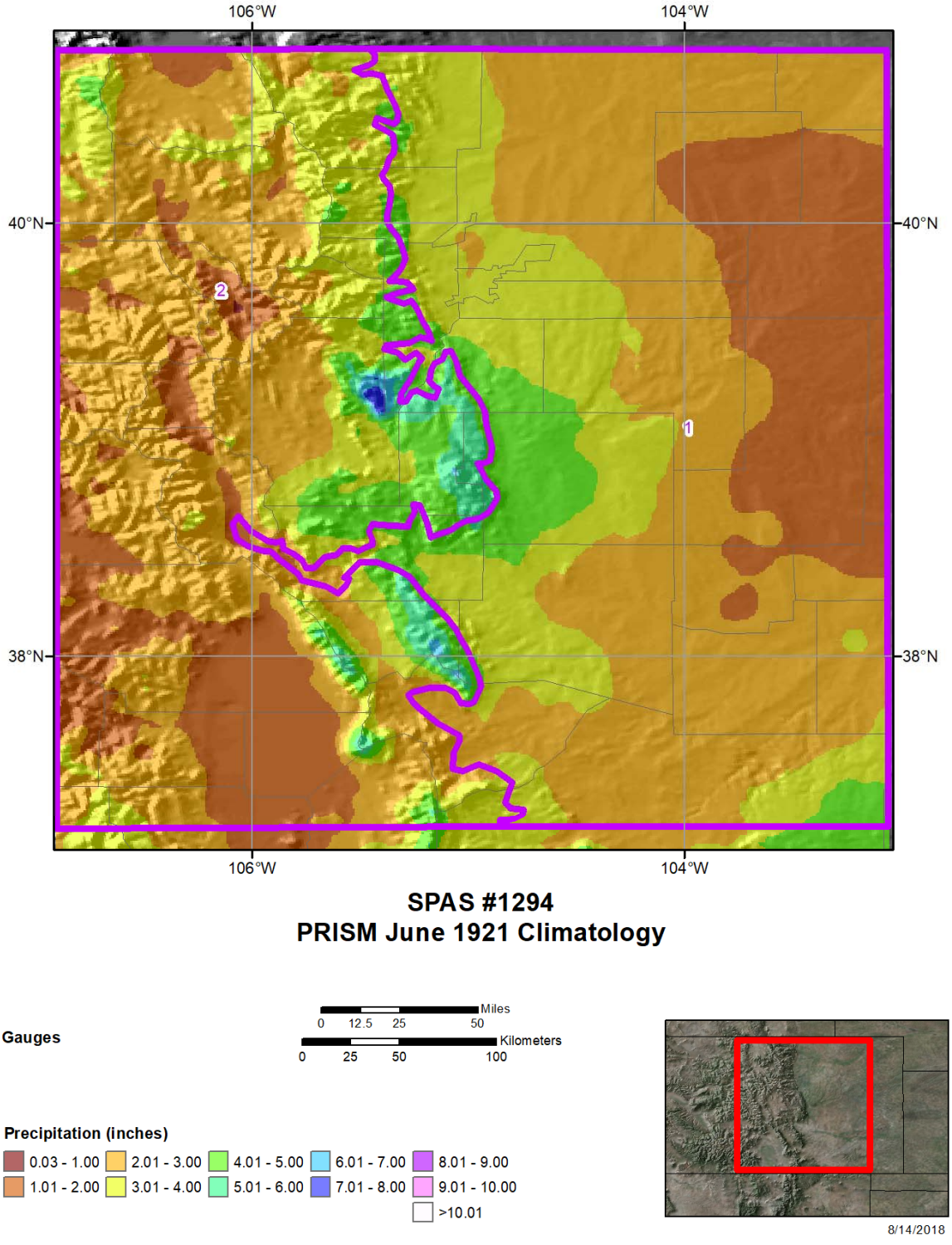

Figure 23: PRISM June 1921 climatology with the anomalously high values evident in the region covering elevation greater than 7500 feet

The WRF spatial output was similar to the original SPAS spatial analysis, especially over the main rainfall center location around Penrose, CO, except that the WRF storm center was shifted to the east approximately 10-miles and the magnitude was substantially less than the observed data (Figures 24 and 25). Figure 25 shows the original SPAS total storm isohyetal with the high elevation regions in question shown (inside the black circles). These are the main areas where the initial investigations demonstrated issues with the PRISM basemap added more rain than was supported by the observations and flood runoff information. These are areas where pseudo rain gauges were adding to constrain the values in those regions to fit the surrounding rain gauge observations.

Considering that the WRF reanalysis produced a reasonable spatial fit over the main rainfall location and along the Front Range in general, it was assumed the spatial pattern and relative magnitudes over the higher elevation locations were similarly more representative, and likely more relevant for defining the spatial pattern than the PRISM monthly climatology used previously. This provided further justification for updating the spatial patterns above 7500 feet for increased precision of dynamically-likely spatial patterns and not allow the precipitation to be inappropriately inflated by PRISM climatological basemaps. Further corroboration of the anomalously high rainfall patterns produced by the PRISM basemap was shown after investigating the USGS report on the storm (Follensbee and Jones, 1992) and the figure showing areas of greatest rainfall during the event. Figure 26 from that report shows the regions of heaviest rainfall from their investigations and flood runoff events. The areas highlighted as having the greatest rainfall are associated with the Penrose center with no suggestion of heavy rainfall over the region above 7500 feet.

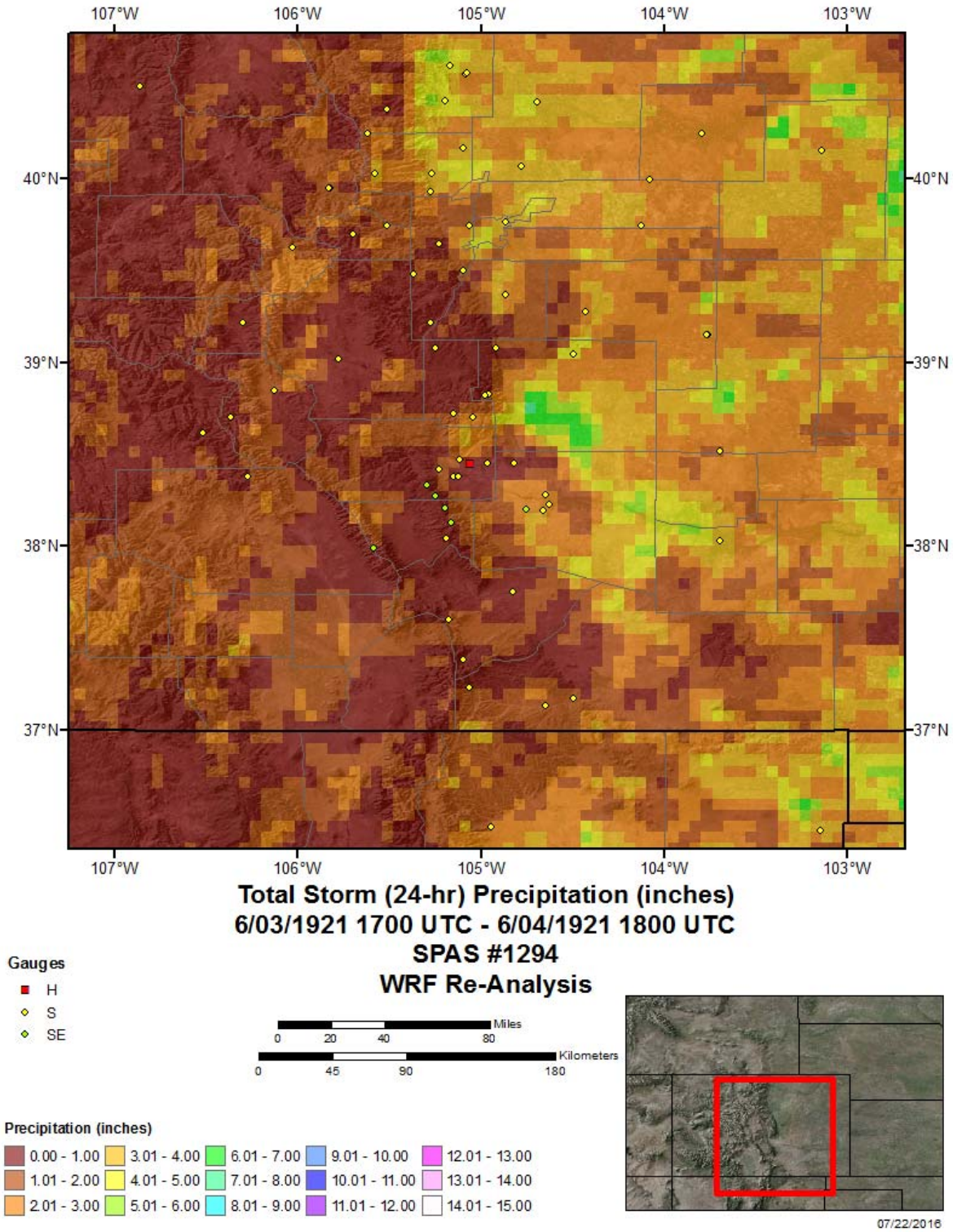

Figure 24: WRF reanalysis precipitation over the SPAS 1294 domain

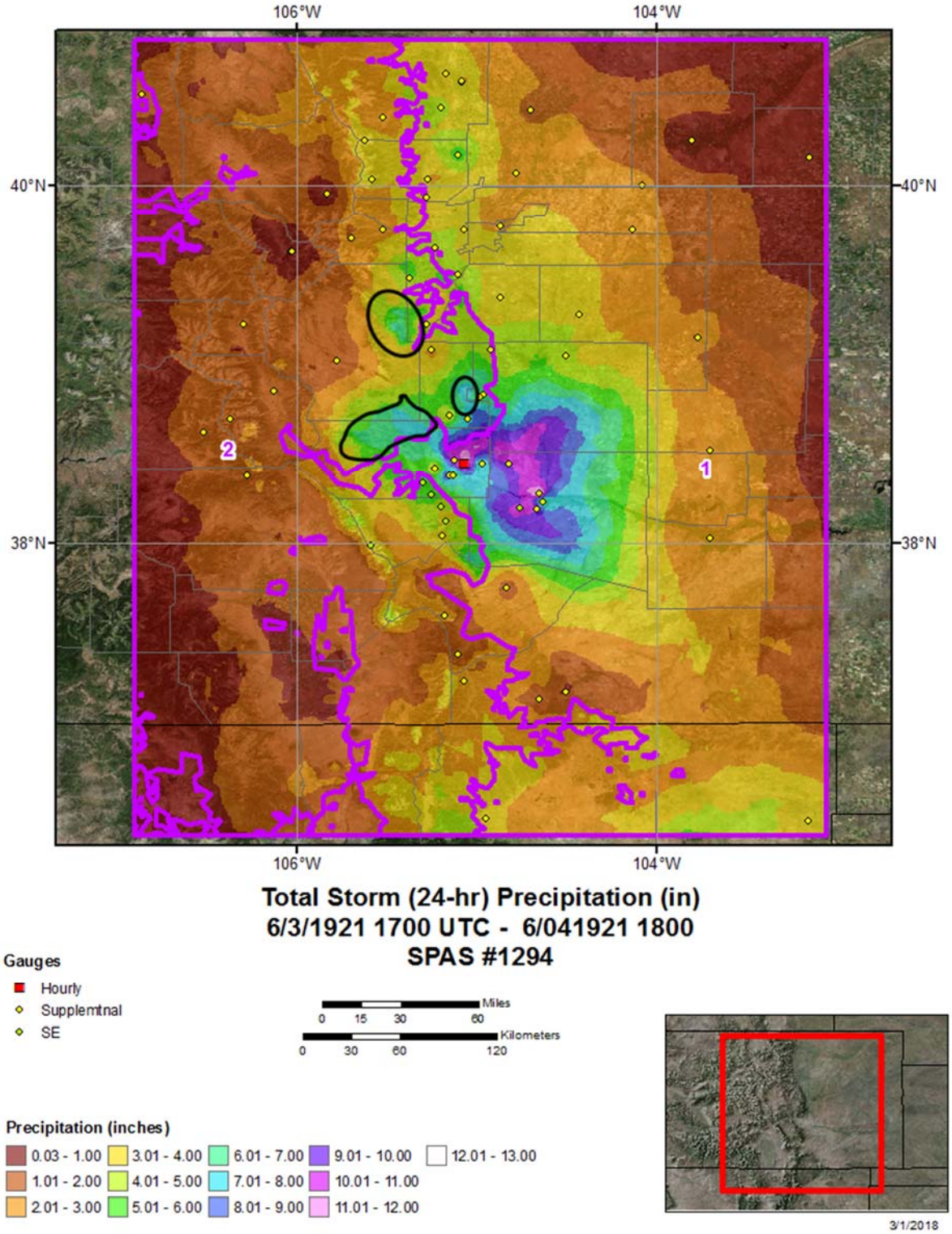

Figure 25: SPAS 1294 total storm isohyetal pattern prior to utilizing the WRF reanalysis information. Note the black circles encompass regions ultimately adjusted to correct for the inappropriate increase resulting from the PRISM June 1921 climatological basemap.

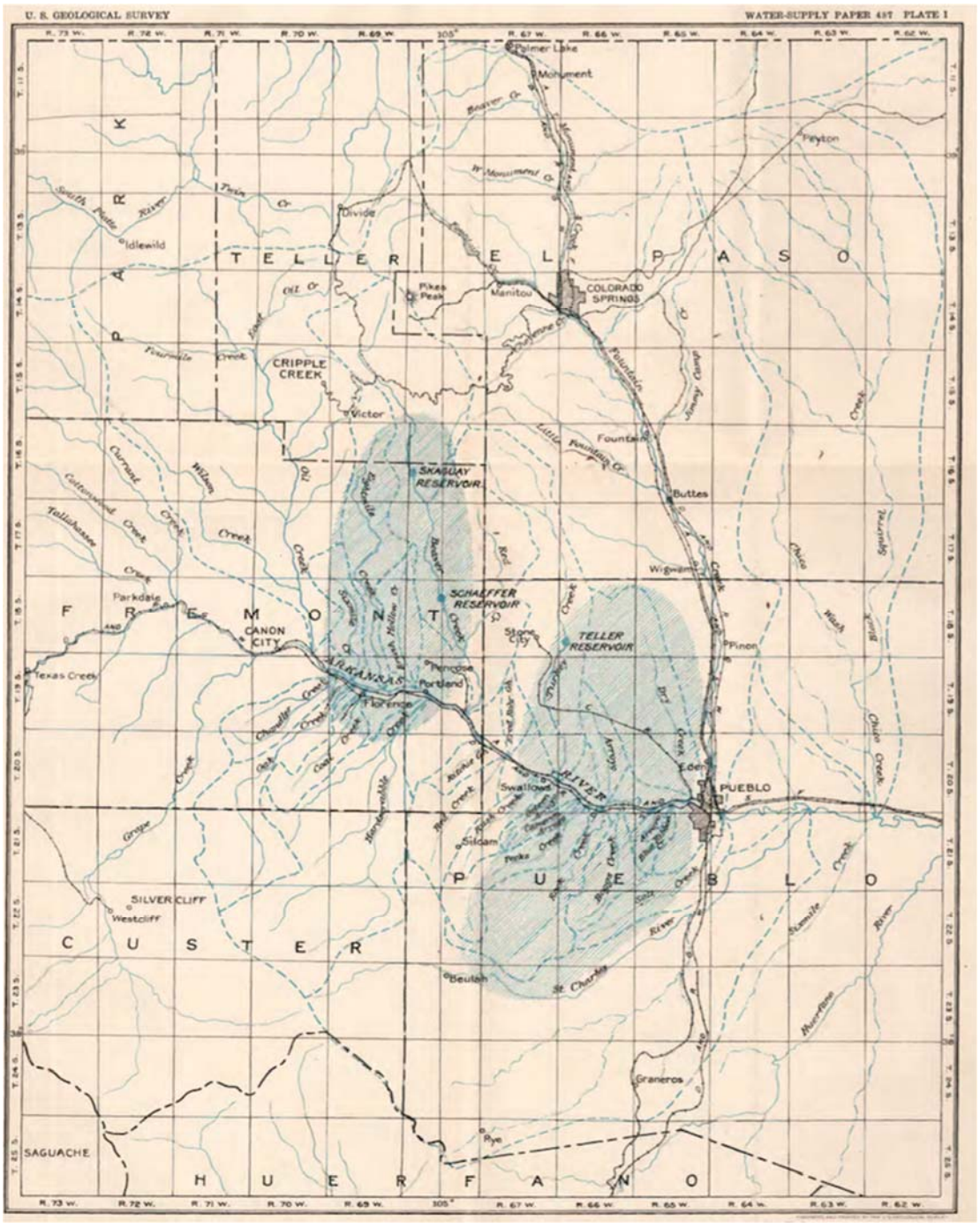

Figure 26: USGS depiction of regions of heavy rainfall causing excessing flooding (reproduced from Follensbee and Jones, 1922). Note, no significant rainfall is depicted around the highest elevation of Pikes Peak or along the Park/Freemont/Teller county area.

Application of the appropriate GTF duration and the updated spatial patterns produced a DAD for the high elevation region (DAD Zone 2) that resulted in a more physically realistic precipitation accumulation pattern. Figure 27 displays the final SPAS analysis after correcting the high elevation spatial patterns and magnitudes.

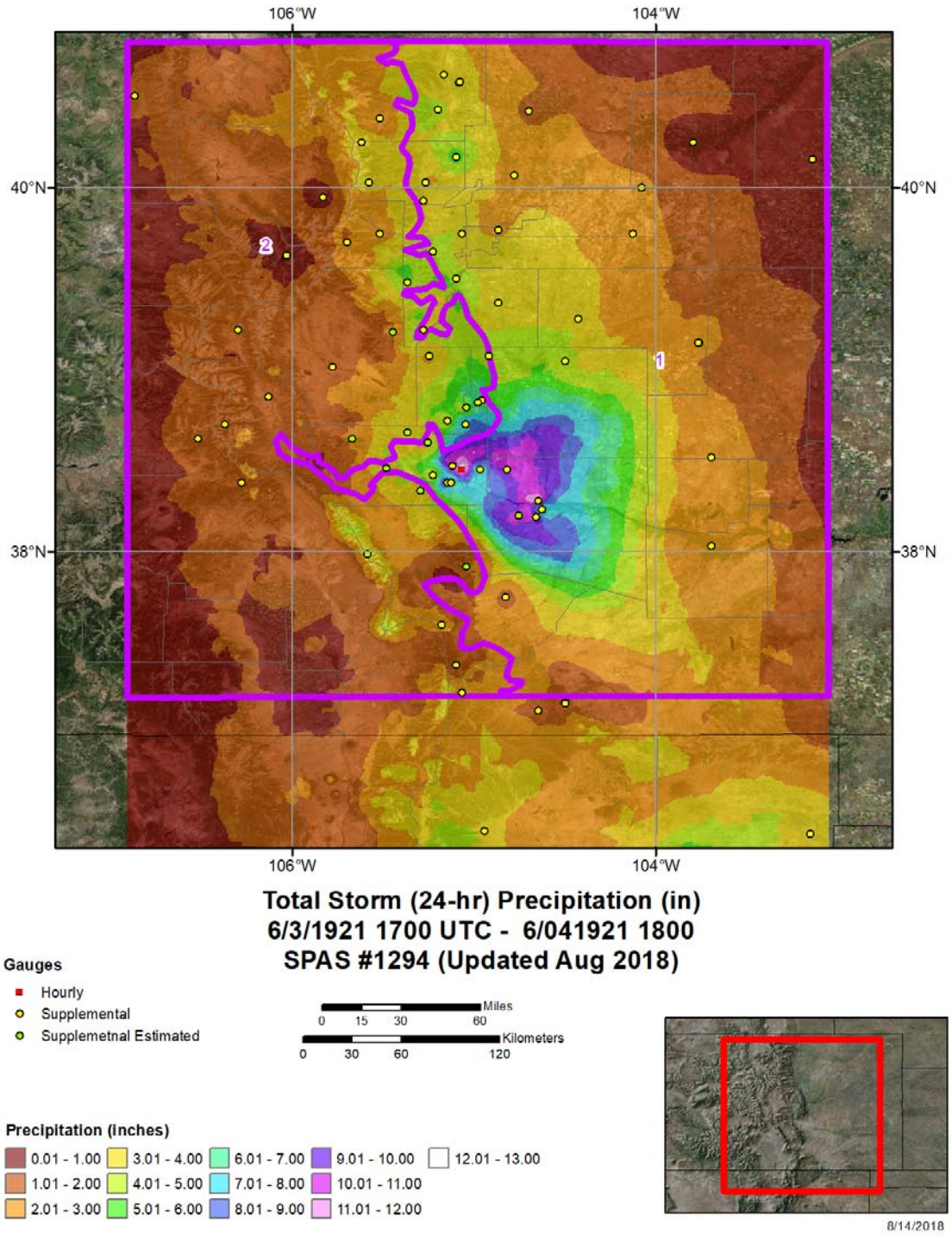

Figure 27: SPAS 1294 total storm isohyetal pattern after adjusting the high elevation spatial patterns

Unfortunately, the WRF reanalysis of the Savageton, WY September 1923 (SPAS 1325); Elbert-Cherry Creek-Genoa-Hale May 1935 (SPAS 1295); Opal, WY August 1990 (SPAS 1264); and Virsylvia, NM August 1922 storms showed little skill in being able to replicate either the spatial pattern or magnitude of the storm. Therefore, the WRF reanalysis results were not used in the SPAS analysis of these storms. Appendix L provides the results of the WRF analyses for each storm evaluated.

7. Storm Adjustments

7.1 In-Place Maximization Process

Maximization was accomplished by increasing surface dew points (or sea surface temperatures when the storm representative location is over the ocean) to a climatological maximum and calculating the enhanced rainfall amounts that could potentially be produced if the climatological maximum moisture had been available during the observed storm period. Additionally, the climatological maximum dew point for a date two weeks towards the season is selected with higher amounts of moisture from the date that the storm actually occurred. This procedure assumes that the storm could have occurred with the same storm dynamics two weeks towards the time in the year when maximum dew points occur. This assumption follows HMR guidance and is consistent with procedures used to develop PMP values in all the current HMR documents (e.g., HMR 55A Section 5.3), the WMO manual (WMO 2009), as well as in all prior AWA PMP studies. The storm data Appendix F provides the individual analysis maps used for each storm adjustment process including the HYSPLIT model output, the surface dew point observations or sea surface temperature (SST) observations, the storm center location, the storm representative location, and the IMPF for each storm.

Each storm used for PMP development was thoroughly reviewed by the PRB to confirm that reasonableness of the storm representative value and location used. As part of this process, AWA provided all the information used to derive the storm representative value for review, including the following:

- Hourly surface dew point observations
- Daily SST observations
- HYSPLIT model output
- Storm adjustment spreadsheets
- Storm adjustments maps with data plotted

These data sets allowed the PRB to conduct an independent review of each storm. Results of this analysis demonstrated that the values AWA utilized to adjust each storm was reasonable for PMP development.

For storm maximization, average dew point values for the appropriate duration that are most representative of the actual rainfall accumulation period for an individual storm (e.g., 6-, 12-, or 24-hour) are used to determine the storm representative dew

point. This value (either dew point or SST) is then maximized using the appropriate climatological value representing the 100-year return interval at the same location moved two weeks towards the season of higher climatological maximum values.

The HYSPLIT model (Stein et al., 2015 and Rolph et al., 2017) provides detailed and reproducible analyses for assisting in the determination of the upwind trajectories of atmospheric moisture that was advected into the storm systems. Using these model trajectories, along with an analysis of the general synoptic weather patterns and available surface dew point temperature data, the moisture source region for candidate storms is determined. The procedure is followed to determine the storm representative location and is similar to the approach used in the HMRs. However, by utilizing the HYSPLIT model, much of the subjectivity found in the HMR analysis process was corrected. Further, details of each evaluation can be explicitly provided, and the HYSPLIT trajectory results based on the input parameters defined are reproducible. Available HYSPLIT model results are provided as part of Appendix F.

The process results in a ratio of observed moisture versus climatological maximum moisture. Therefore, this value is always 1 or greater. In addition, the intent of the process is to produce a hypothetical storm event that represents the upper limit of rainfall that a given storm could have produced with the perfect combination of moisture and maximum storm efficiency (atmospheric processes that convert moisture to precipitation) associated with that storm. This assumes that the storm efficiency processes remain constant as more moisture is added to the storm environment. Therefore, an upper limit of 1.50 (50 percent) is applied to the IPMF with the assumption that increases beyond this amount would change the storm efficiency processes and the storm would no longer be the same storm as observed from an efficiency perspective.

This upper limit is a standard application applied in the HMRs (e.g., HMR 51 Section 3.2.2). HMR 55A “relaxed” this value to 1.70 in orographic regions to account for a lack of data. During this study the 1.50 upper limit was applied in all cases because updated data sets and analysis tools (i.e. HYSPLIT) were available. In addition, investigations from the Dynamical Modeling Task demonstrated that the level when storm efficiency changes as more moisture is added are actually far less than 50 percent for the storms investigated (Mahoney, 2016). Therefore, the use of 1.50 as an upper limit is a conservative application. Table 2 provides the IPMF used for all storms. The 1.50 upper limit was applied to ten of the short list storms.

7.2 Climatological maximum dew point data

HMR and WMO procedures for storm maximization use a representative storm dew point as the parameter to represent available moisture to a storm. Prior to the mid-1980s, maps of maximum 12-hour persisting dew point values from the *Climatic Atlas of the United States* (EDS, 1968) were the source for maximum dew point values. This study uses the 100-year average return interval dew point climatology. Storm precipitation amounts were maximized using the ratio of precipitable water representing the 100-year recurrence interval dew point to precipitable water

representing the dew point associated with the observed storm event, assuming a vertically saturated atmosphere through 30,000 feet. The precipitable water values associated with each storm representative dew point value were determined from the WMO Manual for PMP Annex 1 (1986).

Updated maximum average dew point climatologies used in this study for the storm maximization and adjustment calculations provide 100-year return frequency values for 3-, 6-, 12-, and 24-hour durations. The development of these climatologies and the process to implement these data followed the same reasoning and use as described in the other AWA PMP studies (e.g., Tomlinson, 1993; Tomlinson et al., 2008; Kappel et al., 2013; Kappel et al., 2014; Kappel et al., 2016). These analyses demonstrated that the maximum 12-hour persisting dew point climatology used in HMR 49, HMR 51 and HMR 55A were outdated and more importantly did not adequately represent the atmospheric moisture available in the extreme rainfall storm environments for many of the events and often missed or underestimated the atmospheric moisture available and hence lead to inaccurate maximization calculations. The updated dew point climatologies used in this study more accurately represent the atmospheric moisture associated with a given storm by using maximum average dew point values observed over durations specific to each storm's rainfall duration. The x-hour 100-year recurrence interval dew point values replace the 12-hour persisting dew point values and better represent the intent of the process.

The use of the 100-year x-hour average recurrence interval dew point climatology in the maximization process is appropriate because it provides a sufficiently rare occurrence of moisture levels when combined with the maximum storm efficiency to produce a combination of rainfall producing mechanisms that could physically occur. Use of more rare recurrence intervals was investigated during the Wyoming statewide PMP study (Kappel et al. 2014) and again during this study. In both cases, the review boards agreed with AWA's recommendation that the difference between the 100-year and 1,000-year recurrence values was minimal and the 100-year data best represented the intent of the process and produced the most robust output. The choice to use average recurrence interval and average duration was first determined to be most appropriate during the EPRI Michigan/Wisconsin region PMP study (Section 2-1 and 7, Tomlinson, 1993). That study included original authors of HMR 51 on the review board.

An envelope of maximum dew point values as applied in the development of the 12-hour persisting dew point climatology used in HMR 51 is no longer used because in many cases, the maximum observed dew point values do not represent a meteorological environment that would produce rainfall. Instead these maximum values can represent a local extreme moisture value that is often the result of local evapotranspiration and other factors not associated with a storm environment and saturated atmosphere. Also, the dew point observational data available has changed significantly since the publication of the maximum dew point climatologies used in HMR 51. Hourly dew point observations became standard at all first order NWS weather stations starting in 1948. This has allowed for a sufficient period of record (i.e. 50 years or more) of hourly data to exist from which to develop the climatologies

out to the 100-year average recurrence interval, that were not available during the development of HMR 51.

The final dew point grids used in this project were completed during the previous studies. Details on the development process and data utilized are available in the Arizona statewide report documentation (Kappel et al., 2013), the Wyoming statewide report documentation (Kappel et al., 2014), and the Texas statewide report documentation (Kappel et al., 2016). Appendix D contains the maps used in the development of PMP in this analysis.

7.3 In-Place Maximization Factor (IPMF) Calculation

Storm maximization is quantified by the IPMF using Equation 3.

$$IPMF = \frac{W_{p,max}}{W_{p,rep}} \qquad \text{Equation 3}$$

where,

$W_{p,max}$ = precipitable water for maximum dew point (in.)
$W_{p,rep}$ = precipitable water for representative dew point (in.)

The available precipitable water, Wp, is calculated by determining the precipitable water depth present in the atmospheric column (from sea level to 30,000 feet) and subtracting the precipitable water depth that would not be present in the atmospheric column between sea-level and the surface elevation at the storm location using Equation 4.

$$W_p = W_{p,30,000'} - W_{p,elev} \qquad \text{Equation 4}$$

where,

W_p = precipitable water above the storm location (in.)
$W_{p,30,000'}$ = precipitable water, sea level to 30,000′ elevation (in.)
$W_{p,elev}$ = precipitable water, sea level to storm surface elevation (in.)

7.4 Transposition Zones

PMP-type events in regions of similar meteorological and topographic settings surrounding a location are a very important part of the historical evidence on which a PMP estimate is based. Since most locations have a limited period of record for rainfall data, the number of extreme storms that have been observed over a location is limited. Historic storms that have been observed within similar meteorological and topographic regions are analyzed and adjusted to provide information describing the storm rainfall as if that storm had occurred over the location being studied.

Transfer of a storm from where it occurred to a location that is meteorologically and topographically similar is called transposition. The underlying assumption is that storms transposed to the location could have occurred under similar meteorological

and topographical conditions. To properly relocate such storms, it is necessary to address issues of similarity as they relate to meteorological conditions, moisture availability, and topography. In this study, adjustment factors used in transpositioning of a storm are quantified by using the Geographic Transposition Factor (GTF) and Moisture Transposition Factor (MTF).

The regional transposition zones developed for this study were based on the variable meteorological and topographical characteristics across the domain along with considerations of moisture source region characteristics. National Centers for Environmental Information (formally the National Climatic Data Center) climate regions, USGS physiographic regions, Precipitation Frequency Task precipitation super regions, and adjacent study transposition regions were all investigated to help define the zones.

Figure 28 shows the transposition zones utilized in this study. Note, that the zones were used as a general guidance and for initial evaluations. Storms were ultimately allowed to move between zones and/or were restricted within a given zone for final PMP development.

Transposition zones 1 and 2 represent the eastern plains of Colorado and New Mexico. In these regions topography is generally less important than most of the remainder of the region. These areas also have the most direct access to low-level moisture from the Gulf of Mexico. Transposition zones 3 and 4 represent the highly orographically influenced regions where the High Plains transition to the Rocky Mountains. These areas see some of the most frequent and extreme rainfalls in the entire region because of the preferential access to moisture and increased orographic effects. Transposition zones 5 and 6 represent mountainous regions east of the Continental Divide that do not have direct access to low-level moisture from the Gulf of Mexico because terrain blocks the flow upstream (zones 3 and 4). These regions receive frequent precipitation, often in the form of snow. However, the lack of low-level moisture inflow results in lower relative precipitation amounts. Transposition zones 7 and 8 represent protected inland valleys and are some of the driest regions in the domain analyzed. This is the result of terrain blocking low-level moisture from entering these regions from the east and west. The southern portion of transposition zone 8 (the Rio Grande Valley) is more open to low-level moisture access from the Gulf of Mexico and receives greater amounts of rainfall than the northern sections and the adjacent transposition zone 7. Transposition zone 9 is very similar to zone 5 and 6, except it is located west of the Continental Divide. Therefore, the most important moisture source is the Pacific Ocean. Orographic effects are very important in this region; however moisture availability is very low. This results from storms having to cross several mountain barriers before reaching this region. Transposition zone 9 receives frequent precipitation, but in generally lower intensity and often in the form of snow. In fact, some areas in transposition zone 9 receive the highest mean annual precipitation in the entire study domain. However, much of the precipitation occurs as snowfall. Transposition zones 10-15 represent Basin and Range and Colorado Plateau regions west of the Rocky Mountains in western Colorado and New Mexico. In these regions, a strong seasonality of precipitation occurs, with general storms

common from fall through spring, and the NAM system dominating in summer. General storms in the region originate from the Pacific Ocean and therefore are significantly altered before reaching the area. Precipitation from this storm type is generally less than local and/or tropical storms in these areas. Moisture for local and tropical storms originates from the Gulf of California and/or local recycled moisture. Therefore, there is an increase in frequency and intensity for locations to the south versus the northern areas, especially with the tropical storm type. Finally, transposition zone 16 represents the Uintah and Wind River Ranges in northeastern Utah and southwestern Wyoming. The weather patterns and seasonality are similar to transposition zone 9.

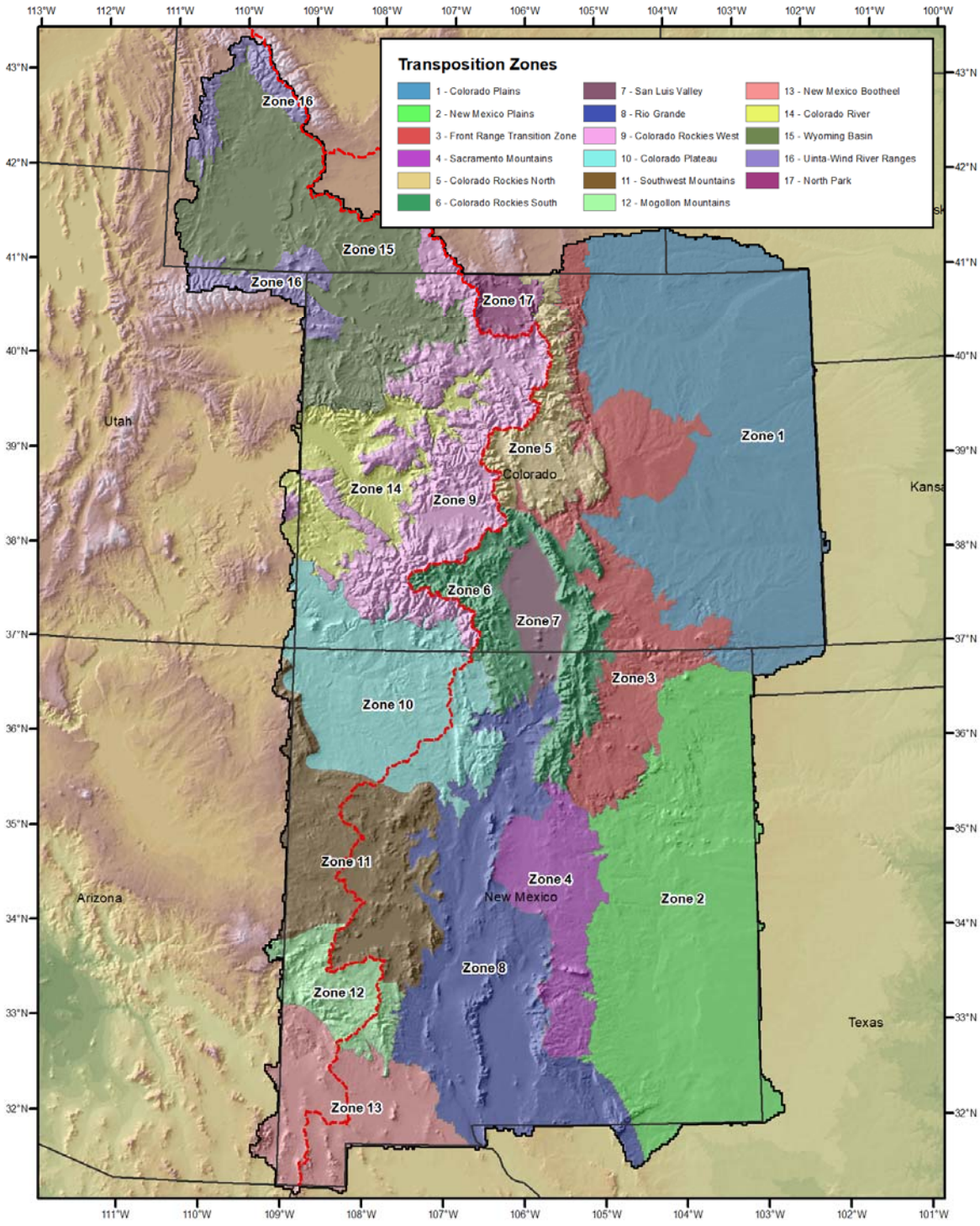

Figure 28: Transposition zones utilized for CO-NM REPS

Initial transposition limits were assigned with the understanding that additional refinements would take place as the data were run through the PMP evaluation process. Numerous sensitivity runs were performed using the PMP database to investigate the results based on the initial transposition limits. Several storms were

re-evaluated based on the results that showed inconsistencies and/or unreasonable values either too high or too low. Examples of inconsistencies and unreasonable values include areas where gradients of PMP depths between adjacent grid points that were significantly different and not specifically related to a similar meteorological or topographical change. When these occur because of excessive GTF and/or MTF values or because a storm was likely moved beyond reasonable transposition limits, adjustments are applied.

Although somewhat subjective, decisions to adjust the transposition limits for a storm were based on the understanding of the meteorology which resulted in the storm event, similarity of topography between the two locations, access to moisture source, seasonality of occurrence, and comparison to other similar storm events. Appendix I provides a description of the iterations and adjustments that were applied during each PMP version to arrive at the final values via the PMP Version Log.

For all storms, the IPMF does not change during this process. The MTF and GTF change as a storm is moved from its original location to a new location. Further, because the MTF represents the horizontal difference in available moisture between the original location and the new location (i.e. no elevation difference component is applied when used with the GTF), this factor does not vary as much as the GTF across the region. Generally, most MTFs result in less than a +/-10 percent change. Therefore, the largest contributing factor to the variation of PMP over a specific area in the transposition process is the GTF. This is to be expected, as the topography across the region varies significantly in elevation, aspect and slope, often over very short distances.

The spatial variations in the GTF were useful in making decisions on transposition limits for many storms. As described previously, values larger than 1.50 for a storm's maximization factor exceed limits that would no longer produce the same storm as the originally observed event. In these situations, changing a storm by this amount is likely also changing the original storm characteristics so that it can no longer be considered the same storm at the new location. The same concept applies to the GTF. GTF values greater than 1.50 indicate that transposition limits have most likely been exceeded. In addition, a lower limit of 0.50 was applied for the same reason, but this inherently affects a much more limited set of storms and regions. Therefore, storms were re-evaluated for transpositionability in regions which results in a GTF greater than 1.50. At high elevation locations where there was a relative lack of extreme rainfall observations, storms were considered transpositionable even if the GTF exceeded the 1.50 values (although the cap of 1.50 was applied) to ensure that enough storm data were available from which to derive adequate information.

The transposition process is one of the most important aspects of PMP development. This step also contains significant subjectivity as the processes utilized to define transposition limits are difficult to quantify. General guidelines are provided in the HMRs (e.g., HMR 51 Section 2.4.1 and HMR 55A Section 8.2). AWA utilized these guidelines as well as updated procedures and data sets developed during the many

PMP studies completed in the region since the HMRs were published. General AWA guidelines included:

- Investigation of previous NWS transposition limit maps
- Experience and understanding of extreme rainfall processes in the study region and how those factors vary by location, storm type, and season
- Understanding of topographical interactions and how those effect storms by location, storm type, and season
- Previously applied transposition limits from adjacent statewide PMP studies
- Limiting transposition to east or west of the Continental Divide
- Use of GTF and MTF values as sensitivity
- Spatial continuity of PMP depths
- Comparisons against NOAA Atlas 14 precipitation frequency climatology
- Information from CO-NM REPS Precipitation Frequency Task precipitation frequency data and annual exceedance probability
- Information from the Dynamical Modeling Task HRRR model output and WRF reanalysis
- Discussions with PRB and Project Sponsors

An important aspect of this study was the involvement of the PRB in evaluating and reviewing individual storm transposition limits. The PRB had initial input in helping to define the overall transposition zones used in the study shown in Figure 28. Once initial transposition limits were applied to each storm, the resulting GTF values were reviewed with the PRB during Workshop #5. Additional discussions regarding transposition limits took place between Workshop #5 and Workshop #6 and after Workshop #6. These were most focused on the controlling storms. Section 5.3 provides an example of the extensive evaluations utilized to determine transposition limits of important storms. The PMP Version Log provided in Appendix I provides the numerous iterations of PMP development and the various transposition limit adjustments that were applied to storms during the PMP development process. In some cases, storms originally considered for a given location were removed after evaluation and in other cases transposition limits were adjusted within a given transposition zone. Table 4 provides the transposition limits that were applied to each storm. In addition, the red hatch area on MTF maps and GTF maps contained in Appendix B and Appendix C, respectively, indicate the final transposition limits applied to each storm.

Table 4: Short storm list

NAME	STATE	LAT	LON	YEAR	MONTH	DAY	ELEVATION (ft)	PMP STORM TYPE	TRANSPOSITION LIMITS
WARD DISTRICT	CO	39.804	-105.329	1894	5	29	8,336	General	Zone 5, 17
LAKE MORAINE	CO	38.804	-104.946	1894	5	30	10,380	General	Zone 5, 6, 17
RATTLESNAKE	ID	43.673	-115.744	1909	11	18	3,297	General	Zone 9, 14, 15, 16, GTF cap of 1.20, MTF cap of 1.0
WAGON WHEEL	CO	37.663	-106.938	1911	10	3	12,500	Tropical	Zone 9, 14 (South of 38.5°N), 10 (north of 37°N)
TAJIQUE 1 to 120h	NM	34.746	-106.413	1915	7	19	8,280	General	Zone (4, 8) > 5,000'; Zone (11, 12) East of Divide; Zone 6 South of 37°N; Zone 13
TAJIQUE 121 to 264h	NM	33.733	-106.968	1915	7	19	4,640	General	Zone 3 (S of 37°), 4, 7, 8, 11, 12, 13, (6 & 9 Southern San Juans - Custom Limits)
MOGOLLON RIM	AZ	33.904	-111.413	1916	1	14	6,668	General	Zone 12, Zone 11 above 5,000'
CIBOLA NF	NM	35.113	-108.196	1916	1	14	8,720	General	Zone 11, Zone 13 above 5,000'
SANTA CATALINA	AZ	32.429	-110.813	1916	1	14	7,863	General	Zone 12, Zone 13
PENROSE	CO	38.464	-105.070	1921	6	2	5,400	HYBRID (G/L)	Zone 3 (<7,500' west of -104.75°)
ADELAIDE	CO	38.630	-104.962	1921	6	2	8,465	HYBRID (G/L)	Zone 3 (above 7,500 feet), Zone 5, 6, 17
VIRSYLVIA (CERRO)	NM	36.804	-105.604	1922	8	17	7,621	Local	Zone 4, 6, 7, 8, (10, 11, 12, 13 east of Divide)
SAVAGETON	WY	43.846	-105.804	1923	9	27	5,056	General	Zone (1 and 3) north of 41°N, MTF cap of 1.0
HUNTERS	WY	44.421	-107.029	1923	9	27	9,330	General	Zone 3 (north of 40°N), 5, 17, MTF cap of 1.0
PALISADE LAKE	CO	37.454	-107.253	1927	6	26	8,211	General	Zone 6 west of 106°W, Zone 9
ELBERT CHERRY CREEK	CO	39.238	-104.488	1935	5	30	6,800	Local	Zone 3
GENOA	CO	39.329	-103.538	1935	5	30	5,560	Local	Zone 1, 2, Zone 3 (<7,500' west of -104.75°)
HALE	CO	39.613	-102.263	1935	5	30	3,700	Local	Zone 1,2
LAS CRUCES	NM	32.304	-106.796	1935	8	30	3,890	Local	Zone 8, 12, 13
SMITH RANCH	CO	40.479	-105.229	1938	8	30	5,471	General	Zone 3 (above 7,500' and west of -104.85°), Zone 5, Zone 6 (east of 105.875°)
MASONVILLE	CO	40.454	-105.196	1938	9	10	5,392	Local	Zone 3, 5
PRAIRIEVIEW	NM	33.138	-103.079	1941	5	20	3,805	General	Zone 2, 4, 8
MCCOLLEUM RANCH	NM	32.146	-104.746	1941	9	20	5,840	General	Zone (1, 2, 3, 4, 5, 8, 12, 13), above storm center -1,000', South of Arkansas Rivver
GOLDEN	CO	39.788	-105.288	1948	6	7	7,109	Local	Zone 3, 5
CONWAY	TX	35.221	-101.396	1951	5	13	3,450	HYBRID (G/L)	Zone (1, 2) +/- 1,000' from storm center
BRADSHAW CITY	AZ	34.204	-112.354	1951	8	26	6,222	Tropical	Zone 9, 10, 11, 12, 13, 14 (South of 38.5° N)
LAKE MALOYA	NM	37.009	-104.341	1955	5	19	7,954	General	Zone 5 (GTF > 0.7), Zone 3 and 6 (east of 105.875°)
SAN LUIS	CO	37.179	-105.413	1957	8	12	8,017	Local	Zone 4, 6, 7, 8, (10, 11, 12 east of Divide)
MORGAN	UT	41.079	-111.654	1958	8	16	7,311	Local	Zone 14, 15
PYRAMID	CO	40.540	-106.721	1961	9	20	9,843	General	Zone 14 above 5,000', Zone 9, 15, 16, 17
GIBSON DAM	MT	48.354	-113.371	1964	6	6	8,000	General	Zone 3 north of Palmer Divide
PLUM CREEK	CO	39.221	-104.896	1965	6	15	7,007	HYBRID (G/L)	Zone 1 above 5,000', Zone 3 (<7,500' west of -104.75°)
RATON	NM	36.754	-104.538	1965	6	16	6,200	HYBRID (G/L)	Zone 1 above 5,000', Zone 3 (<7,500' west of -104.75°)
ELBERT	CO	39.188	-104.296	1965	6	16	6,207	HYBRID (G/L)	Zone 1 above 5,000', Zone 3 (<7,500' west of -104.75°)
HOLLY	CO	37.713	-102.404	1965	6	16	4,100	Local	Zone 1, Zone 2 above 3000 feet
CARLSBAD	NM	32.254	-104.613	1966	8	22	4,360	HYBRID (G/L)	Zone (2, 4, 8, 13) +/- 1,000' from storm center
JUNIPINE	AZ	34.979	-111.771	1966	12	4	6,710	General	Zone 11, Zone 12, Zone 13 above 5,000'
PASTORA PEAK	AZ	36.821	-109.188	1966	12	4	8,189	General	Zone 10 , 11
GRANTS	NM	35.188	-107.754	1967	9	8	7,654	Local	Zone 4, 6, 7, 8, (10, 11, 12 east of Divide)
BLANDING	UT	37.826	-109.543	1968	8	1	10,367	Local	Zone 10, 11, 12, 14
BIG ELK MEADOW	CO	40.267	-105.417	1969	5	4	7,667	General	Zone 3 (above 7,500' and west of -104.85°), Zone 5, Zone 6 (east of 105.875°)

Table 4 (continued): Short storm list

NAME	STATE	LAT	LON	YEAR	MONTH	DAY	ELEVATION (ft)	PMP STORM TYPE	LIMITS
BAYFIELD	CO	37.304	-107.413	1970	9	3	8,950	Tropical	Zone 9, 10, 11, 14 (South of 38.5° N)
MT LEMMON	AZ	32.411	-110.721	1970	9	4	8,080	Tropical	Zone 9, 10, 11, 12, 13, 14 (South of 38.5° N)
WORKMAN CREEK	AZ	33.820	-110.904	1970	9	4	7,250	Tropical	Zone 9, 10, 11, 12, 13, 14 (South of 38.5° N)
INDIAN WELLS	AZ	35.495	-110.421	1970	9	4	5,710	Tropical	Zone 9, 10, 11, 12, 14 (South of 38.5° N)
JOANNE	AZ	33.821	-110.921	1972	10	4	7,140	Tropical	Zone 9, 10, 11, 12, 13, 14 (South of 38.5° N)
SWEETWATER	CO	39.721	-107.038	1976	7	13	6,278	Local	Zone 14, 15
BIG THOMPSON CANYON	CO	40.479	-105.429	1976	7	31	8,133	Local	Zone 3 (North of 39° and West of -105°), Zone 5, 17
PENA BLANCA	NM	35.596	-106.429	1977	7	8	5,986	Local	Zone 4, 6, 7, 8, (10, 11, 12 east of Divide)
NOGALES	AZ	31.339	-110.935	1977	10	6	3,924	Tropical	Zone 13
BEAR SPRING	AZ	34.038	-111.488	1978	2	27	7,000	General	Zone 11, Zone 12, Zone 13 above 5,000'
WHITE SANDS	NM	32.387	-106.529	1978	8	19	4,604	Local	Zone (8, 12, 13) -1,000' elevation constraint
CONRAD RANCH	UT	40.585	-111.590	1979	10	18	9,712	General	Zone 9, 14, 15, 16
ROCK SPRINGS	AZ	34.013	-112.263	1980	2	13	2,892	General	Zone 13 below 5,000'
CROWN KING	AZ	34.221	-112.346	1980	2	13	6,445	General	Zone 11, Zone 12, Zone 13 above 5,000'
BELEN	NM	34.654	-106.821	1980	6	9	5,181	Local	Zone 4, 6, 7, 8, (10, 11, 12 east of Divide)
FRIJOLE CREEK	CO	37.096	-104.379	1981	7	3	5,728	Local	Zone 3
CLYDE	TX	32.479	-99.479	1981	10	10	2,000	Tropical	Zone 1, 2, 3, 4, 6, 7, 8 (south of 38.5°N)
MT TIMPANOGOS	UT	40.404	-111.638	1982	9	26	10,555	General	Zone 9, 14, 15, 16
FLAT TOP MOUNTAIN	UT	40.379	-112.204	1982	9	26	9,062	General	Zone 9, 14, 15, 16
COTTONWOOD	UT	41.604	-112.012	1982	9	26	7,056	General	Zone 9, 14, 15, 16
PRESCOTT	AZ	34.621	-112.554	1983	9	23	5,808	Local	Zone 12, 13
ALTAR	MX	30.646	-111.771	1983	9	27	2,770	Tropical	Zone 12, 13
MT GRAHAM	AZ	33.288	-109.104	1983	9	27	6,371	Tropical	Zone 9, 10, 11, 12, 13, 14 (South of 38.5° N)
ALBUQUERQUE	NM	35.096	-106.479	1988	7	9	6,303	Local	Zone 4, 6, 7, 8, (10, 11, 12 east of Divide)
OPAL	WY	41.738	-110.246	1990	8	16	6,924	Local	Zone 14 (except for San Miguel/Dolores river drainage), 15
KNOLES HOLE SPRING	AZ	33.829	-110.913	1993	1	5	7,395	General	Zone 11, Zone 12, Zone 13 above 5,000'
SPENCER CANYON	AZ	32.413	-110.746	1993	1	5	7,965	General	Zone 13
WOLF CREEK	CO	37.463	-106.721	1993	8	27	10,382	General	Zone 6 west of 106°W, Zone 9
COTOPAXI	CO	38.455	-105.595	1996	8	1	7,652	Local	Zone 3, 5, 6, 17
TUCSON	AZ	32.390	-110.800	1996	9	3	5,750	Local	Zone 13
RUXTON PARK	CO	38.855	-104.965	1997	6	6	9,009	HYBRID (G/L)	Zone 5, 6
FORT COLLINS	CO	40.548	-105.133	1997	7	28	5,135	HYBRID (G/L)	Zone 1 above 5,000', Zone 3 (<7,500' west of -104.75°)
PAWNEE CREEK	CO	40.775	-103.625	1997	7	29	4,500	Local	Zone 1
JOSEPH CITY	AZ	34.945	-110.355	1998	7	31	5,000	Local	Zone 10, 11, 12, 13
SABINO CANYON	AZ	32.385	-110.705	1999	7	14	6,800	Local	Zone 12, 13
SAGUACHE	CO	38.215	-106.295	1999	7	25	8,900	Local	Zone 5, 6, 17
DALLAS CREEK	CO	38.095	-107.915	1999	7	31	9,018	Local	Zone 9, 14, 15, 16

Table 4 (continued): Short storm list

NAME	STATE	LAT	LON	YEAR	MONTH	DAY	ELEVATION (ft)	PMP STORM TYPE	LIMITS
PLACERVILLE	CO	38.005	-107.955	2001	8	8	10,600	Local	Zone 9, 14, 15, 16
BLUFF	UT	37.255	-109.575	2001	8	14	4,907	Local	Zone 10, 11, 14
OGALLALA	NE	41.125	-101.717	2002	7	6	3,215	Local	Zone 1
COLLBRAN	CO	39.285	-107.895	2003	8	15	7,694	Local	Zone 9, 14, 15, 16
ROOSEVELT LAKE	AZ	33.596	-111.065	2003	9	6	2,700	Local	Zone 11, 12
JAVIER	AZ	34.730	-113.020	2004	9	18	5,600	Tropical	Zone 9, 10, 11, 12, 13, 14 (South of 38.5° N)
CEDAR CITY	UT	37.375	-113.075	2006	7	31	8,000	Local	Zone 10, 11, 12, 14
EL PASO	TX	31.935	-106.515	2006	8	1	4,818	Local	Zone 8, 12, 13
SAN LUIS VALLEY	CO	37.525	-105.945	2007	7	19	7,562	Local	Zone 7, 8
PETRIFIED FOREST	AZ	34.725	-109.645	2007	7	27	5,500	Local	Zone 10, 11, 12, 13
COOKS MESA	AZ	34.460	-111.230	2007	11	30	7,472	General	Zone 12, Zone 11 above 5,000'
MARSHALL SADDLE	AZ	32.440	-110.780	2007	11	30	8,834	General	Zone 12, Zone 13
MT HOPE	CO	37.540	-106.870	2007	11	30	12,055	General	Zone 9 & Zone 14 south of 39.5°N, Zone 10 within DAD Zone 4, Zone 6
SUNSPOT	NM	33.335	-105.795	2008	7	26	9,339	Tropical	Zone 1, 2, 3, 4, 6, 7, 8 (south of 38.5°N)
HAVASUPAI	AZ	35.155	-112.575	2008	8	15	4,900	Local	Zone 10, 11, 12
PETERSON RANCH	AZ	33.810	-110.910	2010	1	19	7,450	General	Zone 10, Zone 11, Zone 12, Zone 13 above 5,000'
SANTA RITA EXP RANGE	AZ	31.760	-110.840	2010	1	19	4,576	General	Zone 12 below 5,000', Zone 13
SPEARMAN	TX	36.135	-101.495	2010	6	13	3,263	Local	Zone 1 and 2 (with +/-1,000' elevation constraint)
ANDREW NYMAN MOUNTAIN	UT	42.050	-111.620	2010	10	25	8,290	General	Zone 9, 14, 15, 16
DEER CREEK DAM	UT	41.360	-111.910	2010	10	25	5,756	General	Zone 9, 14, 15, 16
ALTA	UT	40.590	-111.640	2010	10	25	8,680	General	Zone 9, 14, 15, 16
BOULDER	CO	40.015	-105.265	2013	9	8	5,308	General	Zone (1, 3) > 5,000'
CHEYENNE MOUNTAIN	CO	38.745	-104.865	2013	9	8	9,323	General	Zone 3 (above 7,500' and west of -104.85°), Zone 5, Zone 6 (east of 105.875°)
AURORA	CO	39.705	-104.835	2013	9	8	5,573	General	Zone 1, 3
COAL CREEK	CO	39.865	-105.285	2013	9	8	7,333	General	Zone 3 (> 7,500'), 5, 6, 17
GUADALUPE PASS	TX	32.035	-104.555	2013	9	10	3,986	General	Zone 1, 2, 4, 8 (orographic portion of SE region), (Zone 3 < 7,500')
SUMNER LAKE	NM	34.595	-104.475	2013	9	10	4,284	General	Zone (1, 2, 3, 5) < 7,500'
CHAPARRAL	NM	32.145	-105.995	2013	9	10	4,718	General	Zone 4, 8, 13
GAIL	TX	32.725	-101.405	2014	9	21	2,575	Local	Zone 2, 4, 8 (with +/-1,000' elevation constraint)
THE BOWL	TX	31.935	-104.825	2014	9	21	8,008	Tropical	Zone 1, 2, 3, 4, 6, 7, 8, 11, 12, 13 (south of 38.5°N)
TAHOKA	TX	33.105	-101.825	2015	5	5	3,002	Local	Zone 2 (with +/-1,000' elevation constraint)

7.5 Moisture Transposition Factor

The MTF was developed to represent the difference in available moisture from a 100-year recurrence interval climatological perspective between two locations. This was done assuming that the precipitation frequency climatologies used in this study do not necessarily quantify this difference. Numerous discussions have occurred during previous studies and again during this study with the PRB to try and quantify moisture differences. As with previous studies, no definitive answer developed. Therefore to account for the unknown in this process versus how much of the climatological moisture differences are already represented in the precipitation frequency climatologies the decision was made to set a lower limit of 1.00 to the MTF. This decision was made after extensive discussions between the PRB, Project Sponsors, and AWA. In addition, the MTF for the SPAS 1274 Rattlesnake, ID November 1909 and SPAS 1211 Gibson Dam, MT June 1964 storm were held to 1.00. This was done to adjust the significant increase this factor produced because the storms were moved over such a great distance and this factor was inappropriately increasing the storm beyond reasonable limits.

Further information from the PRB perspective can be found in the PRB Review Summary. Appendix B provides the MTF maps for each storm with the lower limitation of 1.00 applied.

Moisture, in the form of precipitable water depths, was determined by extracting the dew point temperatures at each storm representative location and each representative target grid point location. ArcGIS was used to shift the storm center and target grid point locations upwind according to each storm's inflow vector. The monthly dew point temperature was extracted at each representative point for two bounding months and temporally interpolated based on the storm's temporal transposition date. The extracted dew point temperatures were rounded to the nearest ½° Fahrenheit and converted to precipitable water using a lookup table derived from HMR 55A Appendix C (Hansen et al., 1988 p241-242).

Four of the short list storm events (Junipine, AZ December 1966; Peterson Ranch, AZ January 2010; Rattlesnake, ID November 1909; and Nogales, AZ October 1977) have storm representative locations over the ocean. For these cases, a +2σ SST climatology was used as a surrogate for the dew point climatology. These data are downloaded from the ICOADS data server. ICOADS data provided by the NOAA/OAR/ESRL PSD, Boulder, Colorado, USA, from their Web site at https://www.esrl.noaa.gov/psd/.

7.6 Moisture Transposition Factor (MTF) Calculation

The MTF is calculated as the ratio of precipitable water for the maximum dew point at the target location to precipitable water for the storm maximum dew point at the storm center location as described in Equation 5. This MTF represents the change in climatological maximum moisture availability between two locations due to horizontal distance. The change due to vertical displacement is quantified inherently within the

GTF, described in the next section. Elevation is not considered in the MTF calculation; therefore, the precipitable water depth is calculated for the entire atmospheric column, from sea level to 30,000 feet[1].

$$MTF = \frac{W_{p,trans}\,(30{,}000')}{W_{p,\max(30{,}000')}} \qquad \text{Equation 5}$$

where,

$W_{p,trans(30,000')}$ = maximum precipitable water, sea level to 30,000′ elevation, target moisture inflow source location (in.)

$W_{p,max\ (30,000')}$ = maximum precipitable water, sea level to 30,000′ elevation, storm representative moisture source location (in.)

7.7 Geographic Transposition Factor

The GTF process is used to not only capture the difference in terrain effects between two locations but also to capture all processes that result in precipitation reaching the ground at one location versus another location. The GTF is a mathematical representation of the ratio of the precipitation frequency climatology at one location versus another location. The precipitation frequency climatology is derived from actual precipitation events that resulted in the Annual Maximum Series (AMS) at a given station. An upper limit of 1.50 and a lower limit of 0.50 were applied to the GTF as described in Section 7.3. This was done to ensure the storm being adjusted was not adjusted beyond limits, which would change the original storm characteristics in a manner that would violate the PMP process assumptions.

The GTF values were calculated utilizing NOAA Atlas 14 data and the precipitation frequency climatologies developed during the Wyoming and Texas statewide PMP studies (Kappel et al., 2014, Kappel et al., 2016). These data sets were used to ensure consistency in the climatological datasets and to ensure required coverage for all storm locations within the overall storm search domain. The precipitation frequency data derived, as part of CO-NM REPS Precipitation Frequency Task did not provide the overall coverage needed to provide calculations for all storm center locations outside of the study domain and therefore was not used for the GTF process.

The storms used in NOAA Atlas 14 represent observed precipitation events that resulted in an Annual Maximum Series (AMS) accumulation. Therefore, they represent all precipitation producing process that occurred during a given storm event. In HMR terms, the resulting observed precipitation represents both the convergence-only component and any orographic component. The NOAA Atlas 14 gridded precipitation frequency climatology was produced using gridded mean annual maxima (MAM) grids that were developed with the PRISM (Daly et al., 1994). PRISM utilizes geographic information such as elevation, slope, aspect, distance from coast, and terrain weighting for weighting station data at each grid location. The use of the precipitation frequency climatology grids should be reflective of all precipitation producing processes. Further, the use of the gridded precipitation climatology at the

[1] The precipitable water values are taken from Annex I. Tables of precipitable water in saturated pseudo-adiabatic atmosphere (WMO, 2009)

100-year recurrence interval represents an optimal combination of factors, including representing extreme precipitation events equivalent to the level of rainfall utilized in AWA's storm selection process, and providing the most robust statistics given the period of record used in the development of the precipitation frequency climatologies.

Therefore, the GTF does not just represent the difference in topographic effects between two locations, but instead represents the difference in all precipitation processes between two locations. This is one reason it is very important to apply appropriate transposition limits to each storm during the PMP development process.

There are many orographic processes and interactions related to terrain interactions that are not well understood or quantified. Therefore, observed data (precipitation accumulations represented in the precipitation frequency data) are used as a proxy, where it is assumed that the observed precipitation represents all the precipitation processes associated with a storm event. Again, this follows guidance provided by the WMO 2009, Section 3.1.4 and discussed in Section 2.3 of this document. Given this, it seems logical that observed precipitation at a given location represents a combination of all factors that produced the precipitation, including what would have occurred without any terrain influence and what actually occurred because of the terrain influence (if any). Significant judgment is inherent when determining transposition regions because the process of determining similar meteorology and topography is highly subjective.

As part of the GTF process the following assumptions are applied:

- NOAA Atlas 14 and other precipitation frequency climatology represent all precipitation producing factors that have occurred at a location. This is based on the fact that the data are derived from AMS values at individual stations that were the result of an actual storm event. That actual storm event included both the amount of precipitation that would have occurred without topography and the amount of precipitation that occurred because of topography (if any).
- If it is accepted that the precipitation frequency climatology is representative of all precipitation producing processes for a given location, then comparing the precipitation frequency climatology at one point to another will produce a ratio that shows how much more or less efficient the precipitation producing processes are between the two locations. This ratio is called the GTF.
- If there is no orographic influence at either location being compared or between the two locations, then the differences should be a function of (1) storm precipitation producing processes in the absence of topography (thermodynamic and dynamic), (2) how much more or less moisture is available from a climatological perspective, and/or (3) elevation differences at the location.

7.8 HRRR Model Output Used to Convert Precipitation Frequency Data to Rain (for use in GTF calculations)

High Resolution Rapid Refresh (HRRR) model output provided by the CO-NM REPS Dynamical Modeling Task provided a significant advancement in the PMP development process during this study. One aspect where the HRRR data proved extremely valuable was in the adjustment of the precipitation frequency climatologies to represent rainfall only values. This was required because the annual maximum accumulation values at individual stations across high elevation regions of the study domain are highly influenced by snowfall. Comparisons were made at six high-elevation locations (Tower, Joe Wright, Independence Pass, Silver Creek Divide, Hopewell, and Gallegos Peak) that included frequency analyses of six SNOTEL stations using both annual maximum data for rainfall and precipitation (Figure 29). The six sites rainfall AMS all occurred between May and September (Figures 30-35). Site-specific L-moment analysis results confirm precipitation frequency climatologies in high-elevation regions are influenced by snowfall with an average 100-year ratio of rain to snow of 0.73. Figures 36-41 show the at-site 24-hour frequency analysis for rainfall and snowfall for 1-year through 1000-year frequencies. Therefore, the precipitation frequency climatologies in these locations are influenced by data that are not representative of the PMP being developed (snow versus rain).

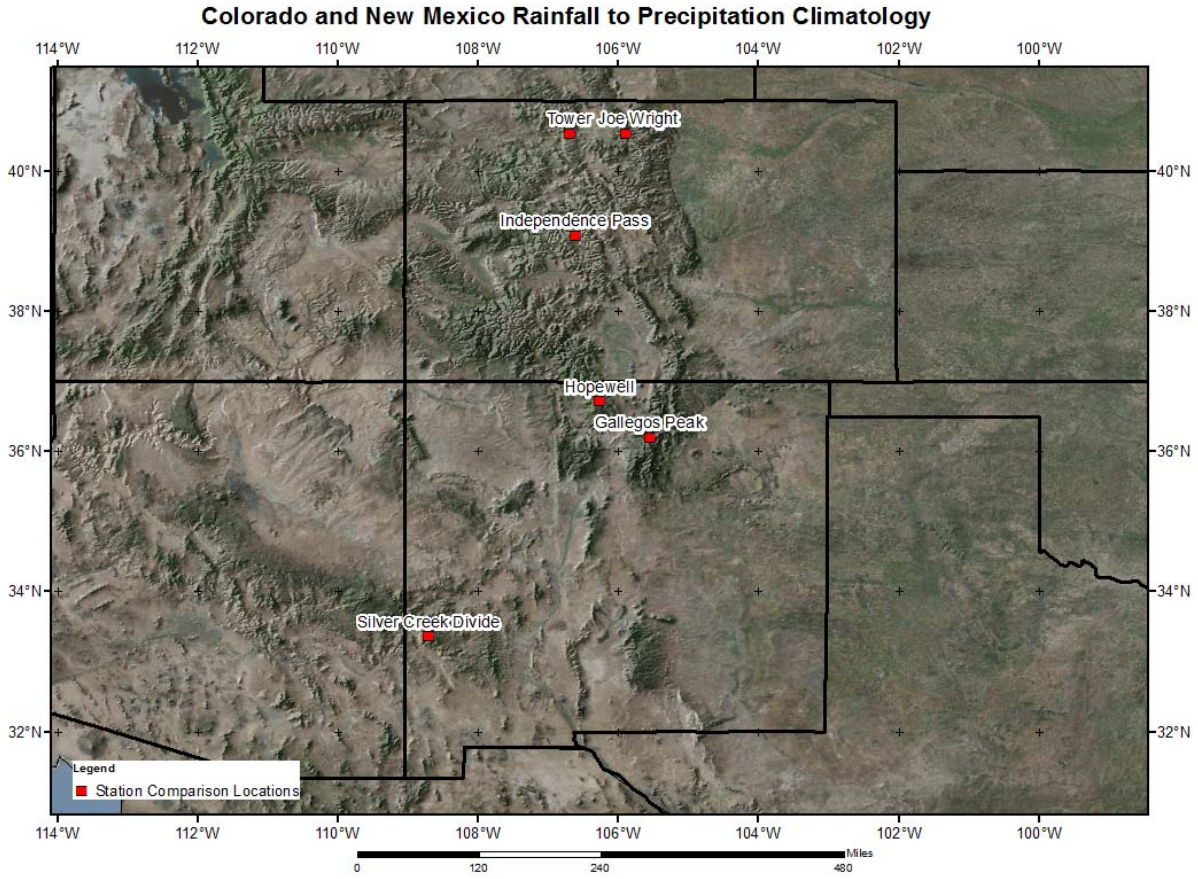

Figure 29: Six stations used to investigate rainfall only versus precipitation frequency

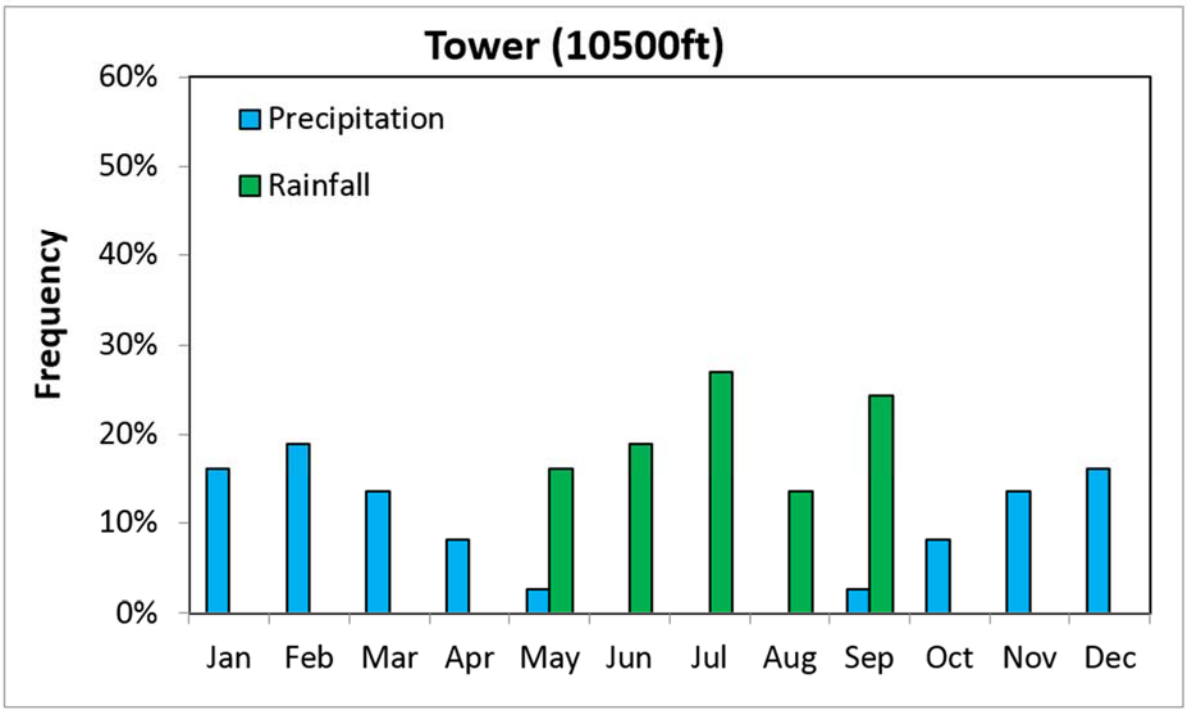

Figure 30: Annual maximum series for rainfall and precipitation at Tower, CO SNOTEL site.

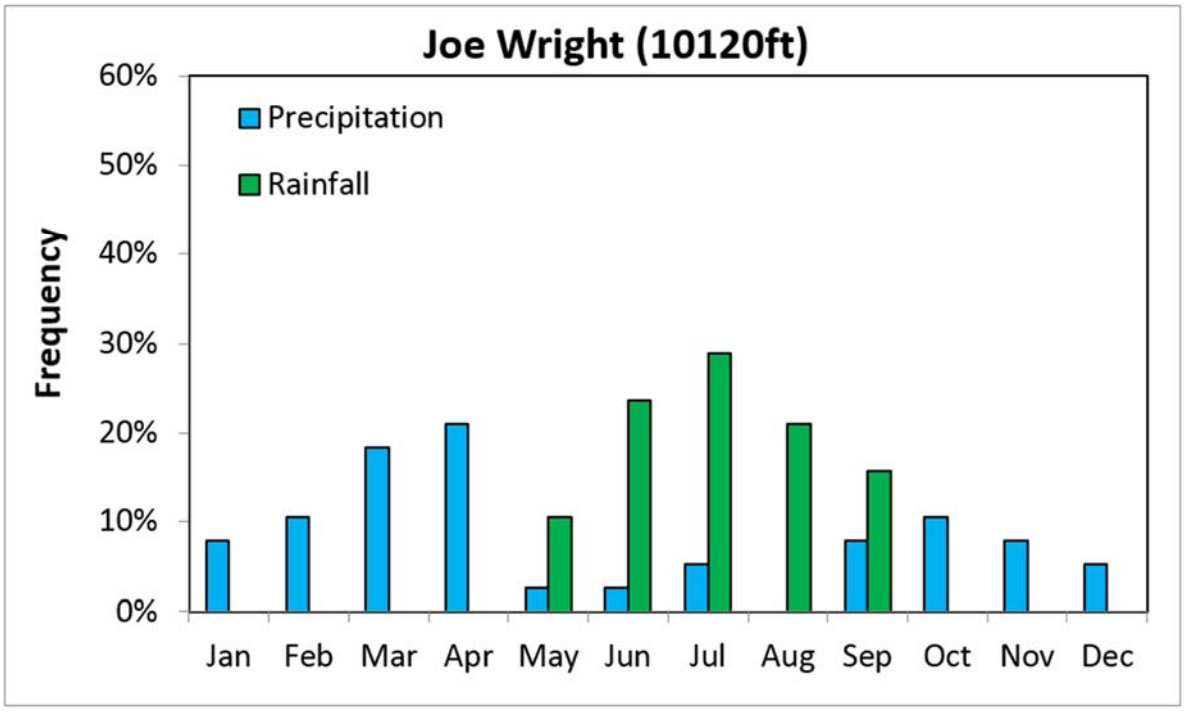

Figure 31: Annual maximum series for rainfall and precipitation at Joe Wright, CO SNOTEL site.

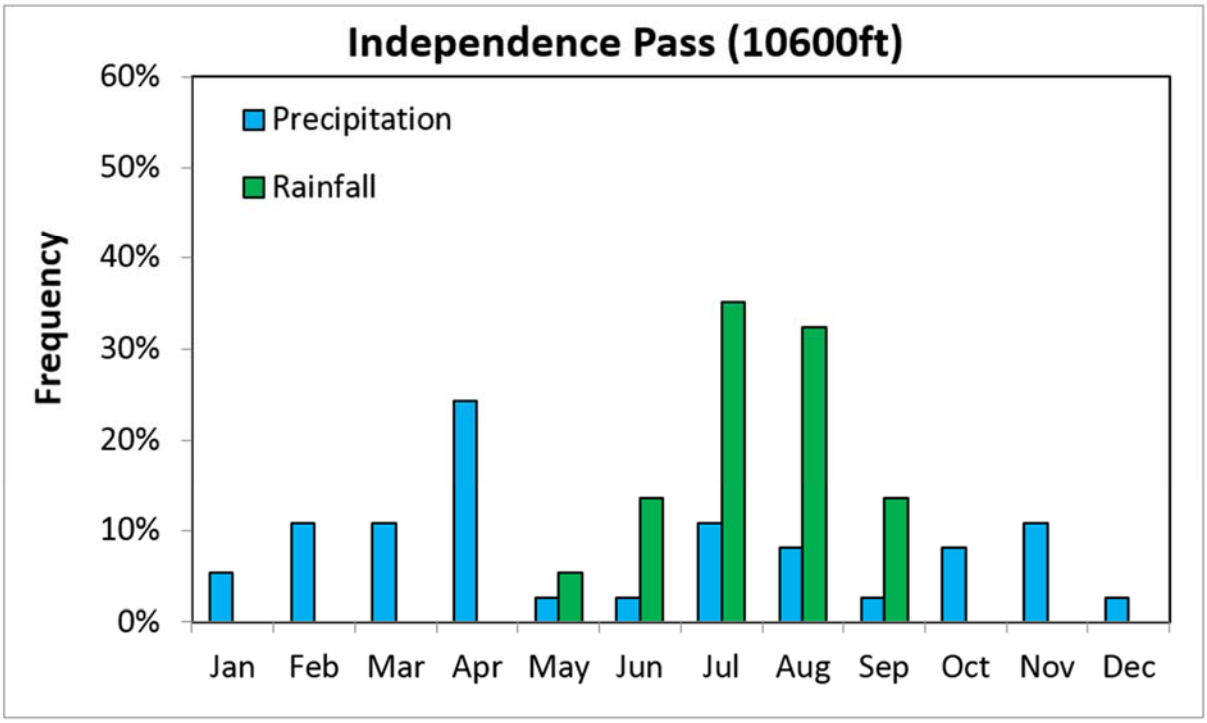

Figure 32: Annual maximum series for rainfall and precipitation at Independence Pass, CO SNOTEL site.

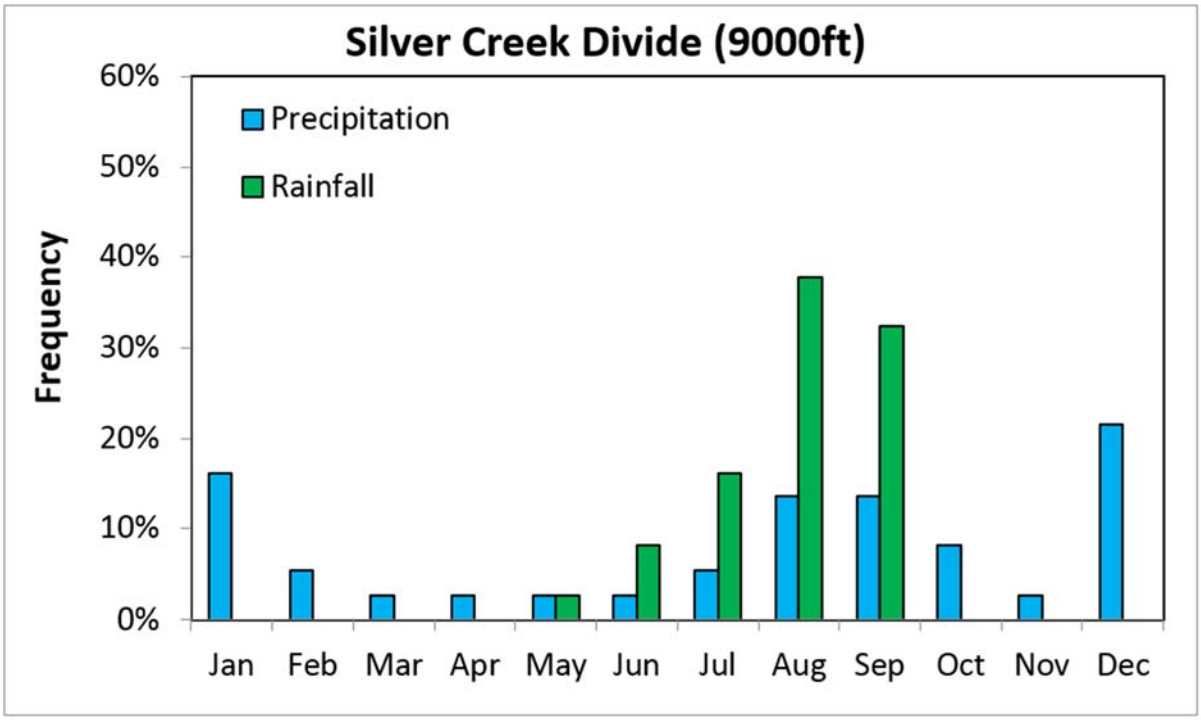

Figure 33: Annual maximum series for rainfall and precipitation at Silver Creek Divide, NM SNOTEL site.

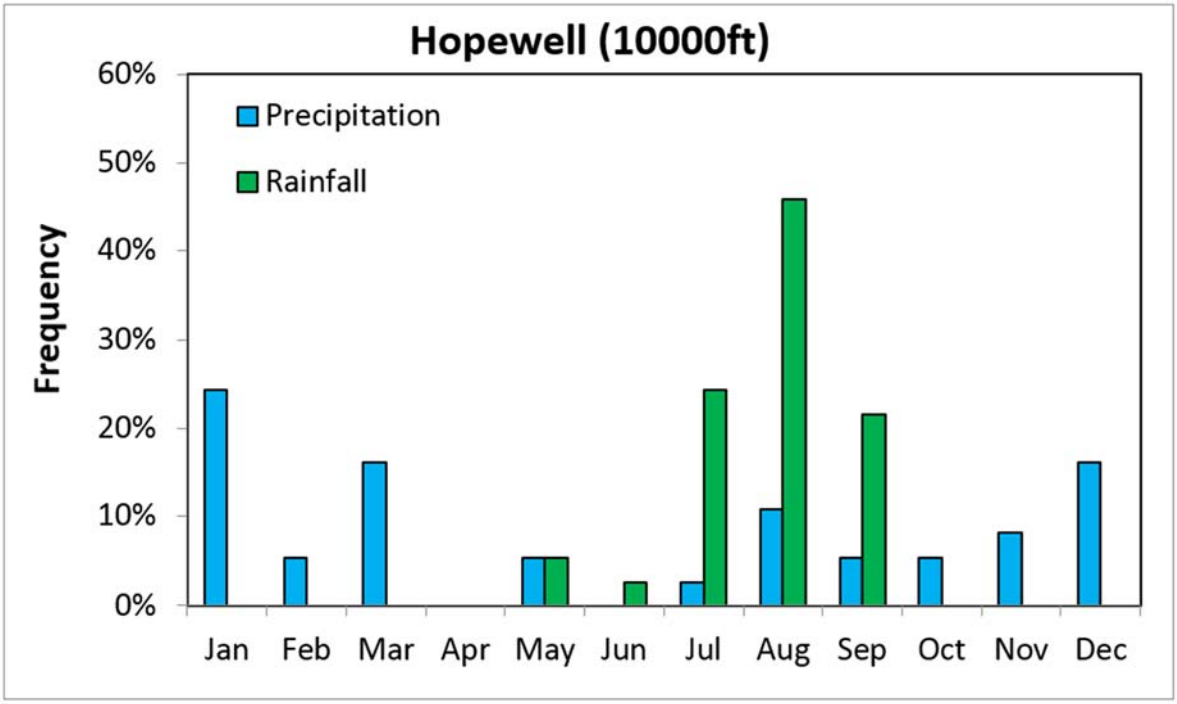

Figure 34: Annual maximum series for rainfall and precipitation at Hopewell, NM SNOTEL site.

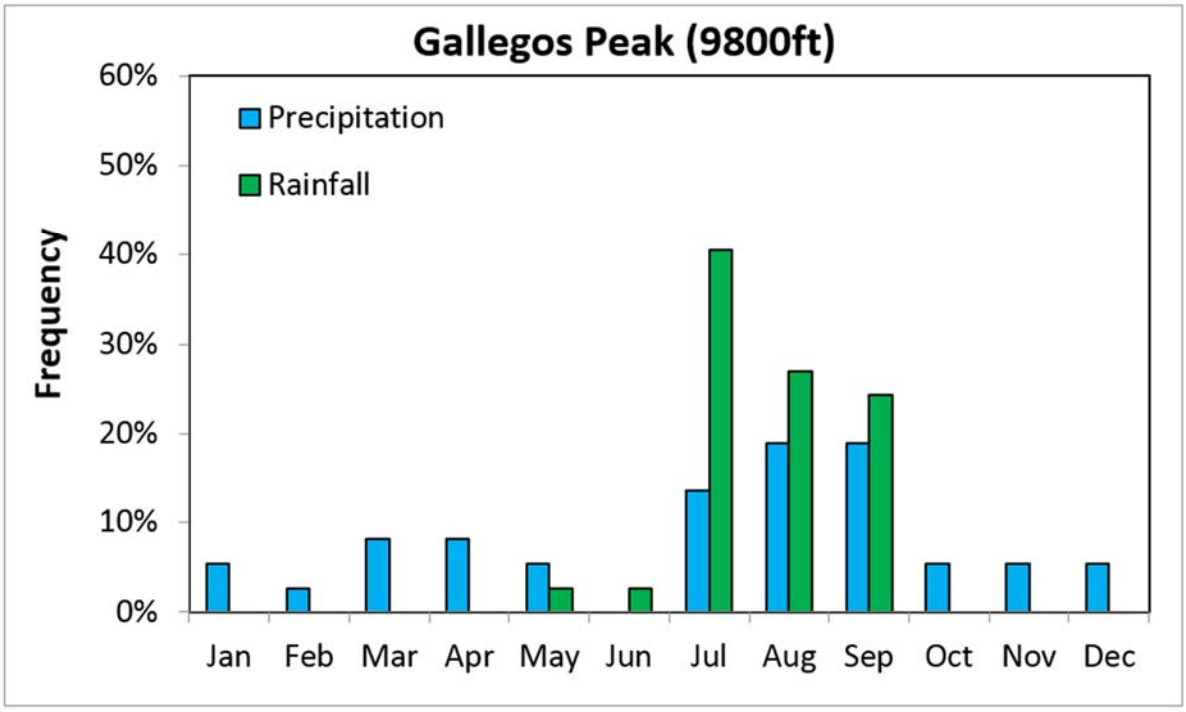

Figure 35: Annual maximum series for rainfall and precipitation at Gallegos Peak, NM SNOTEL site.

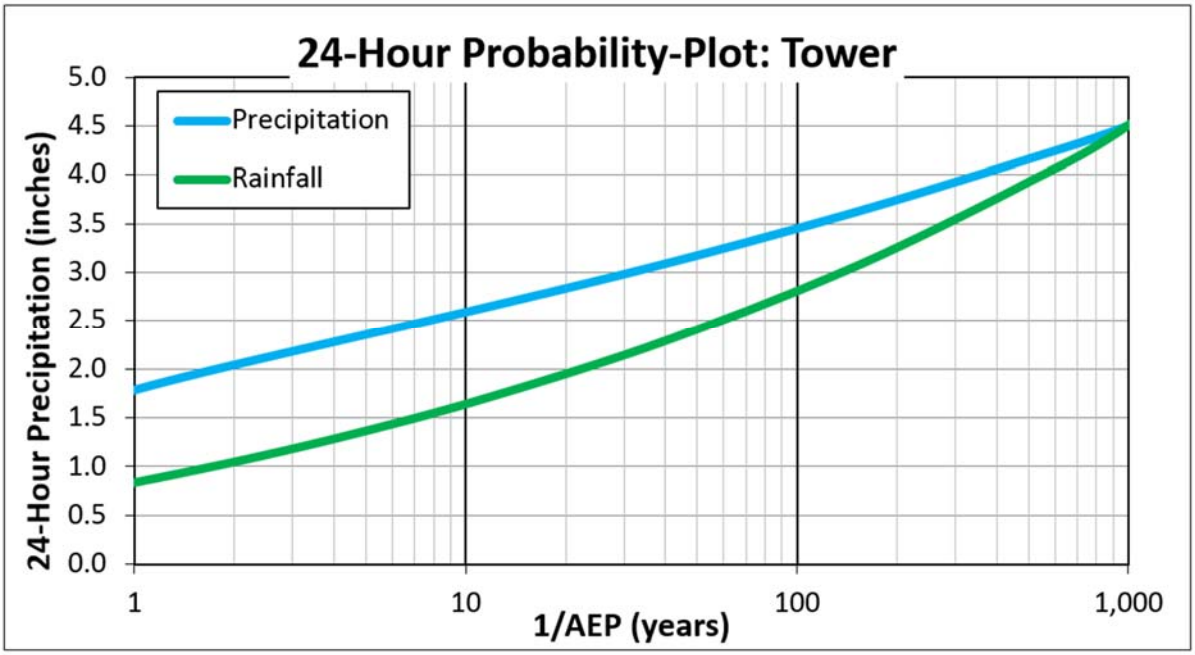

Figure 36: Frequency analysis results rainfall and precipitation annual maximum series at Tower, CO SNOTEL site.

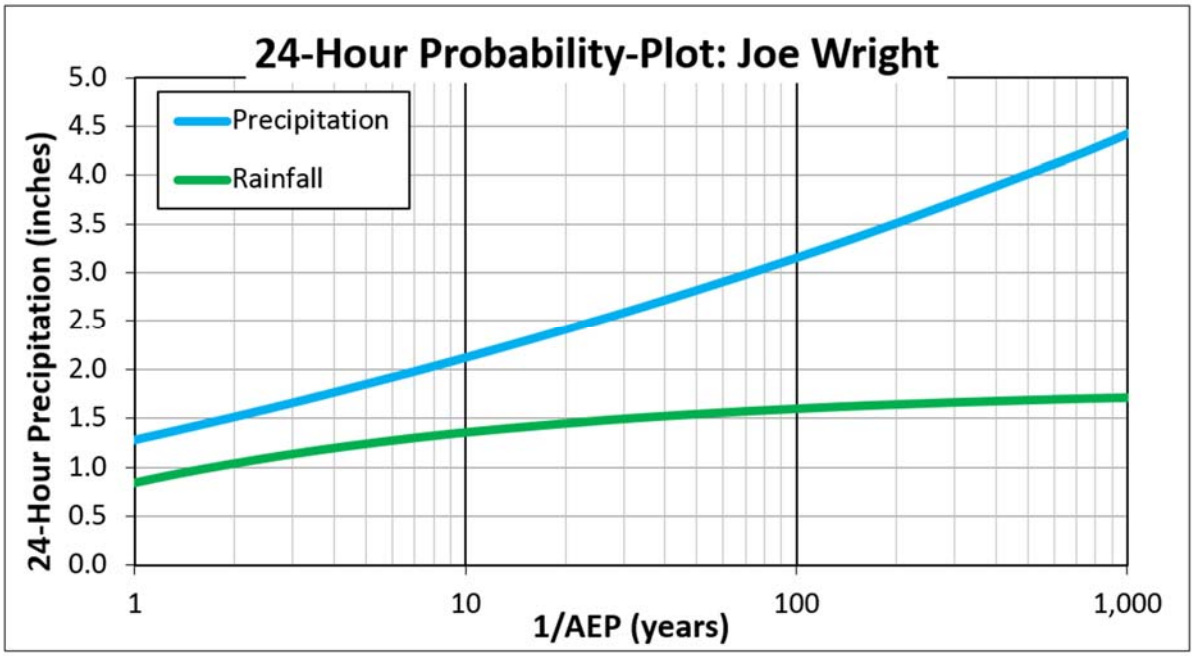

Figure 37: Frequency analysis results rainfall and precipitation annual maximum series at Joe Wright, CO SNOTEL site.

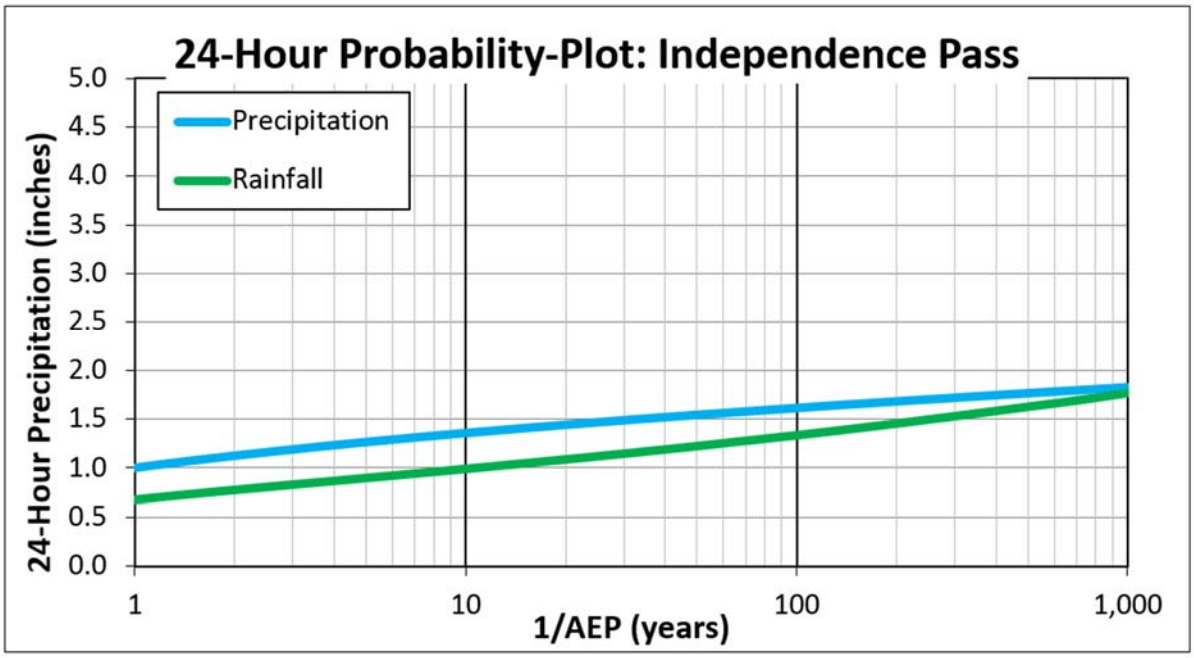

Figure 38: Frequency analysis results rainfall and precipitation annual maximum series at Independence Pass, CO SNOTEL site.

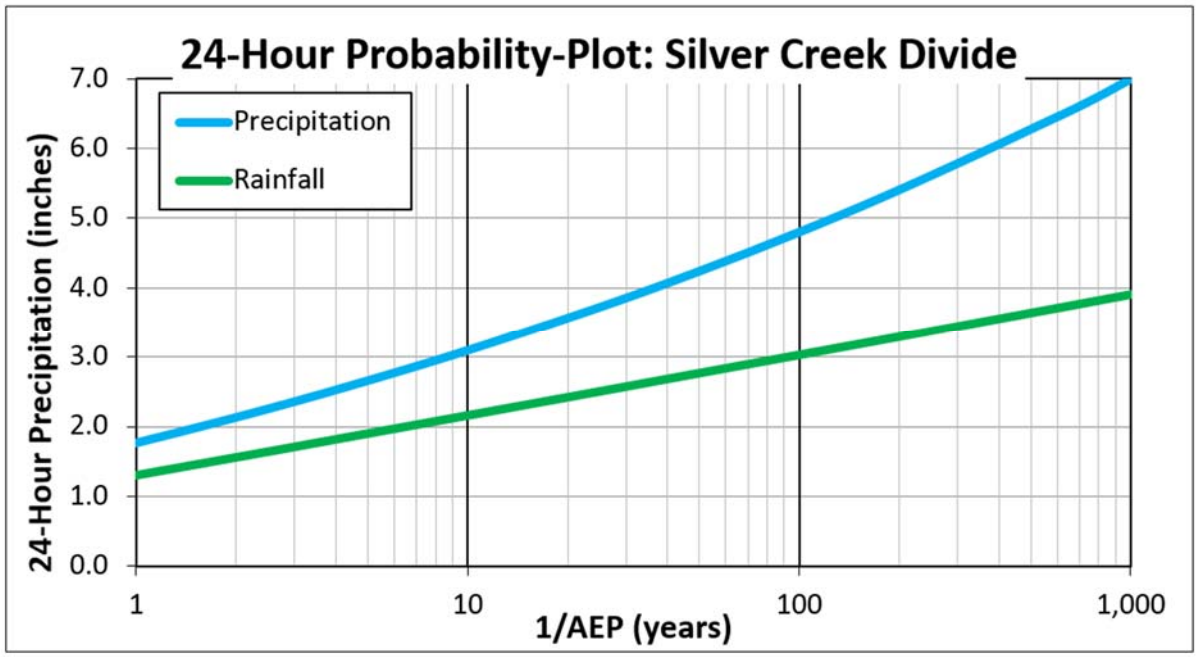

Figure 39: Frequency analysis results rainfall and precipitation annual maximum series at Silver Creek Divide, NM SNOTEL site.

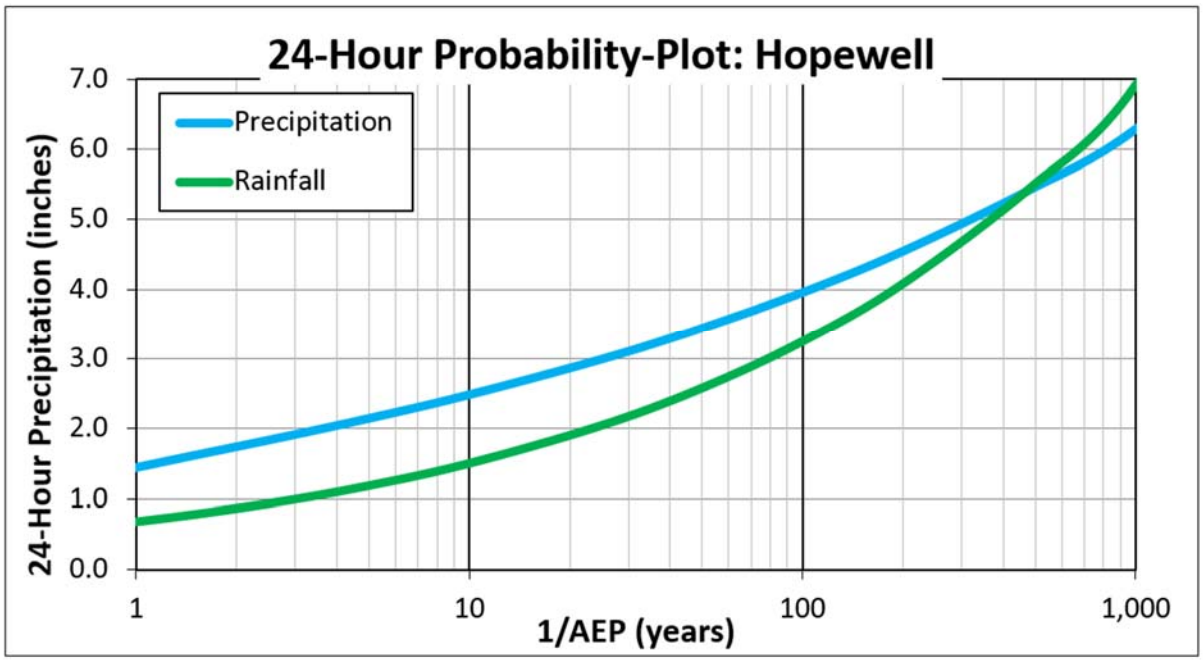

Figure 40: Frequency analysis results rainfall and precipitation annual maximum series at Hopewell, NM SNOTEL site.

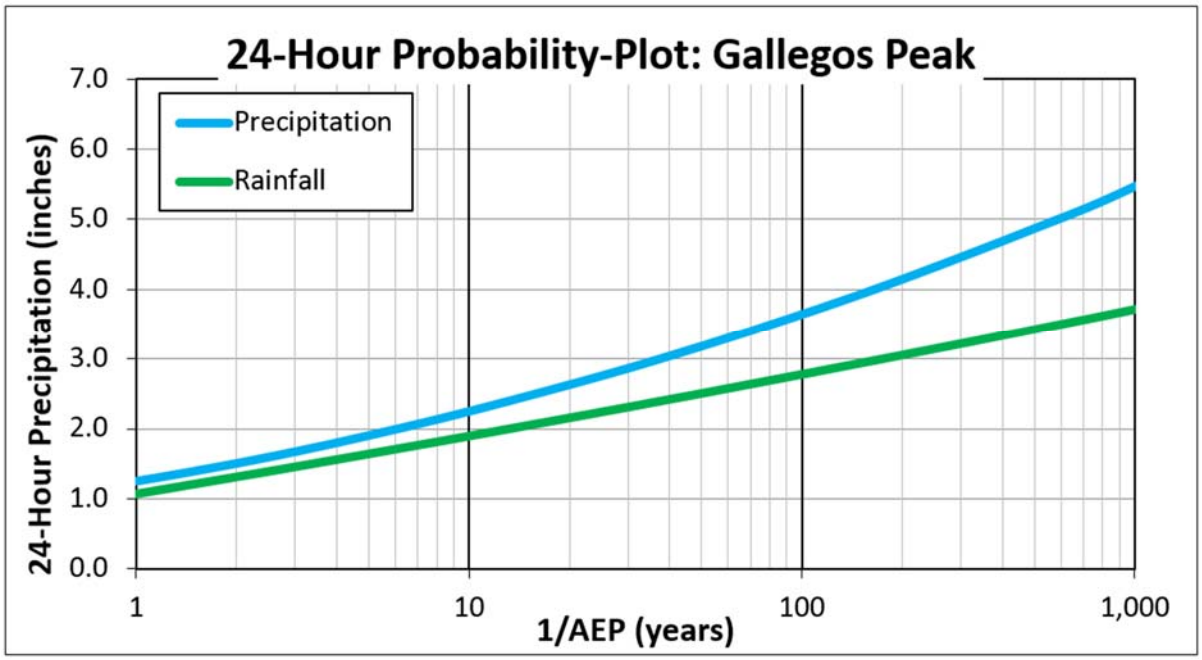

Figure 41: Frequency analysis results rainfall and precipitation annual maximum series at Gallegos Peak, NM SNOTEL site.

This results in precipitation frequency depths that are higher than what they would be if only liquid precipitation (rainfall) had been analyzed and used in the precipitation frequency development process. Because of this issue in regions where snowfall influences precipitation frequency climatology, the precipitation frequency depths

need to be corrected to represent rainfall-only values. The development of rainfall-only precipitation climatology was not part of this study process; therefore, as a surrogate HRRR model output from CO-NM REPS Dynamical Modeling Task was utilized. This provided an excellent climatology of liquid versus frozen precipitation on a high-resolution grid across the entire domain. This output was used to produce a correction factor to convert precipitation frequency depths to represent rainfall-only depths in regions identified as being overly influenced by snowfall/frozen precipitation.

Comparisons were made at several high-elevation locations between HRRR model output and frequency analyses of SNOTEL stations using both annual maximum data for rainfall and precipitation. The comparison of HRRR and station rainfall to precipitation ratios provided support for implementing the HRRR data for rainfall only adjustments. Note that the HRRR datasets only cover the most recent 5-year period. Therefore, it is assumed that the values utilized from the HRRR dataset represent precipitation accumulation patterns and quantities similar to what would result if a longer period of record had been available. These assumptions and limitations were explicitly discussed and reviewed with the PRB and Project Sponsors as part of several workshops and interim teleconferences. Agreement was reached that application of the HRRR model output for adjustment of the precipitation frequency climatologies was acceptable for the use of PMP development in this study.

The ratio of liquid to frozen precipitation was initially calculated on a gridded basis by dividing the HRRR maximum rainfall-only field by the precipitation field for the 6-hour and 24-hour durations. The 6-hour ratio would be applied to the 6-hour 100-year precipitation to convert to 100-year rainfall for use in local storm GTF calculations. Similarly, the 24-hour ratio would be applied to the 24-hour 100-year precipitation. Due to the short period of record of the HRRR output, the resulting gridded ratios contained a few areas of “noise” and inconsistent spatial variations that were unsuitable for application to the GTF calculations. To correct this, the relationship between the rain-only to precipitation ratio and elevation was examined over larger representative regions to provide a smoother spatial field for the ratio development.

Initially, the ratio versus elevation relationship was evaluated over 1,000-foot elevation bands, separated into various regions east and west of the Continental Divide and with various latitudinal constraints. The regions north of 37°N were prioritized as these locations contain most of the areas where snowfall/frozen precipitation has an excessive influence on the precipitation frequency climatologies. Also, there are not enough high-elevation data points south of 37°N to provide a meaningful correlation.

Through workshop discussions and from input from the CO-NM REPS Dynamic Modeling Task, it was determined that the mean annual temperature parameter would be a more appropriate representation of regions where snowfall/frozen precipitation influences precipitation frequency climatologies versus elevation. The PRISM 30-year normal mean annual temperatures were plotted against the rainfall-only to all-precipitation ratios and averaged over 1°C bands. The resulting relationships were

consistent for the critical high-elevation regions of this study on both sides of the Continental Divide.

Figures 42 and 43 show the ratio of HRRR maximum rainfall to all-precipitation versus mean annual temperature averaged over each 1°C temperature band for the 6-hour and 24-hour durations, respectively.

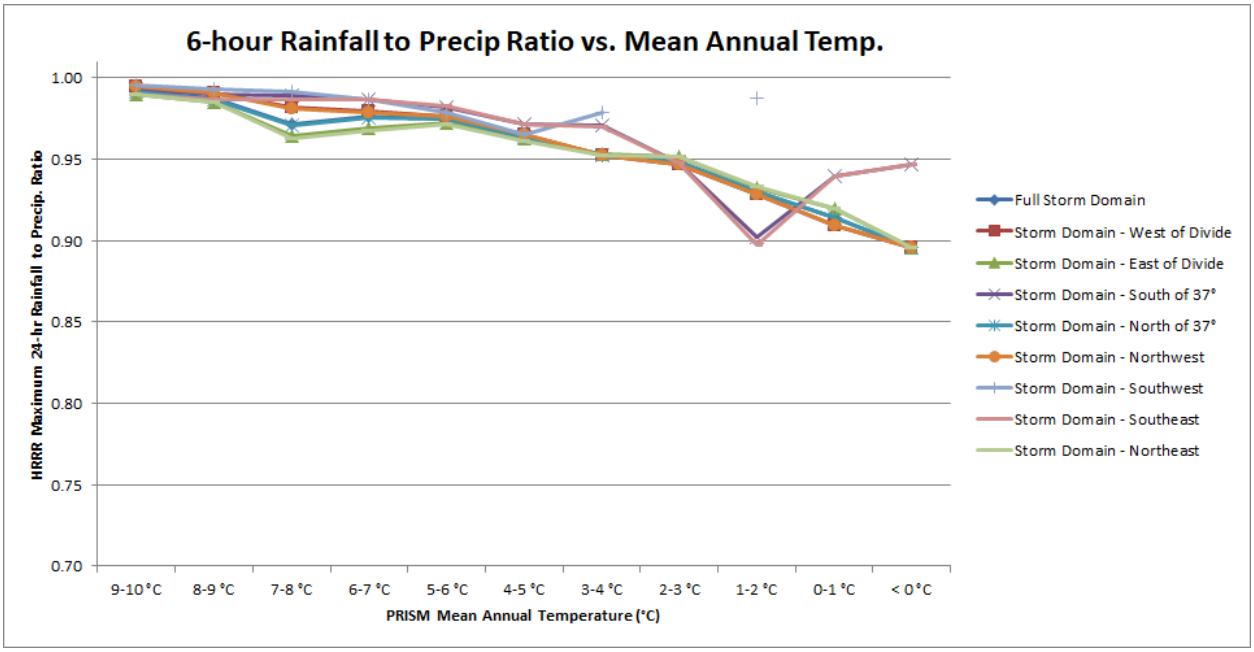

Figure 42: 6-hour rainfall to all-precipitation ratio vs. mean annual temperature

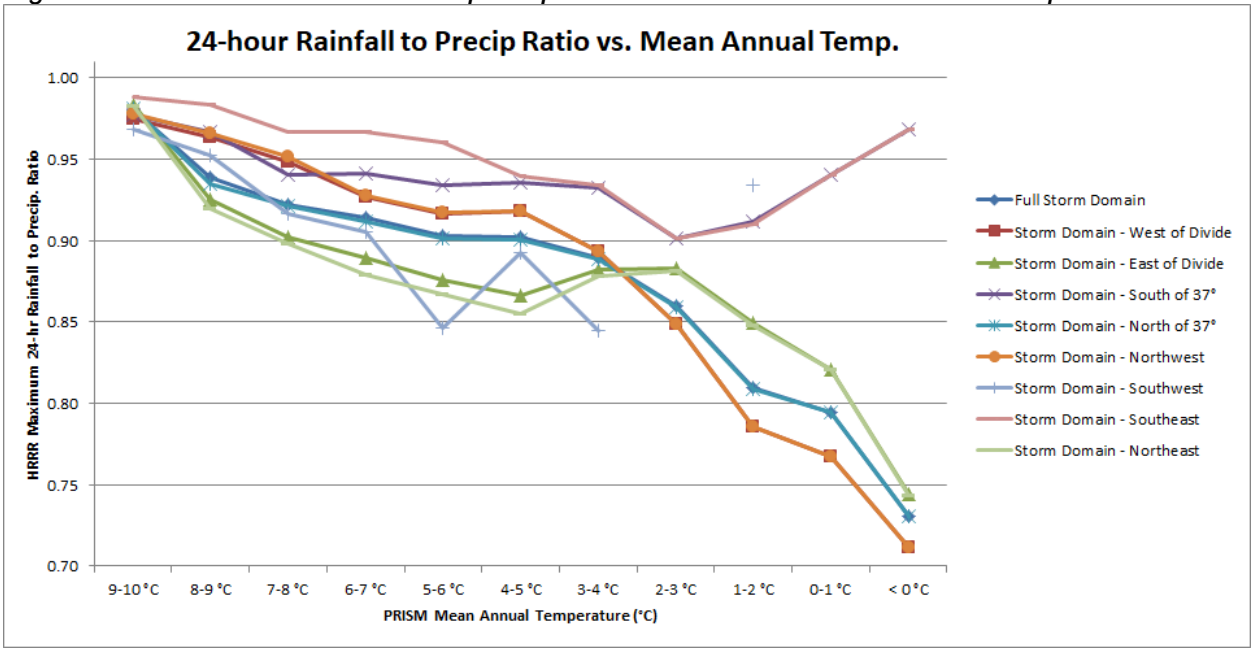

Figure 43: 24-hour rainfall to all-precipitation ratio vs. mean annual temperature

The ratio reduction of 4.3 percent per 1°C was applied to the 100-year 24-hour precipitation for all areas below 5°C mean annual temperature. The ratio reduction of 1.5 percent per 1°C was applied to the 100-year 6-hour precipitation for all areas below 5°C mean annual temperature. The 5°C threshold was geographically consistent with the areas expected to be potentially impacted by non-liquid precipitation. The ratios were applied over 0.1°C temperature bands as areal-averages in 0.0015 and 0.0043 increments to 6-hour and 24-hour 100-year gridded precipitation, respectively.

To illustrate the rainfall-only to precipitation ratio versus elevation relationship, three cross-sectional profiles were constructed at the locations indicated in Figure 44. Transect 1 (Figure 45) was drawn from west to east along 40°N. Transect 2 (Figure 46) was drawn from west to east along 39°N. Transect 3 (Figure 47) was drawn from west to east along 38°N.

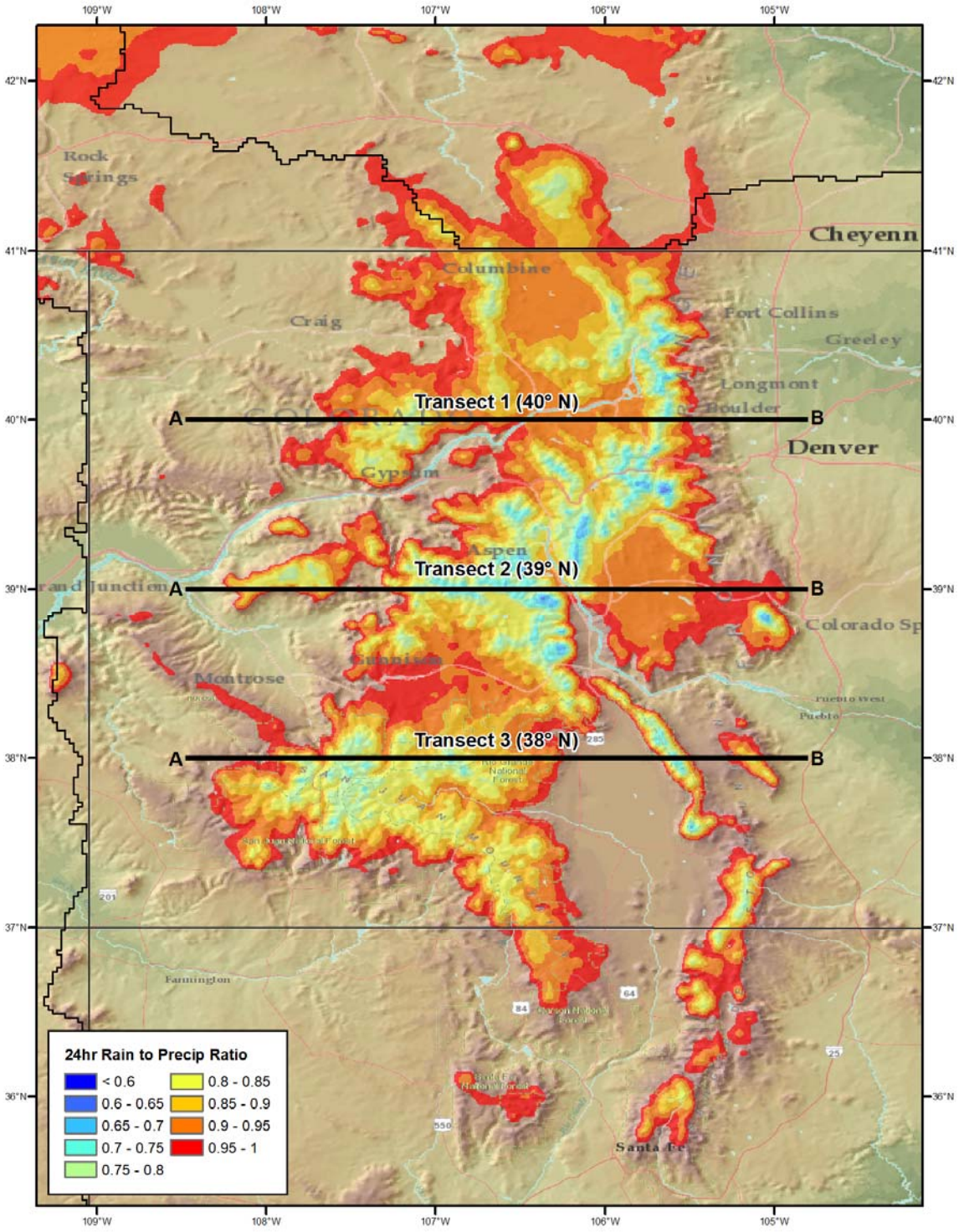

Figure 44: Transect locations of three cross-sectional estimated ratio vs. elevation profiles

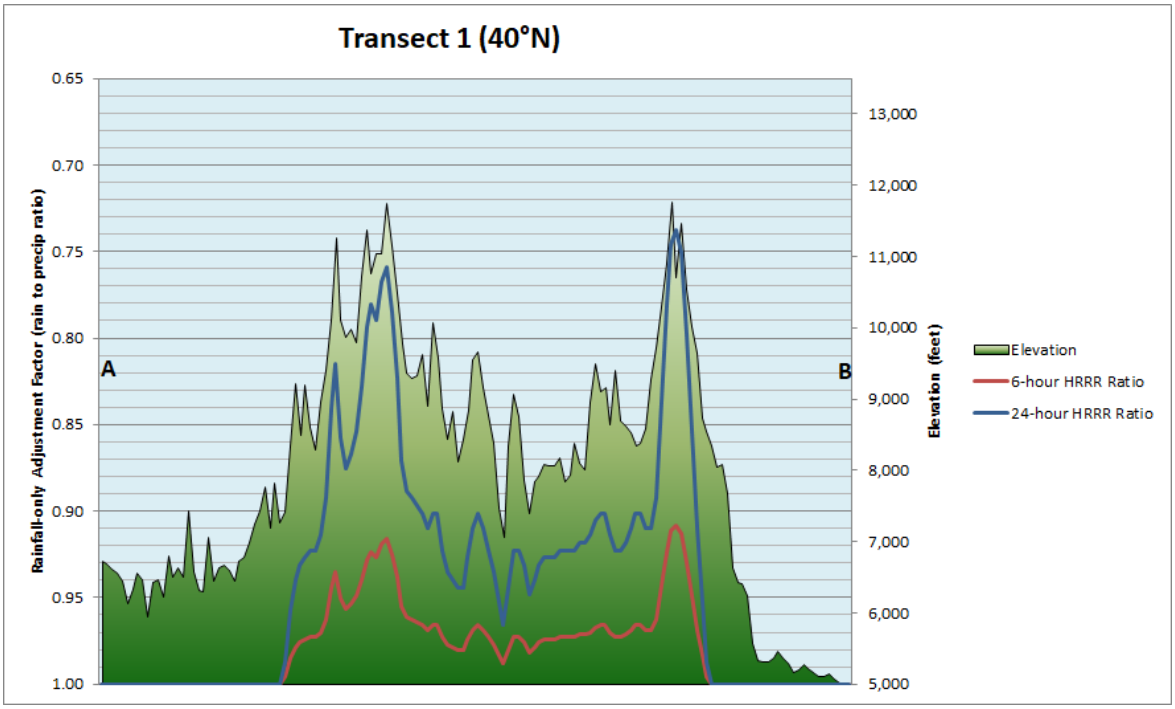

Figure 45: Cross-sectional profile for Transect 1 (40°N)

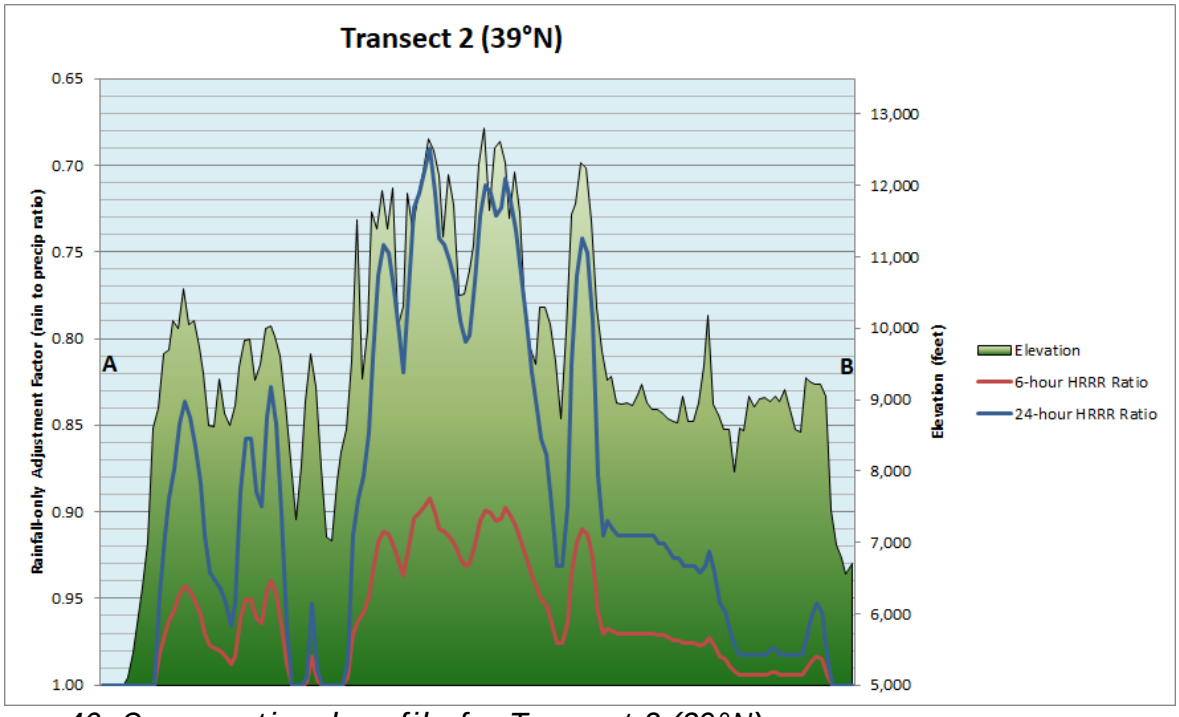

Figure 46: Cross-sectional profile for Transect 2 (39°N)

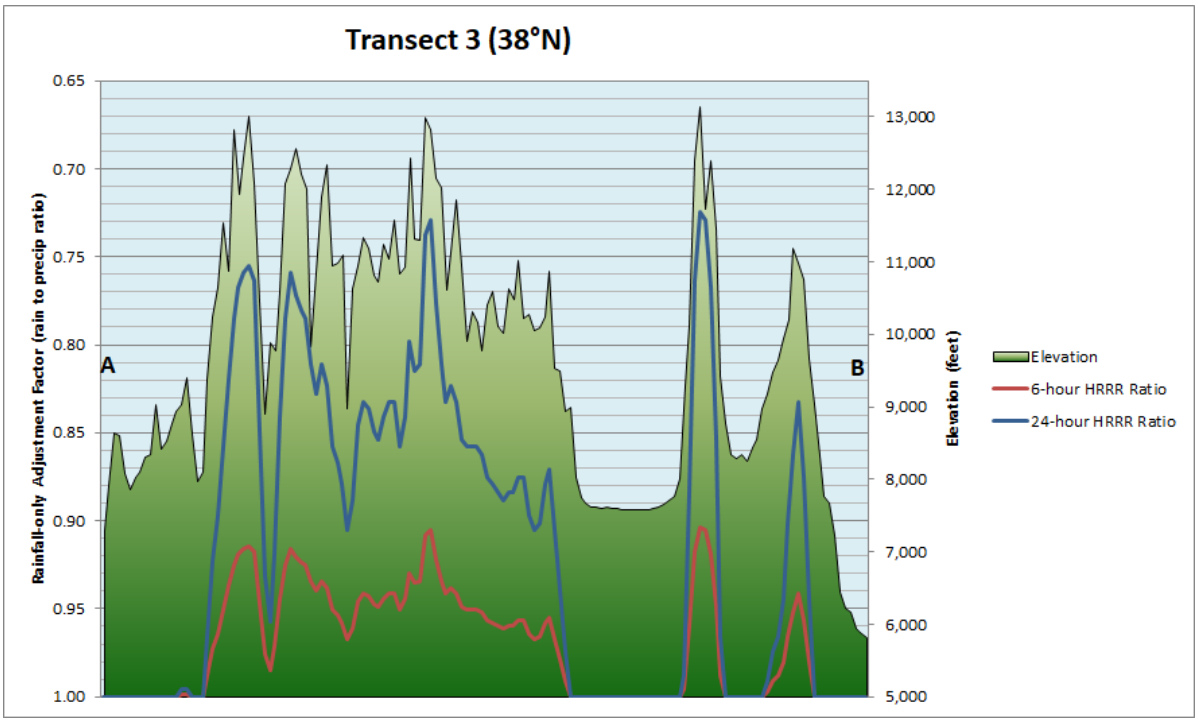

Figure 47: Cross-sectional profile for Transect 3 (38°N)

Figure 48 and Figure 49 show the 6-hour and 24-hour estimated ratios, respectively, over the critical regions. Figure 50 and Figure 51 illustrate the 100-year rainfall-only depths after the HRRR ratio application for 6-hour and 24-hour durations, respectively.

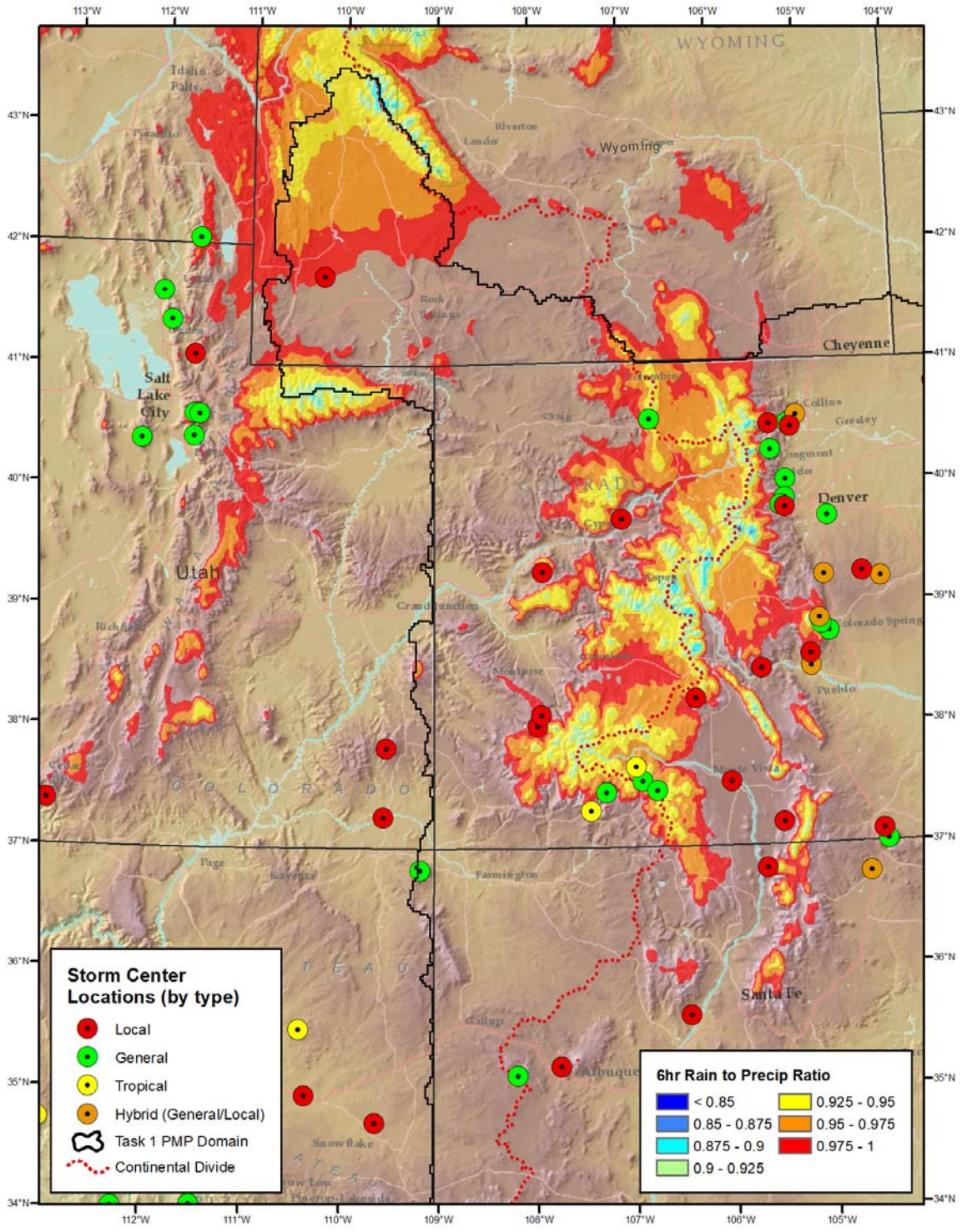

Figure 48: 6-hour estimated ratio of rainfall to all-precipitation with storm center locations

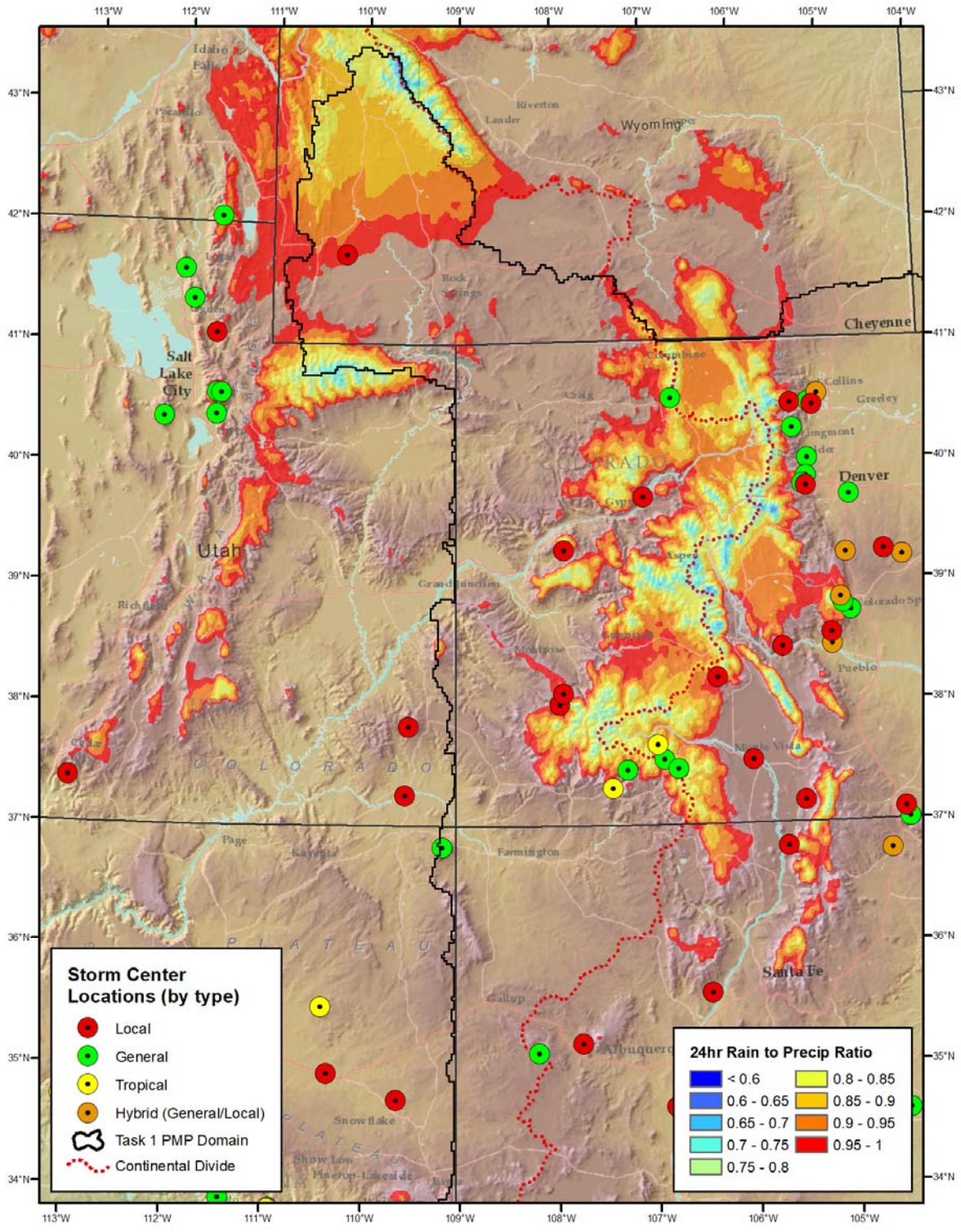

Figure 49: 24-hour estimated ratio of rainfall to all-precipitation with storm center locations

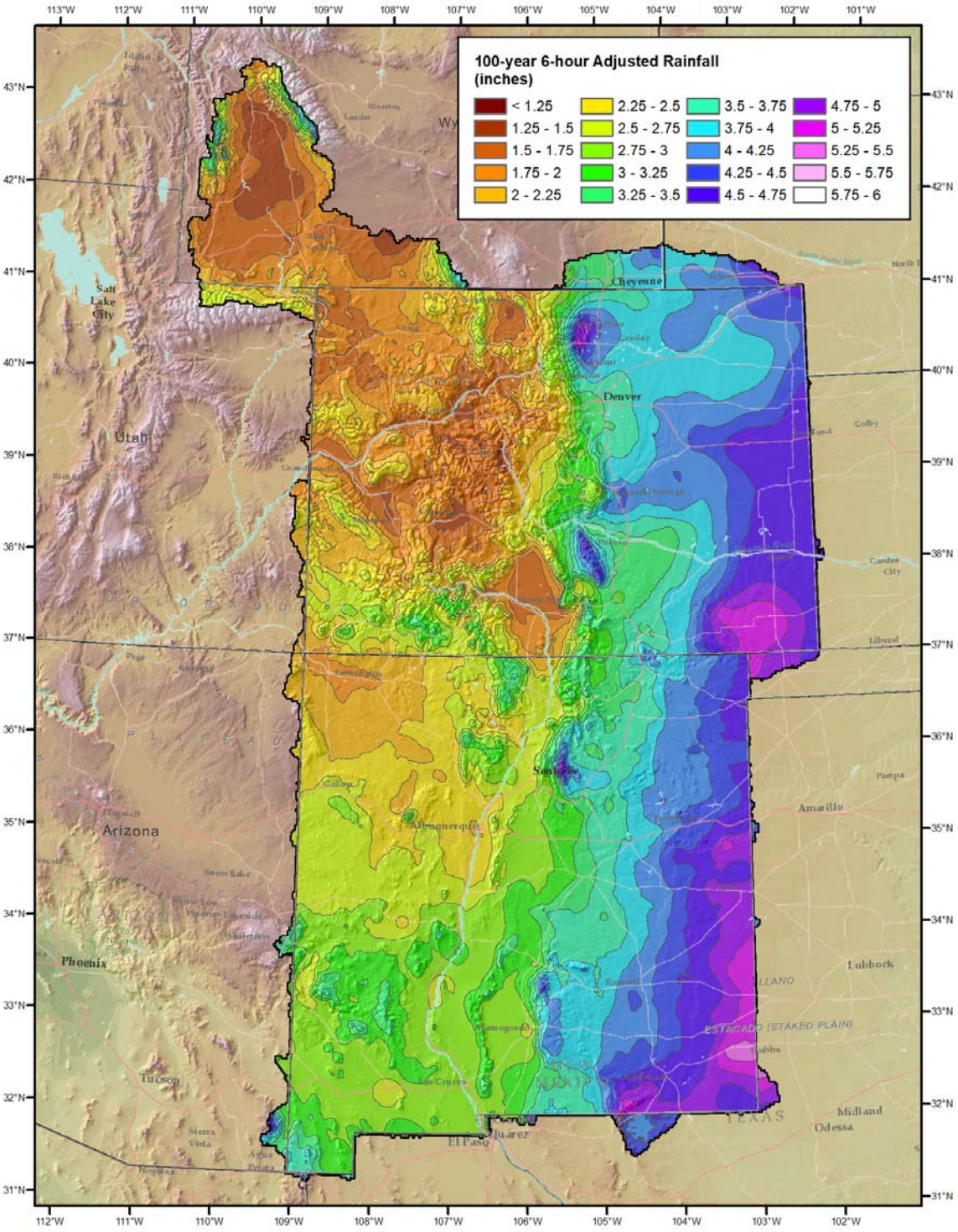

Figure 50: HRRR adjusted 100-year 6-hour rainfall-only depths

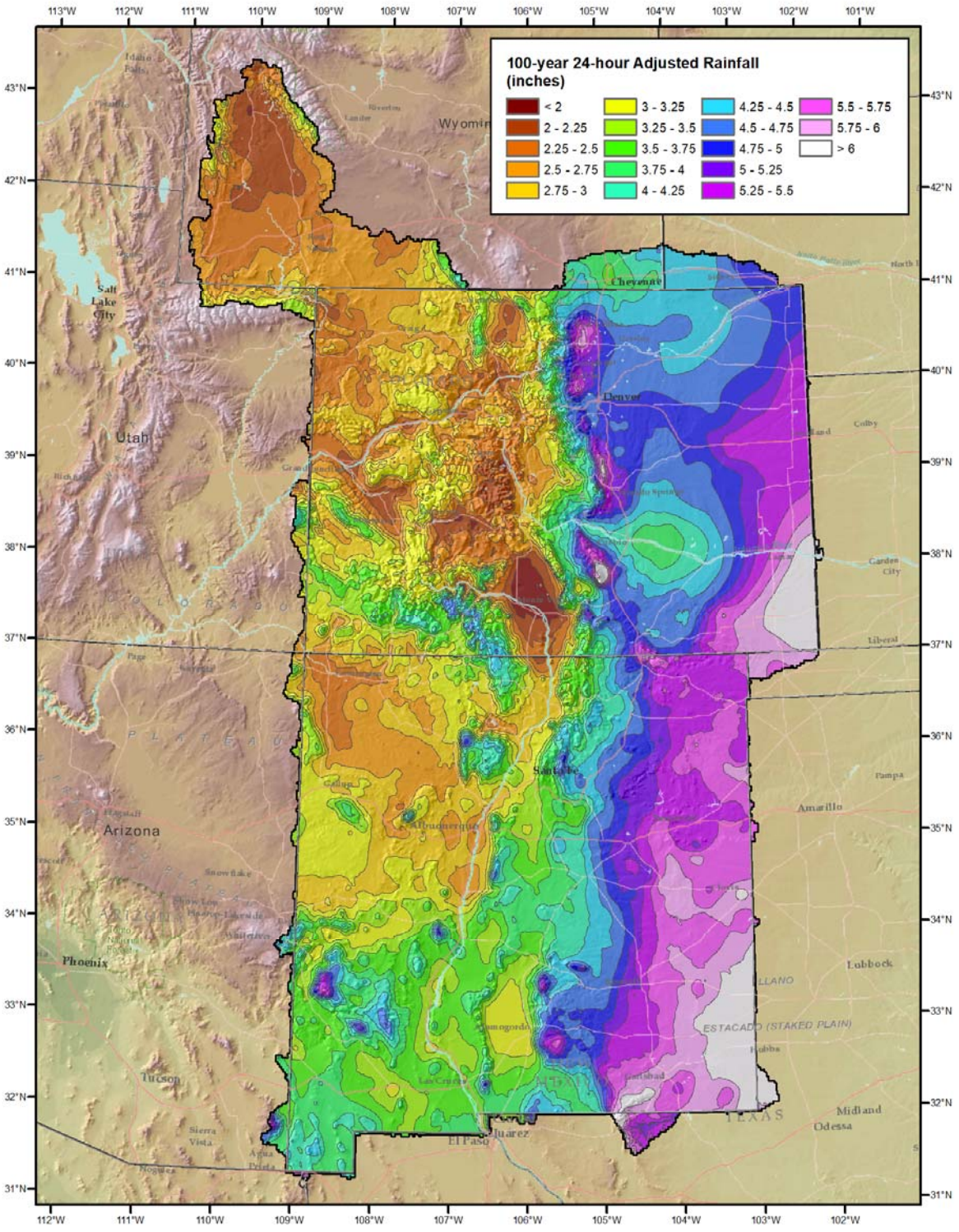

Figure 51: HRRR adjusted 100-year 24-hour rainfall-only depths

7.9 Geographic Transposition Factor (GTF) Calculation

The GTF is calculated by taking the ratio of transpositioned 100-year rainfall to the in-place 100-year rainfall.

$$GTF = \frac{R_t}{R_s} \qquad \text{Equation 6}$$

where,

R_t = climatological 100-year rainfall depth at the target location
R_s = climatological 100-year rainfall depth at the source storm center

The in-place climatological precipitation (R_s) was determined at the grid point located at the SPAS-analyzed total storm maximum rainfall center location. The corresponding transpositioned climatological precipitation (R_t) was taken at each target grid point. The 100-year AEP was used for each transpositioned location and also for the in-place location for storm centers. The 6-hour precipitation frequency climatologies were used for the local storm type. The 24-hour precipitation frequency climatologies were used for the general and tropical storm types. Precipitation frequency (PF) estimates for Arizona, Utah, and New Mexico were taken from NOAA Atlas 14 volume 1 (Bonnin et al., 2011). PF estimates over Colorado and Nebraska were taken from NOAA Atlas 14 volume 8 (Perica et al., 2013). PF estimates over Texas were taken from the precipitation frequency analysis for the Texas Statewide PMP study (Kappel et al., 2016). PF estimates over Wyoming and Idaho were taken from the precipitation frequency analysis for the Wyoming Statewide PMP study (Kappel et al., 2014). PF estimates at high-elevation were adjusted to rainfall-only depths using the methods described in previous section.

7.10 Total Adjustment Factor (TAF)

The TAF is a combination of the total moisture and terrain differences on the SPAS analyzed rainfall after being maximized in-place and then transpositioned to the target grid point.

$$TAR_{xhr} = P_{xhr} \times IPMF \times MTF \times GTF \qquad \text{(from Equation 1)}$$

The TAF, along with the other storm adjustment factors, is exported and stored within the storm's adjustment factor feature class to be accessed by the GIS PMP tool as described in the following section.

8. Development of PMP Values

8.1 PMP Calculation Process

To calculate PMP, the TAF for each storm must be applied to the storm's SPAS analyzed DAD value for the area size and duration of interest to yield a total adjusted rainfall value. The storm's total adjusted rainfall value is then compared with the adjusted rainfall values of every storm in the database transposable to the target grid

point. The largest adjusted rainfall depth becomes the PMP for that point at a given duration. This process must be repeated for each of the grid cells intersecting the input drainage basin for each applicable duration and storm type. The gridded PMP is averaged over the drainage basin of interest to derive a basin average and the accumulated PMP depths are temporally distributed.

A GIS-based PMP calculation tool was developed to automate the PMP calculation process. The PMP tool is a Python scripted tool that runs from a Toolbox in the ArcGIS desktop environment. The tool accepts a basin polygon feature or features as input and provides gridded, basin average, and temporally distributed PMP depths as output. These PMP output elements can be used with hydrologic runoff modeling simulations for PMF calculations. Full documentation of the PMP tool usage and structure is found in Appendix G.

The PMP tool can be used to calculate PMP depths for the following durations.

Local Storm PMP Durations:

- 1-, 2-, 3-, 4-, 5-, 6-, 12-, and 24-hour

General/Tropical Storm PMP Durations:

- 1-, 6-, 12-, 24-, 48-, and 72-hour

The PMP tool provides depths at an areal-average for the drainage basin area size. This area can be overwritten with a specific user-defined area-size within the tool dialogue.

8.1.1 Sample Calculations

The following sections provide sample calculations for the storm adjustment factors for the Big Elk Meadow, CO of May, 1969 (SPAS 1253) general storm event when transpositioned to 39.85°N, 105.675°W (grid point ID #83,789). The target location is about 30 miles southwest of the storm location at an elevation of 11,950 feet near the crest of the Colorado Front Range located in transposition zone 5 (see Figure 52).

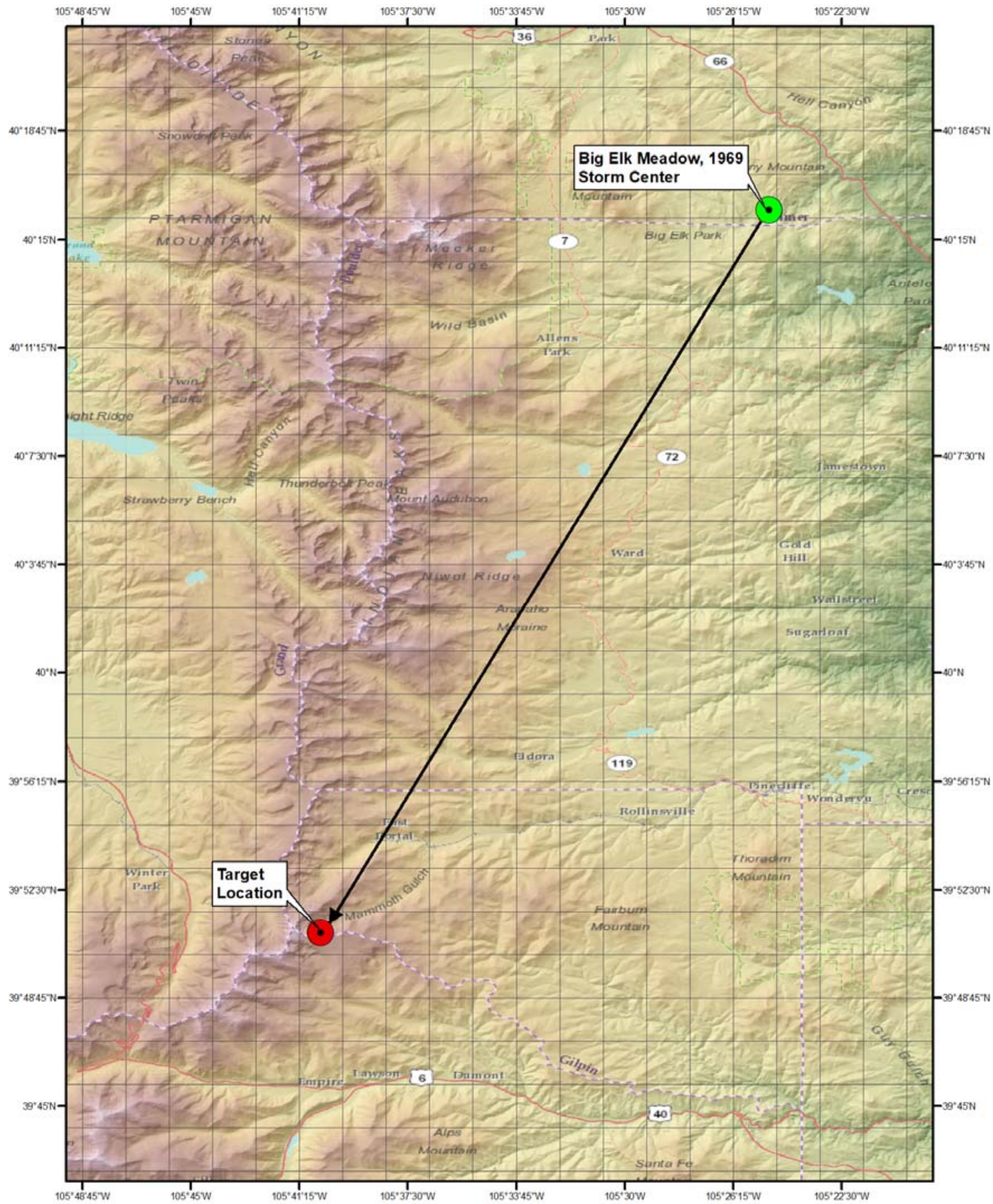

Figure 52: Sample transposition of Big Elk Meadow, CO 1969 storm (SPAS 1253) to grid point #83,789

8.1.2 Sample Precipitable Water Calculation

Using the storm representative dew point temperature and storm center elevation as input, the precipitable water lookup table returns the depth, in inches, used in

Equation 4. The storm representative dew point temperature is 64˚F at the storm representative dew point location 375 miles east-southeast of the storm center (see Appendix F for the detailed storm maximization and analysis information). The storm center elevation is approximated at 7,500 feet at the storm center location of 40.267˚N, 105.417˚W. The storm representative available moisture ($W_{p,\ rep}$) is calculated using Equation 4:

$$W_{p,rep} = W(@64°)_{p,30,000'} - W(@64°)_{p,7,500'}$$

or,

$$W_{p,rep} = 1.680" - 1.000"$$

$$\boldsymbol{W_{p,rep} = 0.680"}$$

The early May storm was adjusted 15 days toward the warm season to a temporal transposition date of May 20th. A weighted average of the May and June 24-hour climatological maximum dew point temperatures was used for the May 20th temporal transposition date. The May climatological 100-year maximum 24-hour average dew point at the storm representative dew point location is 73.5˚F and the June average is 78.2˚F. The two monthly temperatures are averaged (weighted toward May 20th) and rounded to the nearest ½ degree to a climatological maximum dew point temperature of 74.5˚F. The in-place climatological maximum available moisture ($W_{p,\ max}$) is calculated.

$$W_{p,max} = W(@74.5°)_{p,30,000'} - W(@74.5°)_{p,7,500'}$$

$$W_{p,max} = 2.790" - 1.475"$$

$$\boldsymbol{W_{p,max} = 1.315"}$$

The climatological maximum available moisture was determined for the target grid point. The May climatological 100-year maximum 24-hour average dew point for the target dew point location is 73.6˚F and the June average is 78.1˚F. The two monthly temperatures are averaged to 74.4˚F and rounded to a climatological maximum dew point temperature of 74.5˚F. The horizontally transposed climatological maximum available moisture ($W_{p,\ trans}$) is calculated.

$$W_{p,trans} = W(@74.5°)_{p,30,000'}$$

$$\boldsymbol{W_{p,trans} = 2.790"}$$

8.1.3 Sample IPMF Calculation

In-place storm maximization is applied for each storm event using the methodology described in Section 7.2. Storm maximization is quantified by the IPMF using Equation 3:

$$IPMF = \frac{W_{p,max}}{W_{p,rep}}$$

$$IPMF = \frac{1.135"}{0.680"}$$

$$IPMF = 1.93$$

In this case the IPMF is calculated to a factor above 1.50, the maximum upper limit. The IPMF is then set to 1.50.

$$\boldsymbol{IPMF = 1.50}$$

8.1.4 Sample MTF Calculation

Using Equation 5:

$$MTF = \frac{W_{p,trans}}{W_{p,\max(30,000')}}$$

$$MTF = \frac{2.790"}{2.790"}$$

$$\boldsymbol{MTF = 1.00}$$

8.1.5 Sample GTF Calculation

The ratio of the 100-year 24-hour climatological rainfall depth at the target grid point #83,789 location to the Big Elk Meadow, 1969 storm center was evaluated to determine the storm's GTF at the target location. The 24-hour rainfall depth (R_t) of 3.19" was extracted at the grid point #83,789 location from the 100-year 24-hour HRRR-adjusted rainfall-only climatology.

$$R_t = 3.19"$$

Similarly, the 24-hour rainfall depth (R_s) of 4.85" was extracted at the storm center location from the 100-year 24-hour HRRR-adjusted rainfall-only climatology.

$$R_s = 4.85"$$

Equation 6 provides the climatological precipitation ratio to determine the GTF.

$$GTF = \frac{R_t}{R_s}$$

$$GTF = \frac{3.19"}{4.85"}$$

$$\boldsymbol{GTF = 0.66"}$$

The GTF at grid #83,789 is 0.66, or a 34 percent rainfall decrease from the storm center location due to the orographic effects captured within the precipitation frequency climatology. The GTF is then considered to be a temporal constant for the spatial transposition between that specific source/target grid point pair, for that storm only, and can be applied to the other durations for that storm.

8.1.6 Sample TAF Calculation

$$TAF = IPMF \times MTF \times GTF \qquad \text{(from Equation 1)}$$

$$TAF = 1.50 \times 1.00 \times 0.66$$

$$\boldsymbol{TAF = 0.99}$$

The TAF for Big Elk Meadow, CO, 1969 when moved to the grid point at 39.85°N, 105.675°W, representing storm maximization and transposition, is 0.99. This is an overall slight decrease from the original SPAS analyzed in-place rainfall. In this case the amount of GTF reduction due to the transposition to a high-elevation location of lower climatological rainfall is almost inversely proportional to the amount of increase due to the in-place maximization. The MTF has no impact, primarily due to the short distance transpositioned in this example. The TAF can then be applied to the DAD value for a given area size and duration to calculate the total adjusted rainfall. If the total adjusted rainfall is greater than the depth for all other transpositionable storms, it becomes the PMP depth at that grid point for that duration.

9. PMP Results

The PMP tool provides basin-specific PMP based on the area-size of the basin. For each storm type analyzed, the tool provides output in ESRI file geodatabase format. The output includes a basin average PMP table. If the sub-basin average option was checked the tool provides averages for each sub-basin. The depths are calculated for the area-size of the basin, so no further areal reduction should be applied. The tool also provides a point feature class containing PMP depths and controlling storms listed by SPAS ID and storm name, date, and state, in addition to gridded raster PMP depth files. There are also temporally distributed accumulated rainfall tables for each temporal pattern applied to the basin as described in Section 10.7. Finally, a basin average PMP depth-duration chart in the .png image format is also included in the output folder. An example depth-duration chart for Trout Creek basin, located near Buena Vista, Colorado, is shown in Figure 53. Detailed output information is included in the PMP tool documentation in Appendix G.

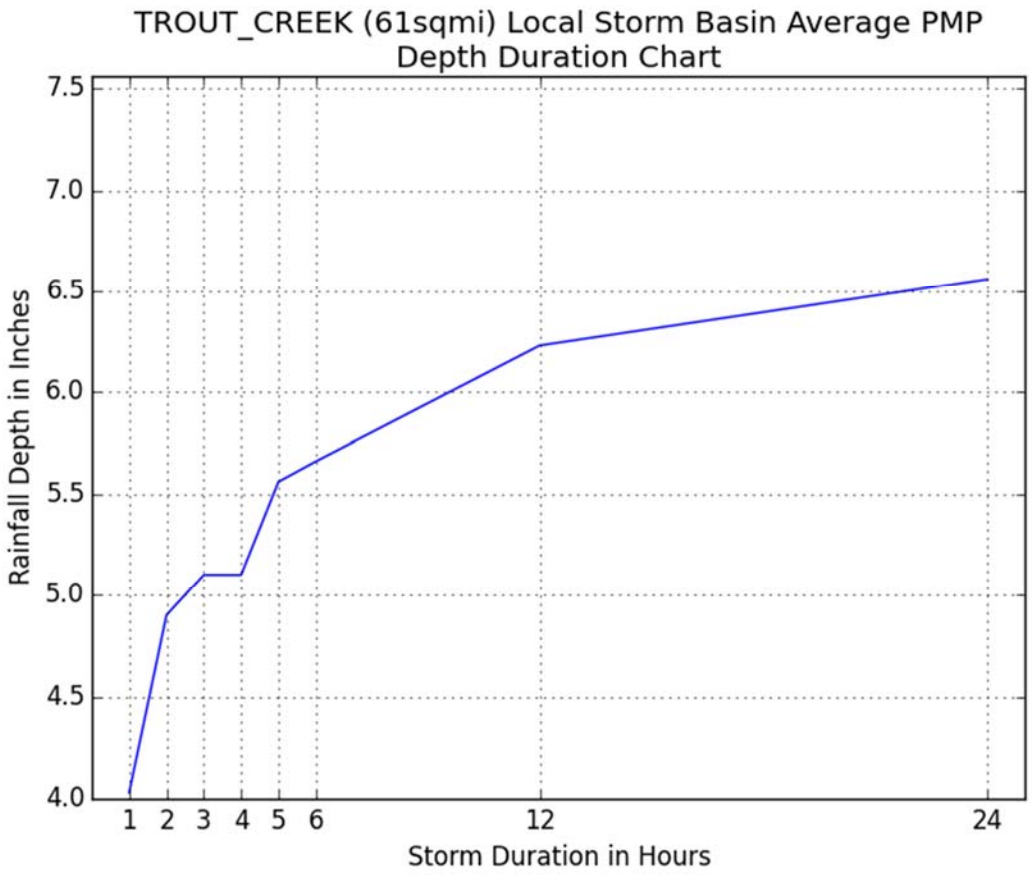

Figure 53: Sample basin average PMP depth-area chart image provided in PMP Tool output folder.

Gridded PMP depths were calculated for the entire study region at various index area-sizes for several durations as a visualization aid. The maps in Appendix A illustrate the depths for 1-, 10-, and 100-square mile area sizes for local storm PMP at 1-, 6-, and 12-hour durations and 1-, 10-, 100-, 1,000-, and 10,000-square mile area sizes for general and tropical storm PMP at 6-, 24-, and 72-hour durations.

10. Development of Temporal Distribution for Use in Runoff Modeling

The development of the site-specific temporal patterns was completed following similar processes as those used in the Wyoming PMP temporal study (Kappel et al., 2015) and the Virginia PMP temporal study (Kappel et al., 2018). All short list storms used in the CO-NM REPS study were used to develop temporal accumulation patterns associated with storm type and general region. Storms were grouped by geographic location (east versus west of the Continental Divide) and by storm type: local, general, tropical, and hybrid.

In terms of storm types, local storms are characterized by short duration (6-hours or less) and small area size high intensity rainfall accumulations. They are often not associated with large scale weather patterns and can be influenced by local moisture sources. General storms produce precipitation over longer durations (greater than 6-hours) and cover larger areas with comparatively lower intensity rainfall accumulations. General storms are produced by large scale synoptic patterns generally associated with areas of low pressure and fronts. In the southern portions of the study domain, storms can also be associated with remnant moisture from decaying tropical systems originating from the eastern Pacific and Gulf of California. Tropical storms rely on warm water from the Gulf of Mexico along with supporting synoptic and upper level weather patterns and occur from June through October. When these storms move slowly over a region, large amounts of rainfall can be produced both in convective bursts and over longer durations. Some storms exhibit characteristics of both the local and general storm or local and tropical rainfall accumulation patterns. These are termed hybrid storms and a unique temporal pattern has been derived to apply to this storm type.

Two methods were used to investigate and derive temporal patterns: i) Synthetic Curves based on SPAS mass curves and ii) Huff Curves based on SPAS mass curves. Investigations were completed by analyzing the rainfall accumulation of each storm and the time over which the main rainfall accumulated. During these analyses, consideration was given to the synoptic meteorological patterns that created each storm type, access to moisture sources, and the general topographical setting. The location of the storm center associated with each SPAS DAD zone was used for the temporal distribution calculations. Hourly gridded rainfall data were used for all SPAS analyzed storms.

HMR 49 and 55A utilized similar qualitative investigations of rainfall accumulation patterns. However, very little background information was provided as to how those rainfall data were analyzed to derive the temporal patterns applied in those documents. HMR 49 Section 4.4 provides background on investigations completed in that study to derive depth-duration information. HMR 49 Section 4.7 provides background on the time distribution of incremental PMP for the local storm type. HMR 55A Section 12.5 addresses local storm incremental accumulation but again provides very limited data and analysis background.

10.1 Synthetic Curve Methodology

Hourly gridded rainfall data were used for all SPAS analyzed storms. The maximum rain accumulations were based on rainfall at the storm center. The rainfall mass curve at the storm center were used for the temporal calculations. The steps used to derive the synthetic curves are described below.

10.1.1 Standardized Timing Distribution by Storm Type

The Significant Precipitation Period (SPP) for each storm was selected by excluding relatively small rainfall accumulations at the beginning and end of the rainfall duration. Accumulated rainfall (R) amounts during the SPP were used in the analysis

for the hourly storm rainfall. The total rainfall during the SPP was used to normalize the hourly rainfall amounts. The time scale (T_S) was computed to describe the time duration when half of the rainfall accumulated (R). The procedures used to calculate these parameters are listed below.

10.1.2 Parameters

SPP - Significant Precipitation Period when the majority of the rainfall occurred
R - Accumulated rainfall at the storm center during the SPP
R_n - Normalized R
T - Time when R occurred
T_s – Time when 50 percent accumulation occurs, value is set to zero. Negative time values precede the time to 50 percent rainfall, and positive values follow
T50 - Time when $R_n = 0.5$

10.1.3 Procedures used to calculate parameters

1. Determine the SPP. Inspect each storm's rainfall data for "inconsequential" rainfall at either the beginning and/or the end of the records. Remove these "tails" from calculations. Generally, AWA used a criterion of less than 0.1 inches/hour intensity to eliminate non-intense periods. No internal rainfall data were deleted.
2. Recalculate the accumulated rainfall records for R. This yields the SPP.
3. Plot the SPAS rainfall and R mass curves and inspect for reasonableness.
4. Normalize the R record by dividing all values by the total R to produce R_n for each hour, R_n ranges from 0.0 to 1.0.
5. Determine T50 using the time when $R_n = 0.5$.
6. Calculate T_s by subtracting T50 from each value of T. Negative time values precede the time to 50 percent rainfall, and positive values follow.
7. Determine max24hr and max6hr precipitation, convert accumulations into a ratio of the cumulative rainfall to the total accumulated rainfall for that duration.
8. Visually inspect resulting data to determine a best fit of the curves. This includes both the intensity (steepness) of accumulation and whether most of the accumulations are exhibiting a front, middle, or back loaded accumulation.

Graphs were prepared of a) R vs T, b) R_n vs T, c) R_n vs T_s, and d) maximum point precipitation for General (24-hour), Local (6-hour), Tropical (24-hour) storm events. Evaluations of the resulting rainfall accumulation curves individually and in relation to each other were completed by visually inspecting the data. From these investigations, a rainfall accumulation pattern that represented a significant majority of the patterns with a steep intensity was utilized as the synthetic pattern. This process is highly subjective. The objective of the process is to produce a synthetic pattern that captures the majority of the worst-case runoff scenarios for most basins and represents a physically possible temporal accumulation pattern. However, it is not possible for a single synthetic curve to capture all of the worst-case runoff scenarios for all basins. Therefore, the user should consult with the Colorad0 and New Mexico

dam safety offices for further guidance on temporal applications beyond what is provided in the GIS PMP tool.

10.1.4 Results of the Analysis

Following the procedures and description from the previous section, results are presented as three graphs. The graphs are a) R vs T, b) R_n vs T, and c) R_n vs T_s for Local, Hybrid, General, and Tropical storm types. Figure 54, Figure 55, and Figure 56 show these graphs for local SPAS storm events east of the Continental Divide while Figure 57, Figure 58, and Figure 59 show these graphs for local SPAS storm events west of the Continental Divide.

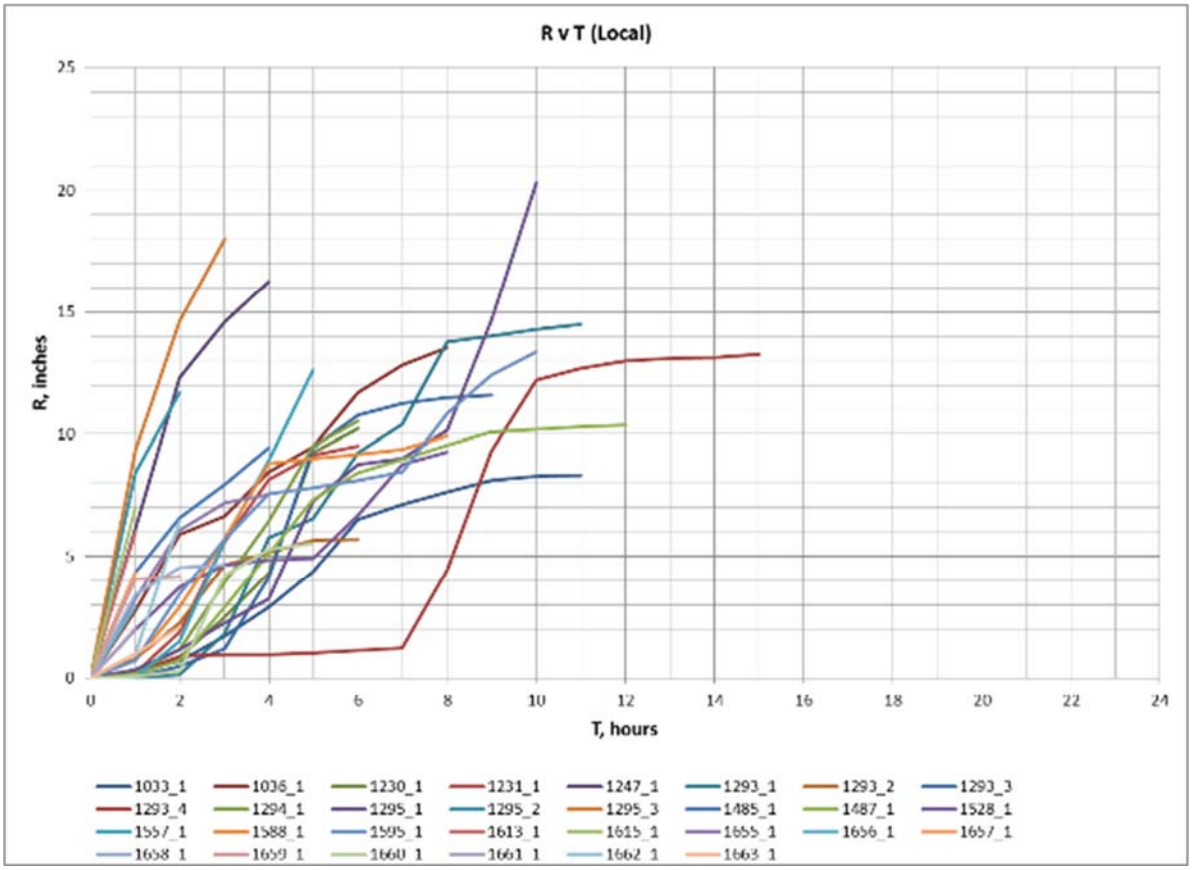

Figure 54: SPAS Rainfall (R) versus time (T) for Local Type Storm east of the Divide

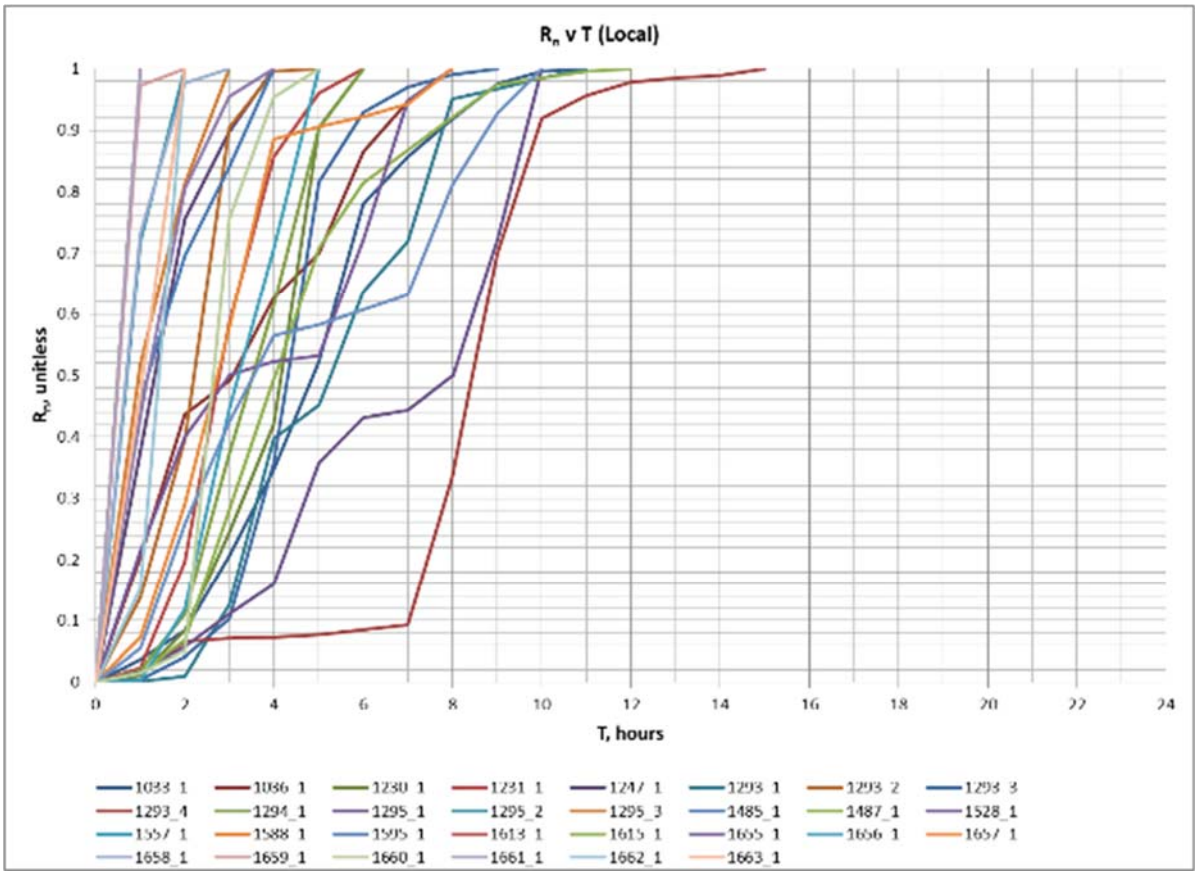

Figure 55: Normalized R (R_n) versus time (T) for Local Type Storm east of the Divide

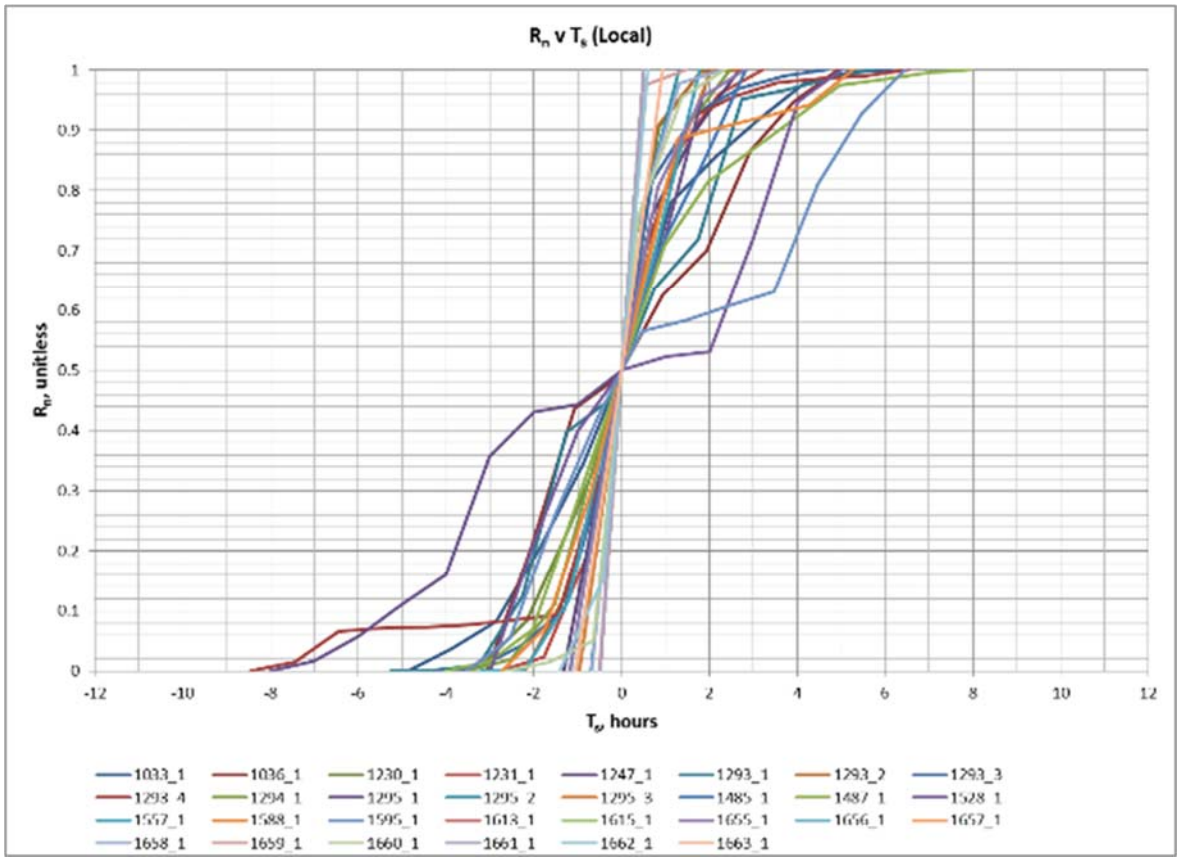

Figure 56: Normalized R (R_n) versus shifted time (T_s) for Local Type Storm east of the Divide

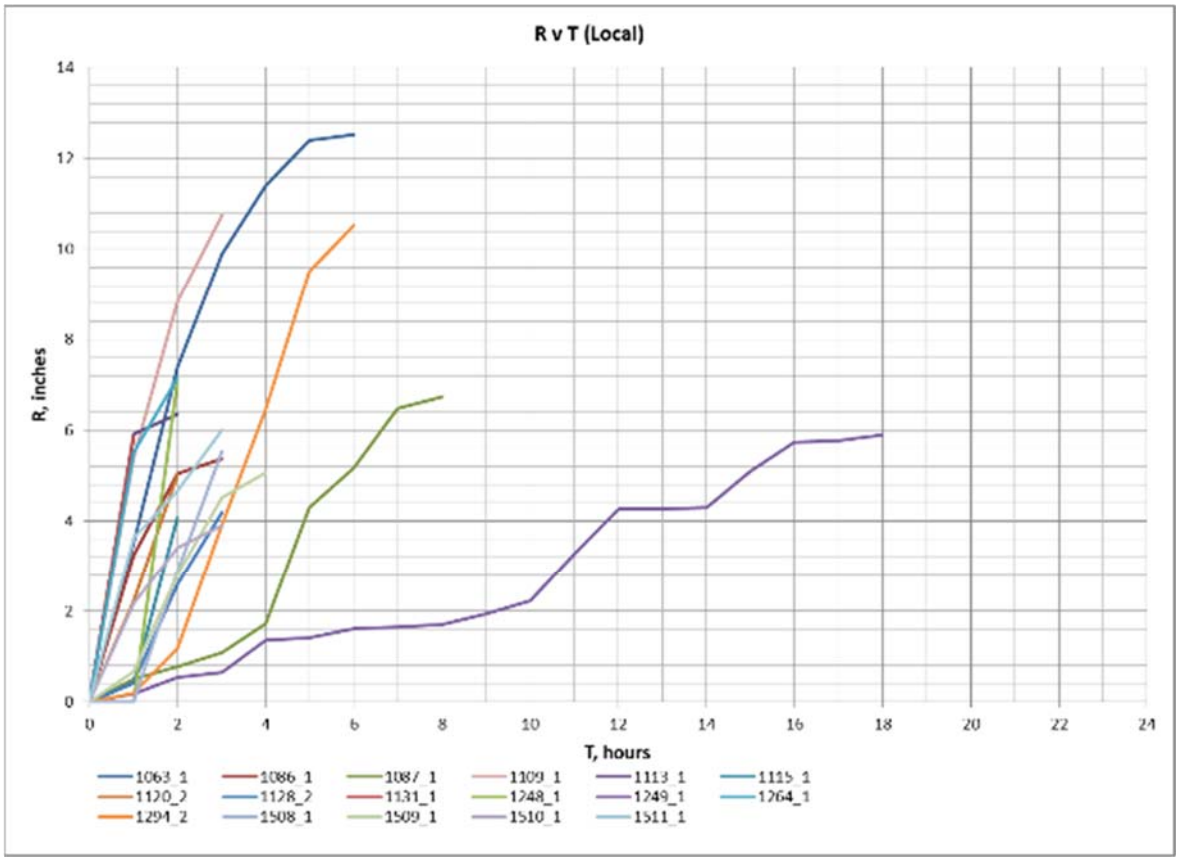

Figure 57: SPAS Rainfall (R) versus time (T) for Local Type Storm west of the Divide

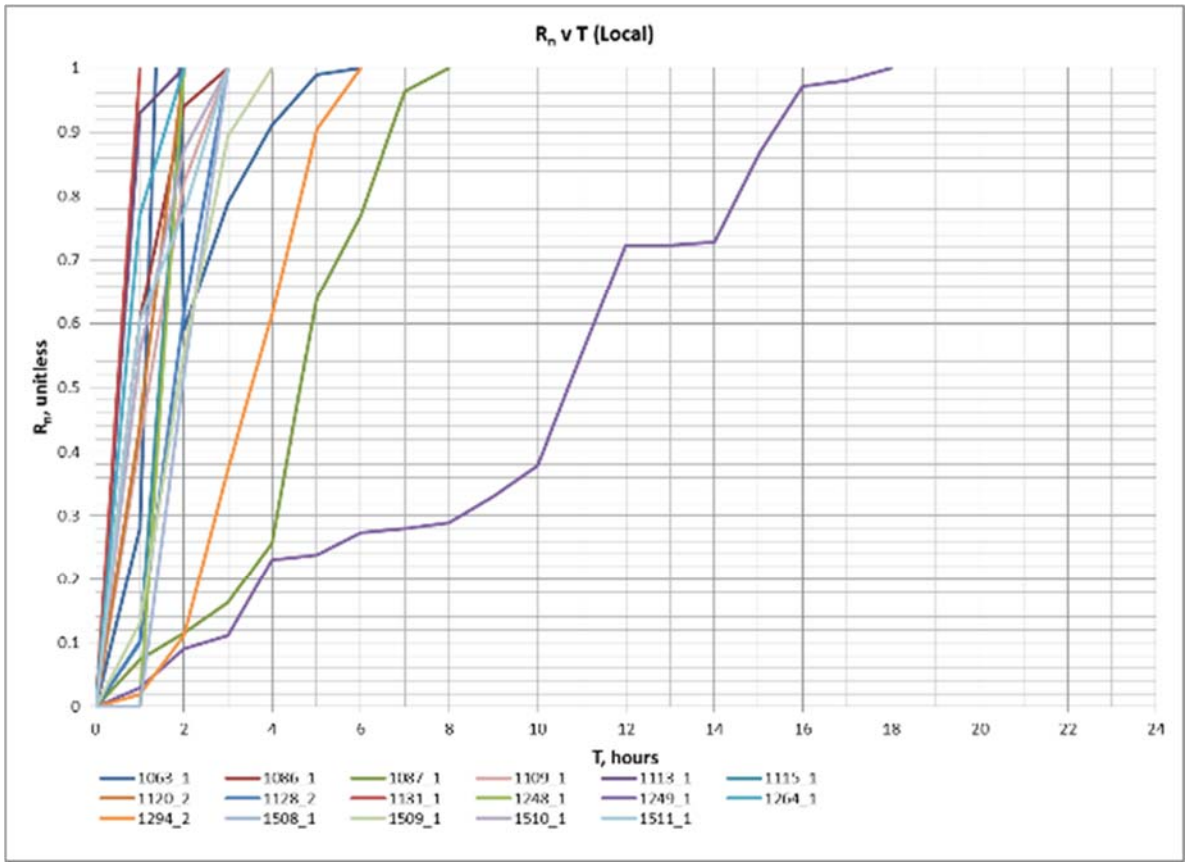

Figure 58: Normalized R (R_n) versus time (T) for Local Type Storm west of the Divide

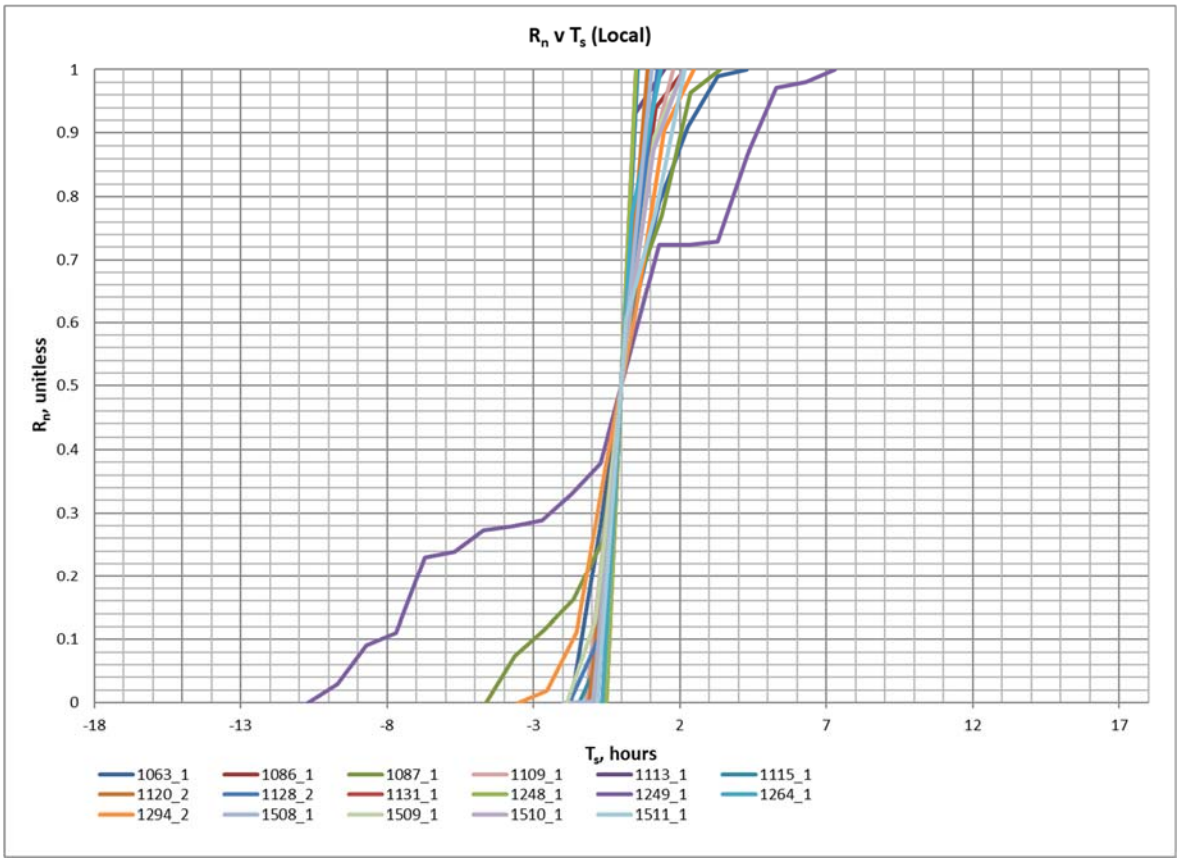

Figure 59: Normalized R (R_n) versus shifted time (T_s) for Local Type Storm west of the Divide

Figure 60, Figure 61, and Figure 62 show graphs for the Hybrid SPAS storm events east of the Continental Divide. There were no Hybrid storm types west of the Divide.

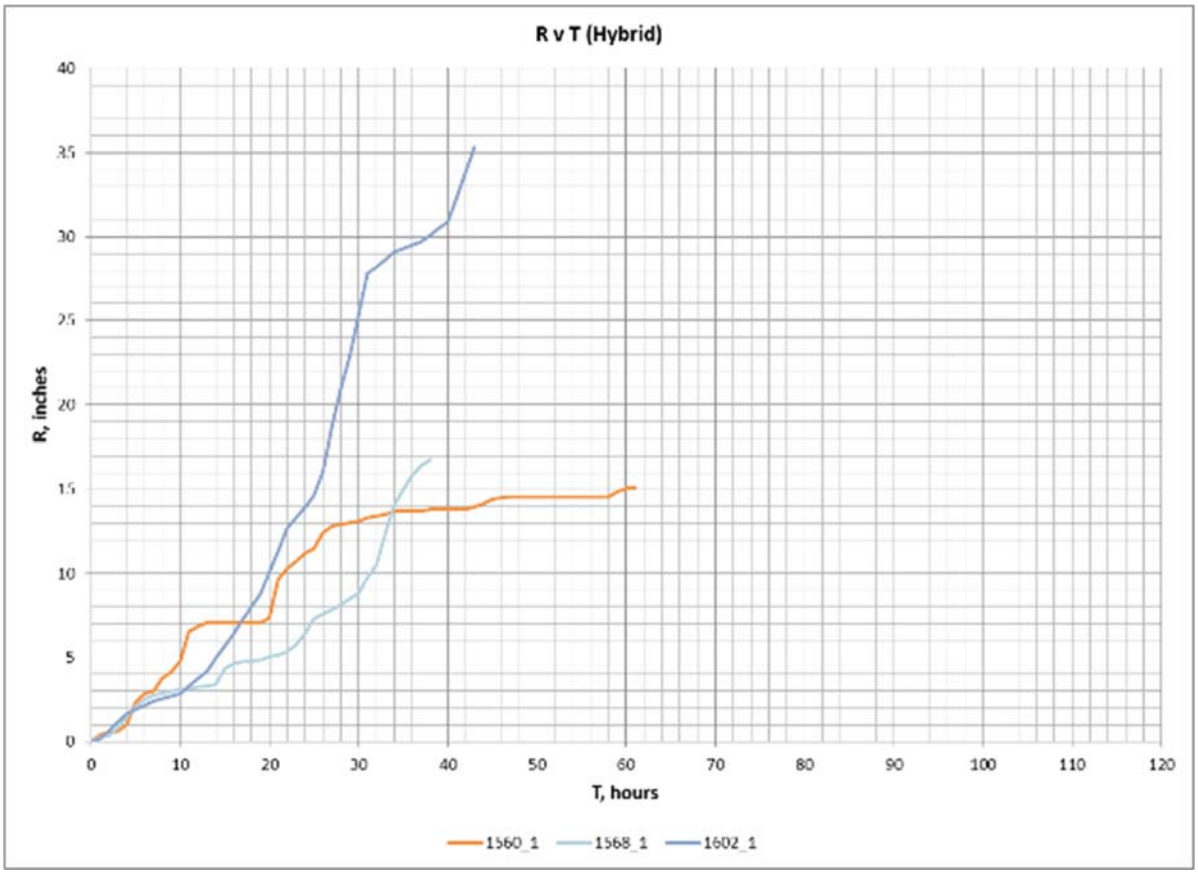

Figure 60: SPAS Rainfall (R) versus time (T) for Hybrid Type Storm east of the Divide

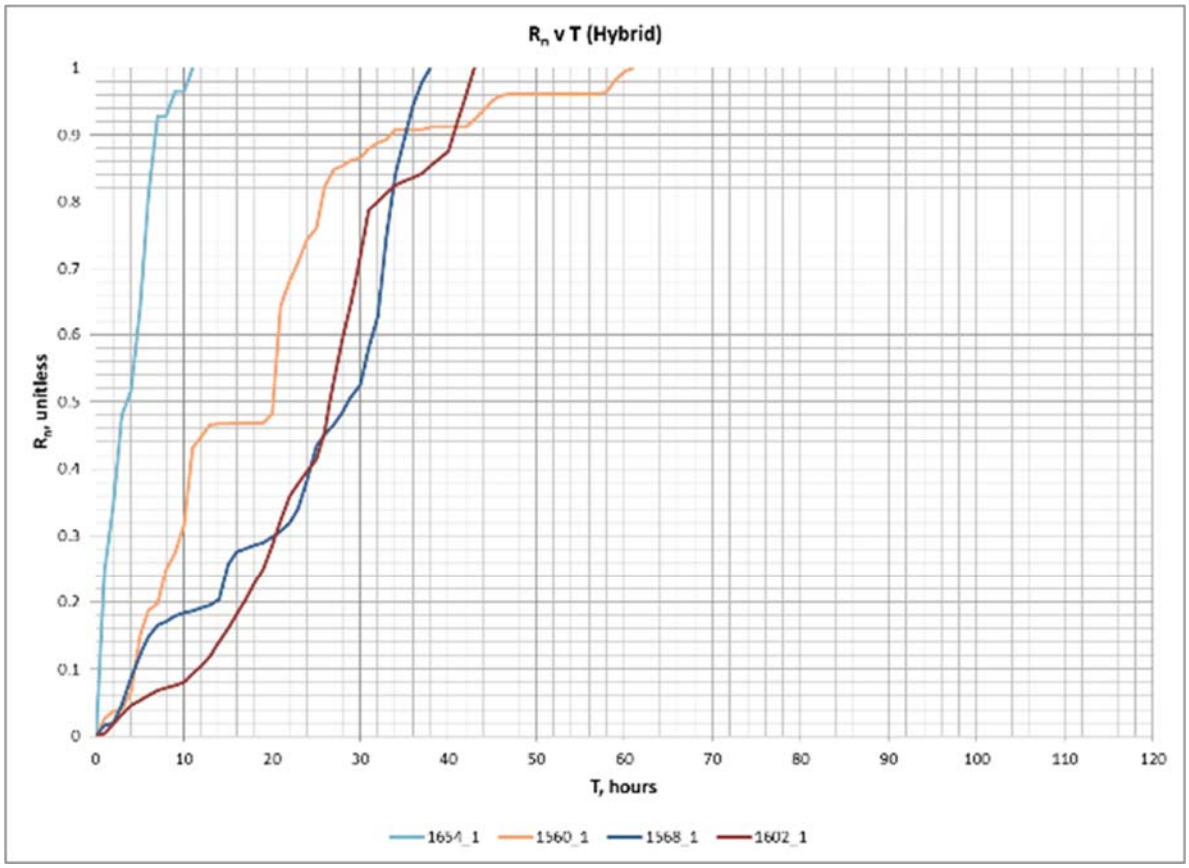

Figure 61: Normalized R (R_n) versus time (T) for Hybrid Type Storm east of the Divide

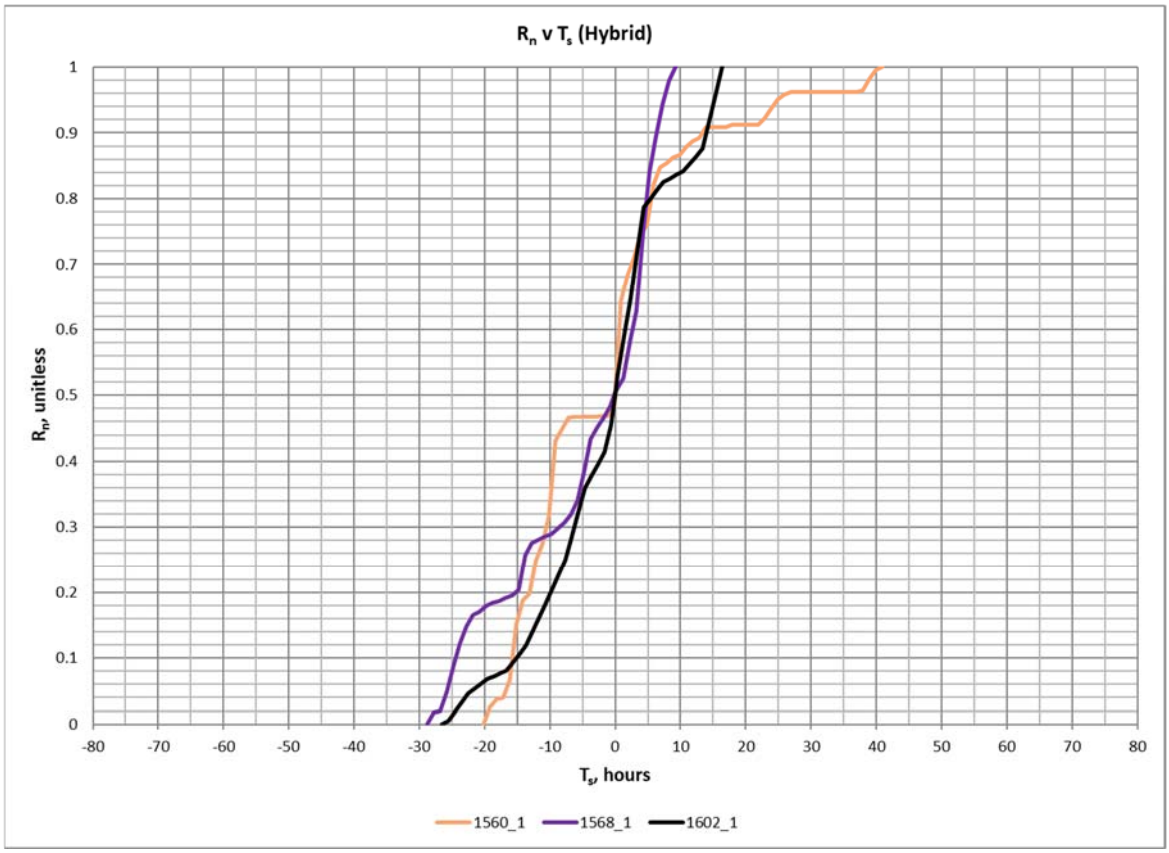

Figure 62: Normalized R (R_n) versus shifted time (T_s) for Hybrid Type Storm east of the Divide

Figure 63, Figure 64, and Figure 65 show graphs for General SPAS storm events east of the Continental Divide while Figure 66, Figure 67, and Figure 68 show these graphs for General SPAS storm events west of the Continental Divide.

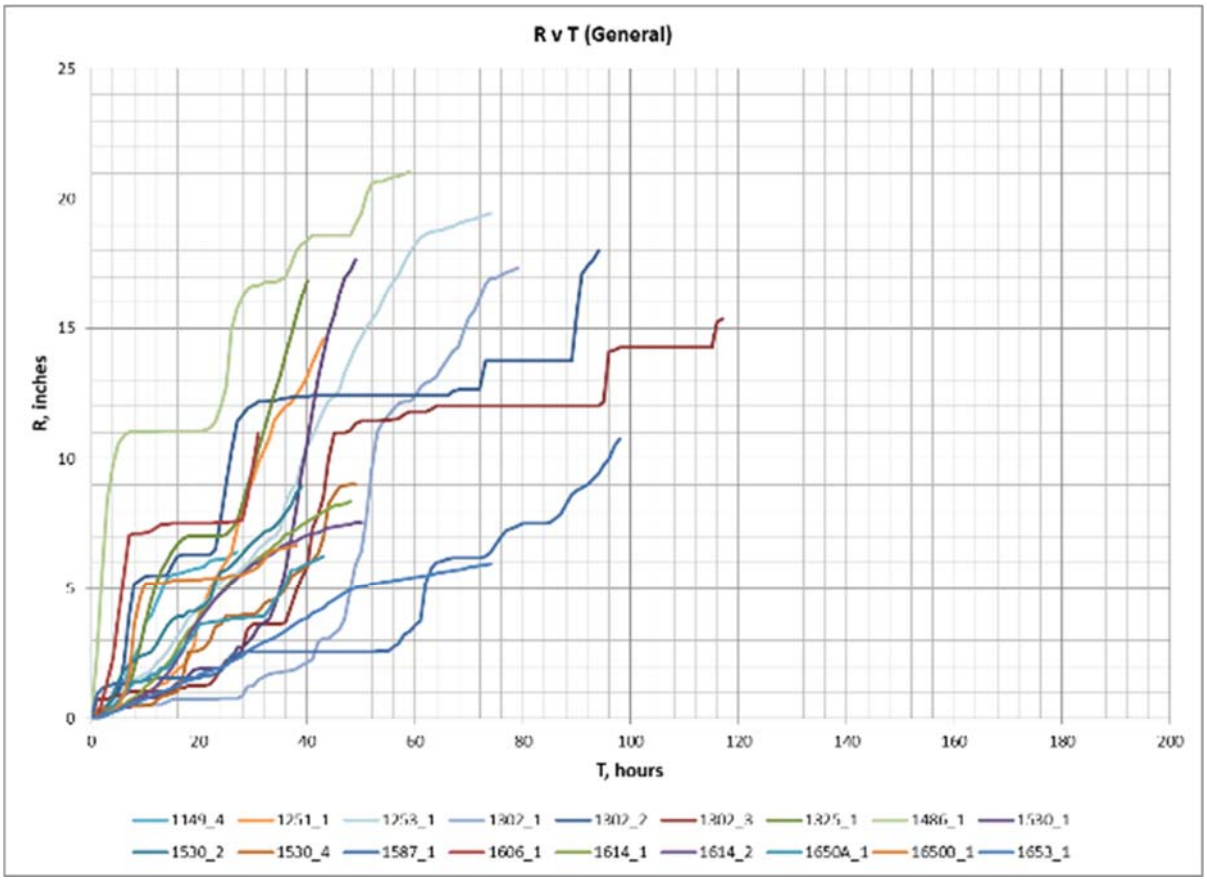

Figure 63: SPAS Rainfall (R) versus time for General Type Storm East of the Divide

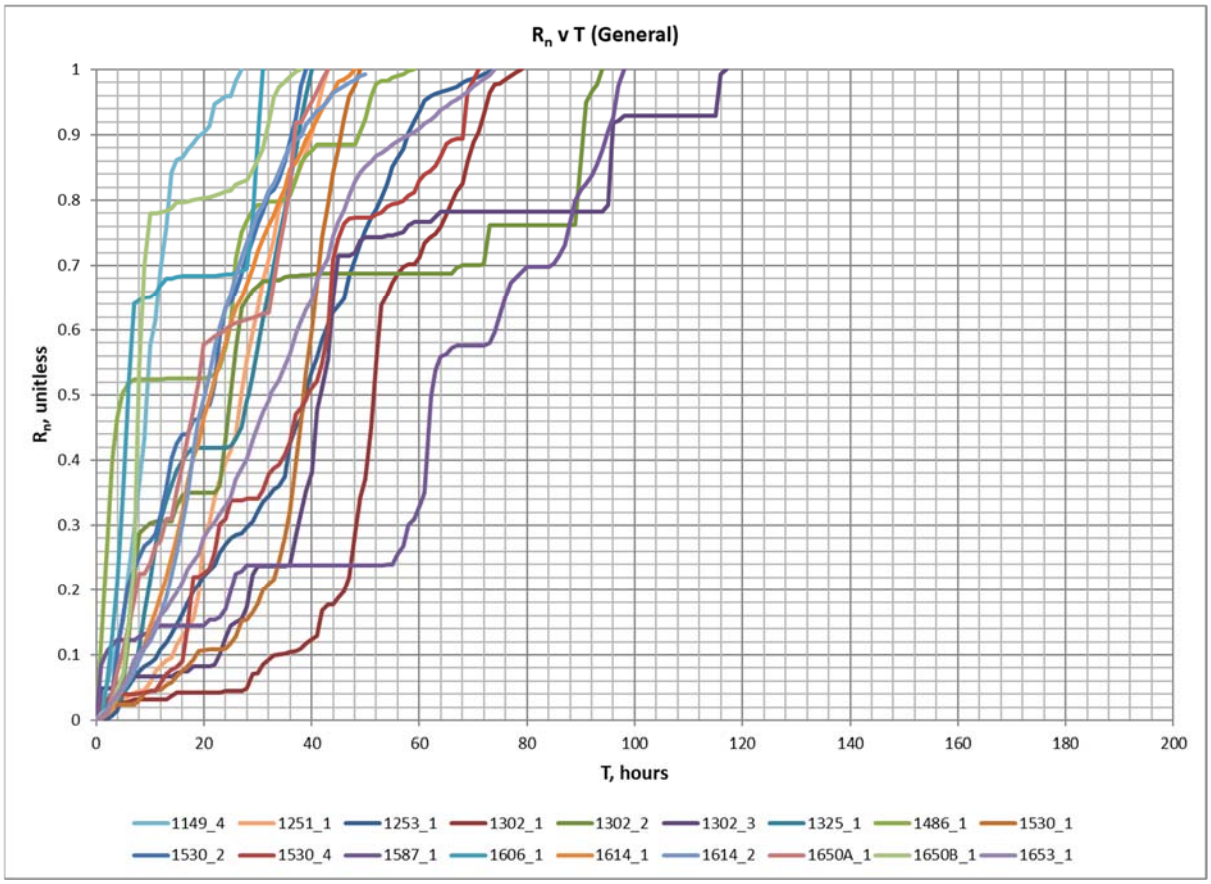

Figure 64: Normalized R (R_n) versus time (T) for General Type Storm East of the Divide

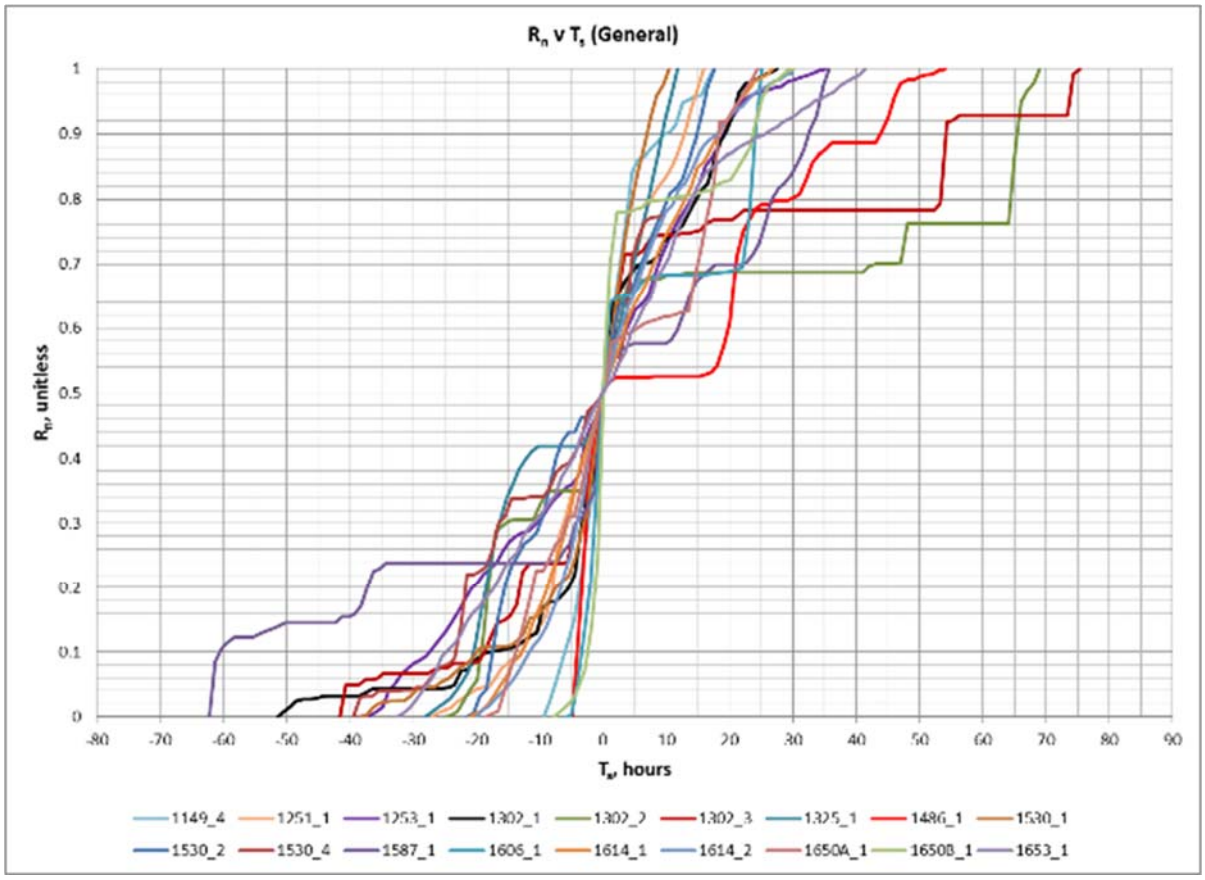

Figure 65: Normalized R (R_n) versus shifted time (T_s) for General Type Storm East of the Divide

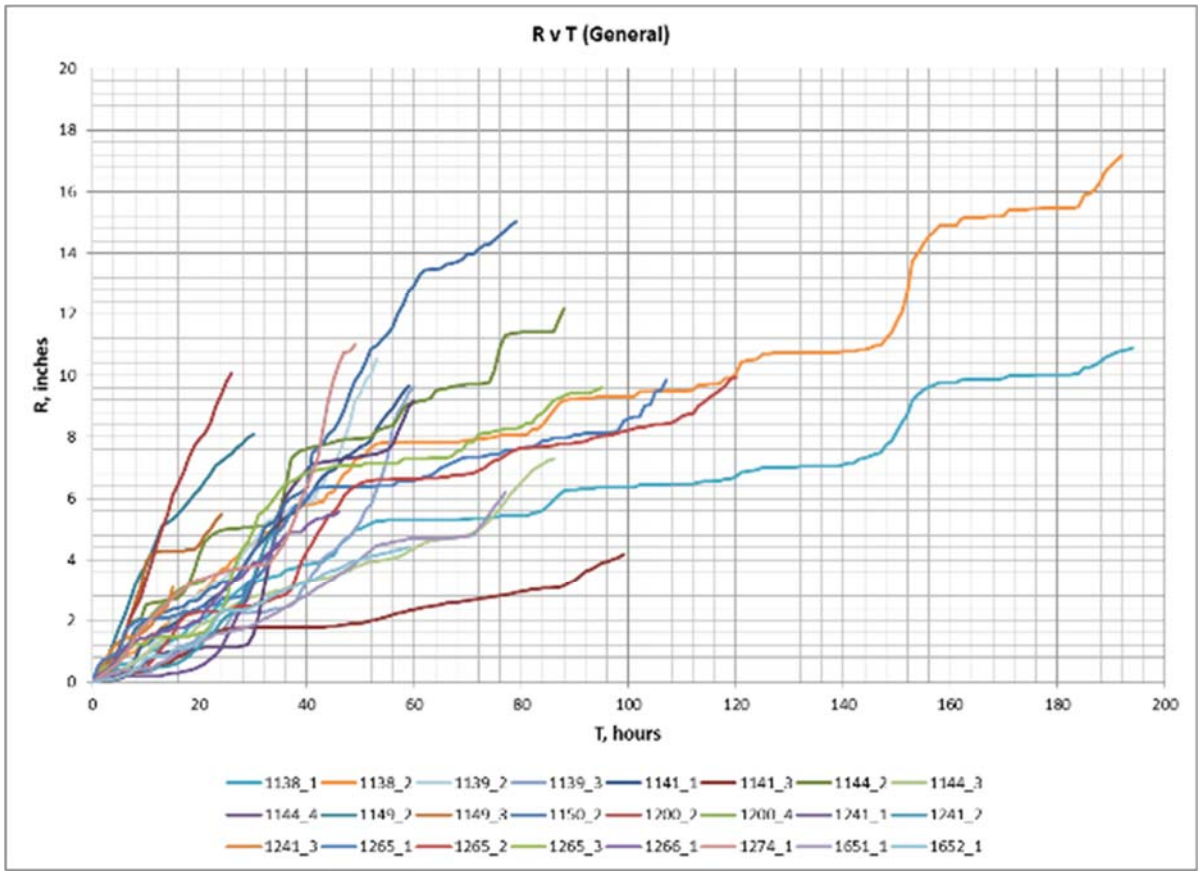

Figure 66: SPAS Rainfall (R) versus time for General Type Storm west of the Divide

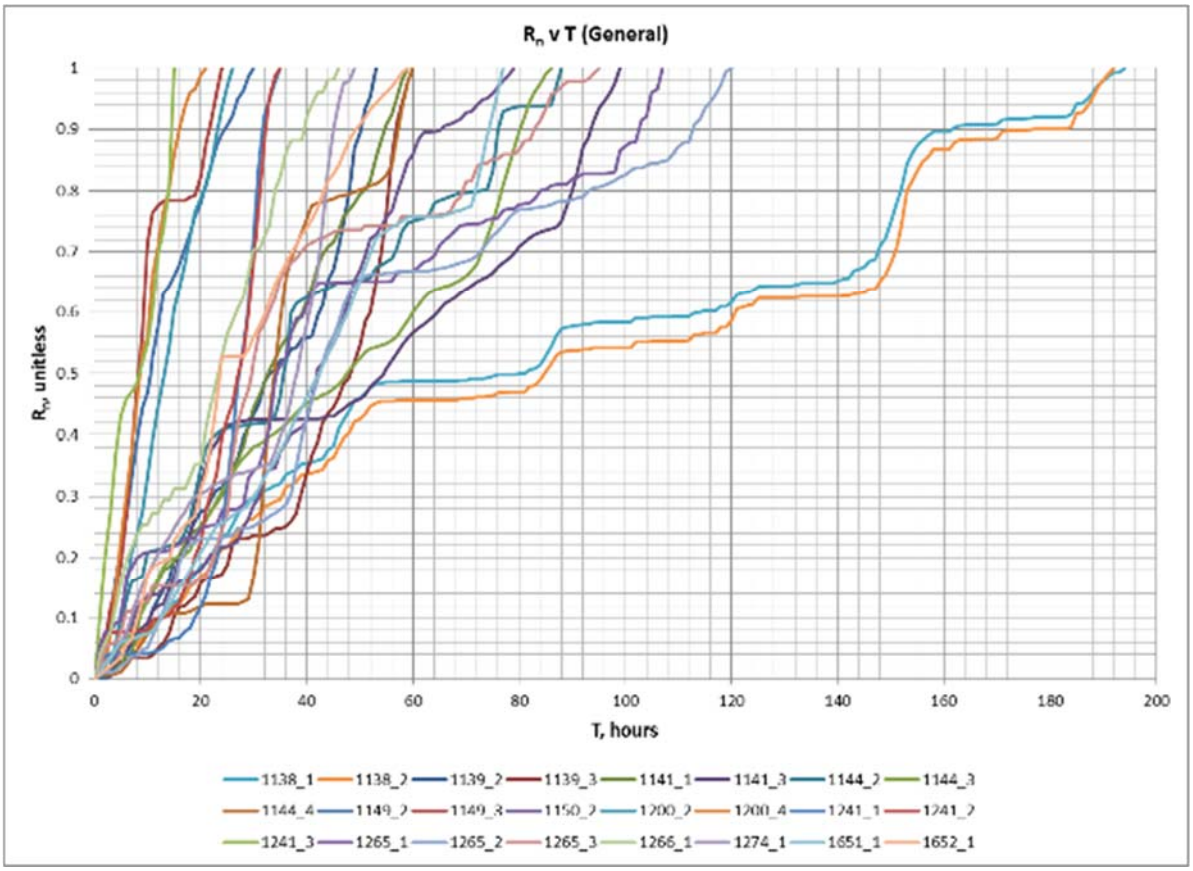

Figure 67: Normalized R (R_n) versus time (T) for General Type Storm west of the Divide

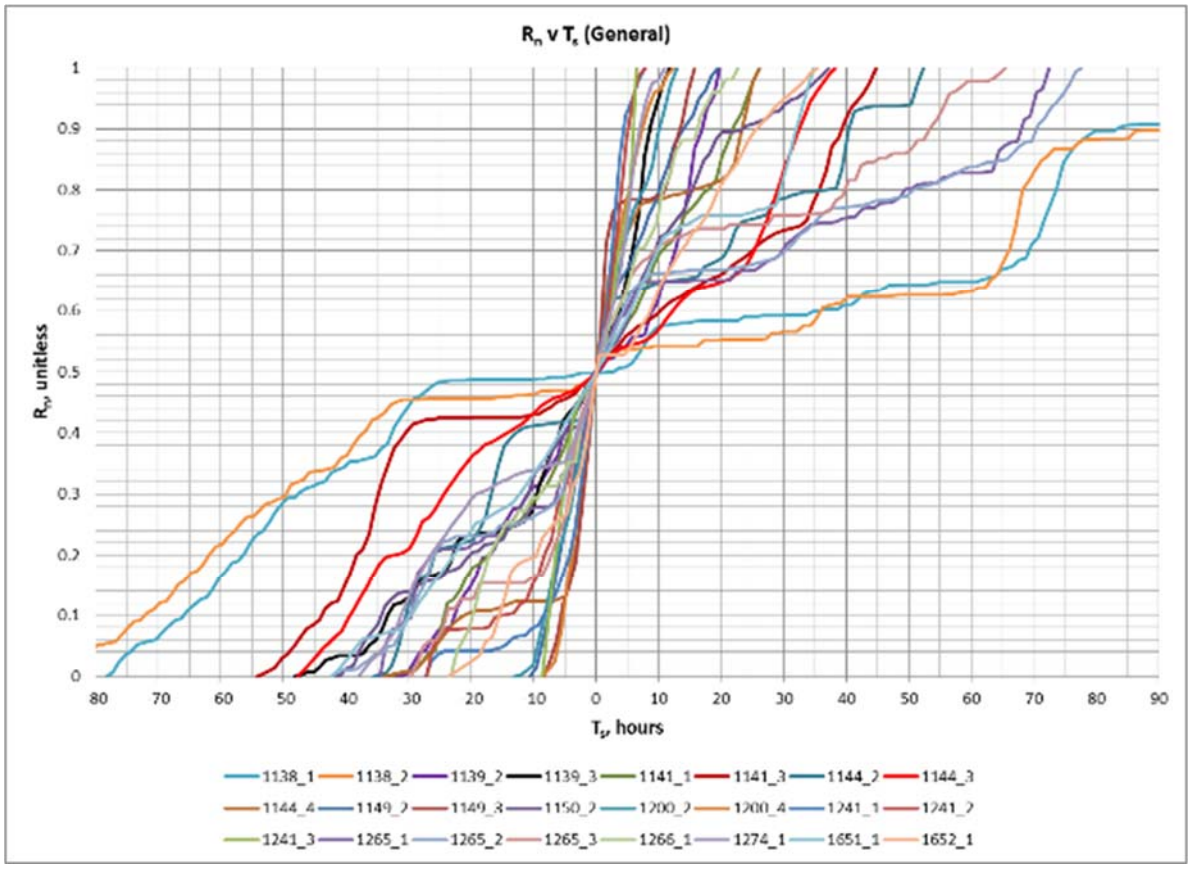

Figure 68: Normalized R (R_n) versus shifted time (T_s) for General Type Storm west of the Divide

Figure 69, Figure 70, and Figure 71 show graphs for Tropical SPAS storm events east of the Continental Divide while Figure 72, Figure 73, and Figure 74 show these graphs for Tropical SPAS storm events west of the Continental Divide.

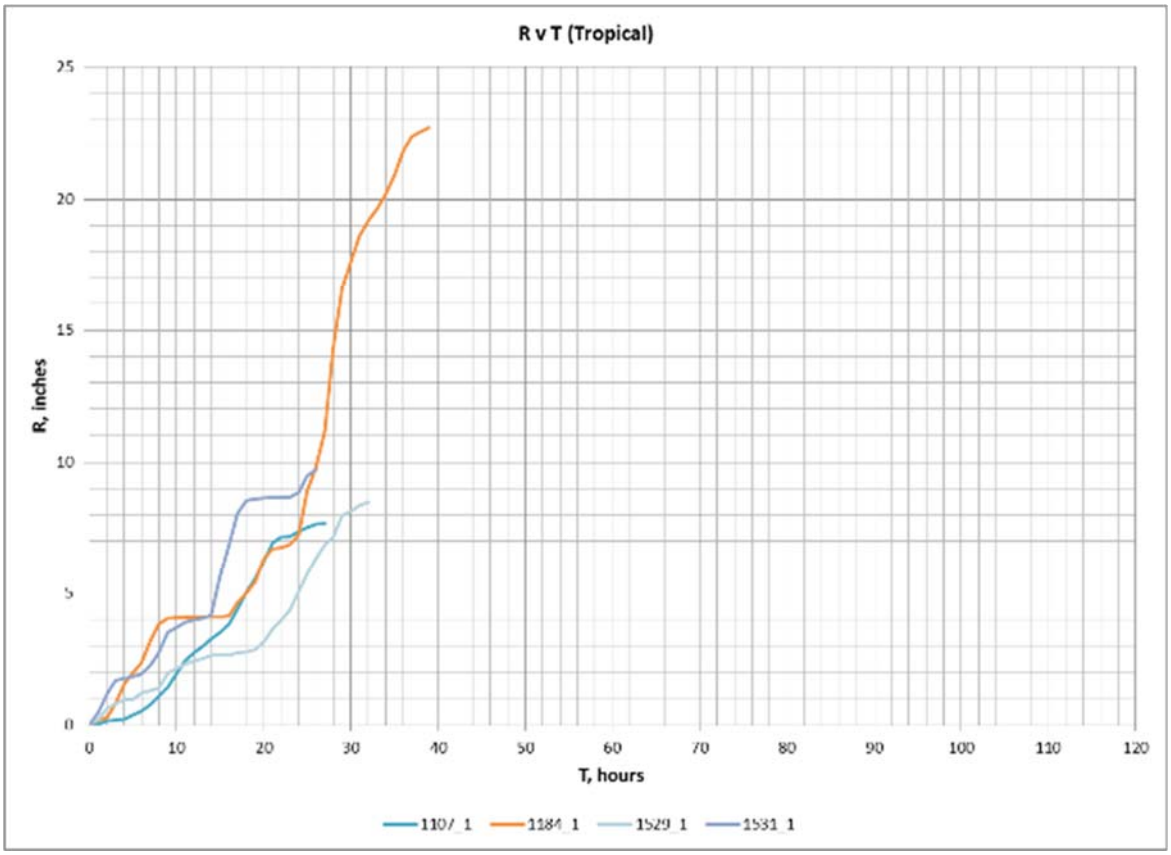

Figure 69: SPAS Rainfall (R) versus time for Tropical Type Storm East of the Divide

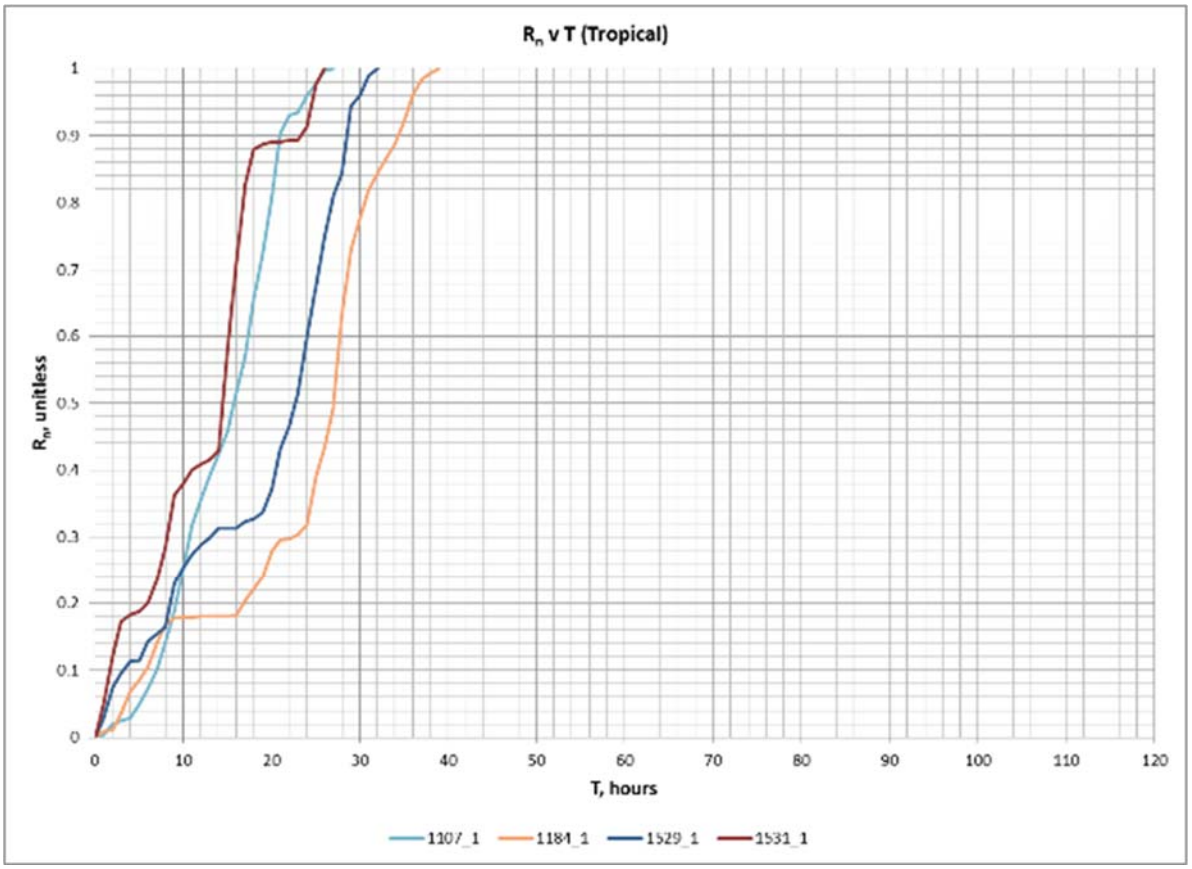

Figure 70: Normalized R (R_n) versus time for Tropical Type Storm East of the Divide

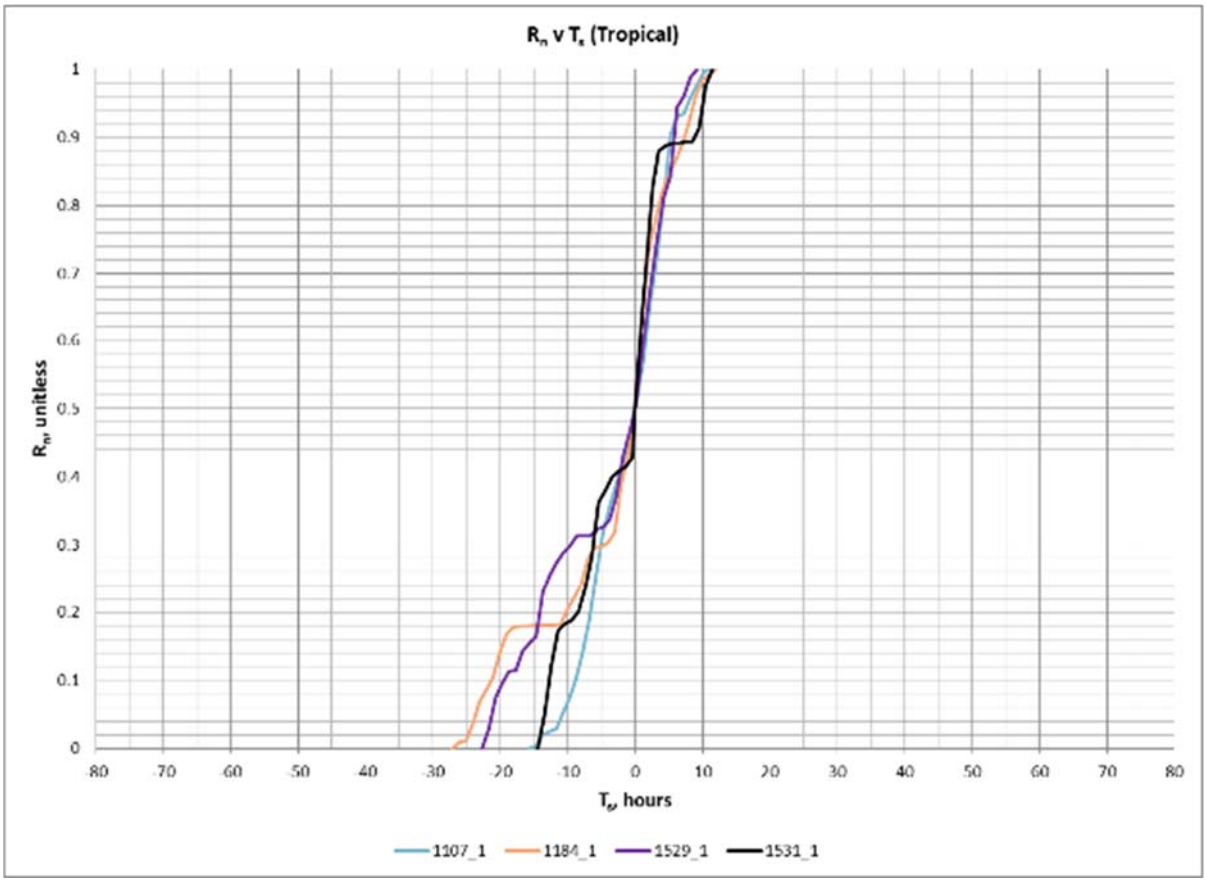

Figure 71: Normalized R (R_n) versus shifted time (T_s) for Tropical Type Storm East of the Divide

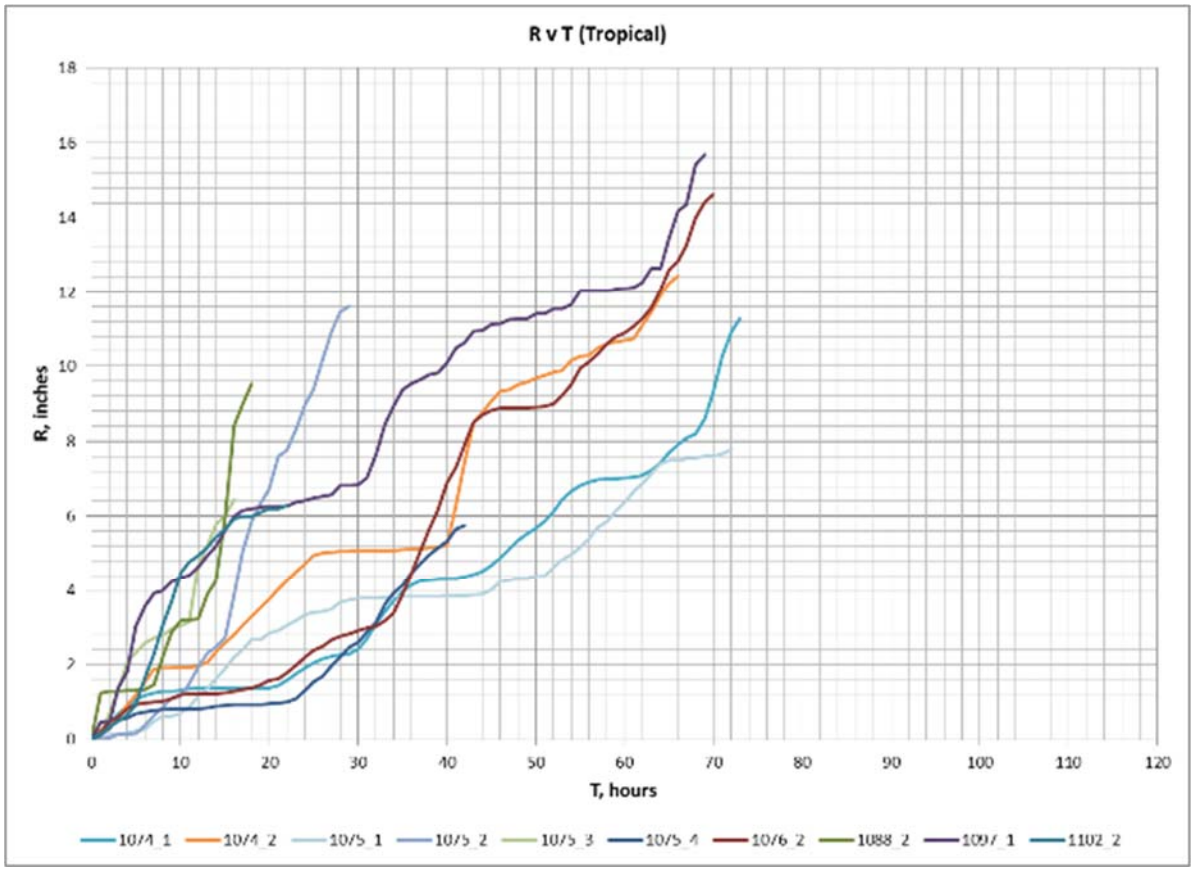

Figure 72: SPAS Rainfall (R) versus time for Tropical Type Storm west of the Divide

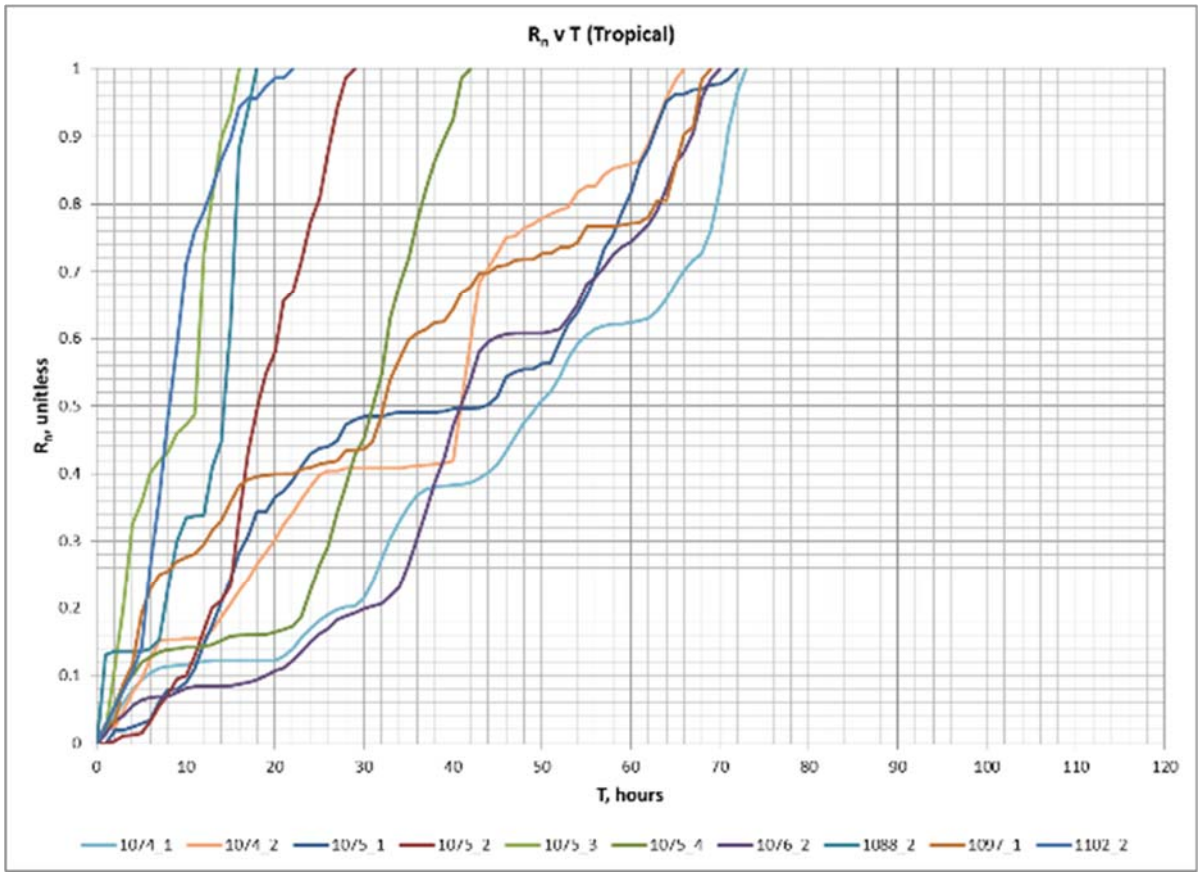

Figure 73: Normalized R (R_n) versus time for Tropical Type Storm west of the Divide

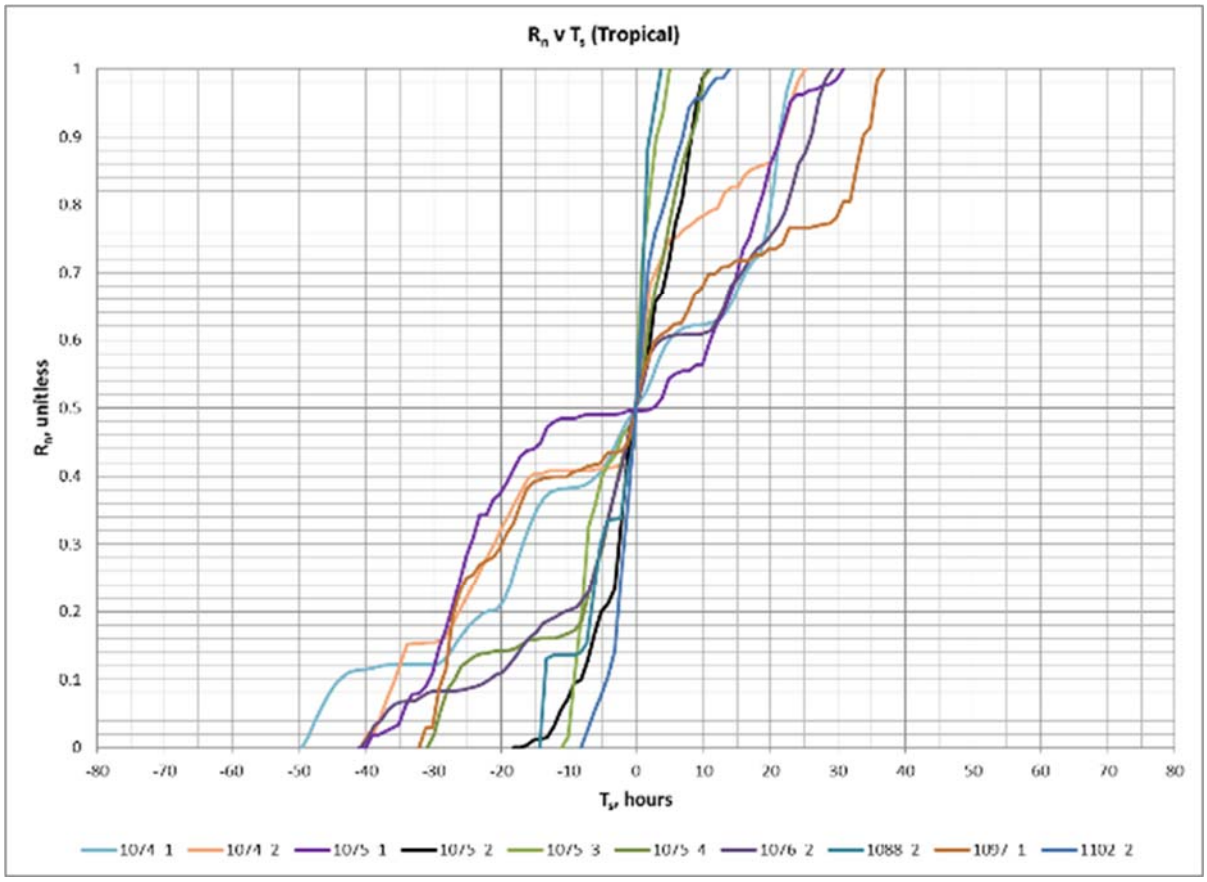

Figure 74: Normalized R (R_n) versus shifted time (T_s) for Tropical Type Storm west of the Divide

10.2 Huff Curve Methodology

Huff curves provide a method of characterizing storm mass curves. They are a probabilistic representation of accumulated storm depths for corresponding accumulated storm durations expressed in dimensionless form. The development of Huff curves are described in detail in Huff (1967) and Bonta (2003), a summary of the steps are listed below.

For each SPAS storm center mass curve, the core cumulative precipitation amounts (R, noted in above section) were identified, the core cumulative rainfall were non-dimensionalized and converted into percentages of the total precipitation amount at one-hour time steps. The non-dimensionalized duration values were interpolated and extracted at 0.02 increments from 0 to 1. Storms were grouped by geographic location (east versus west of the Continental Divide) and by storm type: local, general, tropical, and hybrid. The uniform incremental storm data (by duration and location) were combined and probabilities of occurrence were estimated at each 0.02 increment. Probabilities were estimated as 0.1 increments. The raw recommended curves (90th and 10th) were smoothed using a non-linear regression. Smoothing of the raw curves is performed to account for statistical noise in the analysis (Huff 1967; Bonta 2003).

The curves generated in this study can be generically described as:

- 90th curve - the 90th curve indicates that 10 percent of the corresponding SPAS storms had distributions that fell above and to the left of the90thcurve (front-loaded)
- 50th curve - the 50th curve indicates that 50 percent of the corresponding SPAS storms had distributions that fell above and below the 50th curve (mid-loaded)
- 10th curve - the 10th curve indicates that 10 percent of the corresponding SPAS storms had distributions that fell below and to the right of the 10th curve (back-loaded)

The raw data results are presented below (Figures 75-81), the final curves selected for use were smoothed using non-linear regression and data were provided at 5-minute (local storms) and 15-minute (general, hybrid, tropical) time steps from the non-linear regression equation (data were extracted from the non-linear equation). Some of the Huff curves result in accumulated precipitation at time zero, this is a result of front-loaded storms that generate a significant portion of their precipitation in the first hour, the analysis was performed on hourly data, and the interpolation method for did not force the curve to zero. The final set of Huff curves were set to zero at time zero. The NRCS Type II curve (also known as the SCS curve) is considered a standard temporal pattern for design purposes in many regions of the country; see Section 10.6 for additional description (NRCS, 2005). The Type II curve is added to figures in its native state for comparison (Type II).

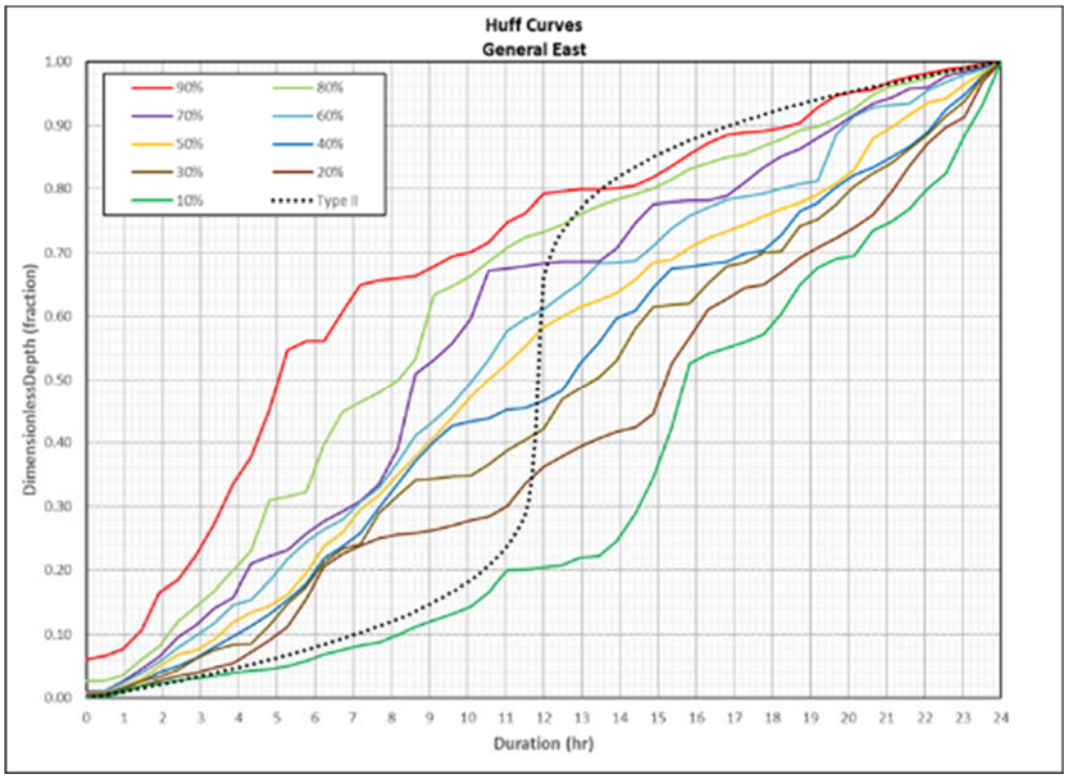

Figure 75: Raw Huff temporal curves for General storms East of the Continental Divide

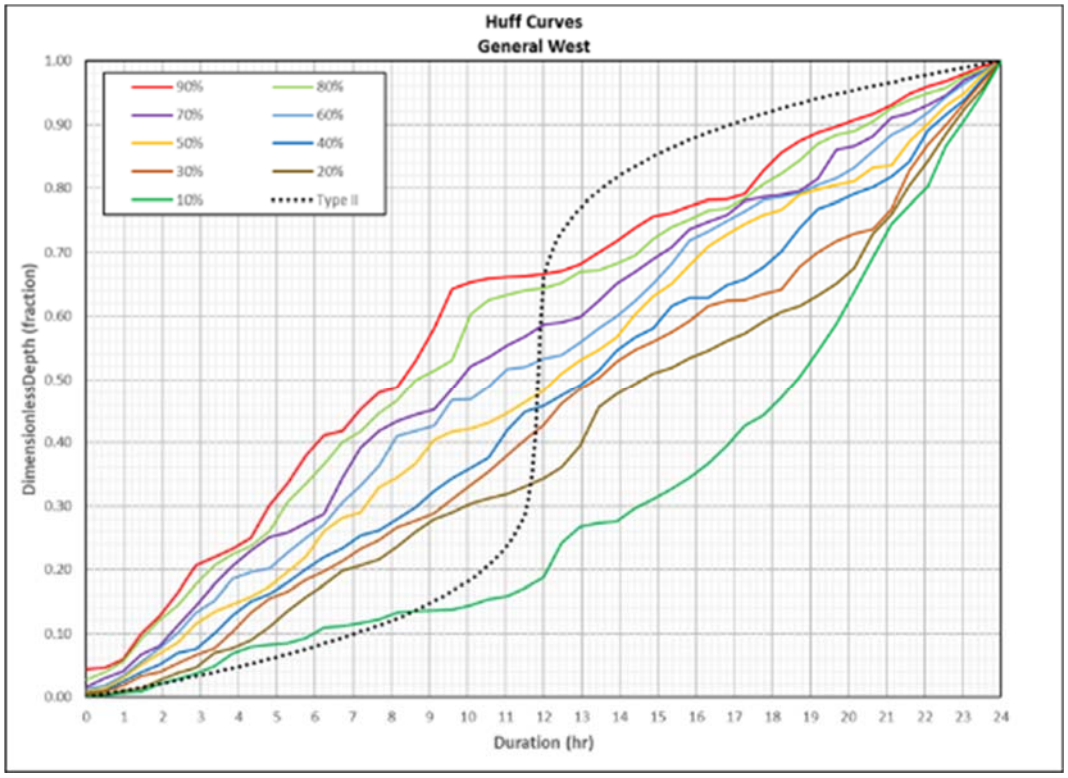

Figure 76: Raw Huff temporal curves for General storms west of the Continental Divide.

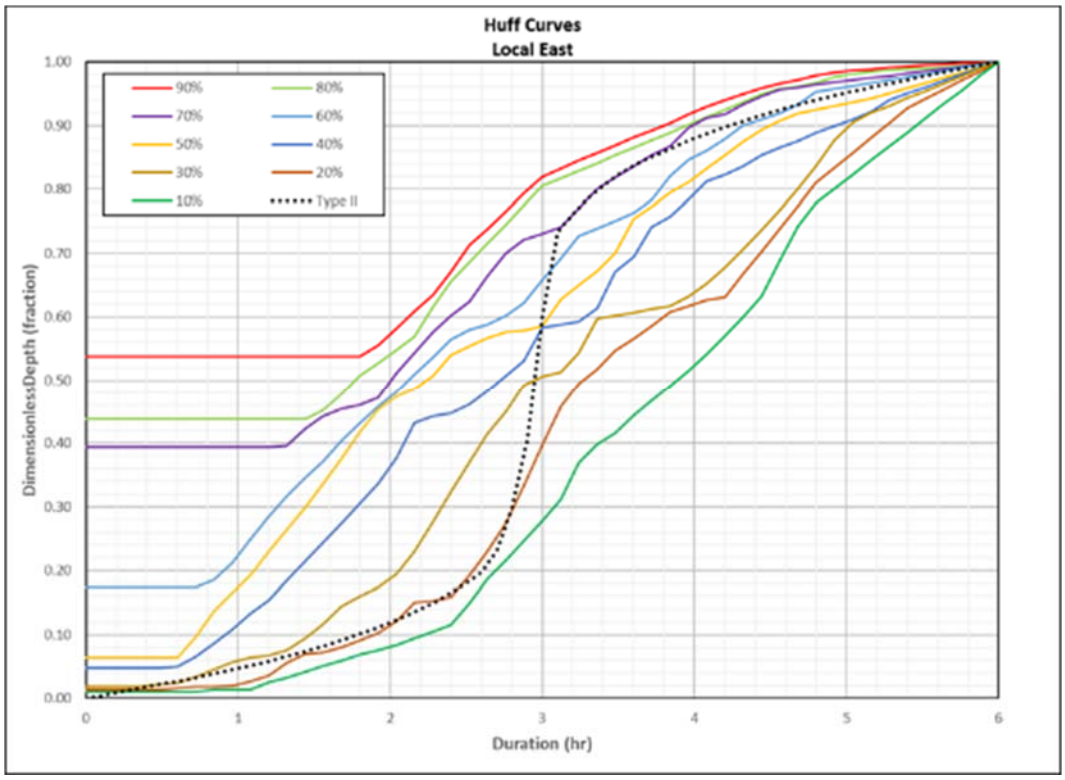

Figure 77: Raw Huff temporal curves for Local storms East of the Continental Divide

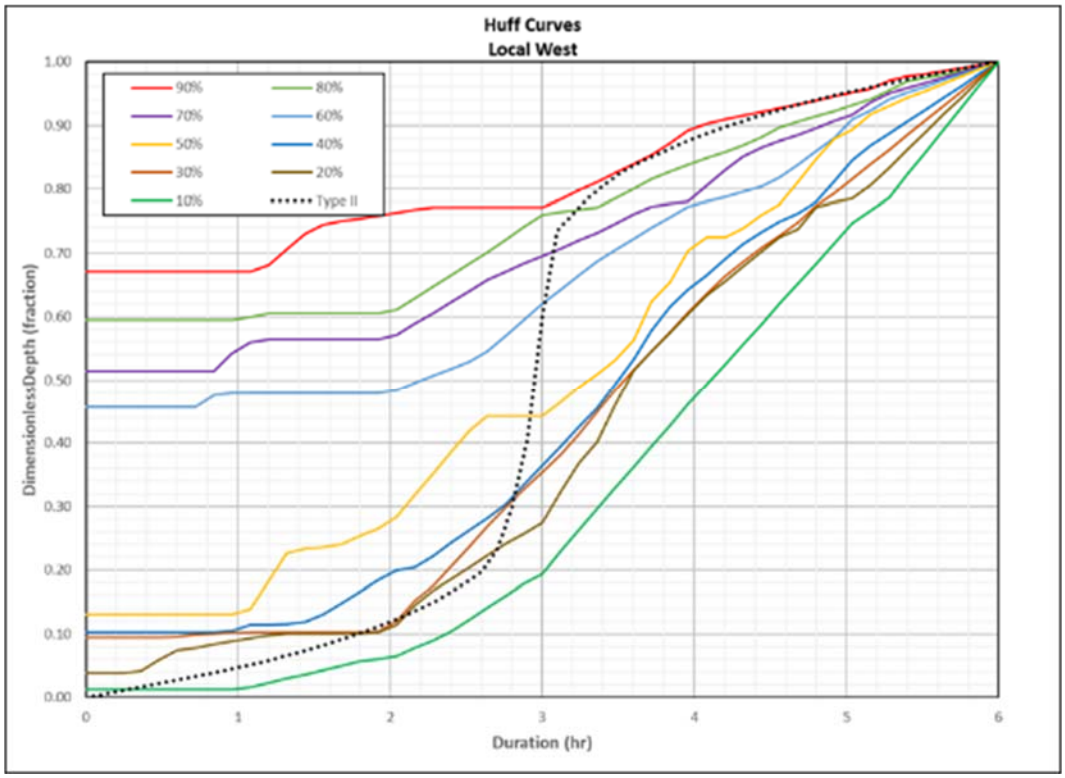

Figure 78: Raw Huff temporal curves for Local storms west of the Continental Divide

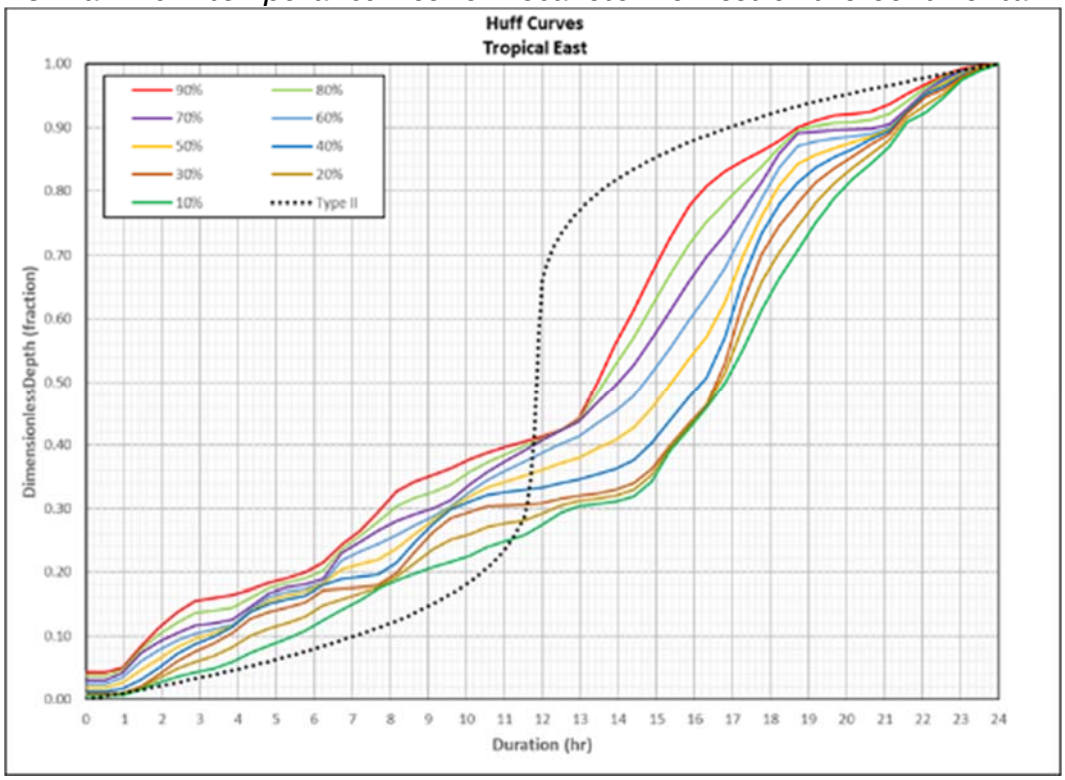

Figure 79: Raw Huff temporal curves for Tropical storms East of the Continental Divide.

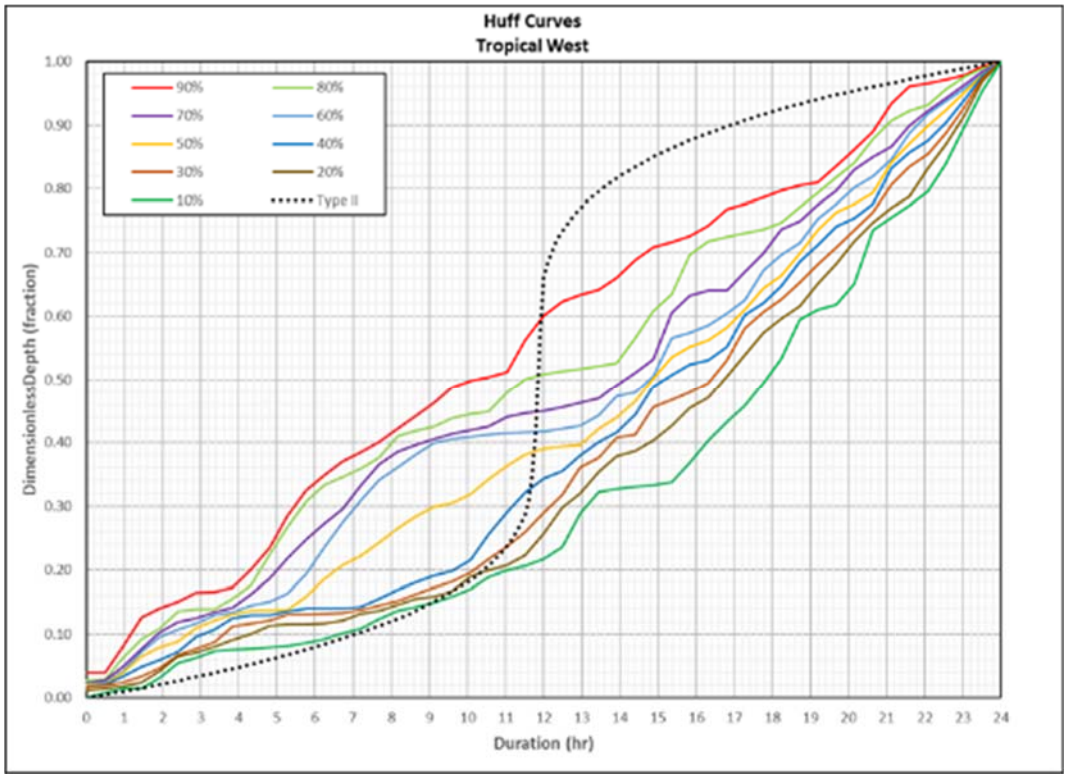

Figure 80: Raw Huff temporal curves for Tropical storms west of the Continental Divide.

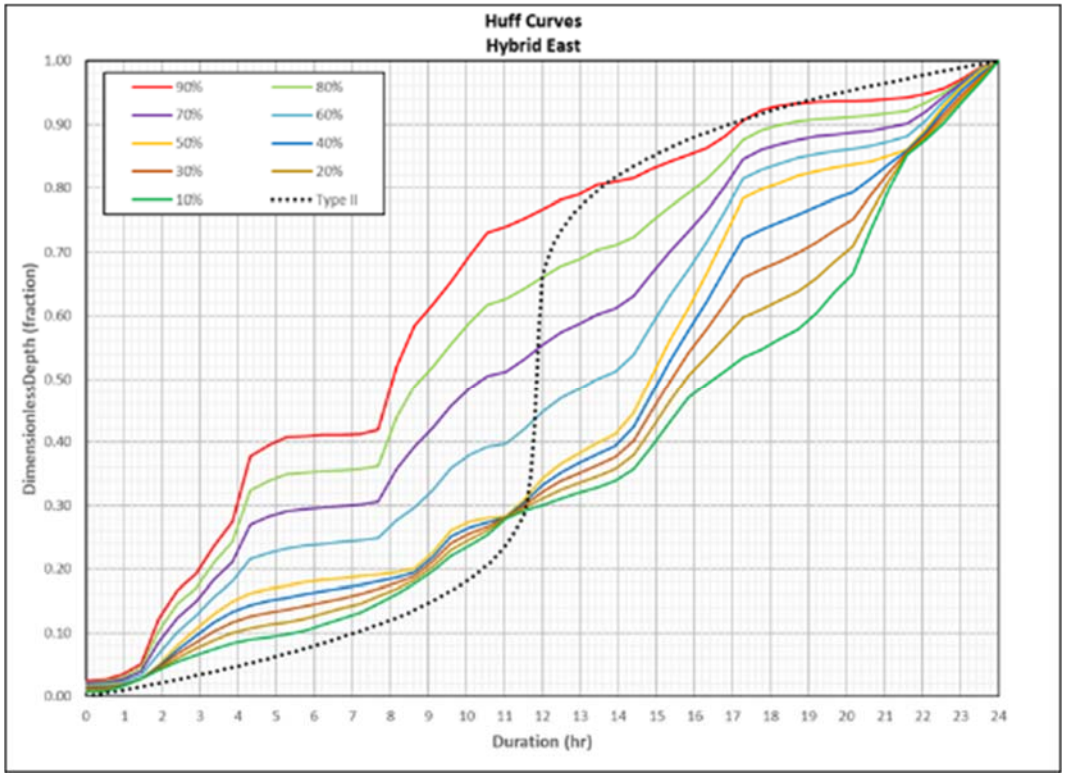

Figure 81: Raw Huff temporal curves for Hybrid storms East of the Continental Divide

10.3 Alternating Block (Critically Stacked) Pattern

Based on HMR 52 (Hansen et al., 1982) procedures and the USBR Flood Hydrology Manual (Cudworth, 1989) a "critically stacked" temporal distribution was developed to try and develop a synthetic rainfall distribution. The critically stacked temporal pattern yields a significantly different distribution than actual distributions associated with the storms used for PMP development in the CO-NM REPS study and in similar analysis of adjacent PMP studies (e.g., Arizona and Wyoming). The critically stacked pattern imbeds PMP values by duration within one another, i.e. the one-hour PMP is imbedded within the 3-hour, which is imbedded within the 6-hour, which is in turn imbedded in the 24-hour PMP. Figure 82 provides a graphical illustration of a critically stacked pattern. The critically stacked procedure has often been chosen in the past for runoff modeling because it represents a worst-case design scenario and ensures PMP depths are equaled at all durations.

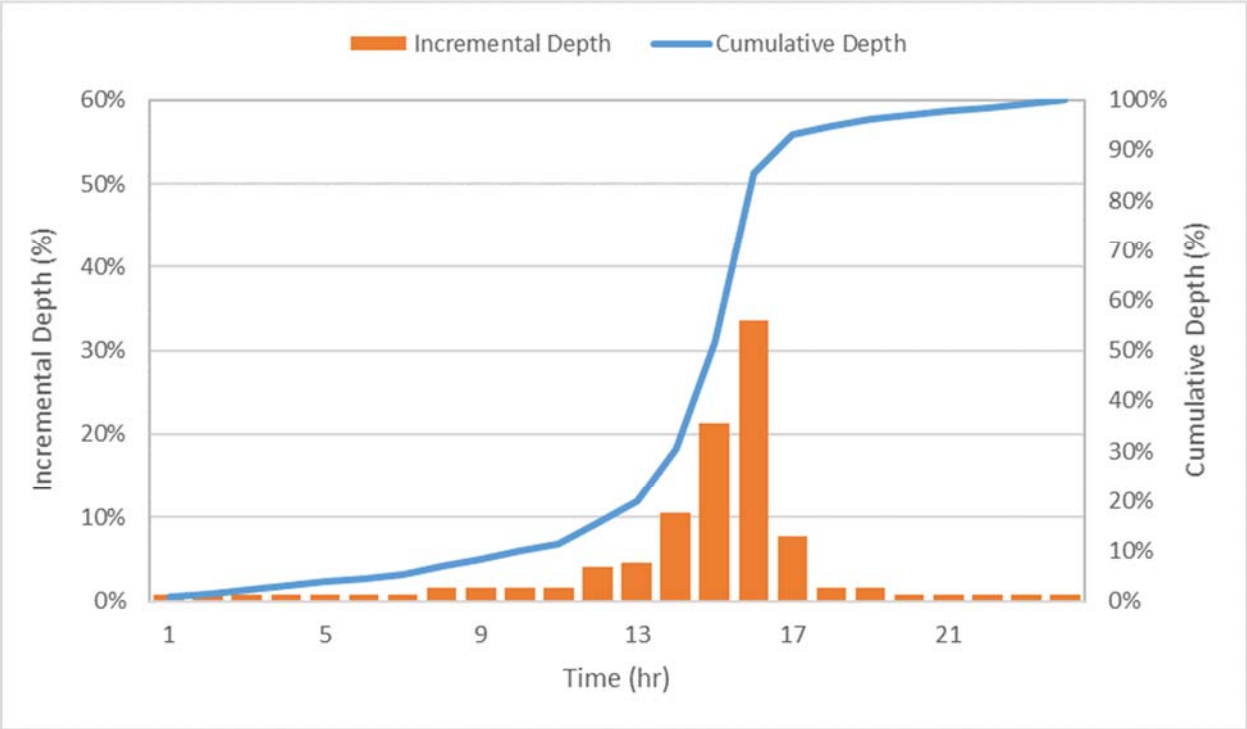

Figure 82: Graphical representation of the critically stacked temporal pattern

10.4 Sub-hourly Timing and 2-hour Local Storm Timing

AWA evaluated the 5-minute incremental rainfall accumulations patterns for twenty-seven storms from the PMP short-list that had been analyzed with SPAS-NEXRAD to identify events that could be used to derive site-specific sub hourly accumulation guidance. This SPAS-NEXRAD 5-minute data was used to derive ratios of the greatest 15-, 30-, and 45-minute accumulations during the greatest 1-hour rainfall accumulation. Data from these twenty-seven storms events allowed a specific evaluation of the sub-hourly rainfall patterns to be evaluated for the CO-NM REPS study region.

For comparison, HMR 55A provided recommended temporal patterns to be applied to the PMP to estimate sub-hourly timing. It is important to note that the 15-minute incremental accumulation ratios derived for the local PMP storm in HMR 55A are based on very limited (almost none) sub-hourly data. HMR 55A referred to the limited amount of available data and suggested using HMR 49 information instead (HMR 55A Section 12.7).

Table 5 displays the results of this analysis. The largest difference between HMR 55A and this study occurs during the greatest 15-minute increment, where HMR 55A provides a value of 68 percent (see HMR 55A Table 12.4), while the actual storm data have an average of 39 percent and a maximum of 64 percent. AWA completed additional sensitivity analysis by comparing the sub hourly ratio data to similar data developed during the Arizona statewide PMP study (Kappel et al., 2013). The results from the Arizona statewide PMP analysis are provided in Table 5 for comparison with the CO_NM REPS results. The 2-hour local storm temporal pattern was developed to account for local storms that are less than 2-hours. The 2-hour local storm temporal pattern utilized the 5-min sub-hourly ratio data (average CO/NM) for the first hour and the second hour was evenly distributed. For example, if a storm event had 8-inches in the first hour and 1-inch in the second hour for a total storm of 9-inches the accumulation pattern is shown in Figure 83.

Table 5: Sub-hourly ratio data from HMR 55A and the Colorado-New Mexico study

Duration (hr)	HMR 55A	Average CO/NM	Maximum CO/NM	Average AZ
0.25	68%	39%	64%	34%
0.50	86%	65%	88%	61%
0.75	94%	84%	100%	82%
1	100%	100%	100%	100%
2	116%			
3	123%			
4	128%			
5	132%			
6	135%			

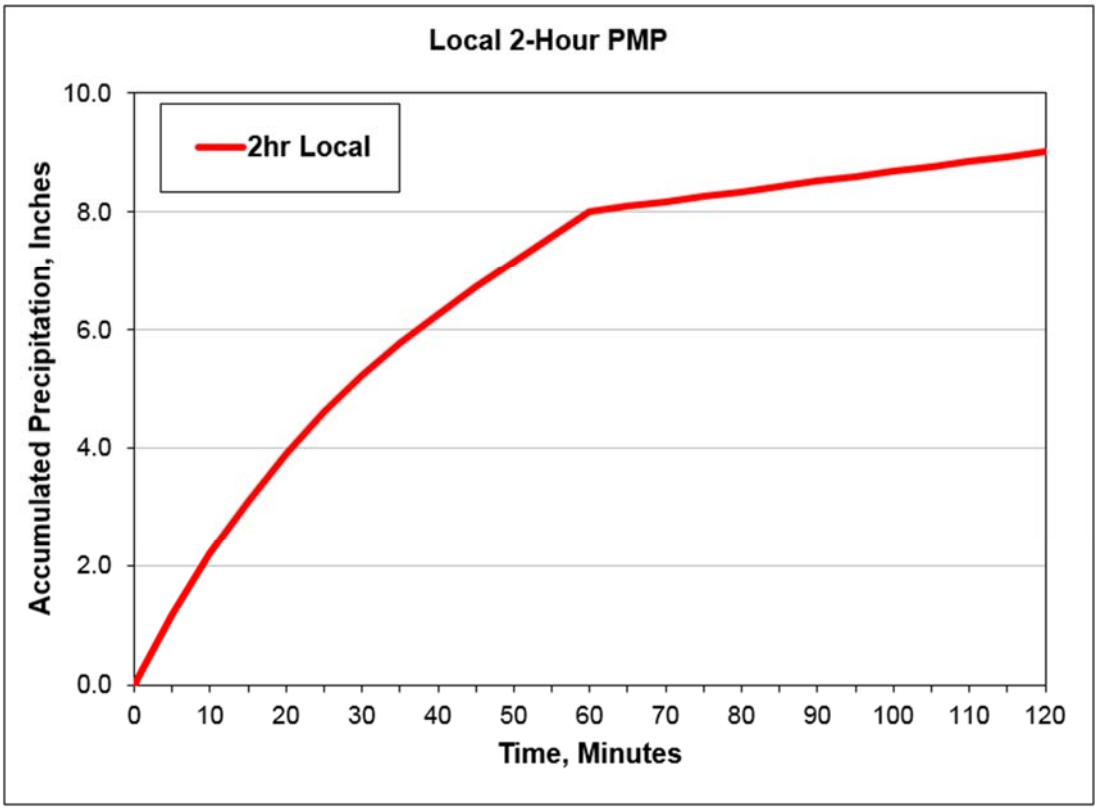

Figure 83: Hypothetical 2-hour local storm distribution

10.5 Meteorological Description of Temporal Patterns

Each of the temporal patterns was derived through visual inspection, meteorological analyses, and comparisons with similar work. Analysis was completed after separating each event by storm type (e.g., general, local, tropical, hybrid). The temporal patterns reflect the meteorological conditions that produce each storm type. These represent observed extreme rainfall accumulation characteristics. It is assumed that similar patterns would occur during a PMP event.

10.6 NRCS Type II Distribution Discussion

Each of the temporal patterns analyzed for all sites were significantly different than the NRCS Type II curve. Figure 84 displays the NRCS Type II curve. The accumulation pattern shown with this curve is much more intense than the patterns shown as part of this analysis. This same finding was evident in previous statewide and site-specific temporal analyses (e.g., Kappel et al., 2015, Kappel et al., 2016, Kappel et al., 2017, Kappel et al., 2018).

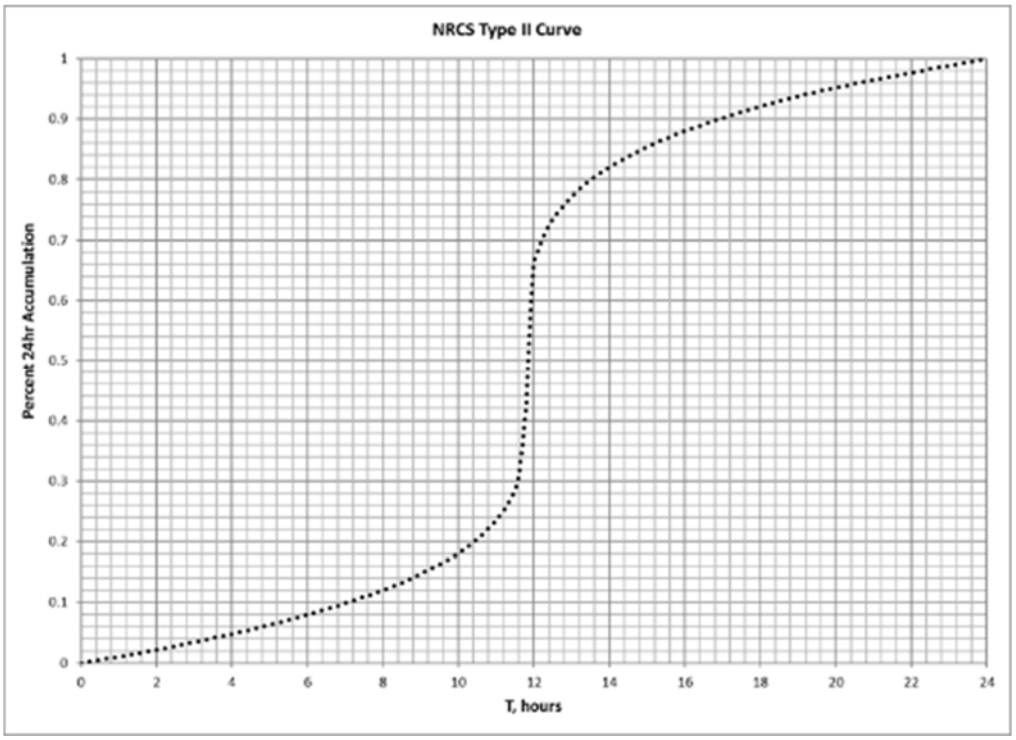

Figure 84: Natural Resource Conservation Service (NRCS) Type II curve

10.7 PMP Tool Temporal Distributions

The output PMP depths are distributed to 5-minute accumulations for local storm PMP and 15-minute accumulations for general and tropical storm PMP for potential use in runoff modeling for dam safety analysis. The distributions are applied by a function within the PMP tool. The development of the temporal distribution patterns is described in Section 10.

The following distributions were developed based on investigation of storm data used in this study. These are recommended patterns based on storm type and basin location:

Local Storm (5-minute Steps)

1. 2-hour Stacked Pattern:
    a. 1st hour:
        i. 1st 15-minute: 39 percent of largest hour evenly distributed[2]
        ii. 2nd 15-minute: 65 percent of largest hour evenly distributed
        iii. 3rd 15-minute: 84 percent of largest hour evenly distributed
    b. 2nd hour: Evenly distributed
2. One of the following:
    a) 6-hour east of Divide – 10th Percentile Huff Curve
    b) 6-hour west of Divide – 10th Percentile Huff Curve

[2] These are accumulation percentages, if 1hr event was 1" then: 15min = 0.39" 30min = 0.65" 45min = 0.84" 60min = 1.00"

3. One of the following:
   a) 6-hour east of Divide – 90th Percentile Huff Curve
   b) 6-hour west of Divide – 90th Percentile Huff Curve
4. One of the following:
   a) 6-hour east of Divide – Synthetic Curve
   b) 6-hour west of Divide – Synthetic Curve
5. 24-hour Eastern Plains – Synthetic Hybrid Curve[3]

General/Tropical Storm (15-minute Steps)

1. One of the following:
   a. 24-hour east of Divide – 10th Percentile Huff Curve (general storm pattern, not enough tropical)
   b. 24-hour west of Divide – 10th Percentile Huff Curve (general storm pattern, not enough tropical)
2. One of the following:
   a. 24-hour east of Divide – 90th Percentile Huff Curve (general storm pattern, not enough tropical)
   b. 24-hour west of Divide – 90th Percentile Huff Curve (general storm pattern, not enough tropical)
3. One of the following:
   a. 24-hour east of Divide – Synthetic Curve
   b. 24-hour west of Divide – Synthetic Curve

The total duration for potential use in runoff modeling for the general storm and tropical storm PMP is 72-hours. The first 24-hour period is the second largest 24-hour PMP evenly distributed. The second 24-hour period are distributed according to the six curves listed above. The final 24-hour period is the third largest 24-hour PMP evenly distributed. The user is reminded to consult the state dam safety programs in Colorado and New Mexico on the accepted application of these distributions for runoff modeling.

The final fourteen storm patterns recommended and included in the PMP Tool are shown in six Figures 85-90 as hypothetical PMP. The final local storm and general/tropical storm patterns are compared to several commonly used temporal patterns. For local 6-hour storms, the east and west temporal patterns are compared against the NRCS Type II, USACE, and HMR 5 temporal patterns Figure 91 and 92. For General/Tropical 24-hour storms, the east and west temporal patterns are compared against the NRCS Type II, USBR, and New Mexico Central distribution temporal patterns Figure 93 and 94. The final temporal patterns analyzed for Colorado-New Mexico were significantly different than the NRCS Type II, USBR, New Mexico Central distribution, USACE, and HMR 5 temporal patterns.

[3] Hybrid curve applied to basins with centroid inside transposition zones 1, 2, 3, 12 or 13

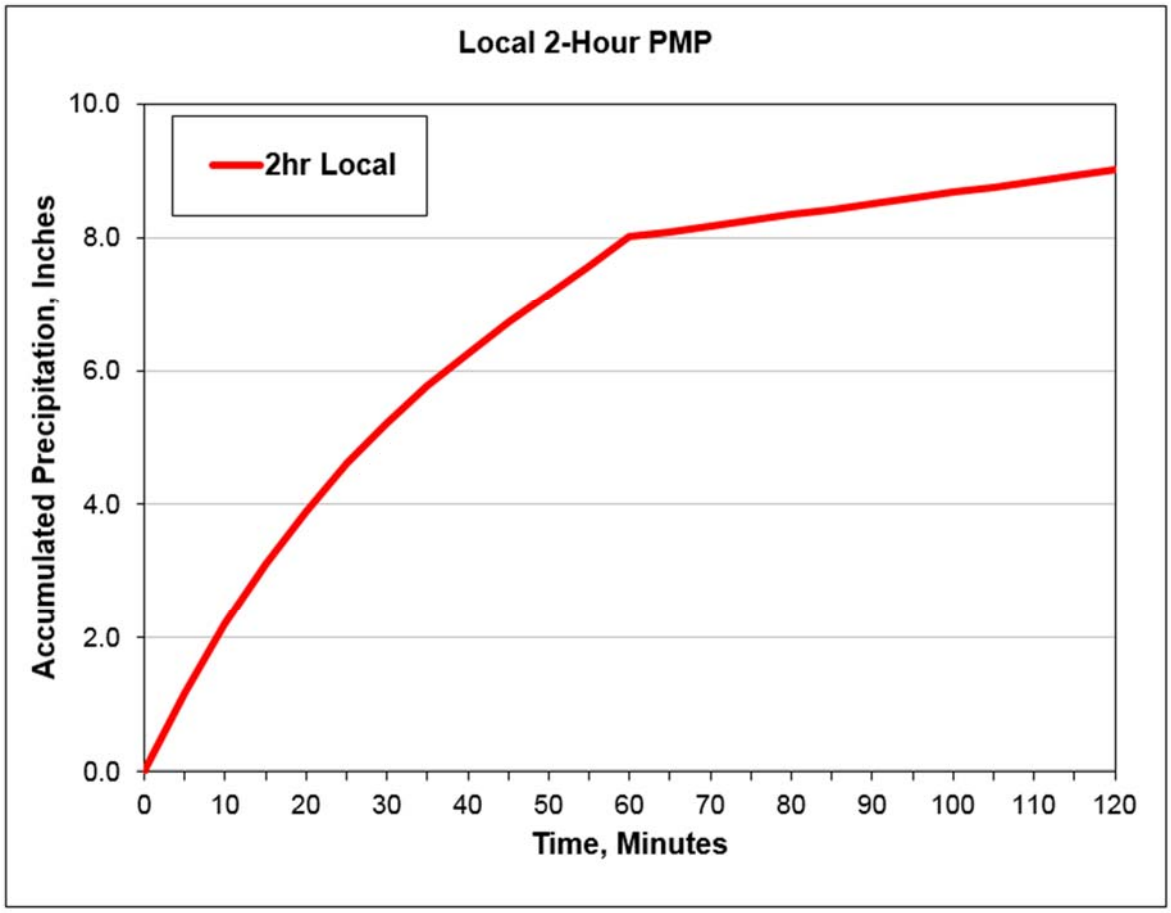

Figure 85: Hypothetical 2-hour local storm pattern at 5-minute time step.

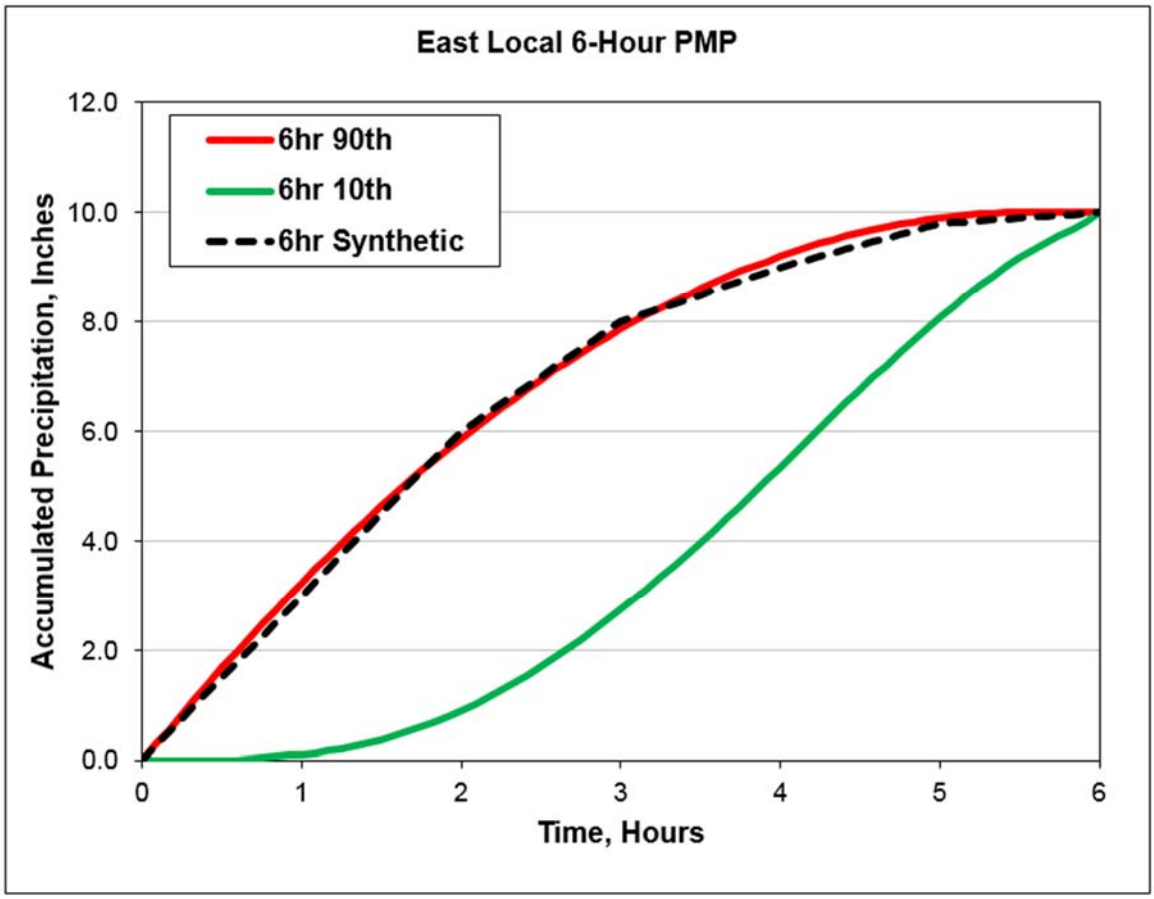

Figure 86: Hypothetical 6-hour local storm east of Continental Divide pattern at 5-minute time step. Red line is the 90th percentile curve, green line is the 10th percentile curve, and black dashed line is the synthetic curve.

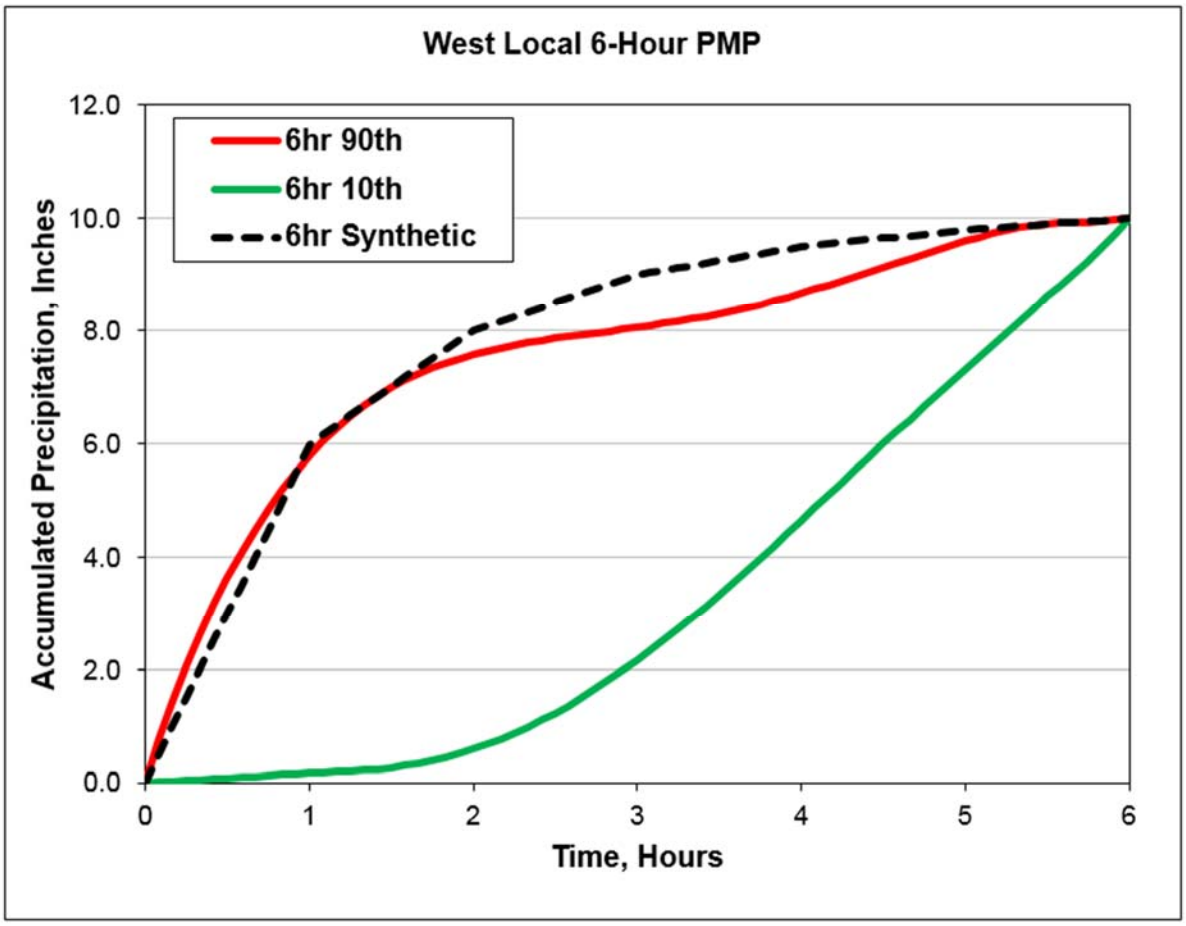

Figure 87: Hypothetical 6-hour local storm west of Continental Divide pattern at 5-minute time step. Red line is the 90th percentile curve, green line is the 10th percentile curve, and black dashed line is the synthetic curve.

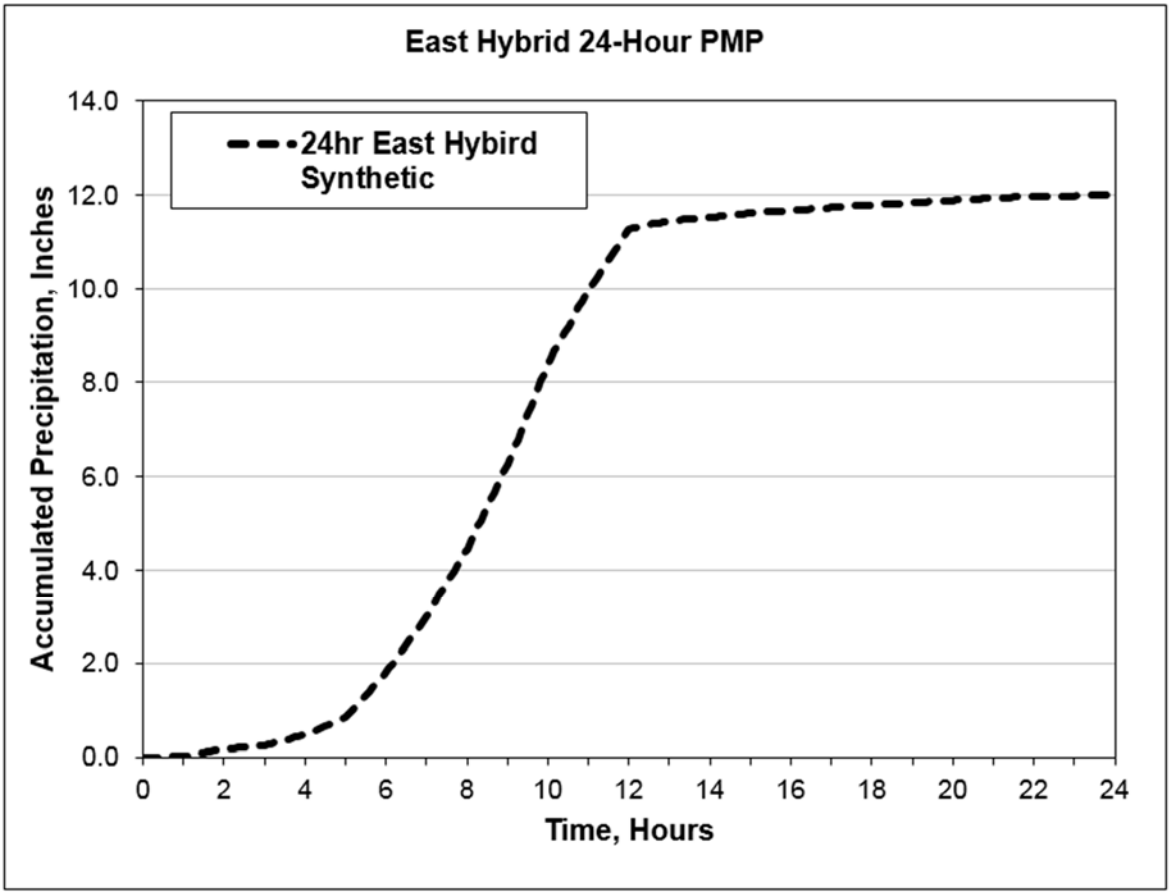

Figure 88: Hypothetical 24-hour Hybrid storm east of Continental Divide pattern at 5-minute time step.

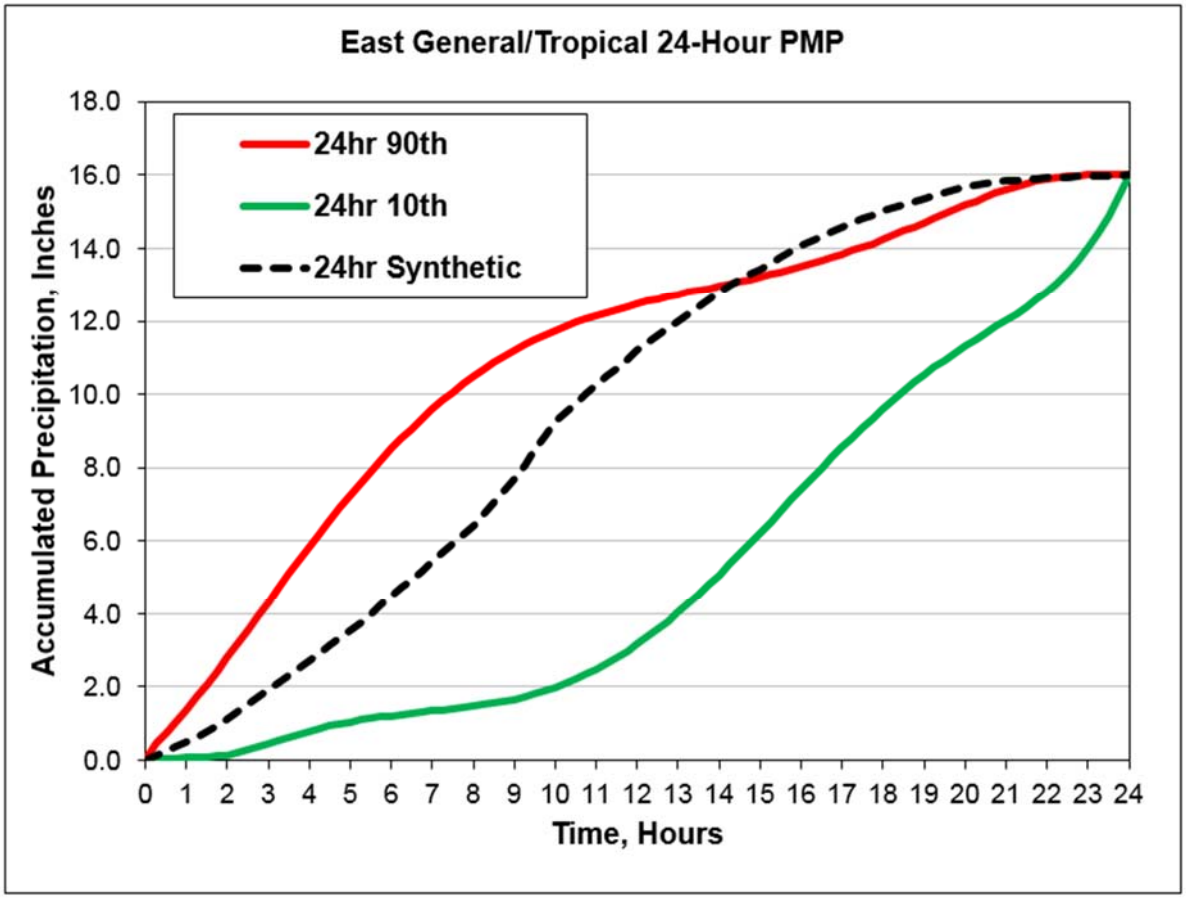

Figure 89: Hypothetical 24-hour general storm east of Continental Divide pattern at 15-minute time step. Red line is the 90th percentile curve, green line is the 10th percentile curve, and black dashed line is the synthetic curve. Note: 24-hour General/Tropical pattern is applied to the largest 24-hour rainfall in the 72-hour PMP.

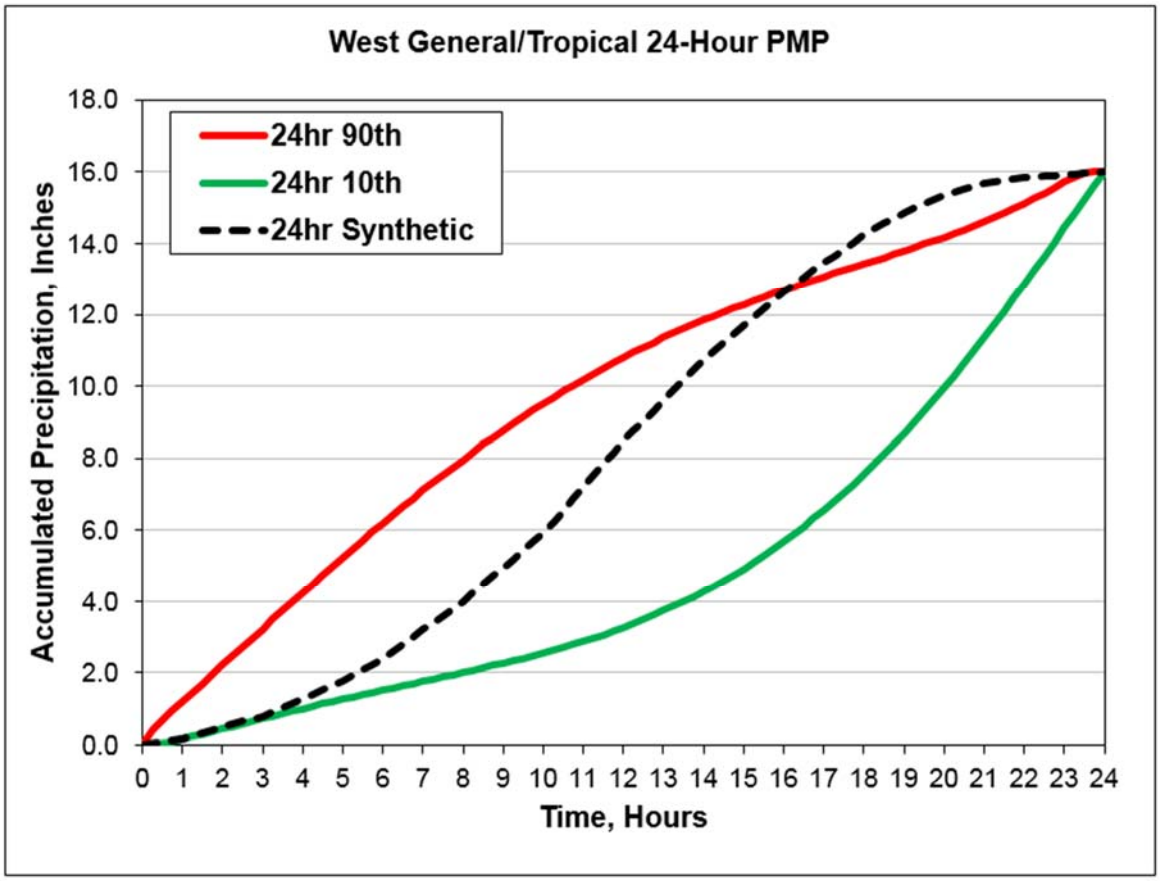

Figure 90: Hypothetical 24-hour general storm west of Continental Divide pattern at 15-minute time step. Red line is the 90th percentile curve, green line is the 10th percentile curve, and black dashed line is the synthetic curve.

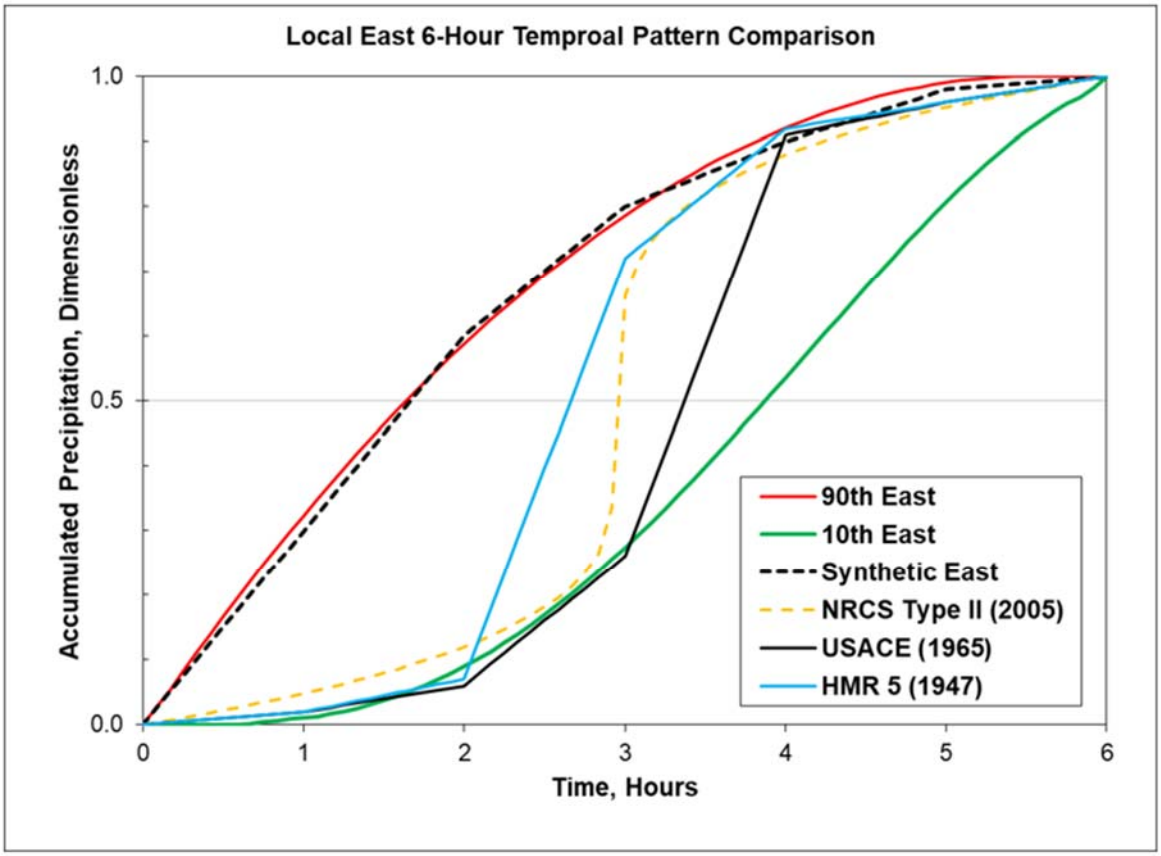

Figure 91: Comparison of final Local east Colorado-New Mexico storm patterns to several commonly used temporal patterns.

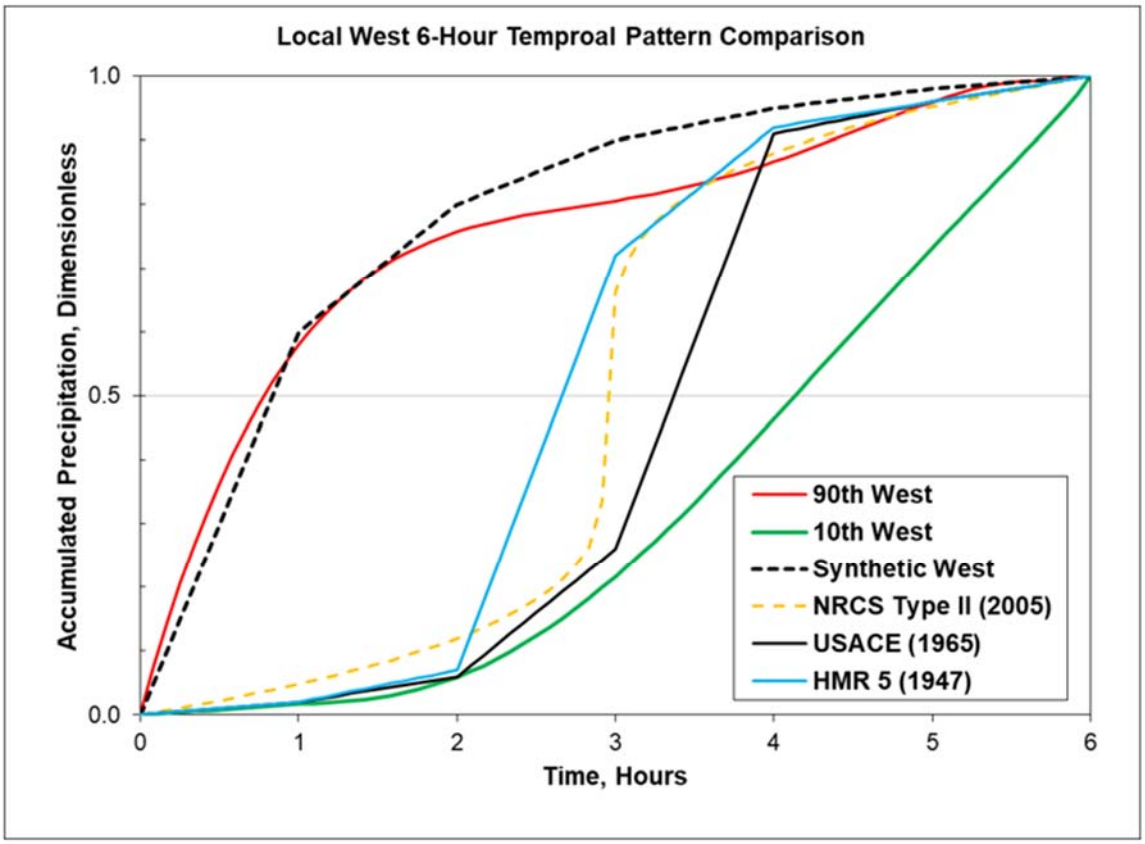

Figure 92: Comparison of final Local west Colorado-New Mexico storm patterns to several commonly used temporal patterns.

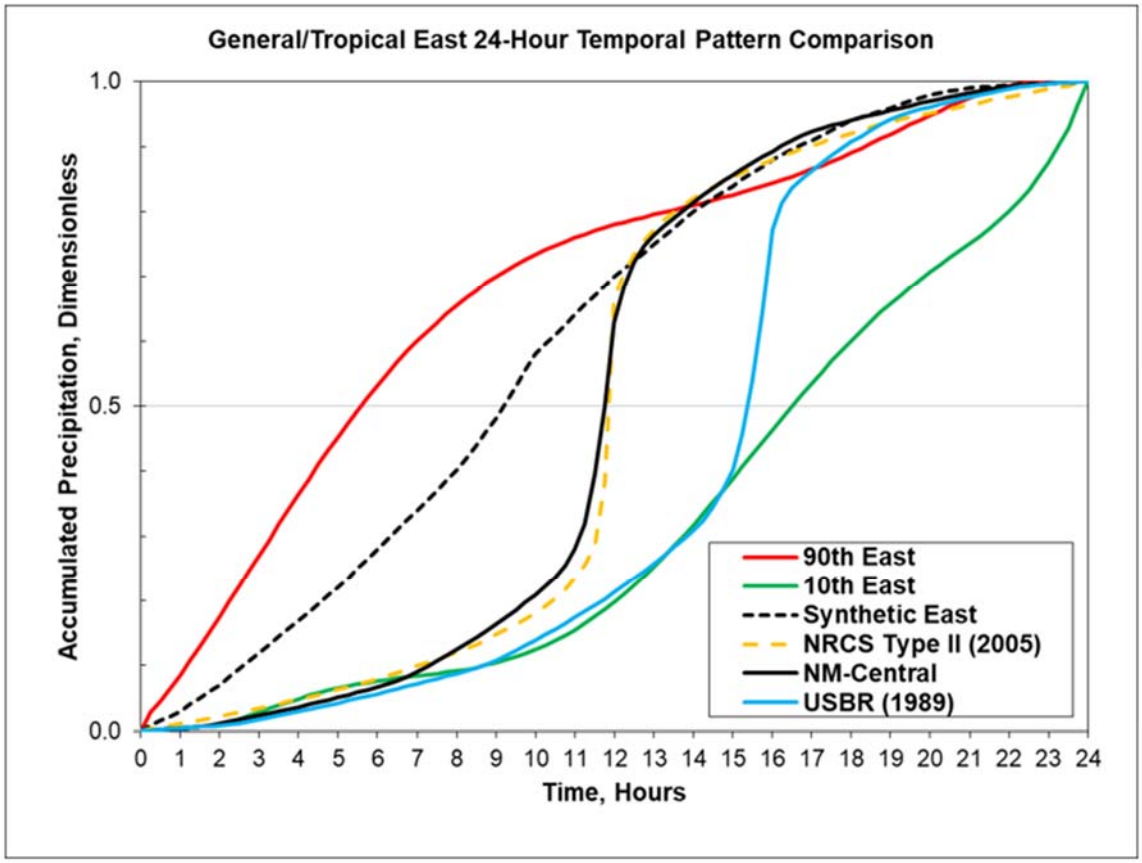

Figure 93: Comparison of final General/Tropical east Colorado-New Mexico storm patterns to several commonly used temporal patterns.

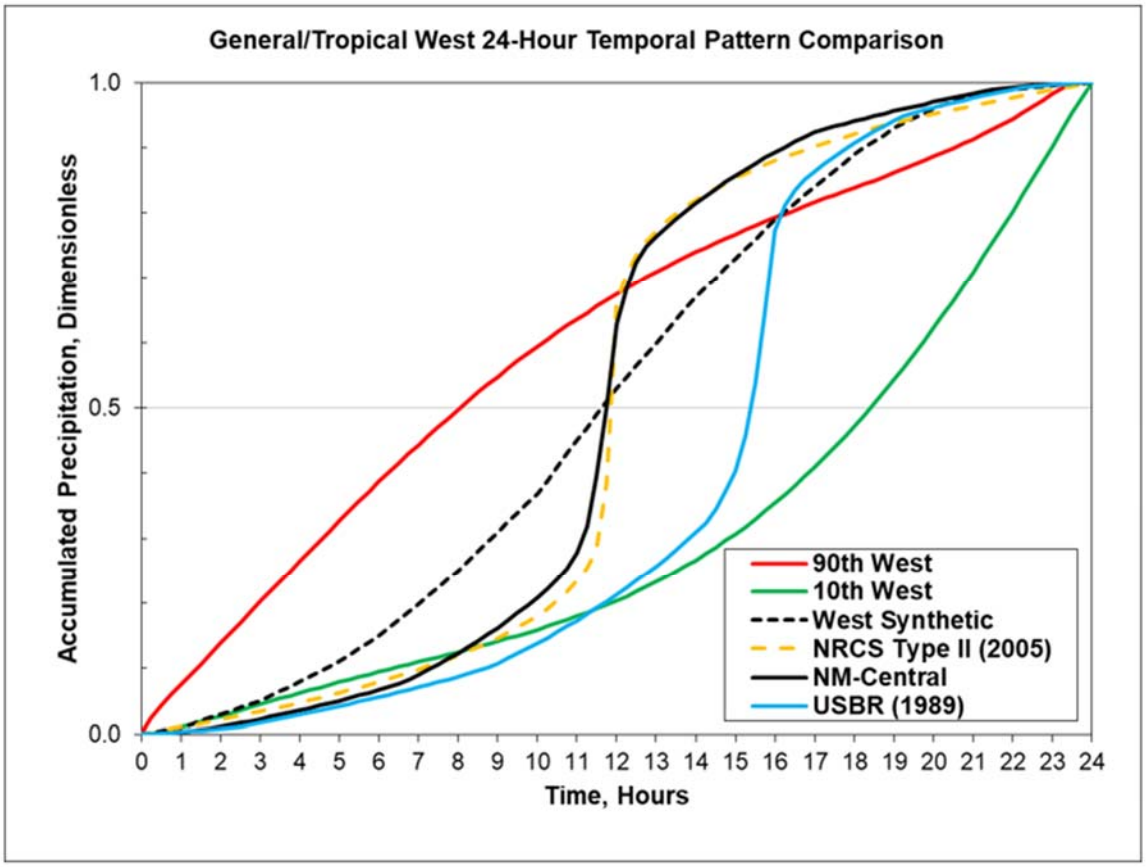

Figure 94: Comparison of final General/Tropical west Colorado-New Mexico storm patterns to several commonly used temporal patterns.

11. Sensitivities and Comparisons

In the process of deriving PMP values, various assumptions and meteorological judgments were made within the framework of state-of-the-practice processes. These parameters and derived values are standard to the PMP development process; however it is of interest to assess the sensitivity of PMP values to assumptions that were made and to the variability of input parameter values.

PMP depths and intermediate data produced for this study were rigorously evaluated throughout the process. ArcGIS was used as a visual and numerical evaluation tool to assess gridded values to ensure they fell within acceptable ranges and met test criteria. Several iterations of maps were produced as visual aids to help identify potential issues with calculations, transposition limits, DAD values, or storm adjustment values. The maps also helped to define storm characteristics and transposition limits, as discussed previously. Over the entire PMP analysis domain, different storms control PMP values at different locations for a given duration and area size.

In some instances, a discontinuity of PMP depths between adjacent grid point locations resulted. This occurs as a result of the binary transposition limits applied to the controlling storms, with no allowance for gradients of transpositionability. Therefore, different storms are affecting adjacent grid points and may result in a shift in values over a short distance. In reality, there would be some transition for a given storm, but the process and definition of transpositionability does not allow for this. It is important to note that these discontinuities make little difference in the overall basin average PMP values as applied for hydrologic analysis purposes for most basins. The discontinuities are only seen when analyzing data at the highest resolution (e.g., individual grid points). Any significant discontinuities would potentially have the most significant effect for small basins where there are a small number of grid points representing the drainage. In those instances, each grid point value would have an exaggerated effect on the basin average PMP.

11.1 Comparison of PMP Values to HMR Studies

This study employs a variety of improved methods when compared to previous HMR studies. These methods include:

- A far more robust storm analysis system with a higher temporal and spatial resolution
- Improved dew point/sea surface temperature (SST) and precipitation climatologies that provide an increased ability to maximize and transpose storms
- Gridded PMP calculations which result in higher spatial and temporal resolutions
- A greatly expanded storm record

Unfortunately, working papers and notes from the HMRs are not available in most cases. Therefore, direct PMP comparisons between the HMRs and the values from this study are somewhat limited. Furthermore, due to the generalization of the regionally-based HMR studies, comparisons to the detailed gridded PMP of this study can vary greatly over short distances. However, comparisons were made for sensitivity purposes where data allowed. The PMP values in this study resulted in a wide range of both reductions and increases as compared to the HMRs.

This study region was covered, in part, by HMR 49, HMR 55A, or HMR 51. Table 6 shows the PMP depth comparisons made to HMR 49 by comparing the 10 square mile 24-hour general/tropical storm PMP and 10 square mile 6-hour local storm PMP at the 1° grid points shown in HMR 49 figure 5.4.

Table 6: Comparison to HMR 49 10 sq. mi. PMP depths (Point_X and Point_Y are longitude and latitude, respectively, in degrees)

Id	POINT_X	POINT_Y	HMR 49 General Storm PMP 24hr 10sqmi	REPS Gen/Trop Storm PMP 24hr 10sqmi	Percent Change from HMR 49	HMR 49 Local Storm PMP 6hr 10sqmi	REPS Local Storm PMP 6hr 10sqmi	Percent Change from HMR 49
1	-109	32	13.2"	10.7"	-18.9%	12.9"	11.0"	-14.7%
6	-108	33	18.4"	11.0"	-40.2%	11.8"	13.8"	16.9%
7	-109	33	16.3"	7.6"	-53.4%	11.3"	10.7"	-5.3%
15	-109	34	12.2"	10.9"	-10.7%	9.9"	13.4"	35.4%
24	-109	35	7.4"	8.0"	8.1%	9.0"	9.9"	10.0%
34	-108	36	9.1"	6.4"	-29.7%	10.6"	7.5"	-29.2%
35	-109	36	12.1"	7.7"	-36.4%	10.6"	9.1"	-14.2%
45	-107	37	10.5"	8.4"	-20.0%	9.1"	9.0"	-1.1%
46	-108	37	9.2"	6.9"	-25.0%	9.6"	7.4"	-22.9%
47	-109	37	9.5"	7.2"	-24.2%	9.6"	7.1"	-26.0%
57	-107	38	10.6"	9.4"	-11.3%	8.4"	7.1"	-15.5%
58	-108	38	10.4"	9.4"	-9.6%	8.2"	6.9"	-15.9%
59	-109	38	9.0"	9.4"	4.4%	8.2"	10.5"	28.0%
70	-107	39	10.9"	9.4"	-13.8%	7.3"	6.1"	-16.4%
71	-108	39	11.2"	9.4"	-16.1%	6.6"	7.9"	19.7%
72	-109	39	9.3"	9.3"	0.0%	8.3"	10.2"	22.9%
84	-106	40	12.0"	9.4"	-21.7%	9.6"	7.1"	-26.0%
85	-107	40	11.5"	9.1"	-20.9%	7.4"	6.0"	-18.9%
86	-108	40	9.3"	9.3"	0.0%	8.0"	8.9"	11.3%
87	-109	40	8.1"	7.6"	-6.2%	8.2"	8.3"	1.2%
99	-107	41	13.0"	9.4"	-27.7%	8.4"	7.4"	-11.9%
100	-108	41	9.7"	8.8"	-9.3%	8.4"	9.2"	9.5%
101	-109	41	9.5"	9.4"	-1.1%	9.1"	6.4"	-29.7%
102	-110	41	8.8"	9.1"	3.4%	8.8"	10.0"	13.6%
113	-109	42	9.8"	8.8"	-10.2%	8.6"	9.5"	10.5%
114	-110	42	7.3"	7.3"	0.0%	9.7"	6.4"	-34.0%
121	-110	43	10.6"	7.4"	-30.2%	9.6"	7.5"	-21.9%

Gridded index PMP depths were available over the HMR 51 and 55A coverage areas allowing a direct gridded comparison with the depths produced for this study. A gridded percent change was calculated for the area-sizes and durations common with the HMR index PMP maps. The CO-NM REPS maximum PMP depth from either the general storm or local storm types were used for the HMR 51 comparisons to account for differences in storm typing between the CO-NM REPS and HMR study.

The HMR 51 overlap area covered the portion of Colorado and New Mexico from 103°W eastward. Table 7 provides the average PMP percent change from HMR 51.

Table 7: Average gridded percent change from HMR 51 for overlap region

Area-size Duration	Percent Change from HMR 51 All-Season PMP
10-sqmi 6-hour	-21.8%
10-sqmi 12-hour	-28.8%
10-sqmi 24-hour	-33.2%
10-sqmi 48-hour	-38.1%
10-sqmi 72-hour	-39.4%
200-sqmi 6-hour	-21.4%
200-sqmi 12-hour	-27.6%
200-sqmi 24-hour	-28.0%
200-sqmi 48-hour	-28.7%
200-sqmi 72-hour	-29.1%
1,000-sqmi 6-hour	-30.0%
1,000-sqmi 12-hour	-33.2%
1,000-sqmi 24-hour	-27.4%
1,000-sqmi 48-hour	-29.5%
1,000-sqmi 72-hour	-30.1%
5,000-sqmi 6-hour	-49.0%
5,000-sqmi 12-hour	-45.5%
5,000-sqmi 24-hour	-37.7%
5,000-sqmi 48-hour	-36.7%
5,000-sqmi 72-hour	-36.5%
10,000-sqmi 6-hour	-50.4%
10,000-sqmi 12-hour	-48.5%
10,000-sqmi 24-hour	-35.4%
10,000-sqmi 48-hour	-32.2%
10,000-sqmi 72-hour	-33.6%

The HMR 55A overlap area covered the region from 103°W to the Continental Divide. Table 8 provides the average 10 square mile CO-NM REPS PMP percent change from the gridded PMP derived from the HMR 55A index plates I-IV (General Storm PMP) averaged over the transposition zones.

Table 8: Average gridded percent change from HMR 55A for overlap region

Transposition Zone	Percent Change from HMR 55A 1-hour 10-sqmi Index PMP	Percent Change from HMR 55A 6-hour 10-sqmi Index PMP	Percent Change from HMR 55A 24-hour 10-sqmi Index PMP	Percent Change from HMR 55A 72-hour 10-sqmi Index PMP
1 - Colorado Plains	-39.2%	-31.4%	-41.3%	-45.5%
2 - New Mexico Plains	-33.3%	-24.8%	-41.9%	-41.6%
3 - Front Range Transition Zone	-46.4%	-26.2%	-26.5%	-44.1%
4 - Sacramento Mountains	-27.5%	-28.5%	-47.5%	-45.1%
5 - Colorado Rockies North	21.6%	-26.4%	-52.0%	-33.6%
6 - Colorado Rockies South	26.7%	-0.7%	-42.4%	-39.7%
7 - San Luis Valley	3.4%	-21.3%	-43.6%	-40.5%
8 - Rio Grande	-0.7%	-13.8%	-40.6%	-43.0%
17 - North Park	11.5%	-30.6%	-61.8%	-59.8%

For General Storm PMP in the regions covered by HMR 55A, values appear to be far too high compared to maximized storm data used in this study. This is most likely the result of a lack of storm data and the highly subjective process used to quantify the effects of topography (the HMR 55A Storm Separation Method or SSM). Similar findings of significant reductions from HMR 55A have been realized in other AWA studies (e.g., Kappel et al., 2014). In this region, the GTF process more accurately accounts for the lack of moisture available to storms, where topography has a significant influence on low-level moisture access. In these situations, the HMR 55A SSM process does not allow for values less than 1 and therefore, does not properly represent a physically possible storm in these regions where terrain affects would decrease rainfall.

11.2 Comparison of PMP Values with Previous Studies

The gridded PMP calculation process used in this study closely follows the methods applied to the surrounding Texas statewide PMP Study (2016), Wyoming statewide PMP Study (2014), and the Arizona statewide PMP Study (2013). Several recent site-specific studies within the study domain have also utilized the gridded approach, including Rio Grande (2014), Sylvan Dam (2015), Glade Reservoir (2017), Lake Maloya (2017), Bradner Dam (2017), and Gross Reservoir (2017). However, in all these cases there were updates and differences in storm lists, storm typing, storm analysis methods, maximization methods, source data, transposition methods, and/or transposition limits. In addition, site-specific considerations can contribute to discrepancies from PMP provided in the previous studies in areas of overlap.

Efforts have been made to be consistent with previous work. However, the PMP depths provided in this study should be considered more reliable in cases where differences occur. Figure 95 shows the differences in PMP depths in areas where the CO-NM REPS study overlaps with the Arizona, Wyoming, and Texas statewide studies.

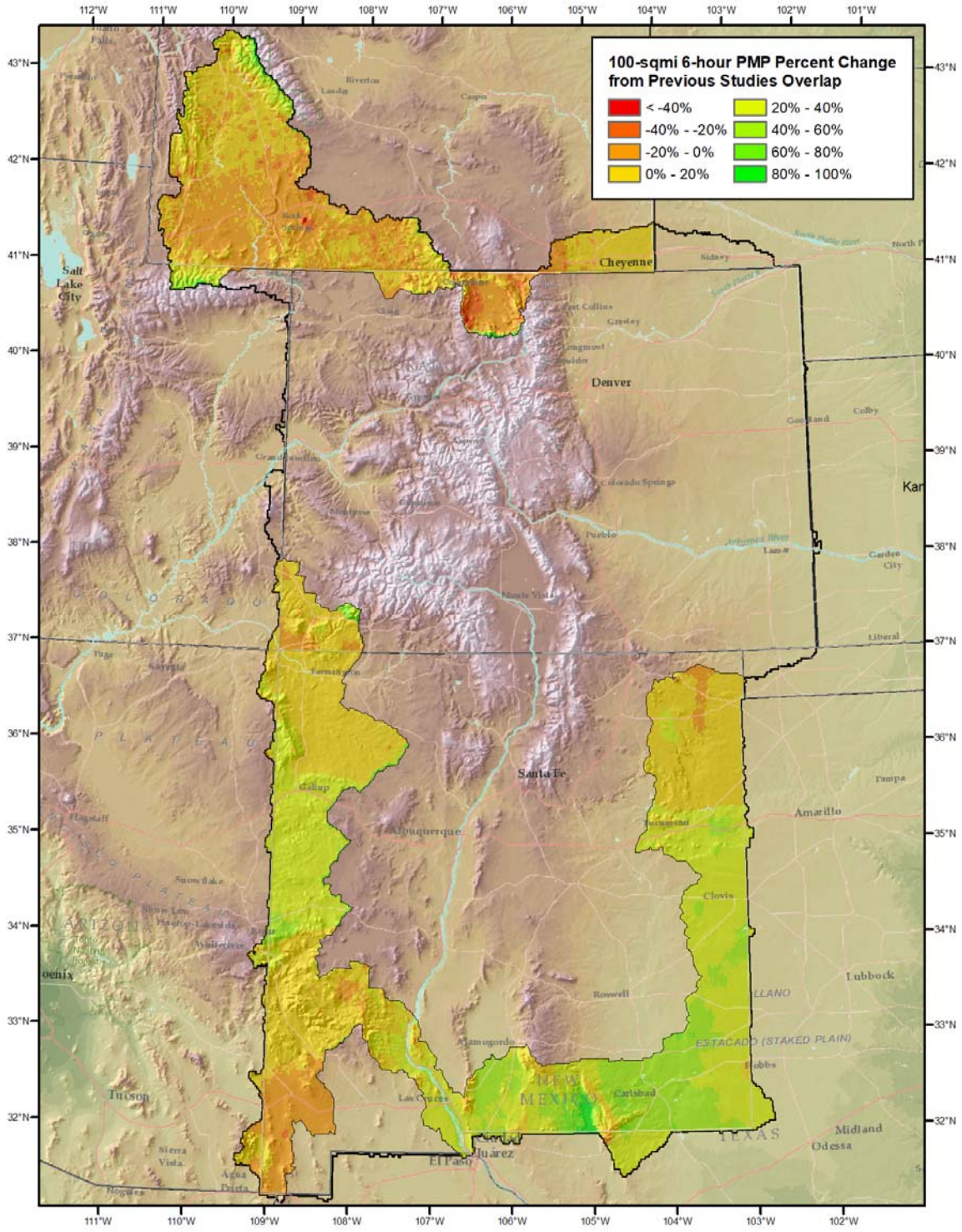

Figure 95: Percent change in combined storm type 100 square mile 6-hour PMP from previous statewide studies

11.3 Comparison of PMP Values with Precipitation Frequency

The ratio of the PMP to 100-year return period precipitation amounts is generally expected to range between two and four, with values as low as 1.7 and as high as 5.5 for regions east of 117°W found in HMR 57 and HMR 59 (Hansen et al., 1994; Corrigan et al., 1999). Further, as stated in HMR 59 "*…the comparison indicates that larger ratios are in lower elevations where short-duration, convective precipitation dominates, and smaller ratios in higher elevations where general storm, long duration precipitation is prevalent*" (Corrigan et al., 1999, p. 207).

For this study, the maximum 24-hour 1/3-square mile PMP was compared directly to the 100-year 24-hour rainfall-only values on a grid-by-grid basis for the entire analysis domain using a GIS. The comparison was presented as a ratio of PMP to 100-year rainfall, and it was determined for each grid point. Average zonal statistics were summarized for each transposition zone. Figure 96, Figure 97, and Figure 98 illustrate the PMP to 100-year rainfall ratios for 6-hour local storm PMP, 24-hour general storm PMP, and 24-hour tropical storm PMP, respectively. The PMP to 100-year return period rainfall ratios vary from 2.60 to 5.40, after combining storm types. The values are in reasonable proportion expected for the study area and demonstrate the PMP values are at appropriately rare levels.

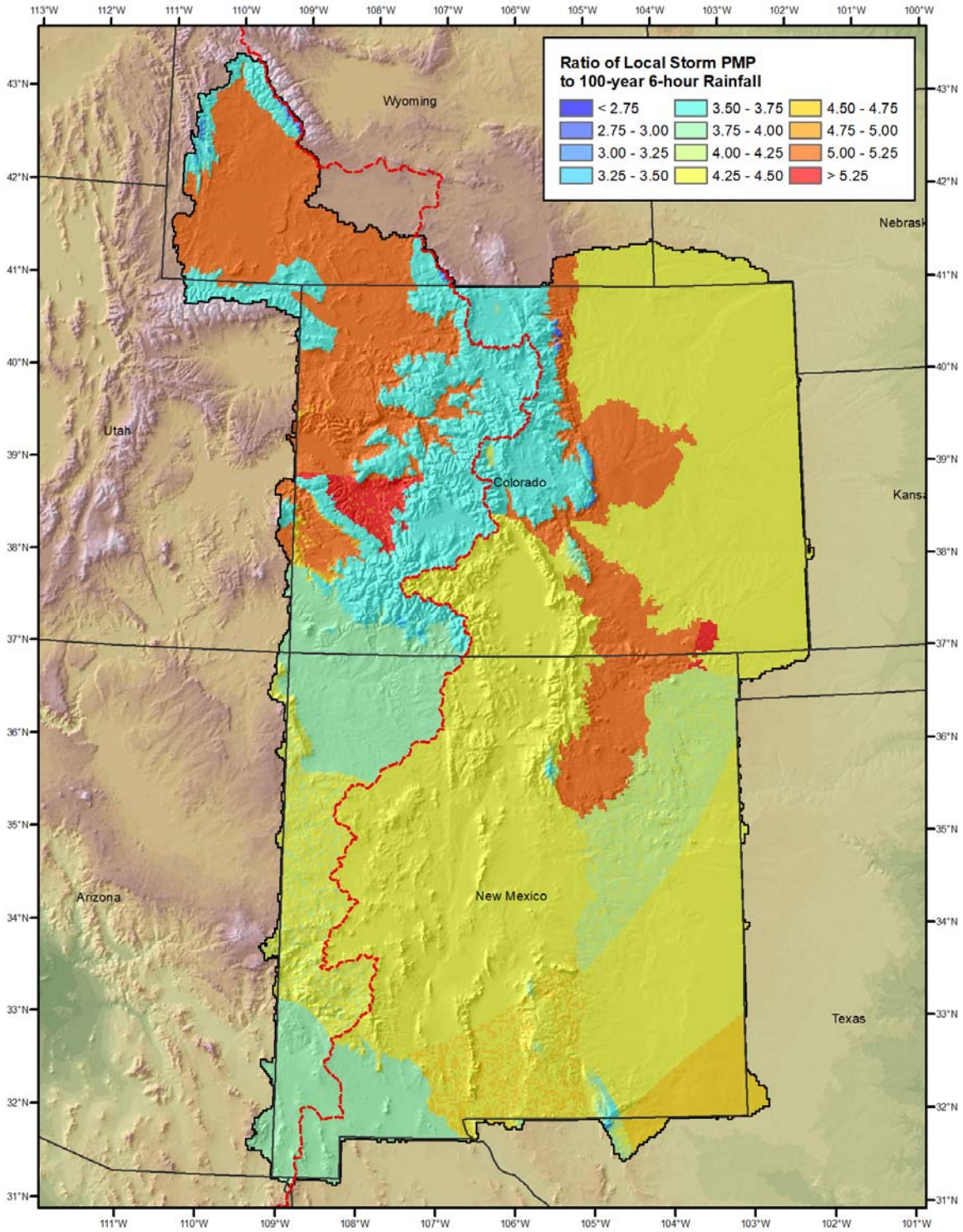

Figure 96: Ratio 6-hour 1-square mile local storm PMP to 100-year precipitation

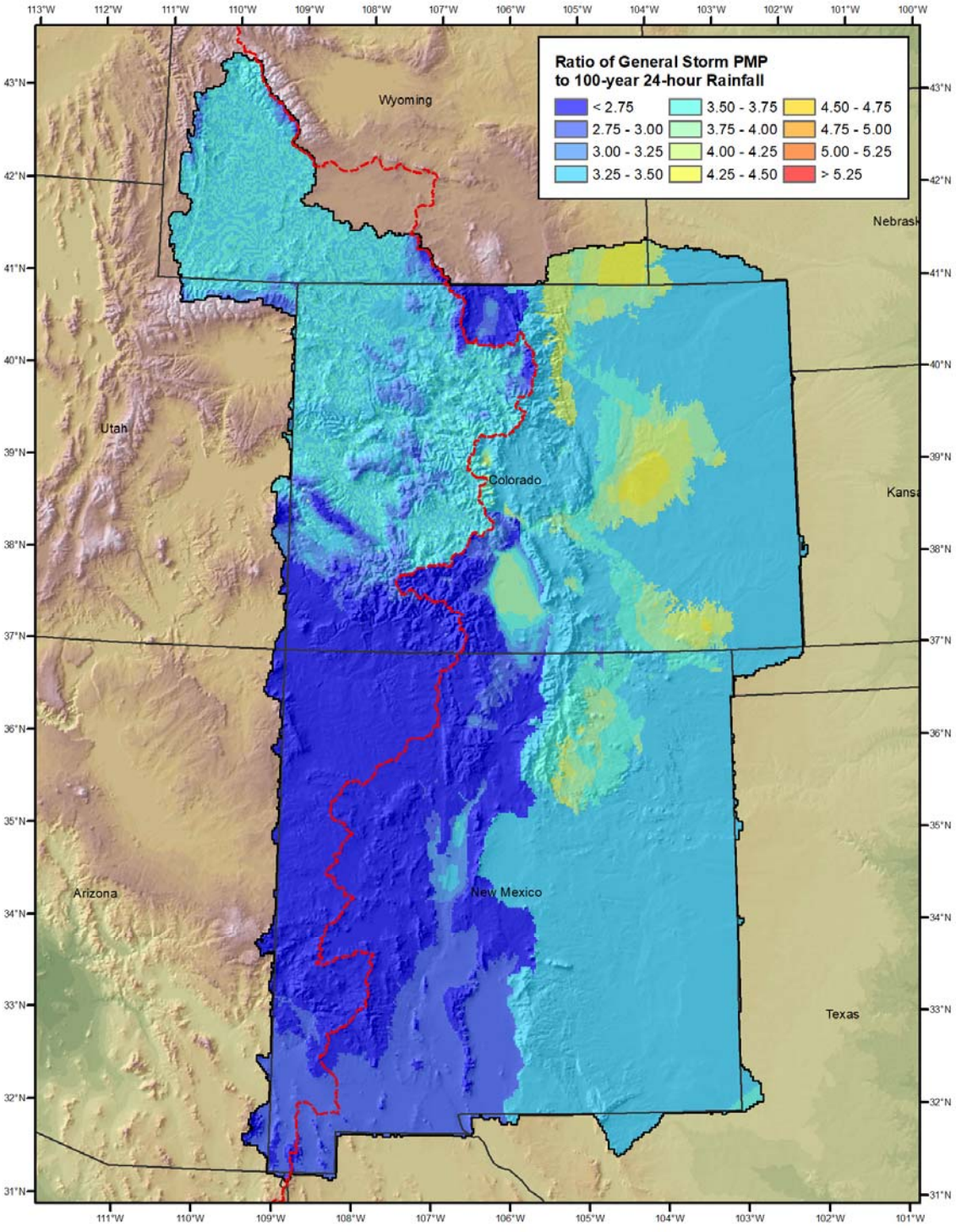

Figure 97: Ratio 24-hour 1-square mile general storm PMP to 100-year precipitation

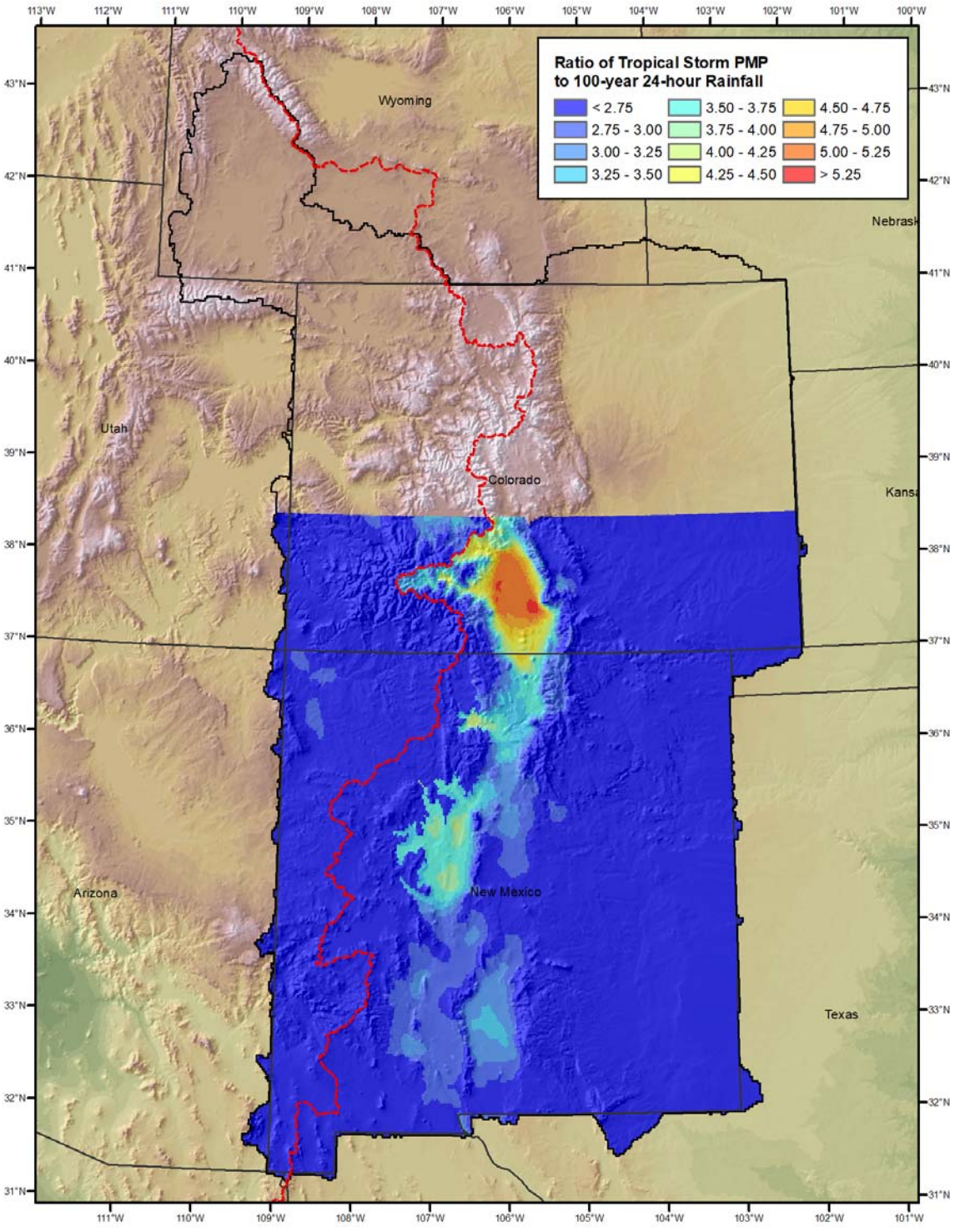

Figure 98: Ratio 24-hour 1-square mile tropical storm PMP to 100-year precipitation

11.4 Average Recurrence Interval of Probable Maximum Precipitation

The average recurrence interval (ARI) was calculated for the 1/3 square mile PMP depths at various durations on a gridded basis using the CO-NM REPS Precipitation Frequency Task precipitation frequency estimates. The REPS local storm precipitation frequency estimates were used to estimate the 2-hour Local Storm PMP ARI, the meso-scale with embedded convection (MEC) storm type from the CO-NM REPS Precipitation Frequency Task precipitation was used for the 6-hour Local Storm PMP ARI comparisons, and the REPS mid-latitute cyclone (MLC) precipitation frequency was used to calculate ARI for PMP durations above 6-hour. A log-linear fit was used to extrapolate ARI values to a maximum of 1×10^{10} years.

Figures 99 and 100 illustrate the 2-hour and 6-hour local storm PMP ARI calculated using the 2-hour local storm precipitation frequency and 6-hour MEC precipitation frequency, respectively. Figure 101 illustrates the 48-hour general storm PMP ARI calculated using the 48-hour MLC precipitation frequency. Figure 102 illustrates the 48-hour tropical storm PMP ARI calculated using the 48-hour MLC precipitation frequency.

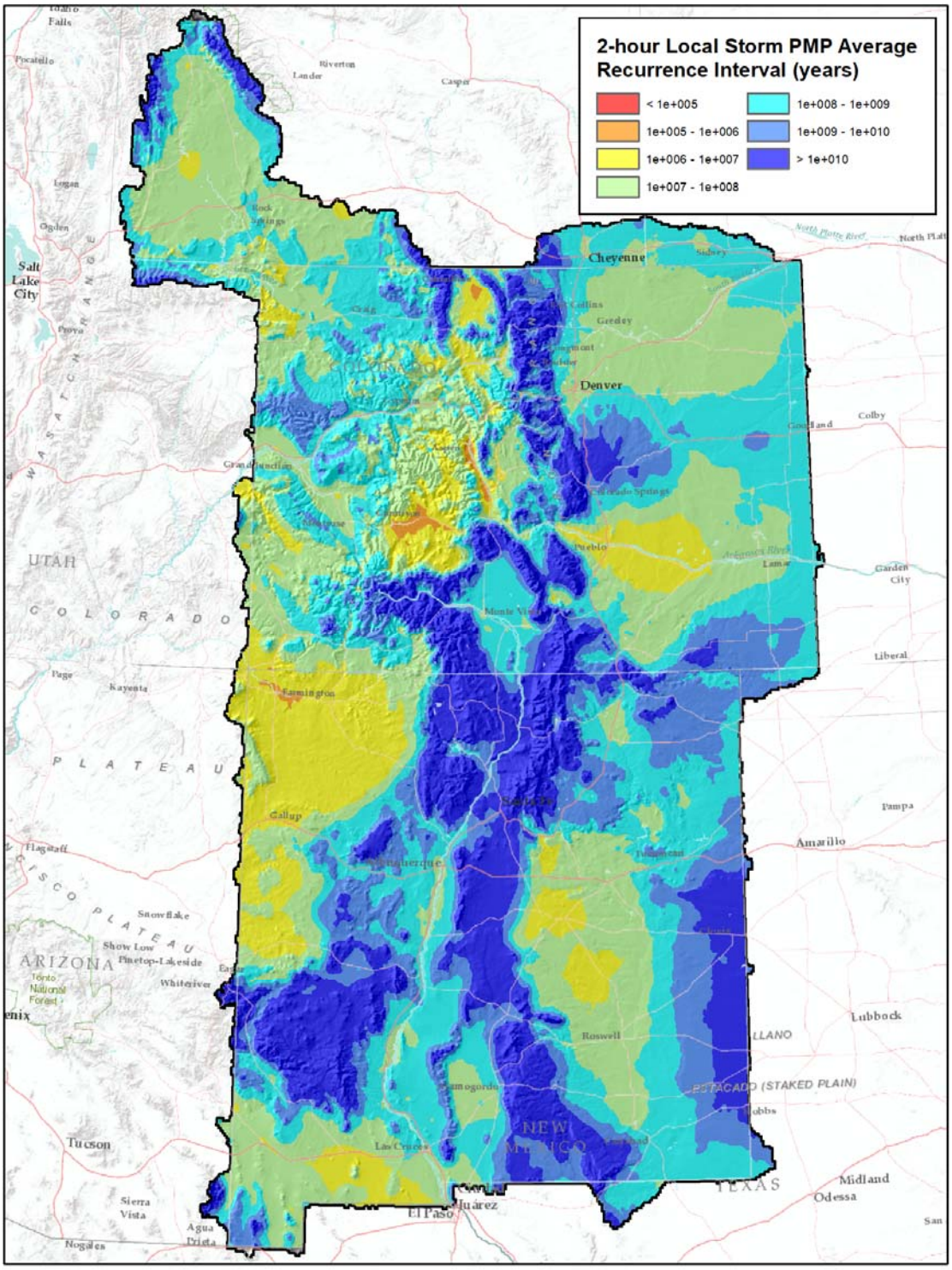

Figure 99: 2-hour local storm PMP estimated average recurrence interval

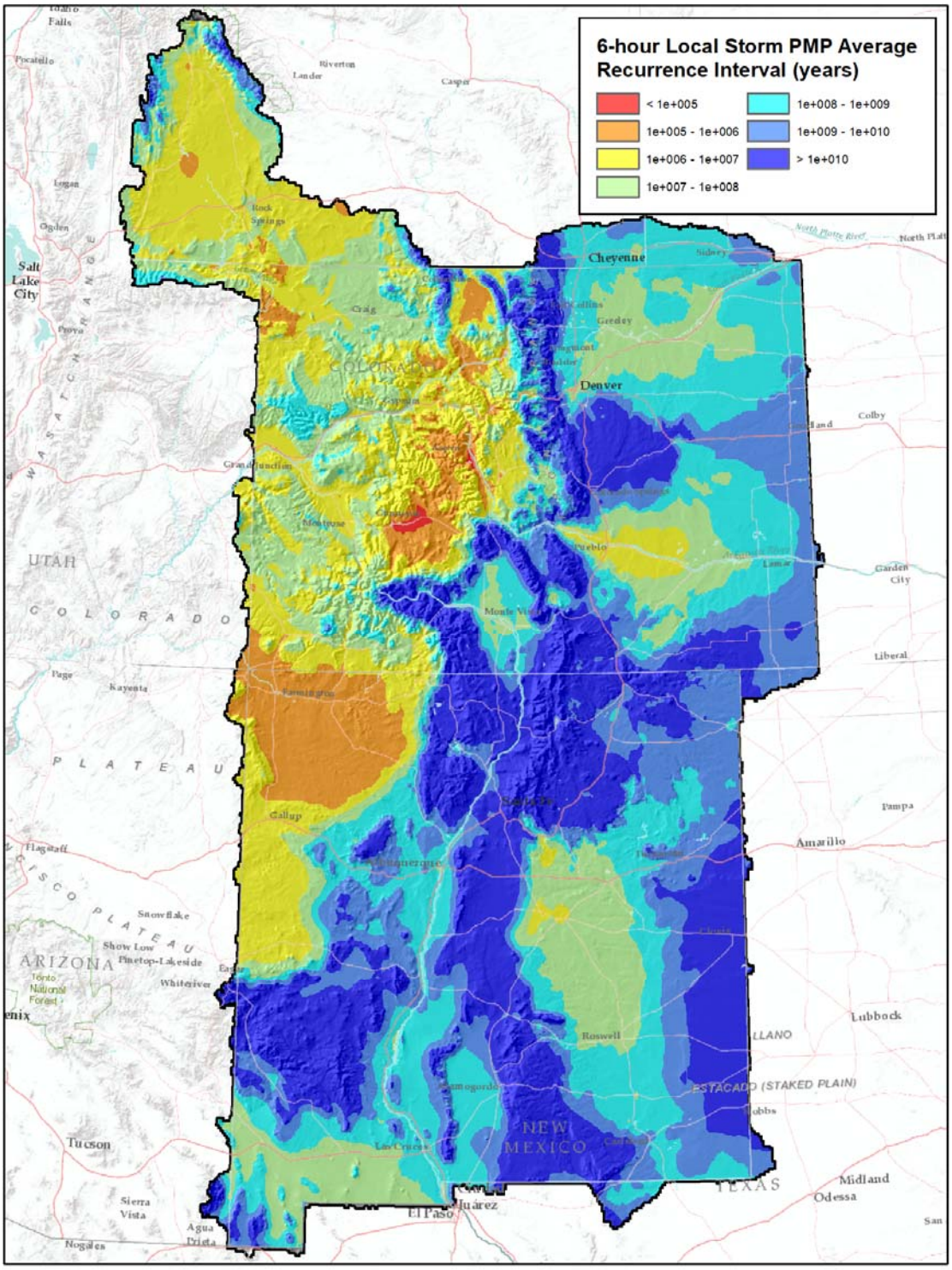

Figure 100: 6-hour local storm PMP estimated average recurrence interval

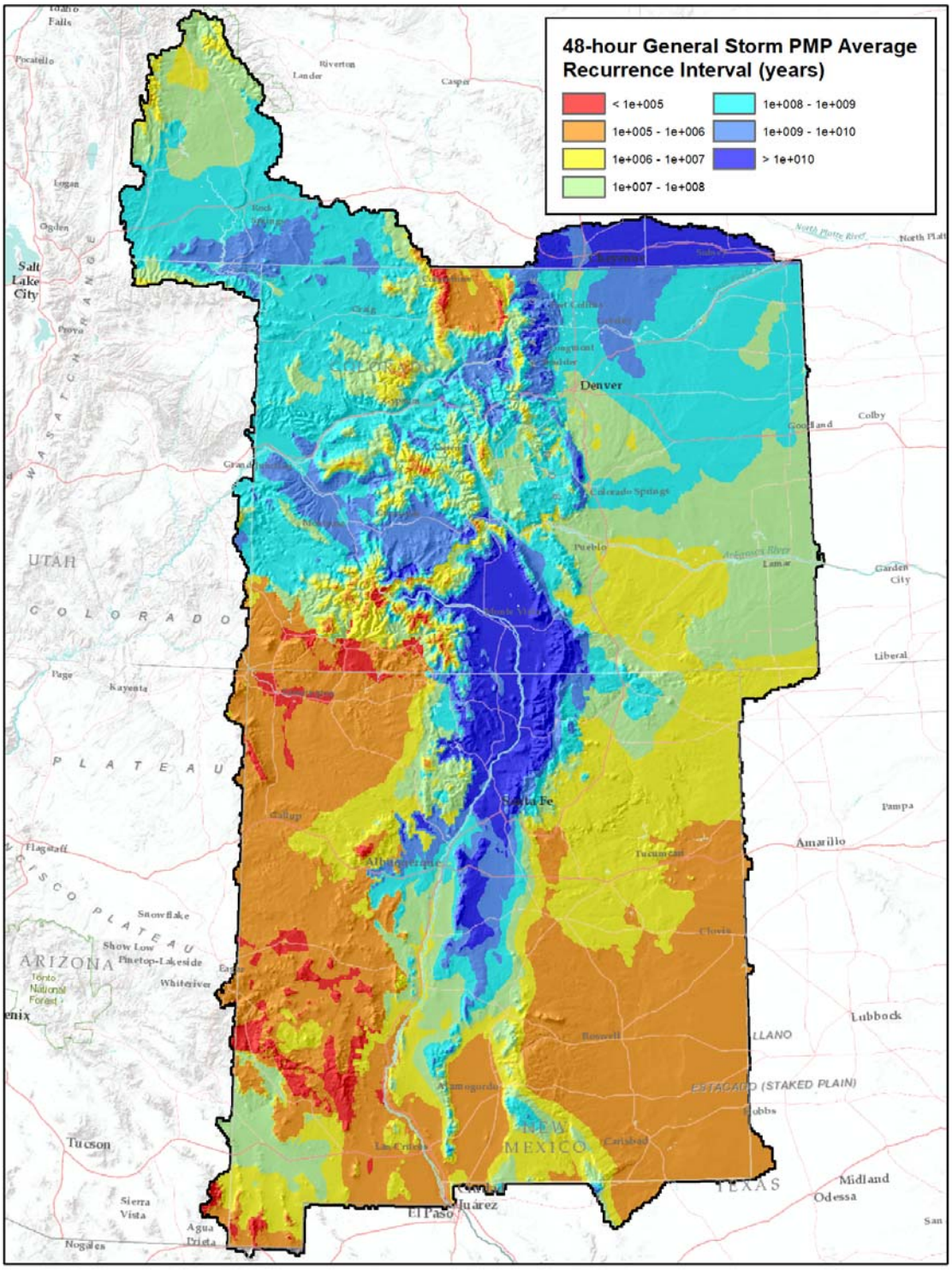

Figure 101: 48-hour general storm PMP estimated average recurrence interval

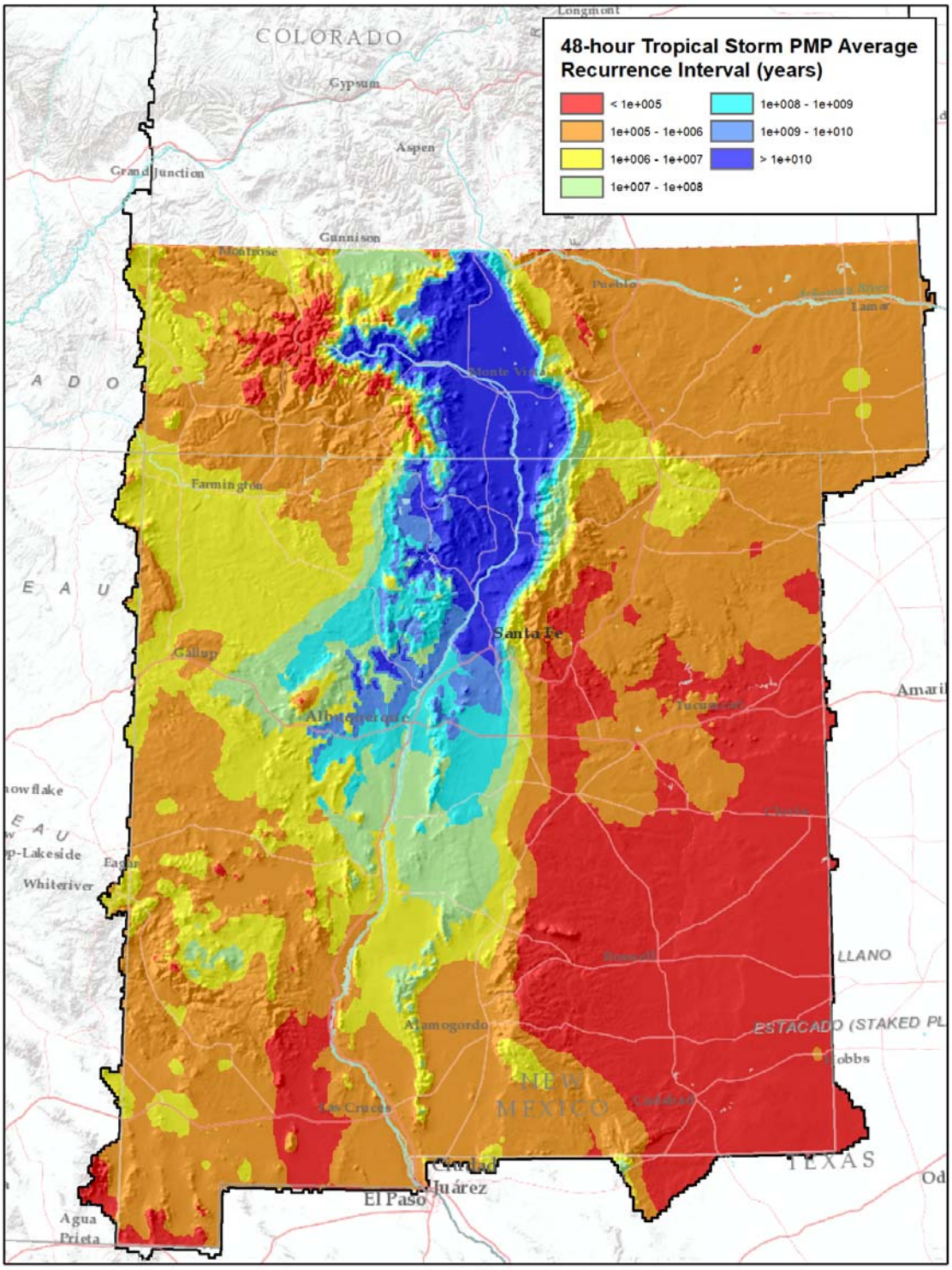

Figure 102: 48-hour tropical storm PMP estimated average recurrence interval

12. Uncertainty and Limitations

12.1 Sensitivity of Parameters

In the process of deriving PMP values, various assumptions and meteorological judgments were made. Additionally, various parameters and derived values were used in the calculations, which are standard to the PMP development process. It is of interest to assess the sensitivity of PMP values to assumptions that were made and to the variability of parameter values.

12.2 Saturated Storm Atmosphere

Atmospheric air masses that provide available moisture to both the historic storm and the PMP storm are assumed to be saturated through the entire depth of the atmosphere and to contain the maximum moisture possible based on the surface dew point. This assumes moist pseudo-adiabatic temperature profiles for both the historic storm and the PMP storm. Limited evaluation of this assumption in the Electric Power Research Institute (EPRI) Michigan/Wisconsin PMP study (Tomlinson, 1993) and the Blenheim Gilboa study (Tomlinson et al., 2008) indicated that historic storm atmospheric profiles are generally not entirely saturated and contain somewhat less precipitable water than is assumed in the PMP procedure. It follows that the PMP storm (if it were to occur) would also have somewhat less precipitable water available than the assumed saturated PMP atmosphere would contain. The *ratio* of precipitable water associated with each storm is used in the PMP calculation procedure. If the precipitable water values for each storm are both slightly overestimated, the ratio of these values will be essentially unchanged. For example, consider the case where instead of a historic storm with a storm representative dew point of 70°F having 2.25 inches of precipitable water and assuming a saturated atmosphere, it actually had 90 percent of that value or about 2.02 inches. The PMP procedure assumes the same type of storm with similar atmospheric characteristics for the maximized storm but with a higher dew point, say 76°F. The maximized storm, having similar atmospheric conditions, would have about 2.69 inches of precipitable water instead of the 2.99 inches associated with a saturated atmosphere with a dew point of 76°F. The maximization factor computed, using the assumed saturated atmospheric values, would be 2.99/2.25 = 1.33. If both storms were about 90 percent saturated, the maximization factor would be 2.69/2.02 = 1.33. Therefore, any potential inaccuracy of assuming saturated atmospheres (whereas the atmospheres may be somewhat less than saturated) should have a minimal impact on storm maximization and subsequent PMP calculations.

12.3 Maximum Storm Efficiency

The assumption is made that if a sufficient period of record is available for rainfall observations, at least a few storms would have been observed that attained or came close to attaining the maximum efficiency possible in nature for converting atmospheric moisture to rainfall for regions with similar climates and topography. The further assumption is made that if additional atmospheric moisture had been

available, the storm would have maintained the same efficiency for converting atmospheric moisture to rainfall. The ratio of the maximized rainfall amounts to actual rainfall amounts would be the same as the ratio of precipitable water in the atmosphere associated with each storm.

There are two issues to be considered. First relates to the assumption that a storm has a rainfall efficiency close to the maximum possible. Unfortunately, state-of-the-science in meteorology does not support a theoretical evaluation of storm efficiency. However, if the period of record is considered (generally over 100 years), along with the extended geographic region with transpositionable storms, it is accepted that there should have been at least one storm with dynamics that approached the maximum efficiency for rainfall production.

The other issue pertains to the assumption that storm efficiency does not change if additional atmospheric moisture is available. Storm dynamics could potentially become more efficient or possibly less efficient depending on the interaction of cloud microphysical processes with the storm dynamics. Offsetting effects could indeed lead to the storm efficiency remaining essentially unchanged. For the present, the assumption of no change in storm efficiency seems acceptable.

12.4 Storm Representative Dew Point and Maximum Dew Point

The maximization factor depends on the determination of storm representative dew points, along with maximum historical dew point values. The magnitude of the maximization factor varies depending on the values used for the storm representative dew point and the maximum dew point. Holding all other variables constant, the maximization factor is smaller for higher storm representative dew points as well as for lower maximum dew point values. Likewise, larger maximization factors result from the use of lower storm representative dew points and/or higher maximum dew points. The magnitude of the change in the maximization factor varies depending on the dew point values. For the range of dew point values used in most PMP studies, the maximization factor for a particular storm will change about 5 percent for every 1ºF difference between the storm representative and maximum dew point values. The same sensitivity applies to the transposition factor, with about a 5 percent change for every 1ºF change in either the in-place maximum dew point or the transposition maximum dew point.

12.5 Judgment and Effect on PMP

During the process of PMP development several aspects include professional judgment. These include the following:

- Storms used for PMP development
- Storm representative dew point value and location
- Storm transposition limits
- Tropical storm type region of influence
- Application of the HRRR data for rainfall only correction

- Use of precipitation frequency climatologies to represent differences in precipitation processes (including orographic effects) between two locations
- PMP comparison to ARI grids

Each of these processes were discussed and evaluated during the PMP development process internally within the PMP task consultant group and with the PRB and Project Sponsors. The resulting PMP values derived as part of the CO-NM REPS PMP task reflect the most defensible judgments based on the data available and current scientific understanding. The CO-NM REPS PMP results represent defensible, reproducible, reasonable, and appropriately conservative estimates.

13. References

Adams, D.K., and A.C. Comrie, 1997: The North American Monsoon, Bulletin of the American Meteorological Society, Vol. 78, 2197-2212.

Alexander et al., 2015: The High-Resolution Rapid Refresh (HRRR): The operational implementation, in 95th Annual meeting of the American Meteorological Society.

Bonnin, G., D. Martin, B. Lin, T. Parzybok, M. Yekta, and D. Riley, 2011: NOAA Atlas 14 Volume 1 Version 5.0, Precipitation-Frequency Atlas of the United States, Semiarid Southwest. NOAA, National Weather Service, Silver Spring, MD.

Bontà, V., 2003: Estimation of parameters characterizing frequency distributions of times between storms. Transactions of the ASAE. 46.

Colorado State Engineers Office (2007), Extreme Precipitation Analysis Tool (EPAT): Final Report, Colorado State Engineers Office: Dam Safety Division – HDR Engineering Inc.

Corps of Engineers, U.S. Army, 1945-1973: Storm Rainfall in the United States, Depth-Area-Duration Data. Office of Chief of Engineers, Washington, D.C.

Corrigan, P. J.L. Vogel, 1993: Meteorological Analysis of a Local Flash Flood Near Opal, Wyoming 16 August, 1990, National Weather Service, Office of Hydrology, Silver Spring, MD. 5pp.

Corrigan, P., D.D. Fenn, D.R. Kluck, and J.L. Vogel, 1999: Probable Maximum Precipitation for California, Hydrometeorological Report Number 59, National Weather Service, National Oceanic and Atmospheric Administration, U. S. Department of Commerce, Silver Spring, Md, 392 pp.

Costa, J.E., and R.D. Jarrett, 2008: An Evaluation of Selected Extraordinary Floods in the United States Reported by the U.S. Geological Survey and Implications for

Future Advancement of Flood Science, http://pubs.er.usgs.gov/usgspubs/sir/sir20085164/.

Cudworth, A.G., 1989: Flood Hydrology Manual, Water Resources Technical Publication, United States Dept, of the Interior, United States Bureau of Reclamation, Denver office, 243pp.

Daly, C., R.P. Neilson, and D.L. Phillips, 1994: A Statistical-Topographic Model for Mapping Climatological Precipitation over Mountainous Terrain. J. Appl. Meteor., 33, 140–158.

Daly, C., Taylor, G., and W. Gibson, 1997: The PRISM Approach to Mapping Precipitation and Temperature, 10th Conf. on Applied Climatology, Reno, NV, Amer. Meteor. Soc., 10-12.

Dickens, J., 2003: On the Retrieval of Drop Size Distribution by Vertically Pointing Radar. American Meteorological Society 32nd Radar Meteorology Conference, Albuquerque, NM.

Doesken, N.J., Pielke, R.A., and O.A.P. Bliss, 2003: Climate of Colorado, Climatography of the United States No. 60, Colorado Climate Center, Atmospheric Science Dept. Colorado State University, Fort Collins, CO., 14pp.

Douglas, M.W., 1995: The Summertime Low-Level Jet over the Gulf of California, Monthly Weather Review, Vol. 123, 2334-2346.

Douglas, M.W., Maddox, R.A., K. Howard, 1993: The Mexican Monsoon, Journal of Climate, Vol. 6, 1665-1667.

England, J.F, Klawon, J.E, Klinger, R.E., and T.R. Bauer, 2006: Flood Hazard Study Pueblo Dam, Colorado, US Bureau of Reclamation, 333pp.

Follansbee, R., and E. Jones, 1922: The Arkansas River Flood of June 3-5, 1921, U.S. Geological Survey Water Supply Paper 487, 52pp.

Follansbee, R., Spiegel, J. B., 1937: Flood on Republican and Kansas Rivers, May and June 1935, U.S. Geological Survey Water Supply Paper WSP 796-B, 52pp.

Follansbee, R., and L.R. Sawyer, 1948: Floods in Colorado, U.S. Geological Survey Water Supply Paper 997, 149pp.

Grantz, K., B. Rajagopalan, M. Clark, and E. Zagona, 2007: Seasonal Shifts in the North American Monsoon. J. Climate, 20, 1923–1935

Hales, J.E., Jr., 1972: Surges of Maritime Tropical Air Northward over the Gulf of California, Monthly Weather Review, Vol. 100, 298-306.

Hansen, E.M, F.K. Schwarz, and J.T Reidel, 1977: Probable Maximum Precipitation Estimates. Colorado River and Great Basin Drainages. Hydrometeorological Report No. 49, NWS, NOAA, U.S. Department of Commerce, Silver Spring, MD, 161 pp.

Hansen, E.M, and F.K. Schwartz, 1981: Meteorology of Important Rainstorms in the Colorado River and Great Basin Drainages. Hydrometeorological Report No. 50, National Weather Service, National Oceanic and Atmospheric Administration, U.S. Department of Commerce, Silver Spring, MD, 167 pp.

Hansen, E.M., L.C. Schreiner and J.F. Miller, 1982: Application of Probable Maximum Precipitation Estimates – United States East of the 105th Meridian. Hydrometeorological Report No. 52, U.S. Department of Commerce, Washington, D.C., 168 pp.

Hansen, E.M, Fenn, D.D., Schreiner, L.C., Stodt, R.W., and J.F., Miller, 1988: Probable Maximum Precipitation Estimates, United States between the Continental Divide and the 103rd Meridian, Hydrometeorological Report Number 55A, National weather Service, National Oceanic and Atmospheric Association, U.S. Dept. of Commerce, Silver Spring, MD, 242 pp.

Hansen, E.M, Schwarz, F.K., and J.T. Riedel, 1994: Probable Maximum Precipitation-Pacific Northwest States, Columbia River (Including portion of Canada), Snake River, and Pacific Drainages. Hydrometeorological Report No. 57, National Weather Service, National Oceanic and Atmospheric Administration, U.S. Department of Commerce, Silver Spring, MD, 353 pp.

Hidalgo, H.G., and J.A. Dracup, 2003: ENSO and PDO Effects on Hydroclimatic Variations of the Upper Colorado River Basin, Journal of Hydrometeorology, Vol. 4, 5-22.

Higgins, R.W., Y. Yao, and X.L. Wang, 1997: Influence of the North American Monsoon System on the U.S. Summer Precipitation Regime. J. Climate, 10, 2600–2622.

Higgins, R.W., Y. Chen, and A.V. Douglas, 1999: Interannual Variability of the North American Warm Season Precipitation Regime. J. Climate, 12, 653–680.

Higgins, R.W., W. Shi, and C. Hain, 2004: Relationships between Gulf of California Moisture Surges and Precipitation in the Southwestern United States. J. Climate, 17, 2983–2997.

Huff, F.A., 1967: Time Distribution of Rainfall in Heavy Storms, Water Resources Research.

Jarrett, R.D., 1987. Flood Hydrology of Foothill and Mountain Streams in Colorado.

Ph.D. Dissertation, Department of Civil Engineering, Colorado State Univ., Fort Collins, Colorado, 239p.

Jarrett, R. D., J. E. Costa, 1987: Evaluation of the flood hydrology in the Colorado Front Range using precipitation, streamflow, and paleoflood data, U.S. Geol. Surv. Water Resour. Invest. Rep.87-4117, 37.

Jarrett, R.D., 1993: Flood Elevation Limits in the Rocky Mountains, Reprinted from Engineering Hydrology Symposium sponsored by the Hydraulics Division/ASCE, July 25-30, 1993, San Francisco, CA.

Jarrett, R. D., and E. M. Tomlinson, 2000: Regional interdisciplinary paleoflood approach to assess extreme flood potential, Water Resources Research, 36(10), 2957–2984.

Javier, J .R. N., J.A. Smith, J. England, M. L. Beck, M. Steiner, and A.A. Ntelekos, 2007: Climatology of Extreme Rainfall and Flooding from Orographic Thunderstorm Systems in the Upper Arkansas River Basin, Water Resources Research, 43, W10410.

Kappel, W.D., Hultstrand, D.M., Muhlestein, G.A., Steinhilber, K., McGlone, D., E.M. Tomlinson, and T. Parzybok. July 2013: Probable Maximum Precipitation Study for Arizona. Prepared for the Arizona Dept. of Water Resources, Dam Safety Division.

Kappel, W.D., Hultstrand, D.M., Muhlestein, G.A., Steinhilber, K., and D. McGlone, July 2014: Site-Specific Probable Maximum Precipitation (PMP) Study for the College Lake Basin, Colorado, prepared for Colorado State University.

Kappel, W.D., Hultstrand, D.M., Muhlestein, G.A., Steinhilber, K., McGlone, D., Parzybok, T.W, and E.M. Tomlinson, December 2014: Statewide Probable Maximum Precipitation (PMP) Study for Wyoming.

Kappel, W.D., Hultstrand, D.M., Muhlestein, G.A., Steinhilber, K., and McGlone, D., December 2015: Application of Temporal Patterns of PMP for Dam Design in Wyoming. Prepared for the Wyoming State Engineer's Office.

Kappel, W.D., Hultstrand, D.M., Rodel, J.T., Muhlestein, G.A., Steinhilber, K., McGlone, D., Rodel, J., and B. Lawrence, November 2015: Statewide Probable Maximum Precipitation or Virginia. Prepared for the Virginia Department of Conservation and Recreation.

Kappel, W.D., Hultstrand, D.M., Muhlestein, G.A., Steinhilber, K., and McGlone, D, February 2016: Site-Specific Probable Maximum Precipitation for Hebgen Dam, MT.

Kappel, W.D., Hultstrand, D.M., Muhlestein, G.A., Steinhilber, K., Rodel, J.T., McGlone, D., Parzybok, T.W., and B. Lawrence, September 2016: Statewide Probable Maximum Precipitation for Texas. Prepared for the Texas Commission of Environmental Quality.

Kappel, W.D., Hultstrand, D.M., Muhlestein, G.A., Rodel, J.T., Steinhilber, K., McGlone, D., and Lawrence, B., May 2017: Site-Specific Probable Maximum Precipitation and Annual Exceedance Probability Assessment for the Gross Reservoir Basin, Colorado. Prepared for Denver Water.

Kappel, W.D., Hultstrand, D.M., Muhlestein, G.A., Rodel, J.T., Steinhilber, K., and Lawrence, B., May 2018: Site-Specific Probable Maximum Precipitation and Annual Exceedance Probability Assessment for the Painted Rocks and East Fork Basins, Montana. Prepared for AECOM and Montana Dept. of Natural Resources.

Kohn, M.S., Jarrett, R.D., Krammes, G.S., and A. Mommandi, 2016: Colorado Flood Database, USGS OFRD 2012-1225, https://pubs.usgs.gov/of/2012/1225/.

Maddox, R. A., Canova, F., and L. R. Hoxit, 1980: Meteorological Characteristics of Flash Flood Events over the Western United States, Monthly Weather Review, Vol. 108, 1866-1877.

Mahoney, Kelly, Michael Alexander, James D. Scott, and Joseph Barsugli, 2013: High-Resolution Downscaled Simulations of Warm-Season Extreme Precipitation Events in the Colorado Front Range under Past and Future Climates*. J. Climate, 26, 8671–8689.

Mahoney, K., Ralph, F.M., Wolter, K., Doesken, N., Dettinger, M., Gottas, D., Coleman, T., White, A., 2014. Climatology of extreme daily precipitation in Colorado and its diverse spatial and seasonal variability. J. Hydrometeorol.

Mahoney, Kelly, 2016: Examining terrain elevation assumptions used in current extreme precipitation estimation practices: A modeling study of the 2013 Colorado Front Range floods. Amer. Meteor. Soc. 30th Conf. on Hydrology, January 2016, New Orleans, LA.

Mahoney, Kelly, Darren L. Jackson, Paul Neiman, Mimi Hughes, Lisa Darby, Gary Wick, Allen White, Ellen Sukovich, and Rob Cifelli, 2016: Understanding the Role of Atmospheric Rivers in Heavy Precipitation in the Southeast, Monthly Weather Review 2016 144:4, 1617-1632.

Martner, B.E, and V. Dubovskiy, 2005: Z-R Relations from Raindrop Disdrometers: Sensitivity to Regression Methods and DSD Data Refinements. 32nd Radar Meteorology Conference, Albuquerque, NM.

Matthai, H.F., 1969: Floods of June 1965 in South Platte River Basin, Colorado, U.S. Geological Survey Water Supply Paper 1850-B, 73pp.

McKee, T.B., and N.J. Doesken, 1997: Colorado Extreme Storm Precipitation Data Study, Climatology Report #97-1, Colorado Climate Center, Atmospheric Science Dept. Colorado State University, Fort Collins, CO, 112pp.

Miller, J.F., R.H. Frederick and R.S. Tracey, 1973: NOAA Atlas 2, Precipitation: Frequency Atlas of the Western United States. U.S. Dept. of Commerce, NOAA, National Weather Service, Washington DC.

Minty, L.J., Meighen, J. and Kennedy, M.R. (1996) Development of the Generalised Southeast Australia Method for Estimating Probable Maximum Precipitation, HRS Report No. 4, Hydrology Report Series, Bureau of Meteorology, Melbourne, Australia, August 1996.

Mueller, M., K. M. Mahoney, M. R. Hughes, 2017: High-resolution model-based investigation of moisture transport into the Pacific Northwest during a strong atmospheric river event. Mon. Wea. Rev.

National Climatic Data Center (NCDC). NCDC TD-3200 and TD-3206 datasets - Cooperative Summary of the Day

National Climatic Data Center (NCDC) Heavy Precipitation Page http://www.ncdc.noaa.gov/oa/climate/severeweather/rainfall.html#maps

National Oceanic and Atmospheric Association, Forecast Systems Laboratory FSL Hourly/Daily Rain Data, http://precip.fsl.noaa.gov/hourly_precip.html

Natural Resources Conservation Service (NRCS), Conservation Engineering Division. (2005, July). Earth Dams and Reservoirs, TR-60.

Osborn, H.B and W.N. Reynolds, 1963: CONVECTIVE STORM PATTERNS IN THE SOUTHWESTERN UNITED STATES, Hydrological Sciences Journal, 8:3, 71-83.

Perica, S. Martin, D., Pavlovic, S., Roy, I., Laurent, M.S., Trypaluk, C., Unruh, D., Yekta, M., and G. Bonnin, 2013: NOAA Atlas 14 Volume 8 version 2, Precipitation-Frequency Atlas of the United States, Midwestern States NOAA, National Weather Service, Silver Spring, MD.

PRISM Mapping Methodology http://www.ocs.oregonstate.edu/prism/index.phtml

Reich, B.J., Shaby, B.A., 2012. A hierarchical max-stable spatial model for extreme precipitation. Ann. Appl. Statist. 6 (4), 1430–1451.

Rolph, G., Stein, A., and Stunder, B., 2017: Real-time Environmental Applications and Display System: READY. Environmental Modeling & Software, 95, 210-228.

Rostvedt, J.O., and Others, 1971: Summary of Floods in the United States During 1966, U.S. Geological Survey Water-Supply Paper 1870-D, 108pp.

Rutz, Jonathan J., W. James Steenburgh, and F. Martin Ralph, 2014: Climatological Characteristics of Atmospheric Rivers and Their Inland Penetration over the Western United States. Mon. Wea. Rev., 142, 905–921.

Rutz, J. J., W. J. Steenburgh, and F. M. Ralph, 2015: The inland penetration of atmospheric rivers over western North America: A Lagrangian analysis. Mon. Wea. Rev., 143, 1924–1944.

Schreiner, L.C., and J.T. Riedel, 1978: Probable Maximum Precipitation Estimates, United States East of the 105th Meridian. Hydrometeorological Report No. 51, U.S. Department of Commerce, Silver Spring, Md, 242 pp.

Smith, W.P., and R.L. Gall, 1989: Tropical Squall Lines of the Arizona Monsoon, Monthly Weather Review, Vol. 117, 1553-1569.

Snipes, H.F., and others, 1974: Floods of June 1965 in Arkansas River Basin, Colorado, Kansas, and New Mexico, U.S. Geological Survey Water Supply Paper 1850-D, 104pp.

Stein, A. F., R. R. Draxler, G. D. Rolph, B. J. B. Stunder, M. D. Cohen, and F. Ngan, 2015: NOAA's HYSPLIT Atmospheric Transport and Dispersion Modeling System. Bull. Amer. Meteor. Soc., 96, 2059–2077.

Storm Studies – Pertinent Data Sheets, and Isohyetal Map, U.S. Department of Interior, Bureau of Reclamation, Denver, CO.

Tomlinson, E.M., 1993: Probable Maximum Precipitation Study for Michigan and Wisconsin, Electric Power Research Institute, Palo Alto, CA, TR-101554, V1.

Tomlinson, E.M., Kappel W.D., and Parzybok, T.W., February 2008: Site-Specific Probable Maximum Precipitation (PMP) Study for the Magma FRS Drainage Basin, Prepared for AMEC, Tucson, Arizona.

Tomlinson, E.M., Kappel W.D., Parzybok, T.W., Hultstrand, D., Muhlestein, G., and P. Sutter, December 2008: Statewide Probable Maximum Precipitation (PMP) Study for the state of Nebraska, Prepared for Nebraska Dam Safety, Omaha, Nebraska.

Tomlinson, E.M., Kappel, W.D., and Parzybok, T.W., February 2011: Site-Specific Probable Maximum Precipitation (PMP) Study for the Magma FRS Drainage Basin, Arizona.

Tomlinson, E.M., Kappel, W.D., and Parzybok, T.W., March 2011: Site-Specific Probable Maximum Precipitation (PMP) Study for the Tarrant Regional Water District, Texas.

Tomlinson, E.M., Kappel, W.D., Hultstrand, D.M., Muhlestein, G.A., S. Lovisone, and Parzybok, T.W., March 2013: Statewide Probable Maximum Precipitation (PMP) Study for Ohio.

Tye, M.R and D. Cooley, 2015: A Spatial Model to Examine Rainfall Extremes in Colorado's Front Range, Journal of Hydrology, 530, 15-23.

Vaill, J.E., 1999. Analysis of the Magnitude and Frequency of Floods in Colorado. U.S. Geological Survey Water-Resources Investigations Report 99-4190, 35 p.

Weaver, J.F., Gruntfest, E., and G.M. Levy, 2000: Two Floods in Fort Collins, Colorado: Learning from a Natural Disaster, Bull. Amer. Meteor. Soc., 81, 2359–2366.

World Meteorological Organization, 1986: Manual for Estimation of Probable Maximum Precipitation, Operational Hydrology Report No 1, 2nd Edition, WMO, Geneva, 269 pp.

World Meteorological Organization, 2009: Manual for Estimation of Probable Maximum Precipitation, Operational Hydrology Report No 1045, WMO, Geneva, 259 pp.

Wu, M.L.C., S.D. Schubert, M.J. Suarez, and N.E. Huang, 2009: An Analysis of Moisture Fluxes into the Gulf of California. J. Climate, 22, 2216–2239.